AD NUMBER

AD878619

NEW LIMITATION CHANGE

TO

Approved for public release, distribution unlimited

FROM

Distribution authorized to U.S. Gov't. agencies and their contractors; Critical Technology; JAN 1970. Other requests shall be referred to Naval Ship Systems Command, Washington, DC.

AUTHORITY

USNSRDC ltr, 15 Jul 1971

NAVAL SHIP RESEARCH AND DEVELOPMENT CENTER
Washington, D.C. 20034

ENGINEERING GUIDE AND COMPUTER PROGRAMS FOR DETERMINING TURBULENCE-INDUCED VIBRATION AND RADIATION OF PLATES

by
Ralph C. Leibowitz
and
Dolores R. Wallace

This document is subject to special export controls and each transmittal to foreign governments or foreign nationals may be made only with prior approval of Naval Ship Systems Command, SHIPS 037.

DEPARTMENTS OF ACOUSTICS AND VIBRATION
AND APPLIED MATHEMATICS
RESEARCH AND DEVELOPMENT REPORT

January 1970 Report 2976

323

The Naval Ship Research and Development Center is a U.S. Navy center for laboratory effort directed at achieving improved sea and air vehicles. It was formed in March 1967 by merging the David Taylor Model Basin at Carderock, Maryland and the Marine Engineering Laboratory (now Naval Ship R & D Laboratory) at Annapolis, Maryland. The Mine Defense Laboratory (now Naval Ship R & D Laboratory) Panama City, Florida became part of the Center in November 1967.

Naval Ship Research and Development Center
Washington, D.C. 20034

MAJOR NSRDC ORGANIZATIONAL COMPONENTS

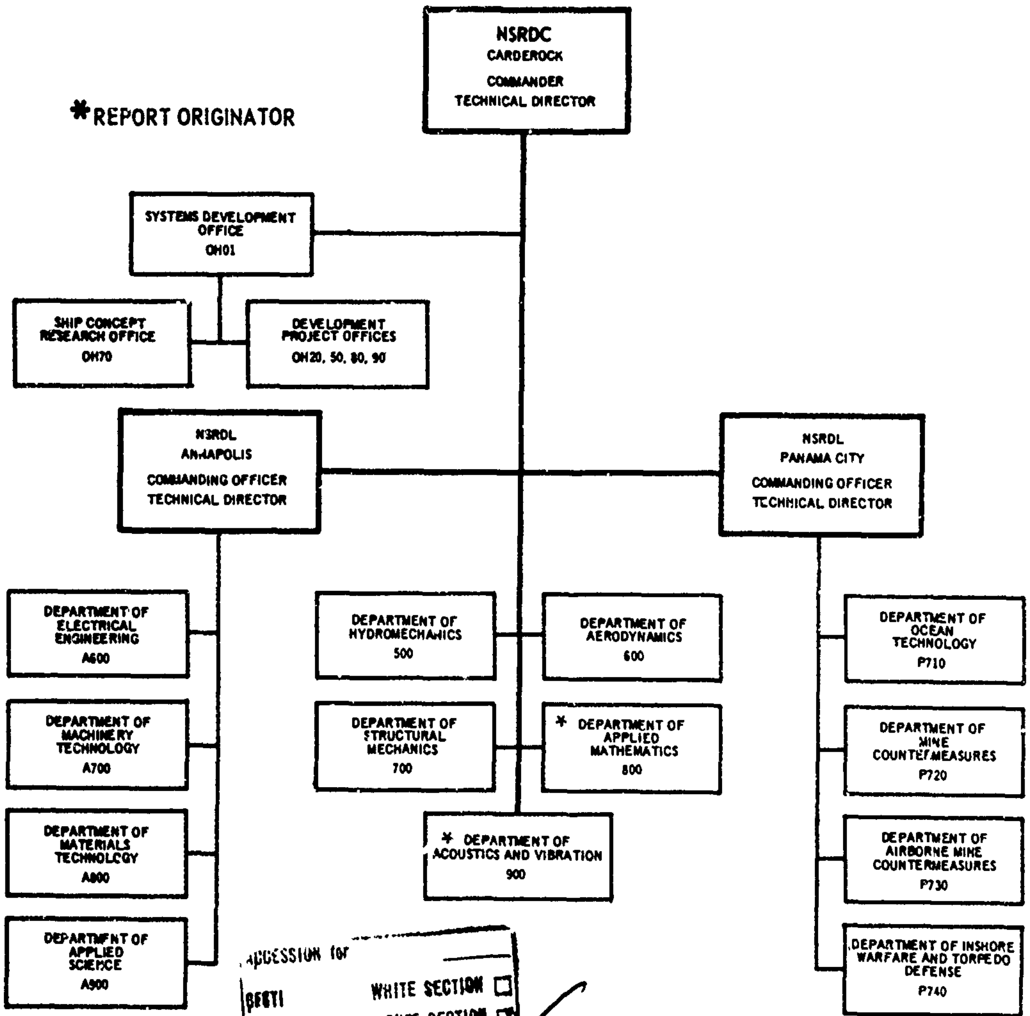

NDW-NSRDC 3960/43 (10-67)

DEPARTMENT OF THE NAVY
NAVAL SHIP RESEARCH AND DEVELOPMENT CENTER
WASHINGTON, D.C. 20034

ENGINEERING GUIDE AND COMPUTER PROGRAMS FOR DETERMINING TURBULENCE-INDUCED VIBRATION AND RADIATION OF PLATES

by

Ralph C. Leibowitz
and
Dolores R. Wallace

Wash, D.C. 20360

January 1970

Report 2976

TABLE OF CONTENTS

LIST OF FIGURES

LIST OF TABLES

ABSTRACT

This report is an engineering guide to the use of the Dyer method of manual computation and to several computer programs for determining turbulence-induced vibration and radiation of finite plates in air and in water. Both simple and clamped boundary conditions are treated. The Dyer method and the computer programs are presented in a series of appendixes:

A. Bolt Beranek and Newman Manual Method (Dyer)
B. Boeing Program I (Masestrello)
C. Electric Boat Program (Izzo)
D. Underwater Sound Laboratory Program (Strawderman)
E. Boeing Program II – Finite Element (Jacobs and Lagerquist)

The documentation is intended to facilitate the performance of flow-induced vibroacoustic computations as well as to furnish the groundwork for future research. It should also act as a theoretical guide for experimentalists. In the broader view, the documentation represents the initial steps of an effort to use computer programs to bridge the gap between vibroacoustic research results and design needs for structures that are subject to excitation by turbulence. Research tending to improve and extend the present program is recommended.

ADMINISTRATIVE INFORMATION

This study was sponsored by the Naval Ship Systems Command (NAVSHIPS) Code 037. Funding was provided by NAVSHIPS 0311 under Subproject S-R003 10 01, Task 11701.

INTRODUCTION

For several years, the Naval Ship Research and Development Center (NSRDC) has been concerned with computing the vibration and acoustic radiation of plates excited by fully developed turbulence. As indicated in Reference 1, the naval need for achieving accurate methods of computation exceeds the current state of the art for performing such computations.* Accurate computational methods for plates can provide a useful foundation for extension to more complex naval structures, e.g., ribbed sonar domes.

It is of interest to document the flow-induced vibroacoustic digital computer solutions that have been the subject of investigation by researchers outside NSRDC and that are germane to naval needs. These constitute a convenient reference for application and a base for

*References are listed on page 313. Technical notes are ordinarily not used as formal references in NSRDC reports. However, Reference 1 was authorized for inclusion by the Head, Department of Acoustics and Vibration and is releasable on request to him. This review of the state of the art shows that accurate methods of prediction have not yet been confirmed because of the lack of experimental data, particularly for plates in water. The rationale motivating the present study is discussed and corresponding experimental studies are recommended.

further development. Accordingly, the primary objective of this report is to present a documentation that provides

1. Theoretical methods of computation for immediate application by researchers who are interested in comparing theory and experiment, observing trends, etc.

2. Theoretical methods of computation for use as a guide in designing experiments.

3. Computational frameworks that can be modified and extended through additional research to meet naval needs in an increasingly realistic manner.

4. Initial steps of an effort to use computer programs to bridge the gap between vibroacoustic research results and design needs for structures that are subject to excitation by turbulence.

The documentation is essentially a user's guide to the Dyer method of manual computation and to several digital computer programs for determining turbulence-induced vibration and radiation of finite plates. Simple and clamped boundary conditions are treated, and the fluid medium surrounding a plate is either air or water. The following titles identify the manual method and the computer programs treated and indicate their location in the report:

Appendix A – Bolt Beranek and Newman Manual Method (Dyer)

Appendix B – Boeing Program I (Maestrello)

Appendix C – Electric Boat Program (Izzo)

Appendix D – Underwater Sound Laboratory Program (Strawderman)

Appendix E – Boeing Program II – Finite Element – (Jacobs and Lagerquist)

Each appendix includes the appropriate notation, the mathematical development of the equations underlying the program, descriptions of input and output data and of units, computer program listings, the time required to run particular computations, flow charts and operations and rules of the computer program. Methods are also presented for determining computer program input data from either experimental or analytical results. Test runs are included to verify the results (published response curves) of the original developers of the programs and hence to indicate the successful operation of the programs at NSRDC.

The physical foundations on which the development of the equations rest are not included. The references cited in the present report direct the interested reader to appropriate literature.

The report has been organized to meet the needs of the program user.

DISCUSSION AND RECOMMENDATIONS

For convenience, the salient features of the documentation are summarized in Table 1 which identifies and compares the various methods. This table makes it easy for the potential user to identify the various features of a program that are of interest to him and to select the

TABLE 1

Comparison of the Computational Methods

Program Designation	Location in Report	Theoretical Approach	Major Assumptions	Plate Bounda[ry] Condition[s]
Bolt Beranek and Newman Manual Method (Dyer)	Appendix A	Green function normal mode analysis (Lyon-Dyer theoretical model)	1 The turbulent field is not affected by plate motion, this is based on the provision that the plate vibratory displacements are small compared to the boundary layer displacement thickness. 2 The boundary layer pressure field has the following characteristics. a. The pressure field is a stationary random process. b. The pressure correlation decays with time. c The pressure correlation has a spatial extent small compared with the plate size of interest, i.e., $v\theta << L_x$, where $v\theta$ is essentially the greatest distance in the convection direction along which the forcing field is correlated. d The pressure correlation is convected along the surface of the plate in the direction of the free-stream velocity e. The spatial correlation is homogeneous depending on the difference in the spatial coordinates in a frame of reference moving with the mean convection speed. 3 The correlation area is much smaller than the plate area. This permits the boundary layer pressure field to be formulated in terms of delta functions which are analytically simple but admittedly imprecise. Moreover, as a consequence, the modes are statistically independent. 4 For low density fluids (only), e.g., air, the radiation reaction on the plate may be neglected, i.e., $p_1 - p_2 << l$ Then, the sound field external to the plate and the vibration field on the plate can be considered independently For high density fluids, e.g., water, the radiation reaction on the plate is included in the analysis. 5 Damping restrictions are $\eta < 1/3$ and $\frac{\beta_o}{2\omega_{mn}M} < 1/3$ 6 Orthogonal modes. 7 Convection velocity is a constant given by $v = 0.8\ U_\infty$	Simple supports
Boeing Program I (Maestrello)	Appendix B	Green function–normal mode analysis (Lyon-Dyer theoretical model) and Fourier transform relationships between cross spectral density and cross correlation of the exciting pressures	1. Same as Items 1, 2, and 3 of Dyer assumptions, model representing turbulence excitation consists of convected wall pressure pattern, space and time dependent which retains the characteristics of the superposition of a wave system, with phase and amplitude associated with wavenumber and frequency spectrum 2. Lightly damped panel 3 Orthogonal modes (except for case of coupled modes, Item 4) 4 Negligible cross-modal effect (except that in obtaining the displacement cross power spectral density the modal cross coupling can be included). 5. Convection velocity is a constant given by $U_o = 0.8\ U_\infty$	Simple supports [...] that in obtaining th[e] displacement cross [...] spectral density, s[...] and clamped supp[...] are included.
Electric Boat Program (Izzo et al.)	Appendix C	Green function–normal mode analysis (Lyon-Dyer theoretical model), Rayleigh formulation for acoustic pressure-plate acceleration relationship, and Fourier Transform relationship between cross spectral density and cross correlation of the acoustic field pressures	1 Same as Items 1, 2, 3, 5, 6, and 7 of Dyer assumptions. 2. Viscous and radiation damping are negligible.	Simple and clamp[ed] supports
Underwater Sound Laboratory Program (Strawderman)	Appendix D	Frequency domain analysis of spectral properties of the random variables	1 Same as Item 1 of Dyer assumptions, boundary layer thickness over the plate is considered constant. 2. Turbulent boundary layer is a homogeneous stationary random process. 3 Zero (or small) pressure gradient. 4 Cavity acoustic pressure provides negligible excitation to the plate, i.e., the only forces exciting the plate are those associated with the turbulent boundary layer pressure fluctuations. 5. Convection velocity is a constant given by $U_c = 0.65_\infty$ 6 The effective mass and damping, due to the combined effect of plate and water, is assumed constant; acoustic damping effects are neglected in the derivation of the cavity acoustic spectral density, the only damping effects being associated with the plate	Simple supports
Boeing Program II Finite Element (Jacobs and Lagerquist)	Appendix E	Finite element matrix structural analysis in the frequency domain	1. Same as Item 1, 3, and 4 of Maestrello assumptions; a frozen turbulence model (Taylor hypothesis) and small-scale distributed and convected random loading of the turbulent boundary layer on a simple panel are assumed, the loading is considered to be a stationary ergodic and homogeneous random pressure. 2. Lightly damped panel; damping proportional to inertia, stiffness or both 3 Mass of the panel is assumed to be concentrated at the node points. 4 Convection velocity is a constant given by $U_c = 0.88\ U_\infty$.	Simple and clamp[ed] supports

	Plat - Boundary Conditions	Fluid Media	Excitation Function Cross Correlation Function and/or Cross Spectral Density for Pressure (no distinction between normalized and unnormalized forms)	Response Function Most General Computer Output Data	Geometry and Coordinate System for Theoretical Model	Test Runs (Specific Computations)
...e premise that the plate vibratory ...thickness. ...the plate are of interest, i.e., $v\theta << L_x$, ...along which the forcing field is correlated. ...in the direction of the free-stream velocity. ...in the spatial coordinates in a frame of ...the boundary layer pressure field to be ...admittedly imprecise. Moreover, as a ...plate may be neglected, i.e., $p_1 - p_2 << f$. ...plate can be considered independently. ...included in the analysis.	Simple supports	Air and Water	$\langle f(r,t) f^*(r',t') \rangle = A t^2 \delta(\zeta - v\tau)\,\delta(\xi)\, e^{-\frac{\tau}{\theta}}$	Space-time correlation of displacements Mean square pressure within a closed space (Figure 1)	Figure 1	See sample problem
...turbulence excitation consists of convected ...characteristics of the superposition of a wave ...frequency spectrum ...test cross power spectral density the model	Simple supports except that in obtaining the displacement cross-power spectral density, simple and clamped supports are included.	Air	1. Model A - convected semifrozen pattern $R(\xi\ \eta\ \tau) = \dfrac{e^{-\frac{\lvert\xi\rvert}{U_c\theta}} \left\{ \sum_{\gamma=1}^{3} \frac{A_\gamma K_\gamma}{K_\gamma^2 + \left(\frac{1}{FU_c}\right)^2 \left[(\xi - U_c\tau)^2 + \eta^2\right]} \right\}}{\sum_{\gamma=1}^{3} \frac{A_\gamma}{K_\gamma}}$ $P(k_1, \omega) = \dfrac{\frac{\theta}{1+\theta^2(\omega + K_1 U_c)^2} \left(\frac{FU_c}{2\pi}\right) \sum_{\gamma=1}^{3} A_\gamma e^{-\lvert\omega\rvert K_\gamma F}}{\sum_{\gamma=1}^{3} \frac{A_\gamma}{K_\gamma}}$ Note. The more general expression $p(k_1, k_2, \omega)$ has been derived and was presented in Reference 15, but was not used in computation. Moreover, in deriving the displacement cross power spectral density, Model A was slightly modified in accordance with recent data for a flat smooth plate (Reference 22) 2. Model B - - unsteady convection Note Expressions for $R(\xi\ \eta\ \tau)$ and $P(k_1, k_2, \omega)$ are presented in this report. Programming of these equations can be easily done at the users request.	Mean square displacements Cross-power spectral density of turbulence pressure, i.e., cross pressure spectra in k, ω space Displacement cross-power spectral density (only the case of model uncoupling has been run)	Same geometry as Figure 1	Figures 7 - 10
	Simple and clamped supports	Air and Water	Same as Dyer equation, but different notation $R_{tp}(r, \tau) = p^2 A \delta\left[(x_o - x_o) - U_c\tau\right] \delta(y_o - y_o)\, e^{-\frac{\lvert\tau\rvert}{\theta}}$	Space-time correlation of acoustic pressures Power spectrum of acoustic pressure	Figure 11	Figures 12 - 14
...r the plate is considered constant. ...ness. ..., i.e., the only forces exciting the plate ...ations. ...te and water, is assumed constant; ...acoustic spectral density, the only	Simple supports	Air and Water	$S_{pp}(\xi\ \eta\ \omega) = 0.75 \times 10^{-5} \alpha^2 \rho_f^2 U_o^3 \delta^* \left[e^{-0.115\lvert\frac{\omega\xi}{U_c}\rvert}\right]\left[e^{-0.7\lvert\frac{\omega\eta}{U_c}\rvert}\right] e^{-i\left(\frac{\omega\xi}{U_c}\right)}$ $\omega < 1.256\,\frac{U_o}{\delta^*}$ $= 1.5 \times 10^{-5} \alpha^2 \frac{\rho_f^2 U_o^6}{\omega^3 \delta^{*2}} \left[e^{-0.115\lvert\frac{\omega\xi}{U_c}\rvert}\right]\left[e^{-0.7\lvert\frac{\omega\eta}{U_c}\rvert}\right] e^{-i\left(\frac{\omega\xi}{U_c}\right)}$ $\omega > 1.256\,\frac{U_o}{\delta^*}$ where $\alpha = 1.0$ for water $\alpha = 3.0$ for air	Plate velocity power spectrum Cavity acoustic pressure power spectrum	Figure 15	Figures 16 - 18
...ence model (Taylor hypothesis) and small- ...dary layer on a simple panel are assumed, ...random pressure. ...both.	Simple and clamped supports	Air	Same as Maestrello equation (Model A), but different notation $\rho(\xi, \eta\ \tau) = \dfrac{e^{-\frac{\lvert\xi\rvert}{U_c\theta}} \left\{ \sum_{n=1}^{3} \frac{A_n K_n}{K_n^2 + B^2\left[(\xi - U_c\tau)^2 + \eta^2\right]} \right\}}{\sum_{n=1}^{3} \frac{A_n}{K_n}}$ Note: The pressure cross-power spectral density is given in various forms in Appendix E.	Mean square displacements Power spectral density of displacement Cross power spectral density of turbulence pressures Cross spectral density of displacement	Figures 19, 20, 21	Figures 27, 28

program that most nearly meets his needs. Of course evaluation of the capability of a program for making accurate predictions with respect to naval problems requires comparison between theory and actual experiments in water.

Based on an evaluation of the computer program presented herein as well as the investigation made in Reference 1, the following recommendations are made:

1. Immediate application should be made of the programs considered to be most relevant to naval needs. A range of geometric, structural, and flow data representing naval plating under actual operating (or scaled) conditions should be submitted as input to the programs. The results of a variation in parameters should be analyzed and evaluated. Comparison of such results from different programs may yield meaningful *qualitative* information or trends. The conclusions drawn from such trends may provide insight into the physical nature of the problem and/or act as a guide to the design of associated experiments. Moreover, when compared with corresponding experimental results, the theoretical results will yield *quantitative* information on the degree of accuracy of the methods of computation. Thus, the theory in conjunction with the experimental results may lead either to modification of the existing analysis or to determination of correction factors for the theoretical results. It may also lead to determination of scaling factors for different geometries and media.

2. The methods considered to be most useful for solving naval problems should be modified and extended to include improvements that enable incorporation of the following parameters, structures, and effects:

a. Radiation resistance
b. Internal damping
c. Fluid loading (added or virtual mass)
d. Shear and rotary inertia (thick plate theory)
e. Convection velocity
f. Ribs
g. Rough plates, protuberances, openings, and indentations
h. Orthotropic plates and inhomogeneous plates
i. Combination of plate materials (composite plates)
j. Complex structures
k. Boundary conditions (other than fixed or simply supported)
l. Cross-modal coupling
m. Surface curvature and fairness
n. Reverberant and nonreverberant (anechoic) media

Improvements in the theory should result in the evolution of design data for selecting plate materials and geometry and structural arrangements for sonar domes and submarine hulls that will have minimum vibratory and acoustic response to turbulence excitation. In particular, design charts of vibroacoustic response as a function of structural parameters (properties and geometry) can be obtained by using a computer. These charts can be useful in establishing acoustical design criteria.

CONCLUSION

The Dyer manual method and several computer programs for determining fully developed turbulence-induced vibration and radiation of finite plates have been documented. The treatments include simple and clamped boundaries, and the environment of the plates is either air or water. Methods have also been given for determining computer input data from either experimental results or analysis. The methods are useful for immediate application by theoretical and experimental researchers and also provide a basis for modification and extension to more accurate programs that are capable of meeting naval needs in an increasingly realistic and practical manner. These achievements can be attained (1) through a better understanding of the physical foundations of the problem and hence an improved representation of the models used and the quantities to be included in the analyses, (2) through improved (new) methods of mathematical analysis as well as practical extension of presently used methods of analysis, and (3) through improvements in computer programing techniques and computer capabilities.

ACKNOWLEDGMENTS

Various personnel played significant roles in the successful completion of this project. The authors are indebted for the supervisory aid and encouragement of Messrs. G.J. Franz and G. H. Gleissner and Drs. E. H. Cuthill, F. N. Frenkiel, and F. Theilheimer. In the initial stages of the work, Dr. Theilheimer also provided mathematical assistance with respect to many phases of the computer program and so merits special appreciation.

For the provision of computer programs and additional assistance relevant to their successful operation, the authors gratefully acknowledge the help of Mr. L. Maestrello, Mrs. F. Gasche, Mr. L. Jacobs, Mr. D. Lagerquist, Mr. K. Tsurusaki, and Mr. M. C. Young of Boeing Company; Mr. Budzyk and the members of his staff at the Electric Boat Division of General Dynamics Corporation; Dr. W. A. Strawderman of the U. S. Navy Underwater Sound Laboratory; and Messrs. Dave Smith, Nelson Wolfe, Mel Eifert, and Ralph Shemovitz of Wright-Patterson Air Force Base.

APPENDIX A

BOLT BERANEK AND NEWMAN MANUAL METHOD (DYER)

APPENDIX A1 – MATHEMATICAL ANALYSIS

APPENDIX A2 – SAMPLE PROBLEM

APPENDIX A3 – METHOD FOR DETERMINING INPUT DATA

NOTATION

A	Correlation area
$A_{mn}(r_0,\omega)$	A coefficient
a'_{mn}	Total modal damping due to structure and fluid coupling
a_{mn}	Modal structural damping, positive and real
B	Bending stiffness equal to $\dfrac{Eh^3}{12(1-\sigma^2)}$
C_B	Free flexural phase velocity for a thin plate equal to $\omega^{\frac{1}{2}}(B/M)^{\frac{1}{4}}$
c	Velocity of sound in fluid
c_L	Longitudinal bar velocity (17,000 ft/sec in steel or aluminum)
D_{pq}	A coefficient
d	Displacement boundary thickness
E	Young's modulus
F	Force on plate due to external and sound pressure fields
f	External pressure field
f_c	Sound coincidence frequency
$f_{rms}, \overline{f^2}$	Root-mean-square and mean-square boundary-layer pressure, respectively
$G(r,r_0,\omega)$	Green function, which is Fourier transform of impulse response g
g	Acceleration due to gravity
$g\left(\dfrac{r,t}{r_0,t_0}\right)$ or $g\left(\dfrac{x,y,t}{x_0,y_0,t_0}\right)$	Impulse response of plate
H_{mn}	A coefficient
h	Plate thickness
$I_{mn}(\tau)$	Time correlation integral
k	Acoustic wave number equal to ω/c
k_{mn}	Wave number equal to $\sqrt{k^2-\Gamma_{mn}^2}$
L	Equal to $\frac{1}{2}(L_xL_y)^{\frac{1}{2}}$
L_x,L_y,L_z	Dimensions of plate along x,y, and z, respectively, as shown in Figure 1.

M	Plate structural mass per unit area
M'	Total effective mass per unit area of plate due to structure and fluid coupling
M_1	Free-space added mass per unit area
M_2	Added mass per unit area associated with coupling to sound waves in the closed liquid-filled volume
m, n or p, q or μ, ν	Mode numbers
$N(\Gamma_{mn}), \Delta N(\Gamma_{mn})$	Number of modes included up to wave number Γ_{mn} and average number of modes in a frequency band $\Delta\nu$, respectively
$n(\Gamma_{mn})$	Modal density
P^2_{mn}	Modal mean-square pressure (a time averaged quantity)
$\overline{P^2_{mn}}$	Spatial average of the modal mean-square pressure P^2_{mn} (a space-time average quantity)
$\overline{p^2}$	Equal to $P^2_{mn}\,\Delta N$, the average mean square pressure for all modes ΔN in a frequency band $\Delta\nu$
p_j	Sound pressure on either side of plate at $z = L_z$
r	Represents coordinate position x,y
S, ds	Area, differential area equal to $dx\,dy$
s	Radiation efficiency
t	Time
U_∞	Free stream velocity of fluid external to plate
$U(t - t_0)$	Unit step function
$V(x,y,z,\omega)$	Equal to the sum of the plate modal velocities
V_{mn}	Plate modal velocity
v	Mean convection speed along the positive x direction
v_0	Hydrodynamic coincidence speed
$W_{m,n}(x,y,t)$	Normal mode for plate
$w(r,t)$ or $w(x,y,t)$	Displacement of neutral plane of plate
w_s	Weight of steel plate per square foot
x,y,z	Coordinate system for plate (see Figure 1)
Z_{mn}	Plate modal impedance

α_m	Convection frequency equal to $m\pi v/L_x$ and interpreted as the frequency at which the turbulent field is convected past a length of plate equal to the m modal wavelength
β	Damping coefficient, including both viscous and hysteretic damping
β_0	Damping coefficient, representing viscous damping of plate structure only
β_1	Damping coefficient, representing added viscous damping due to radiation of energy in the fluid away from plate
Γ_{mn}	Eigenvalue for plate, taken to be real
γ,μ	Coordinate system for plate (see Figure2)
δ	Dirac delta function
$\delta_{\mu\nu}$	Kronecker delta function
ϵ,η	Positive quantities
ζ	Equals $x - x'$
η	Loss factor
θ	Mean statistical lifetime of the turbulent state
κ	Measure of the inverse radius of the turbulence eddy
ν, $\Delta\nu$	Frequency and frequency band, respectively
ξ	Equals $y - y'$
ρ	Fluid density
ρ_s	Density of plate steel
σ	Poisson's ratio
τ	Equals $t - t'$
$\phi_{mn}(x,y)$	Plate eigenfunction
$\psi_i(x,y,z,t)$	Velocity potential; the space $i = 1$ is taken to be free from boundaries except at $z = L_z$ and the space $i = 2$ is a closed space with reflective boundaries
$\Psi_i(x,y,z,\omega)$	Fourier transform of $\psi_i(x,y,z,t)$
ω	Circular frequency of vibration
ω_c	Sound coincidence circular frequency of vibration
ω_{mn}	Damped resonance frequency, positive and real

ω_0	Characteristic frequency
$< \cdot \cdot \cdot \cdot >$	Symbols for time average operation
$*$	Denotes complex conjugate
$\mathcal{F}$	Symbol for Fourier transformation

APPENDIX A1 – MATHEMATICAL ANALYSIS

The differential equation governing displacement of a thin plate due to turbulent boundary layer pressure excitation on the plate surface (Figure 1) is [2–4]

$$B\nabla^4 w + M\frac{\partial^2 w}{\partial t^2} + \beta\frac{\partial w}{\partial t} = -f - (p_1 - p_2)_{z=L_z} = -F(x,y,t) \tag{A1}$$

The solution of Equation (A1) is [5]

$$w(r,t) = \int_{-\infty}^{t} dt_0 \int_S dS_0\, g(r,t/r_0,t_0)\, F(r_0,t_0) \tag{A2}$$

where g, the impulse response of the plate, is the solution to [5,6] the equation

$$B\nabla^4 g + M\frac{\partial^2 g}{\partial t^2} + \beta\frac{\partial g}{\partial t} = -\delta(x - x_0)\,\delta(y - y_0)\,\delta(z - z_0) \tag{A3}$$

The normal mode W_{mn} for the plate, which has the form

$$W_{mn}(x,y,t) = \phi_{mn}(x,y)\, e^{[-a_{mn}t - i\omega_{mn}t]} \tag{A4}$$

satisfies the homogeneous equation for the freely vibrating plate

$$B(1 - i\eta)\nabla^4 W_{mn} + M\frac{\partial^2 W_{mn}}{\partial t^2} + \beta_0\frac{\partial W_{mn}}{\partial t} = 0 \tag{A5}$$

where explicit division is shown of the damping into its hysteretic and viscous components.

The solution to the nonhomogeneous Equation (A1) will be found by obtaining g, for inclusion in Equation (A2), in terms of a superposition of the normal modes or eigenfunctions, Equation (A4), satisfying the homogeneous Equation (A5).

Substitution of Equation (A4) in (A5) yields the following equation for the eigenfunctions ϕ_{mn}

$$\nabla^4\phi_{mn} - \Gamma_{mn}^4\phi_{mn} = 0 \tag{A6a}$$

where

$$\Gamma_{mn}^4 = -\frac{[M(a_{mn} + i\omega_{mn})^2 - \beta_0(a_{mn} + i\omega_{mn})]}{B(1 - i\eta)} \tag{A6b}$$

The eigenvalue Γ_{mn} is taken to be a real quantity. Multplying both sides of Equation (A6b) by $B(1 - i\eta)$ and equating imaginary and real numbers, we obtain

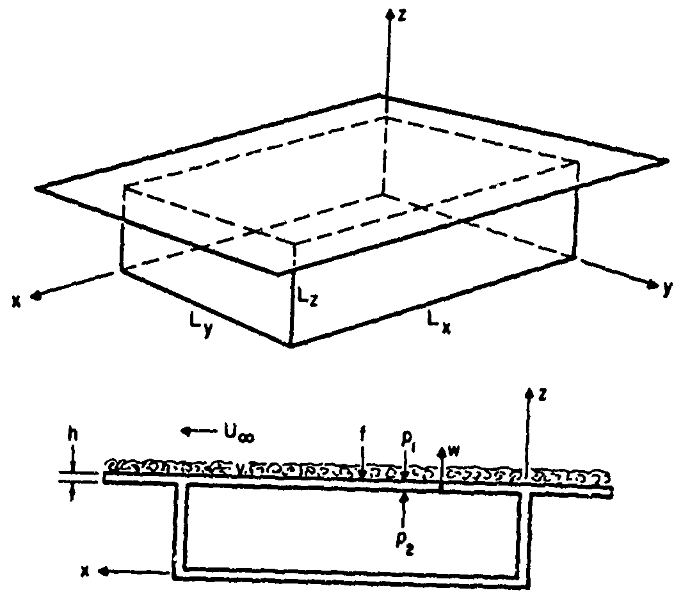

Figure 1 – Geometry and Coordinate System for Boundary Layer Excitation

$$a_{mn} = \frac{\beta_0}{2M} + \frac{\Gamma_{mn}^4 B\eta}{2M\omega_{mn}} \tag{A7}$$

$$\omega_{mn}^2 = \frac{B}{M}\Gamma_{mn}^4 - a_{mn}^2 \approx \frac{B}{M}\Gamma_{mn}^4 \tag{A8}$$

Equations (A7) and (A8) represent two simultaneous equations for a_{mn} and ω_{mn} as functions of the eigenvalues Γ_{mn}^4, which, as will be shown, are determined by the boundary conditions. Equation (A1) is also to obey these conditions.

The Fourier transform pair relating the impulse response g to the Green function G is

$$g(r,t/r_0,t_0) = \frac{1}{2\pi}\int_{-\infty}^{\infty} G(r,r_0,\omega)\, e^{-i\omega(t-t_0)}\, d\omega \tag{A9a}$$

$$G(r,r_0,\omega) = \int_{-\infty}^{\infty} g(r,t/r_0,t_0)\, e^{i\omega(t-t_0)}\, dt \tag{A9b}$$

Taking Fourier transforms of both sides of Equation (A3)* and noting that $\mathcal{F}\left(\frac{d^n g}{dt^n}\right) \to p^n G(\omega)$, where $p = -i\omega$, and $\int_{-\infty}^{\infty} \delta(t-t_0)\, e^{-i\omega(t-t_0)}\, dt = 1$, we obtain

$$\nabla^4 G - \Gamma^4 G = \frac{-\delta(x-x_0)\,\delta(y-y_0)}{B(1-i\eta)} \tag{A10a}$$

where

$$\Gamma^4 = \frac{\omega^2 M + i\omega\beta_0}{B(1-i\eta)} \tag{A10b}$$

Assume that the Green function G can be expanded in terms of the eigenfunctions ϕ_{mn}. Then

$$G(r,r_0,\omega) = \sum_{m,n} A_{mn}(r_0,\omega)\,\phi_{mn}(r) \tag{A11}$$

To evaluate the coefficients A_{mn}, substitute Equation (A11) in (A10a); using Equation (A6a), multiply by ϕ_{pq} and integrate over S, interchanging the summation and integral and normalizing the eigenvalues for convenience thus:

$$\int \phi_{mn}(r)\,\phi_{pq}(r)\,dS = \delta_{mp}\,\delta_{nq} \tag{A12}$$

*Equation (A3) modified to show explicit division of damping as in Equation (A5).

where

$$\delta_{mp}\,\delta_{nq} = 0 \qquad m \neq p \text{ or } n \neq q$$

$$\delta_{mp}\,\delta_{nq} = 1 \qquad m = p,\ n = q$$

These steps give (noting that the summation is dropped, since the final expression is true for all m,n)

$$A_{mn} = \frac{1}{B(1 - i\eta)}\,\frac{\phi_{mn}(r_0)}{\Gamma_{mn}^4 - \Gamma^4} \tag{A13}$$

Substituting Equation (A13) in (A11), we obtain

$$G(r,r_0,\omega) = \frac{1}{B(1 - i\eta)} \sum_{m,n} \frac{\phi_{mn}(r)\,\phi_{mn}(r_0)}{\Gamma_{mn}^4 - \Gamma^4} \tag{A14}$$

Using Equations (A6b) and (A10b), it can be shown that

$$\frac{1}{B(1 - i\eta)}\,\frac{1}{\Gamma_{mn}^4 - \Gamma^4} = \frac{1}{M(p - ia)\,[p - (-ia + \beta_0/M)]}$$

where

$$a = \omega_{mn} - ia_{mn}$$

We also use the approximation, which ignores the hysteretic term $\beta_0/M = 2a_{mn}$; see Equation (A7). Fourier transform tables [7] can now be used to find

$$g(r,t/r_0,t_0) = \sum_{m,n} \frac{\phi_{mn}(r)\,\phi_{mn}(r_0)}{\omega_{mn} M}\; e^{-a_{mn}(t-t_0)} \sin\omega_{mn}(t-t_0)\;\; U(t-t_0) \tag{A15}$$

where the unit step function $U(t - t_0)$ corresponds to $\delta(t - t_0)$ in the excitation.

For a finite plate immersed in a low-density fluid (e.g., air), the radiation reaction on the plate may be neglected, i.e., $p_1 - p_2 << f$. Thus, for *zero fluid load*, Equation (A2) becomes

$$w(r,t) = \int_{-\infty}^{t} dt_0 \int_s dS_0\;\; g(r,t/r_0,t_0)\; f(r_0,t_0) \tag{A16}$$

The cross correlation of the displacement is[8]

$$<w(r,t)\, w^*(r',t')> = \int_{-\infty}^{t} dt_0 \int_{-\infty}^{t'} dt_0' \int_s dS_0 \int_s dS_0'\, g(r, t/r_0\ t_0)$$

$$g^*(r', t'/r_0', t_0')\, <f(r_0, t_0) f^*(r_0', t_0')> \tag{A17}$$

where Dyer used [2-4]

$$<f(r,t)\ f^*(r',t')> = Af^2\, \delta(\zeta - v\tau)\, \delta(\xi)\, e - \frac{|\tau|}{\theta} \tag{A18}$$

We assume simply supported boundaries at the plate edge

$$w = \frac{\partial^2 w}{\partial x^2} = 0 \qquad \text{at } x = 0,\ L_x$$

$$w = \frac{\partial^2 w}{\partial y^2} = 0 \qquad \text{at } y = 0,\ L_y \tag{A19}$$

The eigenfunctions (normalized solutions of Equation (A6a) that obey Equation (A19)) and the corresponding eigenvalues, neglecting the effect of damping, are[9]

$$\phi_{mn}(r) = \frac{2}{(L_x L_y)^{1/2}} \sin \frac{m\pi x}{L_x} \sin \frac{n\pi y}{L_y} \tag{A20}$$

$$\Gamma_{mn}^2 = \left(\frac{m\pi}{L_x}\right)^2 + \left(\frac{n\pi}{L_y}\right)^2 \tag{A21}$$

Equations (A18), (A20), and (A21) are now used to determine the plate vibrations, Equation (A17) . Equation (A17) involves the product of two doubly infinite sums; a typical term is represented by the cross product of two modes (m,n) and (p,q)

$$<w\,(r,t)\ w^*(r',t')>_{mn,pq} = \frac{Af^2\, \phi_{mn}(r)\, \phi_{pq}(r')}{\omega_{mn}\omega_{pq} M^2} \int_{-\infty}^{t} dt_0 \int_{-\infty}^{t'} dt_0'$$

$$\cdot \int_s dS_0 \int_s dS_0'\ \phi_{mn}(r_0)\, \phi_{pq}(r_0') \left[e^{-a_{mn}(t - t_0) - a_{pq}(t' - t_0') - \frac{|\tau_0|}{\theta}} \right]$$

$$\cdot \sin \omega_{mn}(t - t_0) \sin \omega_{pq}(t' - t_0')\, \delta(\zeta_0 - v\tau_0)\, \delta(\xi_0) \tag{A22}$$

If the slope of the plate displacement is small compared to unity, then Equation (A22) is essentially the correlation of the plate normal displacement. Because of the delta function $\delta(\xi_0) = \delta(y_0 - y_0')$, the y_0, y_0' space integrations readily yield the term $(\delta_{nq} L_y)/2$. Further, if it is assumed that $v\theta \ll L_x$, the x_0, x_0' integrations yield the term $\delta_{mp} \frac{L_x}{2} \cos \alpha_m \tau_0$, where

$$\alpha_m = \frac{m\pi v}{L_x} \tag{A23}$$

Thus the result for the spatial integration is $\frac{4}{(L_x L_y)} \left[\frac{(\delta_{nq} L_y)}{2}\right] (\delta_{mp} \frac{L_x}{2} \cos \alpha_m \tau_0)$ $= \cos \alpha_m \tau_0 \, \delta_{mp} \, \delta_{nq}$, and Equation (A22) may now be written

$$\langle w(r,t)\, w^*(r',t')\rangle_{mn,pq} = \frac{Af^2 \phi_{mn}(r)\, \phi_{pq}(r')}{\omega_{mn}\omega_{pq} M^2} \int_{-\infty}^{t} dt_0 \int_{-\infty}^{t'} dt_0'$$

$$\cdot \left[e^{-a_{mn}(t - t_0) - a_{pq}(t' - t_0') - \frac{|\tau_0|}{\theta}} \right]$$

$$\cdot \sin \omega_{mn}(t - t_0) \sin \omega_{pq}(t' - t_0')\, \delta_{mn}\, \delta_{pq} \cos \alpha_m \tau_0 \tag{A24}$$

To facilitate integration, a new coordinate system γ, μ is introduced, where γ and μ are related to the coordinates t_0, t_0' as follows

$$\gamma = (t' - t_0') - (t - t_0) = \tau_0 - \tau$$

$$\mu = (t' - t_0') + (t - t_0) \tag{A25}$$

The differentials of the γ, μ and t_0, t_0' coordinate systems are related by means of the Jacobian

$$dt_0\, dt_0' = \left| \frac{\partial(t_0, t_0')}{\partial(\mu, \gamma)} \right| d\gamma d\mu = \begin{vmatrix} \frac{\partial t_0}{\partial \mu} & \frac{\partial t_0'}{\partial \mu} \\ \frac{\partial t_0}{\partial \gamma} & \frac{\partial t_0'}{\partial \gamma} \end{vmatrix} d\gamma d\mu \quad \begin{vmatrix} -\frac{1}{2} & -\frac{1}{2} \\ +\frac{1}{2} & -\frac{1}{2} \end{vmatrix} d\gamma d\mu$$

$$dt_0\, dt_0' = \frac{1}{2}\, d\gamma\, d\mu \tag{A26}$$

Determination of the limits of integration for μ and γ is intricate. The limits are determined from construction of the μ,γ coordinate system as shown in Figure 2. The figure shows that the limits are $-\mu$ to μ for γ and 0 to ∞ for μ.
Then (letting $\frac{p}{q} \to \frac{m}{n}$ by virtue of the delta functions) Equation (A24) becomes

$$< w(r,t)\, w^*(r', t') >_{mn} = \frac{Af^2\, \phi_{mn}(r)\, \phi_{mn}(r')}{4\omega_{mn}^2\, M^2}\, I_{mn}(\tau) \qquad \text{(A27)}$$

where for the correlation integral $I_{mn}(r)$

$$I_{mn}(\tau) = \int_0^\infty d\mu \int_{-\mu}^{\mu} d\gamma\; e^{\left[-a_{mn}\mu - \frac{|\gamma+\tau|}{\theta}\right]} \cos\alpha(\gamma+\tau)\, [\cos\omega_{mn}\gamma - \cos\omega_{mn}\mu] \quad ; \quad \tau \geq 0$$

(A28)

Because of the absolute value sign in the integrand, Equation (A28) must be integrated in separate regions, depending in part on whether γ is greater or less than $-\tau$(i.e., $\tau_0 > 0$ or $\tau_0 < 0$). Figure 2 shows the regions within which the integral must be evaluated. Thus, Equation (A28) becomes

$$I_{mn}(\tau) = \left\{ \int_\tau^\infty d\mu \int_{-\mu}^{-\tau} d\gamma\; e^{\left[\frac{\gamma+\tau}{\theta}\right]} + \int_\tau^\infty d\mu \int_{-\tau}^{\mu} d\gamma\; e^{\left[\frac{-\gamma-\tau}{\theta}\right]} + \int_0^\tau d\mu \int_{-\mu}^{\mu} d\gamma\; e^{\left[\frac{-\gamma-\tau}{\theta}\right]} \right\} e^{[-a_{mn}\mu]} \qquad \text{(A29)}$$

$$\cdot \cos\alpha(\gamma+\tau)\, [\cos\omega_{mn}\gamma - \cos\omega_{mn}\mu], \qquad \tau \geq 0$$

For $\tau<0$, τ is replaced by $-\tau$ in Equation (A29).

Equation (A29) is laborious to evaluate in generality. Dyer gives the following results for $I_{mn}(\tau)$ for special cases. The results are not directly applicable to underwater problems because the plate is assumed to be immersed in a low-density fluid. However, with modification, they can be used for underwater problems.

MEAN-SQUARE RESPONSE AT COINCIDENCE

The time integral is now specialized to $\tau = 0$ as well as $\alpha_m = \omega_{mn}$, i.e., $v = v_0 = C_B \left[1 + \left(\frac{nL_x}{mL_y}\right)^2\right]^{1/2}$ where v_0 is the hydrodynamic coincidence speed and $C_B = \omega^{1/2}\left(\frac{B}{M}\right)^{1/4}$.

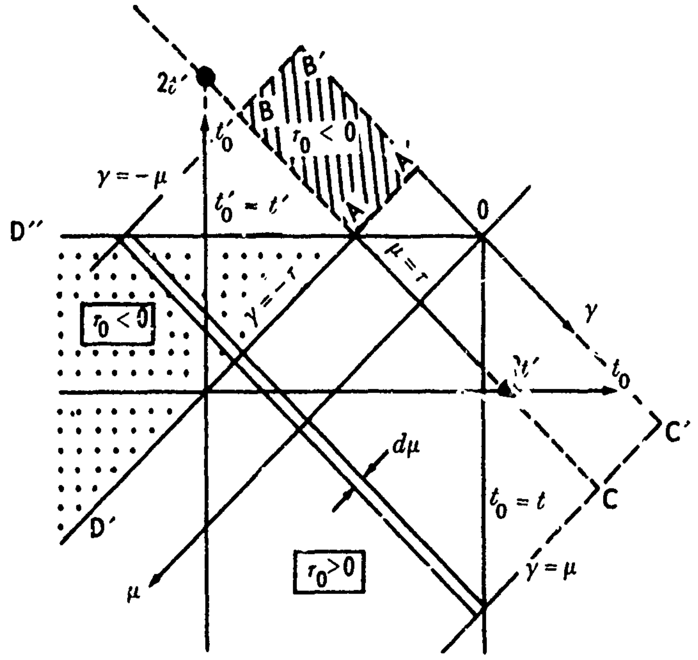

Figure 2 -- Coordinate Systems and Regions of Integration in the Time Domain

Note to Figure 2:

$$\gamma = (t' - t_0') - (t - t_0) = r_0 - r;\ r_0 = t_0 - t_0'$$

$$\mu = (t' - t_0') + (t - t_0)\ ;\ r = t - t'$$

Hence $\gamma = \mu = 0$ corresponds to $t_0 = t,\ t_0' = t'$. The line corresponding to $\mu = 0$ is $t' - t_0' = t_0 - t$ which has the slope $\left(\frac{dt_0'}{dt_0}\right)_{\mu = 0} = -1$. The line corresponding to $\gamma = 0$ is $t' - t_0' = t - t_0$ which has the slope $\left(\frac{dt_0'}{dt_0}\right)_{\gamma = 0} = +1$.

The lines are perpendicular because $\left(\frac{dt_0'}{dt_0}\right)_{\mu = 0}\left(\frac{dt_0'}{dt_0}\right)_{\gamma = 0} = (-1)(1) = -1$. Since $\left(\frac{\partial \gamma}{\partial t_0}\right) = +1, \left(\frac{\partial \mu}{\partial t_0}\right) = -1$ the positive directions are those shown in Figure 2. When $\mu = r = t - t' = (t' - t_0') + (t - t_0)$ then $t_0' = 2t' - t_0$ represents a line with intercepts $t_0 = 2t'$, $t_0' = 2t'$ and slope $\frac{dt_0'}{dt_0} = -1$.

When $\gamma = \mu$ or $(t' - t_0') - (t - t_0) = (t' - t_0') = +(t - t_0)$ then $t_0 = t$. Similarly when $\gamma = -\mu$ then $t_0' = t'$. When $\gamma = -r$, $r_0 = 0$ or $t_0' = t'$.

$$\text{Consider Region AA'BB'} \begin{cases} \mu = r - \epsilon, \epsilon > 0 \\ \gamma = -r - \eta,\ \eta > 0 \end{cases}$$

$\gamma + \mu = 2(t' - t_0')$ or $\gamma = -\mu + 2(t' - t_0')$ or $-r - \eta = -(r - \epsilon) + 2(t' - t_0')$ or $t' - t_0' = \frac{-(\eta + \epsilon)}{2}$ a negative number. Hence $t_0' > t'$. Figure 2 shows that $t_0' > t'$, $\mu = r - \epsilon$, $\gamma < -r$ defines the region AA'BB'. Since $r_0 = \gamma + r$ then $\gamma < -r$ implies $r_0 < 0$ for this region.

Notes for Figure 2 (Continued)

Consider Region OA′ACC′ $\begin{cases} \mu = r - \epsilon;\ \epsilon > 0 \\ \gamma = -r + \eta;\ \eta > 0 \end{cases}$

$\gamma = -\mu + 2(t' - t_0')$ or $-r + \eta = -(r - \epsilon) + 2(t' - t_0')$ or $t' - t_0' = \frac{\eta - \epsilon}{2}$ $\quad t_0' > t'$, $\mu = r - \epsilon$, $\gamma = -r + \eta$ corresponds to region OA′A $\quad t_0' < t'$, $\mu = r - \epsilon$, $\gamma = -r + \eta$ corresponds to region OACC′. Since $r_0 = \gamma + r$ then $\gamma > -r$ implies $r_0 > 0$ for region OA′ACC′.

Consider Region ACDD′ $\begin{cases} \mu = r + \epsilon;\ \epsilon > 0 \\ \gamma = -r + \eta;\ \eta > 0 \end{cases}$

$\gamma = -\mu + 2(t' - t_0')$; $-r + \eta = -r - \epsilon + 2(t' - t_0')$; $t' - t_0' = \frac{\eta + \epsilon}{2}$ a positive number. Hence $t_0' < t'$, $\mu = r + \epsilon$, $\gamma = -r + \eta$ define the region. Since $r_0 = \gamma + r$ then $\gamma > -r$ implies $r_0 > 0$.

Consider Regions (AD′D″ + AD″D‴) $\begin{cases} \mu = r + \epsilon;\ \epsilon > 0 \\ \gamma = -r - \eta;\ \eta > 0 \end{cases}$

$\gamma = -\mu + 2(t' - t_0')$; $t' - t_0' = \frac{\epsilon - \eta}{2}$; $t_0' < t'$, $\mu = r + \epsilon$, $\gamma = -r - \eta$ corresponds to region AD′D″. Since $r_0 = \gamma + r$ then $\gamma < -r$ implies $r_0 < 0$. If $t_0' < t'$ then $\gamma > -\mu$ (see Figure 2). If $t_0' > t'$ then $\gamma < -\mu$ which is an invalid condition since $\gamma = -\mu$ is the lower limit in the integral, Equation (A28), corresponding to $t_0' = t'$. Hence region AD′D‴ is excluded in the integration. From the Figure it is clear that the limits of γ depend on the upper limits of both t_0 and t_0'. Thus when $t_0 = t$ (a limit in Equation (A24)), $\gamma = \mu$ and when $t_0' = t'$, $\gamma = -\mu$. The limits of μ in Equation (A28) are obviously from 0 to ∞ as t_0 and t_0' range from the upper limit $t_0 = t$, $t_0' = t'$ to the lower limit $t_0 = -\infty$, $t_0' = -\infty$ in Equation (A24). That is, the limits are:

$-\mu$ to μ for γ

0 to ∞ for μ

Then

$$I_{mn}(0) \approx \frac{\theta}{a_{mn}(a_{mn}\theta + 1)} + \frac{\theta^2}{(a_{mn}\theta + 1)^2 + 4\omega_{mn}^2\theta^2}\left[\frac{2 - a_{mn}\theta}{4\omega_{mn}^2\theta^2}\right], \qquad \omega_{mn}\theta > 1$$

(A30)

$$I_{mn}(0) \approx \frac{\theta}{a_{mn}}, \qquad a_{mn}\,\theta \ll 1 \text{ (low damping)} \tag{A31}$$

$$I_{mn}(0) \approx \frac{\theta}{a_{mn}(a_{mn}\theta + 1)}, \qquad \omega_{mn}\,\theta \gg 1 \text{ (high frequencies)} \tag{A32}$$

MEAN-SQUARE RESPONSE BELOW COINCIDENCE

The time integral is specialized to $\tau = 0$ as well as $\alpha_m \ll \omega_{mn}$ (i.e., $v \ll v_0$). We get

$$I_{mn}(0) = \frac{2\theta^2}{1 + \omega_{mn}^2\theta^2}\left[\frac{\omega_{mn}^2\theta^2 - (a_{mn}\theta + 1)}{\omega_{mn}^2\theta^2 + (a_{mn}\theta + 1)^2} + \frac{1}{a_{mn}\theta}\right]$$

$$+ \frac{2\theta^2}{1 + \alpha_m^2\theta^2}\left[\frac{a_{mn}\theta + 1}{\omega_{mn}^2\theta^2 + (a_{mn}\theta + 1)^2} - \frac{a_{mn}}{\omega_{mn}^2\theta}\right], \qquad \alpha_m \ll \omega_{mn} \tag{A33}$$

$$I_{mn}(0) \approx \frac{2\theta}{a_{mn}}\,\frac{1}{1 + \omega_{mn}^2\theta^2}, \qquad a_{mn}\theta \ll 1 \text{ (low damping)} \tag{A34}$$

$$I_{mn}(0) \approx \frac{2}{\omega_{mn}^2}\left[1 + \frac{1}{a_{mn}\theta} + \frac{1}{1 + \alpha_m^2\theta^2}\right], \qquad \omega_{mn}\theta \gg 1 \text{ (high frequencies)} \tag{A35}$$

DISPLACEMENT CORRELATION BELOW COINCIDENCE

Here, $\tau \neq 0$ and $\alpha \ll \omega_{mn}$ is considered .

$$I_{mn}(\tau) \approx \frac{2\theta}{a_{mn}}\,\frac{e^{-a_{mn}|\tau|}\cos\omega_{mn}\tau}{1 + \omega_{mn}^2\theta^2}, \qquad a_{mn}\theta \ll 1 \text{ (low damping)} \tag{A36a}$$

When substituted in Equation (A27) the results give the cross correlation of (if $\tau = 0$) mean-square displacement. For the latter case ($\tau = 0$)

$$I_{mn}(0) \approx \frac{2\theta}{a_{mn}} \cdot \frac{1}{1 + \omega_{mn}^2 \theta^2}, \qquad a_{mn}\theta << 1 \text{ (low damping)} \tag{A36b}$$

Now the radiation of boundary layer noise into the closed space shown in Figure 1 is considered, particularly the *underwater case.* The sound field on either side of the plate is governed by the nondissipative linear wave equation of acoustics for a homogeneous, loss- and source-free medium at rest.

$$\nabla^2 \psi_j - \frac{1}{c^2} \frac{\partial^2 \psi_j}{\partial t^2} = 0 \tag{A37}$$

Within the closed space, let $j = 2$. The Fourier transform $\Psi_2(x,y,z,\omega) = \frac{1}{2\pi} \int_{-\infty}^{\infty} \psi_2(x,y,z,t)$ $e^{-i\omega t} dt$ of the velocity potential ψ_2 satisfies the Helmholtz equation

$$\nabla^2 \Psi_2 + k^2 \Psi_2 = \frac{\partial^2 \Psi_2}{\partial x^2} + \frac{\partial^2 \Psi_2}{\partial y^2} + \frac{\partial^2 \Psi_2}{\partial z^2} + k^2 \Psi_2 = 0 \tag{A38}$$

since $\mathfrak{F}\left(\frac{\partial^2 \psi_2}{\partial t^2}\right) \rightarrow -\omega^2 \Psi_2$ and $k = \frac{\omega}{c}$.

Except for the plate, all interior surfaces are assumed to be pressure release surfaces. Therefore, the boundary conditions are

$$\Psi_2 = 0 \begin{cases} x = 0, & L_x \\ y = 0, & L_y \\ z = 0 \end{cases} \tag{A39}$$

Assume a general solution for Equation (A38) in the form of normal modes p,q

$$\Psi_2(x,y,z,\omega) = \sum_{p,q} D_{p,q}\, \phi_{p,q}(r) \sin k_{p,q} z \tag{A40}$$

It will be shown that Equation (A40) satisfies the boundary conditions in Equation (A39). Substitution of Equation (A20) in Equation (A40) and the resultant equation in Equation (A38) gives

$$k_{pq}^2 = k^2 - \left[\left(\frac{p\pi}{L_x}\right)^2 + \left(\frac{q\pi}{L_y}\right)^2\right] = k^2 - \Gamma_{pq}^2 \tag{A41}$$

where ϕ_{pq} and Γ_{pq} are the eigenfunctions and eigenvalues given in Equations (A20) and (A21), respectively.

Equation (A37) is coupled to Equation (A1) by the continuity condition on velocity

$$\frac{\partial w}{\partial t} = \left.\frac{\partial \psi_1}{\partial z}\right|_{z = L_z} = -\left.\frac{\partial \psi_2}{\partial z}\right|_{z = L_z} \tag{A42}$$

Hence

$$-\left.\frac{\partial \Psi_2}{\partial z}\right|_{z = L_z} = \left.\frac{1}{2\pi}\int \frac{\partial w}{\partial t}(x,y,z,t)\, e^{-i\omega t}\, dt\right|_{z = L_z}$$

$$= V(x,y,z,\omega) = \sum_{m,n} V_{mn} = -\sum_{m,n} H_{mn}\,\phi_{mn} \tag{A43}$$

where $H_{mn}\phi_{mn}$ is the plate modal velocity. Using Equation (A40) in Equation (A43)

$$D_{mn} = -\frac{H_{mn}}{k_{mn}\cos k_{mn}L_z} \tag{A44}$$

Substitution of Equations (A44) and (A20) in Equation (A40) gives

$$\Psi_2(x,y,z,\omega) = -\frac{2}{(L_y L_y)^{1/2}}\sum_{m,n}\frac{H_{mn}}{k_{mn}\cos k_{mn}L_z}\sin\frac{m\pi x}{L_x}\sin\frac{n\pi y}{L_y}\sin k_{mn}z \tag{A45}$$

which satisfies the boundary conditions Equation (A39).

Since the pressure $p_2(x,y,z,t) = \rho\,\dfrac{\partial \psi_2(x,y,z,t)}{\partial t}$, then the modal pressure transform is

$$[P_2(x,y,z,\omega)]_{mn} = \frac{1}{2\pi}\left[\int_{-\infty}^{\infty} \rho\,\frac{\partial \psi_2}{\partial t}\, e^{-i\omega t}\, dt\right]_{mn}$$

$$= -i\omega\,\rho[\Psi_2(x,y,z,\omega)]_{mn}$$

Using these equations as well as Equations (A40), (A43), and (A44), the plate modal impedance (at $z = L_z$) is obtained

$$Z_{mn}(x,y,z,\omega) = \frac{P_{mn}(x,y,z,\omega)}{V_{mn}} = \frac{P_{mn}(x,y,z,\omega)}{-H_{mn}\phi_{mn}} = \frac{-i\omega\,\rho[\Psi_2]_{mn}}{-H_{mn}\,\phi_{mn}} = \frac{-i\omega\rho}{k_{mn}}\tan k_{mn}L_z = -i\omega M_2 \tag{A46}$$

From Equations (A41) and (A8) as well as the definition of C_B

$$k_{mn}^2 = k^2 - \Gamma_{mn}^2 = k^2 - \left(\frac{M}{B}\right)^{1/2} \omega_{mn} = \frac{\omega^2}{c^2} - \frac{\omega\omega_{mn}}{C_B^2}$$

Defining a sound coincidence frequency $\omega = \omega_c$, corresponding to $c = C_B$ then

$$k_{mn} = \pm \frac{\omega_c}{C_B}\sqrt{1 - \frac{\omega_{mn}}{\omega_c}}$$

which is real for $\omega_{mn} < \omega_c$ and imaginary for $\omega_{mn} > \omega_c$. Equation (A46) then yields

$$M_2 = \frac{\rho \tanh| k_{mn}L_z|}{|k_{mn}|}, \qquad \omega_{mn} > \omega_c \tag{A47a}$$

$$M_2 = \frac{\rho}{k_{mn}} \tan k_{mn}L_z, \qquad \omega_{mn} < \omega_c \tag{A47b}$$

The added mass M_1 of the free space external to the cavity, provided the mode number is not too low, is taken to be

$$M_1 = \frac{\rho}{|k_{mn}|}, \qquad \omega_{mn} < \omega_c \tag{A48}$$

When the mode number is low, the resistive impedance (viscous damping coefficient) is taken to be

$$\beta_1 = \rho c s \tag{A49}$$

where

$$s = \frac{2}{\pi m} + \frac{2}{\pi n} \frac{\left(\frac{\omega_{mn}L}{c}\right)^2}{1 + \left(\frac{\omega_{mn}L}{c}\right)^2}, \quad \omega_{mn} < \omega_c$$

$$L = \frac{1}{2}(L_x L_y)^{1/2}$$

Equation (A27) gave the modal displacement correlation for a plate in a low-density fluid. The correlation for a high-density fluid is obtained by replacing the structural mass in Equation (A27) by the total mass

$$M' = M + M_1 + M_2 \tag{A50}$$

where M is the plate mass,

M_1 is the free space added mass given by Equation (A48), and

M_2 is the added mass due to the enclosed fluid given by either Equation (A47a) or (47b).

Analogously, the damping in Equation (A7) and, hence, in Equation (A27) becomes for a high-density fluid

$$a'_{mn} = \frac{\beta_0}{2M'} + \frac{\Gamma^4_{mn} B\eta}{2M'\omega_{mn}} + \frac{\beta_1}{2M} \tag{A51}$$

where the first two terms represent the original viscous and hysteretic damping for the plate, except that now $M \to M'$, and the last term is the added viscous damping where β_1 is given by Equation (A49).

APPENDIX A2 – SAMPLE PROBLEM

An example will be given to show how to determine the mean-square pressure ($\tau = 0$) in the liquid-filled cavity ($M \to M'$) adjacent to the plate. Two alternative methods of computation will be treated.

DISCRETE FREQUENCY METHOD

The modal mean-square pressure P_{mn}^2 at the plate is determined from Equations (A46), (A27), (A28), and (A20) as a *time-average* quantity.

$$P_{mn}^2 = \langle P_{mn} P_{mn} \rangle = V_{mn}^2 Z_{mn}^2 = (-i\omega W_{mn})^2 (-i\omega M_2)^2 = W_{mn}^2 \omega_{mn}^4 M_2^2$$

$$= f^2 \frac{A}{L_x L_y} \left(\frac{M_2}{M'}\right)^2 \left[\sin^2 \frac{m\pi x}{L_x} \sin^2 \frac{n\pi y}{L_y}\right] \omega_{mn}^2 I_{mn}(0)$$

The *spatial average* of P_{mn}^2 is

$$\overline{P_{mn}^2} = f^2 \frac{A}{4L_x L_y} \left(\frac{M_2}{M'}\right)^2 \omega_{mn}^2 I_{mn}(0)$$

where* $f^2 = (6 \times 10^{-3} \cdot \frac{1}{2} \rho U_\infty^2)^2$,

$A = \dfrac{2\pi}{\kappa^2}$, and

$\kappa = \dfrac{2}{d}$.

For a steel structure in water, let

$h = \frac{1}{2}$ in. ,

$L_x = L_y = 5$ ft ,

$L_z = 1$ ft ,

$U_\infty = 20$ ft/sec $\doteq$ 12 knots,

$d = 0.02$ ft ,

$\theta \doteq 3 \times 10^{-2}$ sec ,

*See Appendix A3.

$\eta = 10^2$ ($Q = 100$) , and

$\rho = 64.2$ lb/ft^3 .

At coincidence ($C_B = c$, $\omega = \omega_c$)

$$C_B^4 = c^4 = \omega_c^2 \frac{B}{M} = \omega_c^2 \frac{B}{w_s / g} = \omega_c^2 \frac{B}{\rho_s h / g}$$

Hence, ignoring Poisson's ratio σ, the sound coincidence frequency is

$$f_c = \frac{c^2}{2\pi} \sqrt{\frac{\rho_s h / g}{E h^3 / 12}} = \frac{c^2}{2\pi h} \sqrt{\frac{12 \rho_s}{g E}}$$

$$= \frac{(4910 \text{ ft/sec})^2}{2\pi(1/24 \text{ ft})} \sqrt{\frac{12(490 \text{ lb/ft}^3)}{(32.2 \text{ ft/sec}^2)(0.4175 \times 10^{10} \text{ lb/ft}^2)}} \approx 19{,}230 \text{ cps}$$

Now

$$k_{mn}^2 = k^2 - \Gamma_{mn}^2$$

see Equation (A41). From page 174 of Reference 10, we see that for $\omega_{mn} < \omega_c$, $C_B < c$ and $\Gamma_{mn} > k$ (note: k_b and k_a in Reference 10 respectively become Γ_{mn} and k here.) Hence, for frequencies less than 10,000 cps, $| k_{mn}$ may be approximated by Γ_{mn}. Further, restricting attention to frequencies greater than 200 cps, from Equations (A47b), (A48), and (A50)

$$M' = M + M_1 + M_2 = M + \frac{\rho}{| k_{mn} |} + \frac{\rho}{k_{mn}} \tan k_{mn} L_z$$

But

$$k_{mn} = i \Gamma_{mn}, \; i \tan x = \tanh ix, \; \tanh x = - \tanh - x$$

Hence,

$$M_2 = \frac{\rho}{i \Gamma_{mn}} \tan i\Gamma_{mn} L_z = \frac{-\rho}{\Gamma_{mn}} \tanh(-\Gamma_{mn} L_z) = \frac{\rho}{\Gamma_{mn}} \tanh \Gamma_{mn} L_z$$

$$= \frac{\rho}{| k_{mn} |} \tanh \sqrt{\left(\frac{M}{B}\right)^{1/2} \omega_{mn}} \; L_z$$

for ω_{mn} sufficiently high $\tanh \sqrt{\left(\frac{M}{B}\right)^{1/2} \omega_{mn}}\ L_z \to 1$ and $M_2 \to \frac{\rho}{|k_{mn}|}$ (Note: In the NSRDC system of units, $M_2 = \frac{\rho}{g\,|k_{mn}|}$ is used when making computations.) Thus

$$M' = M + \frac{2\rho}{\Gamma_{mn}} \approx M$$

Also, as can be calculated from Equation (A49), for ω_{mn} sufficiently high, we get $\beta_1 \approx 0$. For these conditions and using Equation (A8),

$$\left(\frac{M_2}{M'}\right)^2 \approx \left(\frac{\rho/\Gamma_{mn}g}{M}\right)^2 = \left(\frac{\rho}{M\Gamma_{mn}g}\right)^2 = \left[\frac{\rho/g}{M\left(\frac{M}{B}\right)^{1/4}\omega_{mn}^{1/2}}\right]^2 = \frac{\rho^2/g^2}{\left(\frac{M}{B}\right)^{1/2}\omega_{mn}M^2}$$

but[11]

$$c_L = \left(\frac{E}{\rho_s \cdot \frac{1}{g}}\right)^{1/2} = \sqrt{\frac{12B(1-\sigma^2)}{\frac{\rho_s}{g}h^3}} \approx \frac{\sqrt{12}}{h}\left(\frac{B}{M}\right)^{1/2} \quad \text{(ignoring } \sigma\text{)}$$

Hence,

$$\left(\frac{M}{B}\right)^{1/2} = \frac{\sqrt{12}}{c_L h}$$

and

$$\left(\frac{M_2}{M'}\right)^2 \approx \frac{1}{\sqrt{12}}\,\frac{\frac{\rho^2 c_L h}{g^2}}{\omega_{mn}M^2} = \frac{1}{\sqrt{12}}\,\frac{\frac{\rho^2 c_L h}{g^2}}{\omega_{mn}\frac{\rho_s^2 h^2}{g^2}} = \frac{1}{\sqrt{12}}\,\frac{\rho^2 c_L h}{\omega_{mn}\rho_s^2 h^2}$$

Finally, from Equations (A8) and (A21) for any mode

$$\omega_{mn}^2 \approx \left(\frac{B}{M}\right)\Gamma_{mn}^4 = \left(\frac{B}{M}\right)\left[\left(\frac{m\pi}{L_x}\right)^2 + \left(\frac{n\pi}{L_y}\right)^2\right]^2$$

is calculated, and $I_{mn}(0)$ can be calculated from either Equation (A33) or (A34). In these equations, Equation (A51) is used, noting that in this problem $\beta_1 \approx 0$, $M' \approx M$, $B \approx Eh^3/12$, and $\beta_0 \approx 0$; see page 170 of Reference 2.

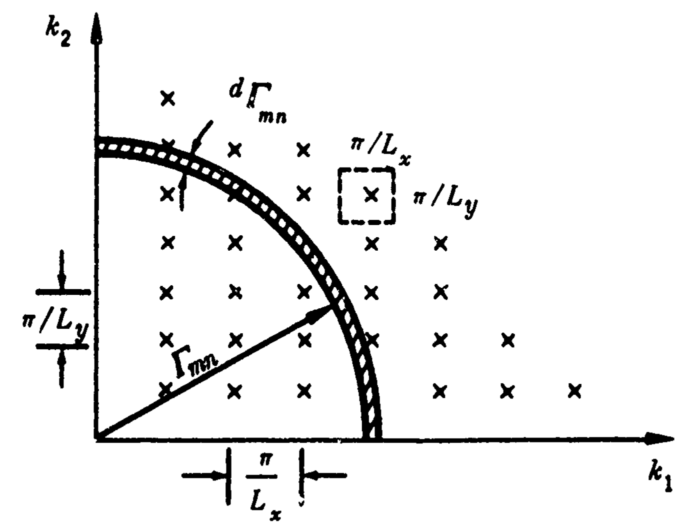

Figure 3 – Modal Lattice and Constant Wave Number Contour for Simply Supported Plate

There is now sufficient data to compute all of the quantities in the equation for $\overline{P^2_{mn}}$. Finally, from Equations (A46) and (A40) and using $k_{mn} = -i\Gamma_{mn}$

$$P_{mn}(x,y,z,\omega) = -i\omega\rho\Psi_{mn}(x,y,z,\omega) = -i\omega\rho D_{mn}\phi_{mn}\sin(-i\Gamma_{mn}z)$$

$$= \omega\rho D_{mn}\phi_{mn}\sinh\Gamma_{mn}z$$

Hence, $P^2_{mn} \propto \sinh\Gamma^2_{mn}$; therefore, the modal mean-square pressure for a location away from the excited plate would be reduced by the factor

$$\frac{\left[P^2_{mn}\right]_{z<L_z}}{\left[P^2_{mn}\right]_{z=L_z}} = \left[\frac{\sinh\Gamma_{mn}z}{\sinh\Gamma_{mn}L_z}\right]^2$$

MODAL DENSITY METHOD

We now determine $\overline{P^2}$, the mean-square pressure as measured by frequency analysis in bands of width $\Delta\nu$. The modal density of a plate found by considering the area included by the quarter circle of radius Γ_{mn} (Figure (3)) is

$$n(\Gamma_{mn}) = \frac{dN(\Gamma_{mn})}{d\Gamma_{mn}} = \frac{\Gamma_{mn}L_xL_y}{2\pi}$$

see page 135 of Reference 10. Hence, using Equation (A8) and the relation $c_L = \frac{\sqrt{12}}{h}\left(\frac{B}{M}\right)^{1/2}$, previously shown, the number of modes included up to wave number Γ_{mn} is

$$dN(\Gamma_{mn}) = \Gamma_{mn}d\Gamma_{mn}\frac{L_xL_y}{2\pi} = \frac{\left(\frac{M}{B}\right)^{1/2}L_xL_y}{4\pi}d\omega = \frac{\sqrt{3}\,L_xL_y}{c_Lh}d\nu$$

where $d\omega = 2\pi\,d\nu$.

Thus, the average number of modes ΔN in a band $\Delta\nu$ is approximately

$$\Delta N = \frac{\sqrt{3}L_xL_y}{c_Lh}\Delta\nu$$

Using the relation $c_Lh = \sqrt{3}L_xL_y\frac{\Delta\nu}{\Delta N}$ and the relation for $\left(\frac{M_2}{M'}\right)$, previously derived, the equation for the modal mean-square pressure per mode is

$$\overline{P^2_{mn}} = \frac{f^2 A}{4L_x L_y} \left(\frac{M_2}{M'}\right)^2 \omega^2_{mn} I_{mn}(0) = \frac{f^2 A}{4L_x L_y} \left(\frac{1}{\sqrt{12}} \frac{\rho^2 c_L h}{\omega_{mn} \rho_s{}^2 h^2}\right) \omega^2_{mn} I_{mn}(0)$$

$$= \frac{f^2 A}{4L_x L_y} \frac{1}{\sqrt{12}} \frac{\rho^2 \sqrt{3}\, L_x L_y \frac{\Delta\nu}{\Delta N}}{\omega_{mn} \rho_s^2 h^2} \omega^2_{mn} I_{mn}(0)$$

For all modes ΔN in the band, the average mean-square pressure is

$$\overline{P^2} = \overline{P^2_{mn}} \Delta N = \frac{f^2 A}{8 h^2} \left(\frac{\rho}{\rho_s}\right)^2 \omega_{mn} I_{mn}(0)\, \Delta \nu$$

where ω_{mn} is now considered to be a continuous frequency variable.

Since all data are known (see Discrete Frequency Method), then for a given frequency bandwidth $\Delta \nu$, $\overline{P^2}$ can be computed. The results of the computation are given for $\Delta \nu = 1$ in terms of spectrum level, $SL = 10 \log_{10} \frac{\overline{P^2}}{P_0^2}\, db$, where reference pressure $p_0 = 1\ \mu\text{bar} = 1\ \text{dyn/cm}^2$ in Reference 2, Figure 7.

APPENDIX A3 – METHOD FOR DETERMINING INPUT DATA

Dyer used the following estimates of input data for the boundary-layer pressure field

$$f_{r.m.s.} = 6 \times 10^{-3} \; \frac{1}{2} \rho U_\infty^2$$

based on measurements by Willmarth[12]

$$\kappa d \approx 2$$

$$\theta \approx 30 \; \frac{d}{U_\infty}$$

$$v \approx 0.8 \; U_\infty$$

$$\omega_0 \approx \kappa v$$

based on a comparison of Equations (A18) and its Fourier transform, which is the spectral density $s(\omega) = 2 \int_{-\infty}^{\infty} < f(r,t) f^* (r',t') > e^{i\omega\tau} d\tau$ with measurements.[12,13]

To determine the cross correlation or mean square pressures, geometric and structural data must also be given as in the sample problem.

APPENDIX B

BOEING PROGRAM 1 (MAESTRELLO)

APPENDIX B1 – MATHEMATICAL ANALYSIS

APPENDIX B2 – METHOD FOR DETERMINING INPUT DATA

APPENDIX B3 – PROGRAM IDENTIFICATION

APPENDIX B4 – TEST RUNS

NOTATION

A_i	Constants
a, b	Length of panel sides
a_{mn}	Plate modal damping
a_1, a_2	Amplitude of temporal fluctuation for unsteady convection
B	Bending stiffness
c	Speed of sound in fluid
E	Young's modulus
F	Equals $\frac{\delta^*}{U_c}$
g	Plate input-response function
g_i	A function
h	Panel thickness
I_ν, K_ν	Integrals
i	Equals $\sqrt{-1}$
J_g	Jacobian
K_a	Bending-wave speed
K_i, K_ν, K_γ	Constants; wave numbers
L_ξ	Characteristic length of pressure field for semifrozen flow (length over which a given turbulent pressure pattern remains distinguishable)
M	Plate mass
m, n	Mode numbers
N	Constant, for piston radiation $N = 4$
P_p	Panel perimeter
P_r	Total length of panel ribs
PWL_{mn}	Sound power level for mn mode
$p(x,y,t)$	Turbulence wall pressure fluctuation
$\overline{p^2}$	Mean-square pressure
$R(\xi,\eta,\tau)$	Correlation coefficient for pressures
$R(\tau)$	Normalized autocorrelation for pressures
t, t'	Time; times at which displacements are measured at points x,y, and x', y', respectively

t_0, t_0'	Times at which pressure measurements are made at points x_0, y_0 and x_0', y_0', respectively
U_c	Broadband convection velocity
U, U_∞	Free-stream velocity
u	Local flow velocity
$u(t - t_0)$	Unit step function
u_τ	Frictional velocity
Vol_{mn}	Volume displacement for a mode
x	Distance from leading edge of plate
$(x, y), (x', y')$	Points on the panel at which displacements are measured
$(x_0, y_0), (x_0', y_0')$	Points on panel at which turbulence pressures are measured
$Y(x,y,t)$	Panel displacement
$\overline{Y}$	Root-mean-square of displacement
$\overline{Y^2}$	Mean square displacement
Y_{mn}	Eigenfunction or orthogonal mode of plate oscillation
y	Distance from wall normal to flow direction
β_{ac}	Acoustic-damping coefficient
β_c	Critical damping
β_{st}	Structural damping coefficient
Γ_{mn}	Eigenvalue
δ^*	Boundary layer displacement thickness
δ_{mn}	Total damping ratio
η	Equals $y - y'$, lateral partial separation
η'	Equals $y_0 + y_0'$
$\theta, \theta_1, \theta_2$	Eddy lifetime for steady convection, i.e., time in which value of correlation coefficient obtained from envelope of correlation maxima (maxima-maximorum) drops to $1/e$
$\overline{\theta_1}, \overline{\theta_2}$	Eddy lifetime for unsteady convection
ν, ν_w	Kinematic viscosity of fluid near wall
ξ	Equals $x - x'$, longitudinal partial separation
ξ'	Equals $x_0 + x_0'$
ρ	Density of fluid
ρ_w	Density of fluid near wall

σ_1, σ_2	Standard deviation of distribution
τ	Equals $t - t'$, time delay
τ_0	Equals $t_0 - t_0'$
τ_0'	Equals $t_0 + t_0'$
τ_w	Local wall-shear stress
$\phi_{mn}(x,y)$ or $\phi(x)\,\phi(y)$	Plate eigenfunctions
ω	Circular frequency equal to $2\pi f$
ω_t	Circular frequency of temporal fluctuation
ω_{mn}	Plate modal frequency
∇^4	Equals $\dfrac{\partial^4 Y}{\partial x^4} + \dfrac{2\partial^4 Y}{\partial x^2 \partial y^2} + \dfrac{\partial^4 Y}{\partial y^4}$
$< \cdots >$	Symbol for time-average operation

APPENDIX B1 – MATHEMATICAL ANALYSIS

Two models were taken from experimental data[14,15] to represent the cross correlation of the turbulence wall-pressure fluctuations in a broad frequency band. The models, designated as Model A-convected semifrozen pattern and Model B-unsteady convection-will be considered in turn.

MODEL A-CONVECTED SEMIFROZEN PATTERN (U_c = CONSTANT)

The normalized cross-correlation function of the pressure fluctuations for this model in a moving frame of reference is represented by the sum of two Gaussian distributions

$$R(\xi,\eta,\tau) = \frac{\overline{<p(x,y,t)\, p(x+\xi, y+\eta, t+\tau)>}}{\overline{p^2}} = e^{\frac{-|\tau|}{\theta}} \left\{ A_1 e^{\frac{-[(\xi - U_c\tau)^2 + \eta^2]}{2\sigma_1^2}} + A_2 e^{\frac{-[(\xi - U_c\tau)^2 + \eta^2]}{2\sigma_2^2}} \right\} \tag{B1}$$

corresponding to measurements made with a series of constant time delays and variable spatial separation; see Reference 16 Figure 4. The convection velocity, obtained from Equation (B1), is defined by

$$\frac{\partial R(\xi,\tau)}{\partial \xi} = 0, \quad \text{when } U_c = \frac{\xi_{max}}{\tau} \tag{B2}$$

Alternatively, the normalized cross-correlation function may also be represented by

$$R(\xi,\eta,\tau) = e^{\frac{-|\xi|}{U_c\theta}} \left\{ A_1 e^{\frac{-[(\xi - U_c\tau)^2 + \eta^2]}{2\sigma_1^2}} + A_2 e^{\frac{-[(\xi - U_c\tau)^2 + \eta^2]}{2\sigma_2^2}} \right\} \tag{B3}$$

corresponding to measurements made with constant spatial separation and variable time delay; see Reference 16 Figure 3. The convection velocity obtained from Equation (B3) is defined by

$$\frac{\partial R(\xi,\tau)}{\partial \tau} = 0, \quad \text{when } U_c = \frac{\xi}{\tau_{max}}. \tag{B4}$$

Since most data were taken at constant spatial separation, the autocorrelation function obtained from Equation (B3) by setting $\xi = \eta = 0$ is

$$R(\tau) = A_1 e^{\frac{-U_c^2\tau^2}{2\sigma_1^2}} + A_2 e^{\frac{-U_c^2\tau^2}{2\sigma_2^2}} \tag{B5}$$

and the corresponding power spectrum is (use Fourier transform Pairs 708 of Reference 7)

$$P(\omega) = \frac{1}{2\pi}\int_{-\infty}^{\infty} R(\tau)\, e^{-i\omega\tau}\, d\tau = \frac{A_1\sigma_1}{U_c\sqrt{2\pi}} e^{\frac{-\sigma_1^2\omega^2}{2U_c^2}} + \frac{A_2\sigma_2}{U_c\sqrt{2\pi}} e^{\frac{-\sigma_2^2\omega^2}{2U_c^2}} \tag{B6}$$

Comparison of theory and experiment shows that the high-frequency resolution of Equation (B3) is poor; see Reference 14 Figure 1. Hence *a more satisfactory empirical representation of the cross correlation of the pressures is constructed as follows from the autocorrelation obtained from the measured power spectral density, with decay in a moving frame of reference. This representation corresponds to a broader range of frequency components than the previous one;* see Reference 14 Figure 2. The measured dimensionless power spectral density can be represented by

$$\frac{P(\omega)U}{\tau_w^{\,2}\,\delta^*} = A_1 e^{-K_1\omega F} + A_2 e^{-K_2\omega F} + A_3 e^{-K_3\omega F} \tag{B7}$$

where

$$\begin{aligned}
A_1 &= 1.6\\
A_2 &= 7.2\\
A_3 &= 12.0\\
F &= \delta^*/U\\
K_1 &= 0.470\\
K_2 &= 3.0\\
K_3 &= 14.0
\end{aligned}$$

Using Fourier Pair 632 of Reference 7, the normalized autocorrelation is found

$$R(\tau) = \frac{R(\tau)_{\text{unnormalized}}}{R(0)}$$

$$= \frac{\left[\dfrac{A_1 K_1}{K_1^2 + (\tau/F)^2} + \dfrac{A_2 K_2}{K_2^2 + (\tau/F)^2} + \dfrac{A_3 K_3}{K_3^2 + (\tau/F)^2}\right]}{\left(\dfrac{A_1}{K_1} + \dfrac{A_2}{K_2} + \dfrac{A_3}{K_3}\right)} \tag{B8}$$

By introducing the spatial decay $e^{\frac{-|\xi|}{U_c\theta}}$ and moving frame of reference $(\xi - U_c\tau)$, the normalized cross-correlation function of the pressure becomes (by analogy with Equation (B3)) with respect to symmetry about the ξ and τ axes:

$$R(\xi,\eta,\tau) = e^{\frac{-|\xi|}{U_c\theta}} \frac{\left\{\displaystyle\sum_{\gamma=1}^{3} \frac{A_\gamma K_\gamma}{K_\gamma^2 + (1/FU_c)^2[(\xi - U_c\tau)^2 + \eta^2]}\right\}}{\displaystyle\sum_{\gamma=1}^{3} \frac{A_\gamma}{K_\gamma}} \tag{B9}$$

By changing the decay rate from $\frac{|\xi|}{U_c\theta}$ to $\frac{|\tau|}{\theta}$ in Equation (B9) , (the Taylor hypothesis), the functional form of $R(\xi,\eta,\tau)$ still fits the experimental results.[17] Hence either form of the exponential may be used to describe the decay of the wall pressure correlation.

MODEL B-UNSTEADY CONVECTION ($U_c \neq$ CONSTANT)

For unsteady convection, the normalized cross correlation has the form

$$R(\xi,\eta,\tau) = A_1\left(e^{\frac{-|\tau|}{\theta_1}} + a_1 e^{\frac{-|\tau|}{\theta_1}} \sin \omega_1 |\tau|\right) e^{\frac{-[(\xi - U_c\tau)^2 + \eta^2]}{2\sigma_1^2}}$$

$$+ A_2\left(e^{\frac{-|\tau|}{\theta_2}} + a_2 e^{\frac{-|\tau|}{\theta_2}} \cos \omega_2 |\tau|\right) e^{\frac{-[(\xi - U_c\tau)^2 + \eta^2]}{2\sigma_2^2}} \tag{B10}$$

and the normalized autocorrelation ($\eta = \xi = 0$) becomes

$$R(\tau) = A_1\left(e^{\frac{-|\tau|}{\theta_1}} + a_1 e^{\frac{-|\tau|}{\bar{\theta}_1}} \sin \omega_1 |\tau|\right) e^{\frac{-U_c^2\tau^2}{2\sigma_1^2}}$$

$$+ A_2\left(e^{\frac{-|\tau|}{\theta_2}} + a_2 e^{\frac{-|\tau|}{\bar{\theta}_2}} \cos \omega_2 \tau\right) e^{\frac{-U_c^2\tau^2}{2\sigma_2^2}} \qquad \text{(B11)}$$

STRUCTURAL RESPONSE TO TURBULENCE EXCITATION

The displacement cross correlation of a plate due to the cross correlation of a random pressure $\overline{<p(x_0,y_0,t_0)\ p(x_0', y_0', t_0')>}$ has been given by Dyer;[2] see Appendix A

$$\overline{<Y(x,y,t)\ Y(x',y',t')>} = \int_{-\infty}^{t} dt_0 \int_{-\infty}^{t'} dt_0' \int_0^a dx_0 \int_0^b dy_0 \int_0^a dx_0' \int_0^b dy_0'$$

$$\cdot\ g(x,y,t/x_0,y_0,t_0)\ g(x',y',t'/x_0',y_0',t_0')$$

$$\cdot <p(x_0,y_0,t_0)\ p(x_0',y_0',t_0')> \qquad \text{(B12)}$$

Using Equation (B9) with $\frac{|\xi|}{U_c} = |\tau| = |t_0 - t_0'|$, the unnormalized cross correlation for *semifrozen* flow becomes

$$\overline{<p(x_0,y_0,t_0)\ p(x_0',y_0',t_0')>} = \frac{\overline{p^2} e^{\frac{-|t_0 - t_0'|}{\theta}}}{\sum_{\nu=1}^{3} \frac{A_\nu}{K_\nu}}$$

$$\cdot \sum_{\nu=1}^{3} \frac{A_\nu K_\nu}{K_\nu^2 + (1/FU_c)^2 \left\{([(x_0 - x_0') - U_c(t_0 - t_0')])^2 + (y_0 - y_0')^2\right\}} \qquad \text{(B13)}$$

As in Appendix A1, the homogeneous equation for plate vibrations has the form

$$B \nabla^4 Y(x, y, t) + M \frac{\partial^2 Y(x, y, t)}{\partial t^2} + (\beta_{ac} + \beta_{st}) \frac{\partial Y(x, y, t)}{\partial t} = 0 \tag{B14}$$

where

$$Y_{mn}(x, y, t) \sim \phi_{mn}(x, y)\, e^{[-a_{mn} t + i\omega_{mn} t]} \tag{B15}$$

is the normal mode solution to Equation (B14). Substitution of Equation (B15) in Equation (B14) yields

$$\nabla^4 \phi_{mn}(x, y) - \Gamma_{mn} \phi(x, y) = 0 \tag{B16}$$

where

$$\Gamma^4_{mn} = \frac{-M(-a_{mn} + i\omega_{mn})^2 - (\beta_{ac} + \beta_{st})(-a_{mn} + i\omega_{mn})}{B} \tag{B17}$$

Equating imaginary and real quantities in Equation (B17),*

$$a_{mn} = \frac{\beta_{ac} + \beta_{st}}{2M} = \frac{\delta_{mn}\omega_{mn}}{2} \tag{B18}$$

and

$$\omega^2_{mn} \approx \frac{B}{M} \Gamma^4_{mn} \tag{B19}$$

---

* *Forced response* of a mode to a sinusoidal force or *3-dB method* was used to measure damping. For small damping, if $\beta = \beta_{ac} + \beta_{st}$, the *decay ratio* $= \frac{\beta}{\beta_c} = \frac{1}{2} \frac{\omega_+ - \omega_-}{\omega_{mn}} = \frac{1}{2} \frac{\Delta\omega}{\omega_{mn}}$, where ω_+ and ω_- are circular frequencies of vibration, when response differs from extreme value by ratio of $\sqrt{2}$ (equivalent to 3dB). In Reference 14, Equation (13) Maestrello defined the total *damping ratio* by $\delta_{mn} = \frac{\Delta\omega}{\omega_{mn}}$. Hence

$$\frac{\beta}{\beta_c} = \frac{1}{2}\frac{\Delta\omega}{\omega} = \frac{\delta_{mn}}{2} = \frac{\beta}{2M\omega_{mn}} = \frac{a_{mn}}{\omega_{mn}} \text{ and } a_{mn} = \frac{\delta_{mn}\omega_{mn}}{2}$$

see Reference 18, pages 14–16.

For low damping, the impulse response function was found (see Appendix A1) to be

$$g(x, y, t/x_0, y_0, t_0) \doteq \sum_{mn} \frac{\phi_{mn}(x, y)\ \phi_{mn}(x_0, y_0)}{\omega_{mn} M}$$

$$\cdot \left[e^{-a_{mn}(t - t_0)} \sin \omega_{mn}(t - t_0) \right] u(t - t_0) \qquad \text{(B20)}$$

Substituting Equations (B13) and (B20) in Equation (B12) and ignoring cross-coupling terms,

$$\overline{\langle Y(x, y, t)\ Y(x', y', t') \rangle} = \frac{\overline{p^2}}{\sum_{\nu=1}^{3} \frac{A_\nu}{K_\nu} M^2} \sum_{mn} \frac{\phi_{mn}(x, y)\ \phi_{mn}(x', y')}{\omega_{mn}^2}$$

$$\cdot \int_{-\infty}^{t} dt_0 \int_{-\infty}^{t'} dt_0' \int_0^a dx_0 \int_0^b dy_0 \int_0^a dx_0' \int_0^b dy_0'\ e^{-a_{mn}(t' - t_0')}$$

$$\cdot [\sin \omega_{mn}(t' - t_0')\ u(t' - t_0')]\ e^{-a_{mn}(t - t_0)} [\sin \omega_{mn}(t - t_0)\ u(t - t_0)]$$

$$\cdot \sum_{\nu=1}^{3} \frac{\phi_{mn}(x_0, y_0)\ \phi_{mn}(x_0', y_0')\ A_\nu K_\nu\ e^{\frac{-|t_0 - t_0'|}{\theta}}}{K_\nu^2 + (1/FU_c)^2 \left\{ [(x_0 - x_0') - U_c(t_0 - t_0')]^2 + (y_0 - y_0')^2 \right\}} \qquad \text{(B21)}$$

Also (see Appendix A1)

$$\phi_{mn} = \frac{2}{(ab)^{1/2}} \sin \frac{m\pi x}{a} \sin \frac{n\pi y}{b} \qquad \text{(B22)}$$

By trigonometric manipulation,

$$\phi_{mn}(x_0, y_0)\ \phi_{mn}(x_0', y_0') = \frac{1}{ab} \left[\cos \frac{m\pi(x_0 - x_0')}{a} - \cos \frac{m\pi(x_0 + x_0')}{a} \right]$$

$$\cdot \left[\cos \frac{n\pi(y_0 - y_0')}{b} - \cos \frac{n\pi(y_0 + y_0')}{b} \right] \qquad \text{(B23)}$$

The space integral in Equation (B21) may then be written

$$I_\nu = \int_0^b dy_0 \int_0^b dy_0' \int_0^a dx_0 \int_0^a dx_0'$$

$$\frac{\frac{1}{ab}\left[\cos\frac{m\pi(x_0 - x_0')}{a} - \cos\frac{m\pi(x_0 + x_0')}{a}\right]\left[\cos\frac{n\pi(y_0 - y_0')}{b} - \cos\frac{n\pi(y_0 + y_0')}{b}\right]}{K_\nu^2 + (1/FU_c)^2 \left\{[(x_0 - x_0') - U_c(t_0 - t_0')]^2 + (y_0 - y_0')^2\right\}}$$

$$= \int_0^b dy_0 \int_0^b dy_0' \int_0^a dx_0 \int_0^a dx_0' \; f(y_0, y_0', x_0, x_0') \tag{B24}$$

To simplify computation of Equation (B21), the variable of integration is changed, thus reducing the number of operations for the integral.

Let

$$\eta' = y_0 + y_0' \qquad \eta' + \eta = 2y_0 \qquad y_0 = \frac{\eta' + \eta}{2} = g_1(\eta, \eta', \xi = 0, \xi' = 0)$$

$$\eta = y_0 - y_0' \qquad \eta' - \eta = 2y_0' \qquad y_0' = \frac{\eta' - \eta}{2} = g_2(\eta, \eta', \xi = 0, \xi' = 0)$$

$$\xi' = x_0 + x_0' \qquad \xi' + \xi = 2x_0 \qquad x_0 = \frac{\xi' + \xi}{2} = g_3(\eta = 0, \eta' = 0, \xi, \xi')$$

$$\xi = x_0 - x_0' \qquad \xi' - \xi = 2x_0' \qquad x_0' = \frac{\xi' - \xi}{2} = g_4(\eta = 0, \eta' = 0, \xi, \xi')$$

In Appendix A1, following Dyer, the transformation of two variables in a multiple integral had the following form. Let

$$x = \phi(u, v), \; y = \psi(u, v)$$

Then

$$\iint f(x,y)\, dx\, dy = \iint f[\phi(u, v)\, \psi(u,v)] \begin{vmatrix} \frac{\partial x}{\partial u} & \frac{\partial x}{\partial v} \\ \frac{\partial y}{\partial u} & \frac{\partial y}{\partial v} \end{vmatrix} du\, dv$$

A similar formulation may be made for any number of variables of transformation.[19,20]

$$I_\nu = \int_{\bar{x}} f(x)\,dx = \int_{g^{-1}(\bar{x})} f[\,g(t)\,] \;\; J_g(t) \;\; dt \tag{B25}$$

where $x = g(t)$ and $t = g^{-1}(x)$ (the inverse function). In this case, from Equation (B24)

$$f(x) = f(y_0\,, y_0'\,, x_0\,, x_0')$$

$$= \frac{\dfrac{1}{ab}\left[\cos\dfrac{m\pi(x_0 - x_0')}{a} - \cos\dfrac{m\,\pi(\,x_0 + x_0')}{a}\right]\left[\cos\dfrac{n\pi(y_0 - y_0')}{b} - \cos\dfrac{n\pi(y_0 + y_0')}{b}\right]}{K_\nu^2 + (1/FU_c)^2\left[\left\{(x_0 - x_0') - U_c(t_0 - t_0')\right\}^2 + (y_0 - y_0')^2\right]}$$

also

$$f[\,g(t)\,] = f[\,g_1(\eta,\eta',\xi,\xi'),\, g_2(\eta,\eta',\xi,\xi'),\, g_3(\eta,\eta',\xi,\xi'),\, g_4(\eta,\eta',\xi,\xi')\,]$$

$$= f\left[\frac{(\eta' + \eta)}{2}\,, \frac{(\eta' - \eta)}{2}\,, \frac{(\xi' + \xi)}{2}\,, \frac{(\xi' - \xi)}{2}\right]$$

Substitute in $f(x)$

$$x_0 - x_0' = \xi,\; x_0 + x_0' = \xi'\,,\; y_0 - y_0' = \eta\,,\; y_0 + y_0' = \eta'$$

to obtain

$$f[\,g(t)\,] = \frac{\dfrac{1}{ab}\left[\cos\dfrac{m\pi\xi}{a} - \cos\dfrac{m\pi\xi'}{a}\right]\left[\cos\dfrac{n\pi\eta}{b} - \cos\dfrac{n\pi\eta'}{b}\right]}{K_\nu^2 + (1/FU_c)^2\left[\left\{\xi - U_c(\,t_0 - t_0')\right\}^2 + \eta^2\right]} \tag{B26}$$

also

$$J_g(t) = \frac{\partial(g_1\,, g_2\,, g_3\,, g_4)}{\partial(\eta, \eta', \xi, \xi')} = \begin{vmatrix} \dfrac{\partial g_1}{\partial\eta} & \dfrac{\partial g_1}{\partial\eta'} & \dfrac{\partial g_1}{\partial\xi} & \dfrac{\partial g_1}{\partial\xi'} \\[2ex] \dfrac{\partial g_2}{\partial\eta} & \dfrac{\partial g_2}{\partial\eta'} & \dfrac{\partial g_2}{\partial\xi} & \dfrac{\partial g_2}{\partial\xi'} \\[2ex] \dfrac{\partial g_3}{\partial\eta} & \dfrac{\partial g_3}{\partial\eta'} & \dfrac{\partial g_3}{\partial\xi} & \dfrac{\partial g_3}{\partial\xi'} \\[2ex] \dfrac{\partial g_4}{\partial\eta} & \dfrac{\partial g_4}{\partial\eta'} & \dfrac{\partial g_4}{\partial\xi} & \dfrac{\partial g_4}{\partial\xi'} \end{vmatrix} = \begin{vmatrix} \frac{1}{2} & \frac{1}{2} & 0 & 0 \\[1ex] -\frac{1}{2} & \frac{1}{2} & 0 & 0 \\[1ex] 0 & 0 & \frac{1}{2} & \frac{1}{2} \\[1ex] 0 & 0 & -\frac{1}{2} & \frac{1}{2} \end{vmatrix} = \frac{1}{4} \tag{B27}$$

To obtain the new limits, transform the limits in the y_0, y_0' plane (for the transverse coordinates) to corresponding quantities in the η, η' plane and the limits in the x_0, x_0' plane (for the longitudinal coordinates) to corresponding quantities in ξ, ξ' plane. The transformation is shown in Figures 4 and 5. From these figures, the limits for the $\underline{x}$ to T planes are set to

$$x = g(t) = (y_0, y_0', x_0, x_0') : 0 \le y_0 \le b,\ 0 \le y_0' \le b,\ 0 \le x_0 \le a,\ 0 \le x_0' \le a$$

$$t = g^{-1}(x) = (\eta, \eta', \xi, \xi') : -b \le \eta \le b, |\eta| \le \eta' \le 2b - |\eta|,\ -a \le \xi \le a,\ |\xi| \le \xi' \le 2a - |\xi|$$

(Note: For $\eta \gtrless 0$, $\eta' = 2b \mp \eta$, respectively, or equal $2b - |\eta|$ along upper branch. For $\eta \gtrless 0$, $\eta' = \pm \eta$, respectively, or equal $|\eta|$ along lower branch. Similarly for ξ'.)

Substituting Equations (B26) and (B27) in Equation (B25) and using the limits for ξ, ξ', η, η' derived above, we get

$$I_\nu = \frac{1}{4ab}\int_{-a}^{a} d\xi \int_{-b}^{b} d\eta \int_{|\xi|}^{2a-|\xi|} d\xi' \int_{|\eta|}^{2b-|\eta|} d\eta' \frac{\left[\cos\frac{m\pi\xi}{a} - \cos\frac{n\pi\xi'}{a}\right]\left[\cos\frac{n\pi\eta}{b} - \cos\frac{n\pi\eta'}{b}\right]}{K_\nu^2 + (1/FU_c)^2 \quad \left[\left\{\xi - U_c(t_0 - t_0')\right\}^2 + \eta^2\right]}$$

Integration with respect to η' and ξ', in turn, reduces the integral to

$$I_\nu = \frac{2}{ab}\int_{-a}^{a}\left[\int_0^b \frac{\left[(a - |\xi|)\cos\frac{m\pi\xi}{a} + \frac{a}{m\pi}\sin\frac{m\pi|\xi|}{a}\right]\left[(b - |\eta|)\cos\frac{n\pi\eta}{b} + \frac{b}{n\pi}\sin\frac{n\pi|\eta|}{b}\right]}{\left[K_\nu^2 + (1/FU_c)^2\right]\left[\left\{\xi - U_c(t_0 - t_0')\right\}^2 + \eta^2\right]} d\eta\right] d\xi \tag{B28}$$

where

$\int_{-b}^{b} \rightarrow 2\int_0^b$ since the trigonometric functions are even functions of their argument and are thus unaffected by the signs of ξ, η.

Equation (B21) is rewritten

$$\overline{\langle Y(x,y,t)\, Y(x',y',t')\rangle} = \frac{\overline{p^2}}{\sum_{\nu=1}^{3}\left(\frac{A_\nu}{K_\nu}\right) M^2} \sum_{mn} \frac{\phi_{mn}(x,y)\, \phi_{mn}(x',y')}{\omega_{mn}^2} \cdot$$

(Equation continued on top of page 48.)

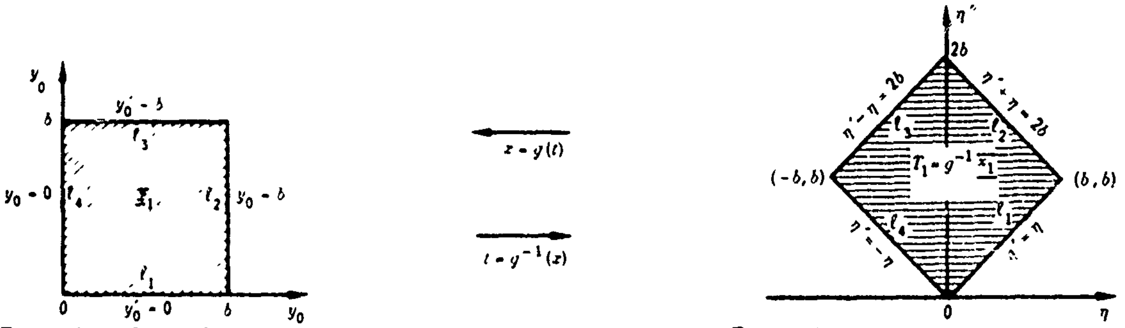

Figure 4A – Original Coordinates and Region of Integration

Figure 4b – Transformed Coordinates and Region of Integration

Figure 4 – Transformation of Transverse Coordinates and Region of Integration

Note to Figure 4:

Line ℓ_1 where $y_0' = 0$ transforms to $\eta' = \eta$
Line ℓ_2 where $y_0 = b$ transforms to $\eta' + \eta = 2b$
Line ℓ_3 where $y_0' = b$ transforms to $\eta' - \eta = 2b$
Line ℓ_4 where $y_0 = 0$ transforms to $\eta' = -\eta$

because
$$\eta' = y_0 + y_0' = g_1^{-1}(y_0, y_0', x_0, x_0')$$
$$\eta = y_0 - y_0' = g_2^{-1}(y_0, y_0', x_0, x_0')$$

Thus these limit points of Equation (B24) for the region y_0, y_0' denoted by $\underline{X}_1$ in Figure 4a transform into the lines enclosing the region T, shown in Figure 4b. The limits for η, η' obtained from the later are based on the following relationships.

Along ℓ_1: $\left.\begin{array}{r} 0 \le y_0 \le b \\ y_0' = 0 \end{array}\right\} \begin{array}{l} \eta' = \eta \quad \frac{d\eta'}{d\eta} = 1 \\ \eta' = y_0 + y_0' = y_0 \end{array}$

Hence η' ranges from 0 to b with slope $\frac{d\eta'}{d\eta} = 1$.

Where $\eta|_{y_0 = 0} = y_0 - y_0'|_{y_0 = 0} = 0$ then $\eta'|_{y_0 = 0} = 0$;

where $\eta|_{y_0 = b} = y_0 - y_0'|_{y_0 = b} = b$ then $\eta' = b$.

Along ℓ_2: $\left.\begin{array}{r} 0 \le y_0' \le b \\ y_0 = b \end{array}\right\} \begin{array}{l} \eta' + \eta = 2b \text{ or } \eta' = 2b - \eta \text{ and } \frac{d\eta'}{d\eta} = -1 \\ \eta' = y_0 + y_0' = b + y_0' \end{array}$

Hence η' ranges from b to $2b$ with slope $\frac{d\eta'}{d\eta} = -1$.

Where $\eta|_{y_0' = 0} = y_0 - y_0'|_{y_0' = 0} = y_0 = b$ then $\eta'|_{y_0' = 0} = b$;

where $\eta|_{y_0' = b} = y_0 - y_0'|_{y_0' = b} = b - b = 0$ then $\eta'|_{y_0' = b} = 2b$.

Along ℓ_3: $\left.\begin{array}{r} 0 \le y_0 \le b \\ y_0' = b \end{array}\right\} \begin{array}{l} \eta' - \eta = 2b \text{ and } \frac{d\eta'}{d\eta} = 1 \\ \eta' = y_0 + y_0' = y_0 + b \end{array}$

Hence η' ranges from b to $2b$ with slope $\frac{d\eta'}{d\eta} = 1$.

Where $\eta|_{y_0 = 0} = y_0 - y_0'|_{y_0 = 0} = -b$ then $\eta'|_{y_0 = 0} = b$;

where $\eta|_{y_0 = b} = y_0 - y_0'|_{y_0 = b} = b - b = 0$ then $\eta'|_{y_0 = b} = 2b$.

Along ℓ_4: $\left.\begin{array}{r} 0 \le y_0' \le b \\ y_0 = 0 \end{array}\right\} \begin{array}{l} \eta' = -\eta \text{ and } \frac{d\eta'}{d\eta} = -1 \\ \eta' = y_0 + y_0' = y_0' \end{array}$

Hence η' ranges from 0 to b with slope $\frac{d\eta'}{d\eta} = -1$.

Where $\eta|_{y_0' = 0} = y_0 - y_0'|_{y_0' = 0} = 0$ then $\eta'|_{y_0' = 0} = 0$;

where $\eta|_{y_0' = b} = y_0 - y_0'|_{y_0' = b} = -b$ then $\eta'|_{y_0' = 0} = b$.

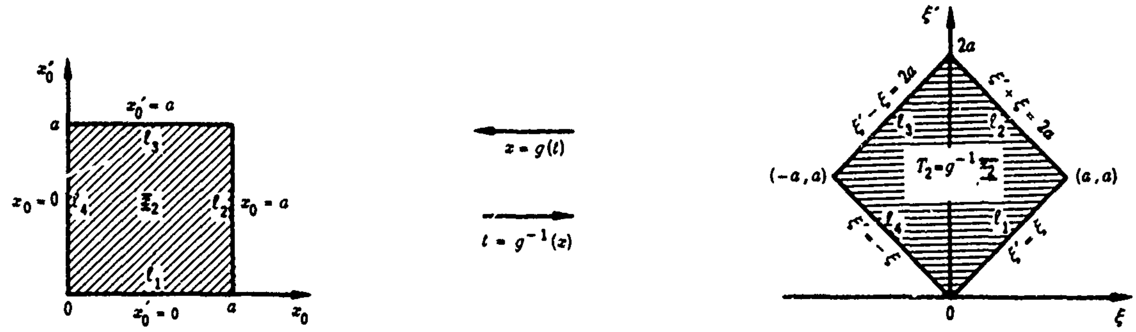

Figure 5a – Original Coordinates and Region of Integration

Figure 5b – Transformed Coordinates and Region of Integration

Figure 5 – Transformation of Longitudinal Coordinates and Region of Integration

Note to Figure 5:

Line ℓ_1 where $x_0' = 0$ transforms to $\xi' = \xi$

Line ℓ_2 where $x_0 = a$ transforms to $\xi' + \xi = 2a$

Line ℓ_3 where $x_0' = a$ transforms to $\xi' - \xi = 2a$

Line ℓ_4 where $x_0 = 0$ transforms to $\xi' = -\xi$

because

$$\xi' = x_0 + x_0' = g_3^{-1}(y_0, y_0', x_0, x_0')$$
$$\xi = x_0 - x_0' = g_4^{-1}(y_0, y_0', x_0, x_0')$$

Thus the limit points of Equation (B24) for the region x_0, x_0' denoted by $\overline{X}_2$ in Figure 5a transform into the lines enclosing the region T_2 shown in Figure 5b. The limits for ξ, ξ' obtained from the latter are based on the following relationships:

Along ℓ_1: $\left.\begin{array}{r} 0 < x_0 \le a \\ x_0' = 0 \end{array}\right\}$ $\begin{array}{l} \xi' = \xi \text{ and } \dfrac{d\xi'}{d\xi} = 1. \\ \xi' = x_0 + x_0' = x_0 \end{array}$

Hence ξ' ranges from 0 to a with slope $\dfrac{d\xi'}{d\xi} = 1$.

Where $\xi|_{x_0 = 0} = x_0 - x_0'|_{x_0 = 0}$ then $\xi'|_{x_0 = 0} = 0$;

where $\xi|_{x_0 = a} = x_0 - x_0'|_{x_0 = a} = a$ then $\xi' = a$.

Along ℓ_2: $\left.\begin{array}{r} 0 \le x_0' \le a \\ x_0 = a \end{array}\right\}$ $\begin{array}{l} \xi' + \xi = 2a \text{ or } \xi' = 2a - \xi \text{ and } \dfrac{d\xi'}{d\xi} = -1 \\ \xi' = x_0 + x_0' = a + x_0' \end{array}$

Hence ξ' ranges from a to $2a$ with slope $\dfrac{d\xi'}{d\xi} = -1$.

Where $\xi|_{x_0' = 0} = x_0 - x_0'|_{x_0' = 0} = x_0 = a$ then $\xi'|_{x_0' = 0} = a$;

where $\xi|_{x_0' = a} = x_0 - x_0' = a - a = 0$ then $\xi'|_{x_0' = a} = 2a$.

Along ℓ_3: $\left.\begin{array}{r} 0 \le x_0 \le a \\ x_0' = a \end{array}\right\}$ $\begin{array}{l} \xi' - \xi = 2a \text{ and } \dfrac{d\xi'}{d\xi} = 1 \\ \xi' = x_0 + x_0' = x_0 + a \end{array}$

Hence ξ' ranges from a to $2a$ with slope $\dfrac{d\xi'}{d\xi} = 1$.

Where $\xi|_{y_0 = 0} = x_0 - x_0'|_{x_0 = 0} = -a$ then $\xi'|_{x_0 = 0} = a$;

where $\xi|_{x_0 = a} = x_0 - x_0'|_{x_0 = a} = a - a = 0$ then $\xi'|_{x_0 = a} = 2a$.

Along ℓ_4: $\left.\begin{array}{r} 0 < x_0' \le a \\ x_0 = 0 \end{array}\right\}$ $\begin{array}{l} \xi' = -\xi \text{ and } \dfrac{d\xi'}{d\xi} = -1 \\ \xi' = x_0 + x_0' = x_0' \end{array}$

Hence ξ' ranges from 0 to a with slope $\dfrac{d\xi'}{d\xi} = -1$.

Where $\xi|_{x_0' = 0} = x_0 - x_0'|_{x_0' = 0} = 0$ then $\xi'|_{x_0' = 0} = 0$;

where $\xi|_{x_0' = a} = x_0 - x_0'|_{x_0' = a} = -a$ then $\xi'|_{x_0' = 0} = a$.

$$\cdot \int_{-\infty}^{t} dt_0 \int_{-\infty}^{t'} dt_0' \left\{ e^{-a_{mn}(t-t_0)} \sin \omega_{mn}(t-t_0)\, u(t-t_0)\, e^{-a_{mn}(t'-t_0')} \sin \omega_{mn}(t'-t_0')\, u(t'-t_0') \right\}$$

$$\cdot \sum_{\nu=1}^{3} \left[A_\nu K_\nu \int_0^a dx_0 \int_0^b dy_0 \int_0^a dx_0' \int_0^b dy_0' \frac{\phi_{mn}(x_0, y_0)\, \phi_{mn}(x_0', y_0')\, e^{\frac{-|t_0 - t_0'|}{\theta}}}{K_\nu^2 + (1/FU_c)^2 \left\{ [(x_0 - x_0') - U_c(t_0 - t_0')]^2 + (y_0 - y_0')^2 \right\}} \right]$$

(B29)

where the space integrals are given by Equation (B28).

Having transformed the space coordinates, now transform the time coordinates. First, change the variable of integration and find the Jacobian

$$\tau_0' = t_0 + t_0' \qquad 2t_0 = \tau_0 + \tau_0' \qquad t_0 = \frac{\tau_0' + \tau_0}{2} = g_1(\tau_0, \tau_0')$$

$$\tau_0 = t_0 - t_0' \qquad 2t_0' = \tau_0' - \tau_0 \qquad t_0' = \frac{\tau_0' - \tau_0}{2} = g_2(\tau_0, \tau_0') \qquad \text{(B30)}$$

$$J(\tau_0, \tau_0') = \frac{\partial(g_1, g_2)}{\partial(\tau_0, \tau_0')} = \begin{vmatrix} \dfrac{\partial g_1}{\partial \tau_0} & \dfrac{\partial g_1}{\partial \tau_0'} \\[2ex] \dfrac{\partial g_2}{\partial \tau_0} & \dfrac{\partial g_2}{\partial \tau_0'} \end{vmatrix} = \begin{vmatrix} \dfrac{1}{2} & \dfrac{1}{2} \\[2ex] -\dfrac{1}{2} & \dfrac{1}{2} \end{vmatrix} = \frac{1}{2} \qquad \text{(B31)}$$

As for the space variables, now obtain the limits of τ_0, τ_0' in the transformed (T_{cd}) plane. The transformation of the limits in the t_0, t_0' plane to corresponding quantities in the τ_0, τ_0' plane is given in Figures 6a and 6b where the limits from the Ξ_{cd} to T_{cd} plane are shown to be

$$\Xi_{cd} = \left\{ (t_0, t_0') : -\infty \le t_0 \le t, \; -\infty \le t_0' \le t' \right\}$$

$$T_{cd} = \left\{ (\tau_0, \tau_0') : \tau_0' - 2t' \le \tau_0 \le 2t - \tau_0', \; -\infty \le \tau_0' \le t + t' \right\} \qquad \text{(B32)}$$

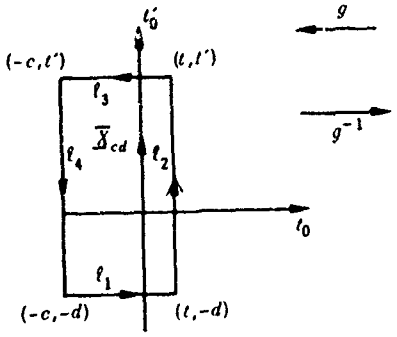

Figure 6a – Original Coordinates and Region of Integration

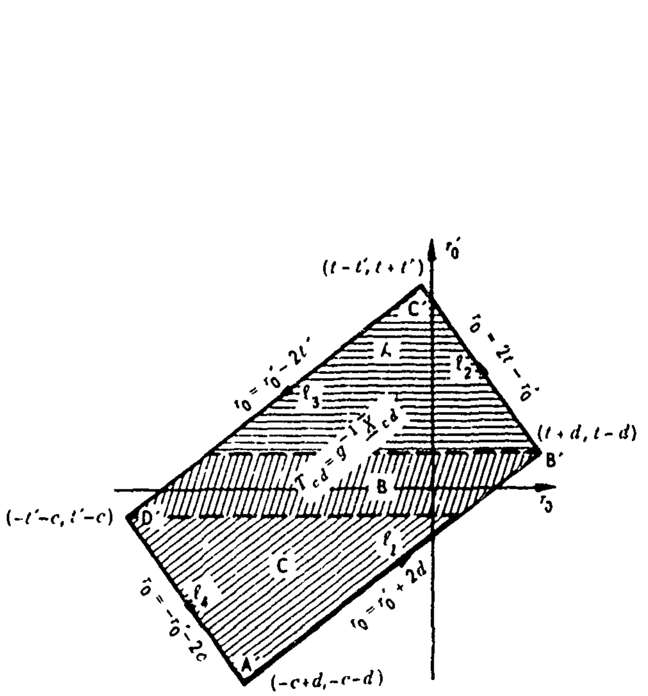

Figure 6b – Transfomed Coordinates and Region of Integration

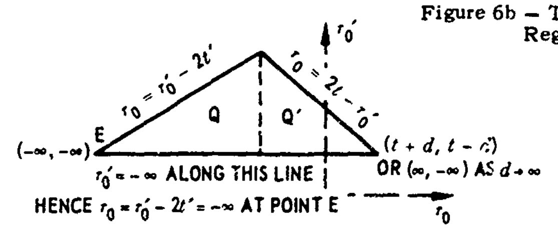

Figure 6c – Subdivision of Region A into Two Parts, Q and Q'

Figure 6 – Transformation of Time Coordinates and Region of Integration

The time limit points of Equation (B29) for the region t_0, t_0' denoted by $\bar{X}_{cd}$ in Figure 6a, where $c \to \infty$, $d \to \infty$, transform into the lines enclosing the region T_{cd} in Figure 6b. The limits obtained from the latter are based on the following relationships, using Equation (B30):

Line ℓ_1 where $t_0' = -d$, $-c \le t_0 \le t$ transforms to $r_0' = t_0 - d$, $r_0 = t_0 + d$, $r_0' = r_0 - 2d$

Line ℓ_2 where $t_0 = t$, $-d \le t_0' \le t'$ transforms to $r_0 = t - t_0'$, $r_0' = t + t_0'$, $r_0 = 2t - r_0'$

Line ℓ_3 where $t_0' = t'$, $t \ge t_0 \ge -c$ transforms to $r_0 = t_0 - t'$, $r_0' = t_0 + t'$, $r_0' = r_0 + 2t'$

Line ℓ_4 where $t_0 = -c$, $t' \ge t_0' \ge -d$ transforms to $r_0 = -c - t_0'$, $r_0' = -c + t_0'$, $r_0' = -2c - r_0$

In Figure 6b, the points of intersection (corners) representing the new limits are found by solving simultaneous equations thus:

Point A': $r_0 = -r_0' - 2c = r_0' + 2d$ yields $r_0' = -c - d$, $r_0 = -c + d$

Point B': $r_0 = r_0' + 2d = 2t - r_0'$ yields $r_0' = t - d$, $r_0 = t + d$

Point C': $r_0 = 2t - r_0' = r_0' - 2t'$ yields $r_0' = t + t'$, $r_0 = t - t'$

Point D': $r_0 = r_0' - 2t' = -r_0' - 2c$ yields $r_0' = t' - c$, $r_0 = -t' - c$

The limits for the transformed variables r_0, r_0' are now obtained from Figure 6b by subdividing the rectangular region into three regions A, B, C, over which the integrations are to be performed. From the figure and letting $c \to \infty$, $d \to \infty$, we have:

For Region A $\begin{cases} r_0' - 2t' \le r_0 \le 2t - r_0' \\ t - d \le r_0' \le t + t' \text{ becomes } -\infty \le r_0' \le t + t' \end{cases}$

For Region B $\begin{cases} r_0' - 2t' \le r_0 \le r_0' + 2d \\ t' - c \le r_0' \le t - d \to -\infty \le r_0' \le -\infty. \end{cases}$ Since the limits for r_0' coincide they will yield a zero contribution to the total integral. Therefore these limits are not considered.

For Region C $\begin{cases} -r_0' - 2c \le r_0 \le r_0' + 2d \\ -c - d \le r_0' \le t' - c \text{ becomes } -\infty \le r_0' \le -\infty. \end{cases}$

Again, these limits are not considered.

Since only the limits for Region A contribute to the total integral, they alone are to be considered.

The limits for T_{cd} shown in Figure 6 correspond to integrations for Region A only, which is the only region that need be treated. To perform the integration in Region A, it is convenient to subdivide the region in two, Q and Q′ as shown in Figure 6c. The limits are then reestablished so that the first is integrated with respect to τ_0' in Region Q (the inner integral) and then with respect to τ_0 in Region A; similar action is taken for Region Q′. The limits are (letting $t - t' = \tau$)

$$\text{In Region Q} \begin{cases} -\infty \leq \tau_0' \leq \tau_0 + 2t' \\ -\infty \leq \tau_0 \leq t - t' = \tau \end{cases}$$

$$\text{In Region Q}' \begin{cases} -\infty \leq \tau_0' \leq 2t - \tau_0' \\ t - t' = \tau \leq \tau_0 \leq \infty \end{cases}$$

The transformed time integral is now obtained from Equation (B25)

$$I' = \int_{\Sigma_{cd}} f(x)\,dx = \int_{g^{-1}(\vec{x})} f[g(t)]\ J_g(t)\ dt \tag{B33}$$

using Equation (B29) to obtain

$$f[g(t)] = e^{\frac{-|t_0 - t_0'|}{\theta}} e^{-a_{mn}|t - t_0|} \sin \omega_{mn}(t - t_0)\, u(t - t_0)\, e^{-a_{mn}(t' - t_0')} \sin \omega_{mn}(t' - t_0')\, u(t' - t_0')$$

$$= -\frac{1}{2} e^{\frac{-|t_0 - t_0'|}{\theta}} e^{-a_{mn}(t + t' - t_0 - t_0')} [\cos \omega_{mn}(t + t' - t_0 - t_0') - \cos \omega_{mn}(t - t' - t_0 + t_0')] \cdot u(t - t_0)\, u(t' - t_0')$$

$$= -\frac{1}{2} e^{\frac{-|t_0 - t_0'|}{\theta}} e^{-a_{mn}(t + t' - \tau_0')} [\cos \omega_{mn}(t + t' - \tau_0') - \cos \omega_{mn}(\tau - \tau_0)] \cdot u\left[t - \frac{(\tau_0' + \tau_0)}{2}\right] u\left[t' - \frac{(\tau_0' - \tau_0)}{2}\right]$$

(B34)

and Equation (B31) to obtain

$$J_g(t) = \frac{1}{2} \tag{B35}$$

The time integral I' then becomes

$$I' = I_1' + I_2' = \underbrace{\frac{1}{2}\int_{-\infty}^{\tau}\left[\int_{-\infty}^{\tau_0+2t'} f[g(t)]\,d\tau_0'\right]d\tau_0}_{\text{For Q}} + \underbrace{\frac{1}{2}\int_{\tau}^{\infty}\left[\int_{-\infty}^{2t-\tau_0} f[g(t)]\,d\tau_0'\right]d\tau_0}_{\text{For Q}'}$$

$$= -\frac{1}{4}\int_{-\infty}^{\tau}\left\{\left[\int_{-\infty}^{\tau_0+2t'} e^{-a_{mn}(t+t'-\tau_0')}\cos\omega_{mn}(t+t'-\tau_0') - \int_{-\infty}^{\tau_0+2t'}\right.\right.$$

$$\left.\left.\cdot\, e^{-a_{mn}(t+t'-\tau_0')}\cos\omega_{mn}(\tau-\tau_0)\right] e^{\frac{-|\tau|}{\theta}}\,d\tau_0'\right\}d\tau_0$$

$$-\frac{1}{4}\int_{\tau}^{\infty}\left\{\left[\int_{-\infty}^{2t-\tau_0} e^{-a_{mn}(t+t'-\tau_0')}\cos\omega_{mn}(t+t'-\tau_0') - \int_{-\infty}^{2t-\tau_0}\right.\right.$$

$$\left.\left.\cdot\, e^{-a_{mn}(t+t'-\tau_0')}\cos\omega_{mn}(\tau-\tau_0)\right] e^{\frac{-|\tau|}{\theta}}\,d\tau_0'\right\}d\tau_0$$

(For convenience the u's are omitted.)

Using Formula 414 of Reference 21 to obtain the first and third integrals (the second and fourth integrations are simply performed) and noting that $t + t' - \tau_0 - 2t' = t - t' - \tau_0 = \tau - \tau_0$ and $t + t' - 2t + \tau_0 = -t + t' + \tau_0 = \tau_0 - \tau$, we get

$$I' = I_1' + I_2' = -\frac{1}{4}\int_{-\infty}^{\tau} e^{-a_{mn}(\tau-\tau_0)}\,\frac{[a_{mn}\cos\omega_{mn}(\tau-\tau_0) - \omega_{mn}\sin\omega_{mn}(\tau-\tau_0)]}{a_{mn}^2+\omega_{mn}^2}\,e^{\frac{-|\tau|}{\theta}}\,d\tau_0$$

$$+\frac{1}{4a_{mn}}\int_{-\infty}^{\tau} e^{-a_{mn}(\tau_0-\tau)}\cos\omega_{mn}(\tau-\tau_0)\,e^{\frac{-|\tau_0|}{\theta}}\,d\tau_0$$

We define

$$f_1(\xi) = (a - |\xi|) \cos \frac{m\pi\xi}{a} + \frac{a}{m\pi} \sin \frac{m\pi|\xi|}{a}$$

$$f_2(\eta) = (b - |\eta|) \cos \frac{n\pi\eta}{b} + \frac{b}{n\pi} \sin \frac{n\pi|\eta|}{b} \tag{B38}$$

Then

$$\overline{\langle Y(x,y,t)\, Y(x',y',t')\rangle} = \frac{\overline{p^2}}{\sum_{\nu=1}^{3}\left(\frac{A_\nu}{K_\nu}\right) M^2} \sum_{mn} \frac{\phi_{mn}(x,y)\,\phi_{mn}(x',y')}{\omega_{mn}^2}$$

$$\cdot \sum_{\nu=1}^{3} A_\nu K_\nu \frac{2}{ab} \int_{-a}^{a} f_1(\xi) \int_0^b f_2(\eta) \frac{d\eta\, d\xi\, [I_1' + I_2']}{K_\nu^2 + (1/FU_c)^2 \left[\left\{\xi - U_c(t_0 - t_0')\right\}^2 + \eta^2\right]} \tag{B39}$$

or

$$\overline{\langle Y(x,y,t)\, Y(x',y',t')\rangle} = \frac{\overline{p^2}}{\sum_{\nu=1}^{3}\left(\frac{A_\nu}{K_\nu}\right) M^2} \sum_{mn} \frac{\phi_{mn}(x,y)\,\phi_{mn}(x',y')}{2ab\, \omega_{mn}^2} [I_1' + I_2'] \tag{B40}$$

where

$$I_1 = \sum_{\nu=1}^{3} A_\nu K_\nu \int_{-a}^{a} f_1(\xi) \left[\int_0^b f_2(\eta)\, d\eta\right] d\xi \frac{4 I_1'}{K_\nu^2 + (1/FU_c)^2 \left[\left\{\xi - U_c(t_0 - t_0')\right\}^2 + \eta^2\right]}$$

$$= \frac{\omega_{mn}}{a_{mn}^2 + \omega_{mn}^2} \int_{-a}^{a} f_1(\xi) \left[\int_0^b f_2(\eta) \sum_{\nu=1}^{3} A_\nu K_\nu\right.$$

$$\left.\cdot \left[\int_{-\infty}^{\tau} \frac{e^{-a_{mn}(\tau-\tau_0)}\left\{\sin \omega_{mn}(\tau-\tau_0) + \frac{\omega_{mn}}{a_{mn}} \cos \omega_{mn}(\tau-\tau_0)\right\} e^{\frac{-|\tau_0|}{\theta}}}{K_\nu^2 + (1/FU_c)^2 \left[\left\{\xi - U_c(t_0 - t_0')\right\}^2 + \eta^2\right]} d\tau_0\right] d\eta\right] d\xi \tag{B41}$$

$$I_2 = \sum_{\nu=1}^{3} A_\nu K_\nu \int_{-a}^{a} f_1(\xi) \left[\int_0^b f_2(\eta)\, d\eta \right] d\xi \, \frac{4 I_2'}{K_\nu^2 + (1/FU_c)^2 \left[\left\{ \xi - U_c(t_0 - t_0') \right\}^2 + \eta^2 \right]}$$

$$= \frac{\omega_{mn}}{a_{mn}^2 + \omega_{mn}^2} \int_{-a}^{a} f_1(\xi) \left[\int_0^b f_2(\eta) \sum_{\nu=1}^{3} A_\nu K_\nu \right.$$

$$\cdot \left[\int_{\tau}^{\infty} \frac{e^{-a_{mn}(\tau_0 - \tau)} \left\{ \sin \omega_{mn}(\tau_0 - \tau) + \frac{\omega_{mn}}{a_{mn}} \cos \omega_{mn}(\tau_0 - \tau) \right\} e^{\frac{-|\tau_0|}{\theta}}}{K_\nu^2 + (1/FU_c)^2 \left[\left\{ \xi - U_c(t_0 - t_0') \right\}^2 + \eta^2 \right]} d\tau_0 \right] d\eta \Bigg] d\xi$$

(B42)

The time integral in I_1 and I_2 can be further simplified by changing the limits of integration. In Equation (B41), for I_1 let

$$\overline{K}_1 = \int_{-\infty}^{\tau} \frac{e^{-a_{mn}(\tau - \tau_0)} \left\{ \sin \omega_{mn}(\tau - \tau_0) + \frac{\omega_{mn}}{a_{mn}} \cos \omega_{mn}(\tau - \tau_0) \right\} e^{\frac{-|\tau_0|}{\theta}}}{K_\nu^2 + (1/FU_c)^2 \left[(\xi - U_c \tau_0)^2 + \eta^2 \right]} d\tau_0$$

let

$$\bar{x} = \tau - \tau_0 \qquad \tau_0 = \tau - \bar{x} \qquad d\bar{x} = -d\tau_0$$

when

$$\tau_0 = \tau, \ \bar{x} = 0$$

$$\tau_0 = -\infty, \ \bar{x} = \infty$$

substituting the previously mentioned quantities in $\overline{K}_1$ and noting that $-\int_{\infty}^{0} = \int_0^{\infty}$

$$\overline{K}_1 = \int_0^{\infty} \frac{e^{-a_{mn}\bar{x}} \left\{ \sin \omega_{mn} \bar{x} + \frac{\omega_{mn}}{a_{mn}} \cos \omega_{mn} \bar{x} \right\} e^{\frac{-|\tau - \bar{x}|}{\theta}}}{K_\nu^2 + (1/FU_c)^2 \left[([\xi - U_c \tau] + U_c \bar{x})^2 + \eta^2 \right]} d\bar{x} \qquad \text{(B43)}$$

Similarly, for the time integral in I_2, set $\bar{x} = \tau_0 - \tau$, $\tau_0 = \tau + \bar{x}$ $d\bar{x} = d\tau_0$, and note that when $\tau_0 = \infty$, $\bar{x} = \infty$ whereas when $\tau_0 = \tau$, $\bar{x} = 0$. The substitutions yield

$$\bar{K}_2 = \int_0^{\infty} \frac{e^{-a_{mn}\bar{x}} \left\{ \sin \omega_{mn}\bar{x} + \dfrac{\omega_{mn}}{a_{mn}} \cos \omega_{mn}\bar{x} \right\} e^{\frac{-|\tau + \bar{x}|}{\theta}}}{K_\nu^2 + (1/FU_c)^2 \left[([\xi - U_c\tau] - U_c\bar{x})^2 + \eta^2 \right]} d\bar{x} \qquad \text{(B44)}$$

When Equations (B43) and (B44) are substituted into Equations (B41) for I_1 and (B42) for I_2, respectively, Equation (B40) becomes

$$\overline{<Y(x,y,t)\,Y(x',y',t')>} = \frac{\overline{p^2}}{2ab \displaystyle\sum_{\nu=1}^{3} \left(\frac{A_\nu}{K_\nu}\right) M^2} \sum_{mn} \frac{\phi_{mn}(x,y)\,\phi_{mn}(x',y')}{\omega_{mn}(a_{mn}^2 + \omega_{mn}^2)}$$

$$\cdot \int_{-a}^{a} f_1(\xi) \left[\int_0^b f_2(\eta) \left[\int_0^{\infty} g_1(\bar{x}) \sum_{\nu=1}^{3} \left\{ \frac{A_\nu K_\nu e^{\frac{-|\tau - x|}{\theta}}}{K_\nu^2 + (1/FU_c)^2 \left\{ [(\xi - U_c\tau) + U_c\bar{x}]^2 + \eta^2 \right\}} \right. \right. \right.$$

$$\left. \left. \left. + \frac{A_\nu K_\nu e^{\frac{-|\tau + \bar{x}|}{\theta}}}{K_\nu^2 + (1/FU_c)^2 \left\{ [(\xi - U_c\tau) - U_c\bar{x}]^2 + \eta^2 \right\}} \right\} d\bar{x} \right] d\eta \right] d\xi \qquad \text{(B45)}$$

where

$$g_1(\bar{x}) = e^{-a_{mn}\bar{x}} \left\{ \sin \omega_{mn}\bar{x} + \frac{\omega_{mn}}{a_{mn}} \cos \omega_{mn}\bar{x} \right\} \qquad \text{(B46)}$$

and it is important to note that

$$\begin{aligned} &\bar{x} = \tau - \tau_0\,; \; d\bar{x} = d\tau_0 \text{ for the first terms in the time integral} \\ &\bar{x} = \tau_0 - \tau\,; \; d\bar{x} = d\tau_0 \text{ for the second terms in the time integral} \end{aligned} \qquad \text{(B47)}$$

Let

$$\bar{y} = \frac{n\pi\eta}{b} \text{ or } \eta = \frac{b\bar{y}}{n\pi}; \quad \bar{z} = \frac{m\pi\xi}{a} \text{ or } \xi = \frac{a\bar{z}}{m\pi} \tag{B48}$$

then

$$\frac{f_1(\xi)}{a} = \cos\frac{m\pi\xi}{a} - \frac{1}{m\pi}\left(\frac{m\pi|\xi|}{a}\right)\cos\frac{m\pi\xi}{a} + \frac{1}{m\pi}\sin\frac{m\pi|\xi|}{a}$$

$$f_{11}(\bar{z}) = \frac{f_1\left(\frac{a\bar{z}}{m\pi}\right)}{a} = \cos\bar{z} + \frac{1}{m\pi}(-|\bar{z}|\cos\bar{z} + \sin|\bar{z}|)$$

$$\frac{f_2(\eta)}{b} = \cos\frac{n\pi\eta}{b} - \frac{1}{n\pi}\left(\frac{n\pi|\eta|}{b}\right)\cos\frac{n\pi\eta}{b} + \frac{1}{n\pi}\sin\frac{n\pi|\eta|}{b}$$

$$f_{21}(\bar{y}) = \frac{f_2\left(\frac{b\bar{y}}{n\pi}\right)}{b} = \cos\bar{y} + \frac{1}{n\pi}(\sin|\bar{y}| - |\bar{y}|\cos\bar{y}) \tag{B49}$$

Note that $f_1(\xi) = af_{11}(\bar{z})$ and $f_2(\eta) = bf_{21}(\bar{y})$

also when

$$\begin{aligned} \xi &= -a, \bar{z} = -m\pi \\ \xi &= a, \bar{z} = m\pi \\ \eta &= 0, \bar{y} = 0 \\ \eta &= b, \bar{y} = n\pi \end{aligned} \tag{B50}$$

and

$$d\eta = \frac{b}{n\pi}d\bar{y}, \; d\xi = \frac{a}{m\pi}d\bar{z}, \; d\eta d\xi = \frac{ab}{mn\pi^2}d\bar{y}\,d\bar{z} \tag{B51}$$

Substituting Equations (B48) through (B51) in Equation (B45), the final result for the displacement cross correlation is

$$\overline{<Y(x,y,t)\,Y(x',y',t')>} = \frac{\overline{p^2}ab}{2\pi^2\left[\sum_{\nu=1}^{3}\left(\frac{A_\nu}{K_\nu}\right)\right]M^2} \sum_{mn} \frac{\phi_{mn}(xy)\,\phi_{mn}(x',y')}{mn\,\omega_{mn}(a_{mn}^2 + \omega_{mn}^2)}$$

$$\cdot \int_{-m\pi}^{m\pi} f_{11}(\overleftrightarrow{z})\left[\int_0^{n\pi} f_{21}(\overline{y})\left[\int_0^{\infty} g_1(\overline{x}) \sum_{\nu=1}^{3} \left\{ \frac{A_\nu K_\nu e^{\frac{-|\tau - \overline{x}|}{\theta}}}{K_\nu^2 + (1/FU_c)^2 \left\{\left[\left(\frac{a\overline{z}}{m\pi} - U_c\tau\right) + U_c\overline{x}\right]^2 + \left(\frac{b\overline{y}}{n\pi}\right)^2\right\}}\right.\right.\right.$$

$$\left.\left.\left. + \frac{A_\nu K_\nu e^{\frac{-|\tau + \overline{x}|}{\theta}}}{K_\nu^2 + (1/FU_c)^2 \left\{\left[\left(\frac{a\overline{z}}{m\pi} - U_c\tau\right) - U_c\overline{x}\right]^2 + \left(\frac{b\overline{y}}{n\pi}\right)^2\right\}}\right\} d\overline{x}\right] d\overline{y}\right] d\overline{z} \qquad \text{(B52)}$$

(Note that in Reference 15, Equation (28), $f_{11}(\overleftrightarrow{z}) \to f(\overleftrightarrow{z})$, $f_{21}(\overline{y}) \to f(\overline{y})$ and $g_1(\overline{x}) \to g(\overline{x})$.)

If the second form of decay is used (for constant partial separation and variable time delay) for the cross correlation of the wall pressure for *semifrozen flow*, then in Equation (B13)

$$e^{\frac{-|t_0 - t_0'|}{\theta}} \to e^{\frac{-|x - x_0'|}{U_c\theta}} = e^{\frac{-|\xi|}{U_c\theta}} = e^{-\left|\frac{a\overline{z}}{m\pi U_c\theta}\right|}$$

so that following a procedure similar to that used in deriving Equation (B52), for this case

$$\overline{<Y(x,y,t)\,Y(x-,y',t')>} = \frac{\overline{p^2}ab}{2\pi^2 \sum_{\nu=1}^{3} M^2} \sum_{mn} \frac{\phi_{mn}(x,y)\,\phi_{mn}(x',y')}{mn\,\omega_{mn}(a_{mn}^2 + \omega_{mn}^2)}$$

$$\cdot \int_{-m\pi}^{m\pi} f_{11}(\overleftrightarrow{z})\left[\int_0^{n\pi} f_{21}(\overline{y})\left[\int_0^{\infty} g_1(\overleftrightarrow{x}) \sum_{\nu=1}^{3} \cdot \left\{ \frac{A_\nu K_\nu}{K_\nu^2 + (1/FU_c)^2 \left[\left(\left[\frac{a\overleftrightarrow{z}}{m\pi} - U_c\tau\right] + U_c\overleftrightarrow{x}\right)^2 + \left(\frac{b\overline{y}}{n\pi}\right)^2\right]}\right.\right.\right.$$

$$\left.\left.\left. + \frac{A_\nu K_\nu}{K_\nu^2 + (1/FU_c)^2 \left[\left(\left[\frac{a\overleftrightarrow{z}}{m\pi} - U_c\tau\right] - U_c\overline{x}\right)^2 + \left(\frac{b\overline{y}}{n\pi}\right)^2\right]}\right\} d\overline{x}\right] d\overline{y}\right] d\overline{z} \qquad \text{(B53)}$$

where

$$f_{11}(\bar{z}) = \frac{f\left(\frac{a\bar{z}}{m\pi}\right)}{b} = \frac{\cos \bar{z} + \frac{1}{m\pi}(-|\bar{z}| \cos \bar{z} + \sin |\bar{z}|)}{e^{-\left|\frac{a\bar{z}}{m\pi U_c \theta}\right|}}$$

$$f_{21}(\bar{z}) = \frac{f\left(\frac{b\bar{y}}{n\pi}\right)}{b} = \cos \bar{y} + \frac{1}{n\pi} (\sin |\bar{y}| - |\bar{y}| \cos \bar{y})$$

$$g_1(\bar{x}) = e^{-a_{mn}\bar{x}} \left[\sin \omega_{mn}\bar{x} + \frac{\omega_{mn}}{a_{mn}} \cos \omega_{mn}\bar{x}\right]$$

Equations (B52) and (B53) have similar numerical results.

If the pressure covariance is used for *unsteady convection* (Model B) given in Equation (B10), the response of a panel *including modal couplings* is given by

$$\overline{\langle Y(x,Y,t)\, Y(x',y',t')\rangle} = \int_{-\infty}^{t} dt_0 \int_{-\infty}^{t'} dt_0' \int_0^a dx_0 \int_0^a dx_0' \int_0^b dy_0 \int_0^b dy_0'$$

$$\cdot \left\{ \frac{\phi_{mn}(x,y)\,\phi_{mn}(x_0,y_0)}{\omega_{mn} M} e^{-a_{mn}(t-t_0)} [\sin \omega_{mn}(t-t_0)\, u(t-t_0)] \right\}$$

$$\cdot \left\{ \frac{\phi_{p,q}(x',y')\,\phi_{p,q}(x_0',y_0')}{\omega_{pq} \mathbf{M}} e^{-a_{pq}(t'-t_0')} [\sin \omega_{pq}(t'-t_0')\; u(t'-t_0')] \right\}$$

$$\cdot \overline{p^2} \left\{ A_1 \left[e^{\frac{-|t_0-t_0'|}{\theta_1}} + a_1 e^{\frac{-|t_0-t_0'|}{\theta_1}} \cdot \sin \omega_1 |t_0 - t_0'| \right] \right.$$

$$e^{\frac{-\left\{[(x_0-x_0')-U_c(t_0-t_0')]^2 + (y_0-y_0')^2\right\}}{2\sigma_1^2}} + A_2 \left[e^{\frac{-|t_0-t_0'|}{\theta_2}} + a_2 e^{\frac{-|t_0-t_0'|}{\theta_2}} \cdot \cos \omega_2(t_0-t_0') \right]$$

$$\left. e^{\frac{-\left\{[(x_0-x_0')-U_c(t_0-t_0')]^2 + (y_0-y_0')^2\right\}}{2\sigma_2^2}} \right\} \tag{B54}$$

Using the modal volume displacement

$$\mathrm{Vol}_{mn} = \sqrt{2}\ \vec{Y} \int_0^a \int_0^b \phi(x)\phi(y)\ dx\ dy \tag{B55}$$

the *modal acoustic power radiated* in a reverberant field can be calculated

$$PWL_{mn} = \frac{N\omega^2 \rho c K_a^2}{4\pi}\ \overline{Y^2}\ \frac{2P_r + P_p}{P_p}\left[\int_0^a \int_0^b |\phi_m(x)|\quad |\phi_n(y)|\ dx\ dy\right] \tag{B56}$$

Finally, using Equation B9, the normalized power spectrum of the turbulence pressures is computed for case of $\eta = 0$. The normalized correlation coefficient is defined as

$$R_y(\xi,\eta,\tau) = \frac{Y(x,y,t)\,Y(x',y',t')}{\left[\overline{Y(x,y,t)^2\ Y(x',y',t')^2}\right]^{1/2}}$$

The normalized power spectrum is then

$$P(K_1,\omega) = \frac{1}{(2\pi)^2} \cdot \int_{-\infty}^{\infty}\int_{-\infty}^{\infty} R(\xi,0,\tau)\ e^{-(K_1\xi+\omega\tau)} d\xi\, d\tau \tag{B57}$$

$$= \frac{1}{(2\pi)^2}\int_{-\infty}^{\infty} \frac{e^{\frac{-|\xi|}{U_c\theta}}}{\sum_{\gamma=1}^{3}\frac{A_\gamma}{K_\gamma}} \sum_{\gamma=1}^{3} A_\gamma K_\gamma F^2 \left[\int_{-\infty}^{\infty} \frac{e^{-i\omega\tau}\, d\tau}{K_\gamma^2 F^2 + \left(\tau - \frac{\xi}{U_c}\right)^2}\right] e^{-iK_1\xi}\ d\xi \tag{B58}$$

From Pair 632.2 of Reference 7, with $p = i\omega$ and $\beta = K_\gamma F$, the quantity in brackets equals $\frac{\pi}{K_\gamma F} e^{-K_\gamma F|\omega| - i\xi\omega/U_c}$. Hence

$$P(K_1,\omega) = \frac{F}{4\pi \sum_{\gamma=1}^{3}\frac{A_\gamma}{K_\gamma}} \sum_{\gamma=1}^{3} A_\gamma e^{-|\omega| K_\gamma F} \int_{-\infty}^{\infty} e^{\frac{-|\xi|}{U_c\theta}} \cdot e^{-iK_1' d\xi} \tag{B59}$$

where $K_1' = \frac{\omega}{U_c} + K_1$.

Using Pair 444 of Reference 7, with $p = iK_1' = i\left(\frac{\omega}{U_c} + K_1\right)$, and $\beta = \frac{1}{U_c\theta}$, the integral equals

$$\frac{-2/U_c\theta}{-(K_1')^2 - (1/U_c\theta)^2} = \frac{2U_c\theta}{1 + \theta^2(\omega + K_1U_c)^2}$$

Hence

$$P(K_1,\omega) = \frac{\theta}{1 + \theta^2\,(\omega + K_1U_c)^2}\,(FU_c/2\pi)\,\frac{\sum_{\gamma=1}^{3} A_\gamma e^{-|\omega|\,K_\gamma F}}{\left(\sum_{\gamma=1}^{3}\frac{A_\gamma}{K_\gamma}\right)} \tag{B60}$$

which agrees with Reference 16, Equation (6).

COMPUTER PROGRAMS

Computer programs for either Equation (B52) or (B53) and Equation (B60) are designated as Subprograms A and B, respectively. Reference 22 presents equations similar to Equations (B52) and (B53) and gives Fourier transforms to yield the displacement cross spectral density; (see Reference 22, Equation (27)). Since the method of derivation is similar to the method presented in this report, the details are omitted here.* The corresponding computer subprograms are designated as Subprograms C (modal coupling excluded) and D (modal coupling included). The latter subprograms treat simple and clamped supports and uncoupled and coupled modes.

APPENDIX B2 – METHOD FOR DETERMING INPUT DATA

The following data are furnished to the computer

Flow data: U_c , τ_w , $\delta^* = FU$, ω , $\overline{p^2}$, θ , A_ν, K_ν where ν = 1, 2, 3

Panel data: $a, b, h, \delta_{mn}, E, M, \phi_{mn}, \omega_{mn}, \xi, \eta, \tau, m, n, \overline{Y}, N, \rho c K_a^2, \frac{2P_r + P_p}{P_p}, x, y, x', y'$

The method for determining the data is now described. Either the data are arbitrarily selected by the user, i.e., the values are chosen to represent the range of interest, or the selections may correspond to experimental values for a parameter.

---

*The mathematical form of the model representing turbulence excitation pressures used in Reference 22 is slightly different from that used by Maestrello in his earlier works.

Parameter	Description
A_ν, K_ν	Prescribed constants used in Equation (B7)
a, b, h	Prescribed quantities
E	A prescribed quantity
M	A prescribed quantity
m,n	Prescribed data
N	Determined as described on page 434 of Reference 15. Maestrello assumed piston radiation for which $N = 4$.
$\dfrac{2P_r + P_p}{P_p}$	Equal to 1 for a plate without ribs
$\overline{p^2}$	Equals $\int_0^\infty P(\omega)\,d\omega$, where $P(\omega)$ is obtained from Equation (B7). This quantity can also be measured directly.
U_c	A parameter whose values are prescribed by the user, $U_c = 0.8\,U_\infty$; see Reference 15 page 427 . A method for measuring this quantity by experimentation is given by Equations (B2) and (B4) or alternately for K, ω space by equations given in Reference 15, page 414.
$x, y\ x', y'$	Prescribed points; the cross correlation of the displacements are computed for these points.
$\overline{Y}$	Determined by taking the square root of the calculated mean-square displacement.
$\delta^*(=FU)$	Equals $0.37/8\,(U_\infty x/\nu)^{-1/5}$; see Reference 25, Equations (21.6) and (21.8). Tables 1.1 and 2.1 of that reference give values of ν in air and water. Using this equation, values of δ^* for a given fluid can be prescribed over a range of U_∞.
δ_{mn}	Total damping ratio obtained in accordance with the methods of Section 3.4 of Reference 14 and further described in the footnote to statement preceding Equation (B18). Note that in Reference 15 Figure 19, $a_{mn} = \delta_{mn}\omega_{mn}/2$, whereas determination of a_{mn} in Figure 16 of the same reference is made from the formula $a_{mn} = 0.5(\omega_{mn})^{1/3}$, which is based on *El* Baroudis data. The latter was considered acceptable for thin plates. In general it is preferable to use the former method in making a theoretical calculation. Value of a_{mn} may be prescribed by the user to determine the effects of damping variations.

*Our equation agrees with that given by Jacobs in Equation (59), of Reference 34 letting $U_c = 0.8$ Mc(M = Mach Number and c = sound velocity) and noting that θ should be in milliseconds in that equation. Our equation differs from that given in Reference 14, Equation 7, by a factor of 10^{-3} , see also Appendix E.

θ — Corresponds to the time in which the value of the measured correlation coefficient of the fluctuating pressures at the wall, obtained from the envelope of the correlation maxima, drop to $1/e$. Plots of θ versus Mach number for broad- and narrow-band frequencies are given in Reference 14, Figure 5. From Figure 5* $\theta \; - 1.37 \times 10^{-3} \; U_c + 1.15$ where θ is in milliseconds and U_c in feet per second. Thus, $\theta = \theta(U_c)$ may also be prescribed for various values of U_c; θ may also be obtained from the plot of $U_c\theta/\delta^*$ versus the Mach number given in Reference 15, Figure 6.

ξ, η, τ — Prescribed data

$\rho C K_a^2$ — The numerical value of this quantity for air has been computed and included in the program. For a water medium, it is necessary to modify this value in the ratio of $(\rho C)_{water}/(\rho C)_{air}$ by adding an instruction to the program.

τ_w — Determination of this quantity is based on the law of the wall described in detail and shown in Reference 23, Figure 1. The Maestrello data given in Reference 24, Figure 2, lie along the universal curve representing this law. (Note that for incompressible flow, the vertical coordinate of this figure equals u/u_τ). From either of the figures, $\dfrac{y u_\tau}{\nu_w} \Big/ \dfrac{u}{u_\tau} = \dfrac{y u_\tau^2}{u \nu_w}$ = constant = inverse slope of the curve, which is measured. Hence if the velocity profile of the users data agrees with the universal curve, then for a known value of ν_w, selecting a value of u corresponding to a value of y yields the value of u_τ. By definition $\tau_w = \rho_w u_\tau^2$.

$\phi_{mn}(xy)\,\phi_{mn}(x',y')$ — The data required for the computer program are calculated by the digital computer for a range of prescribed values of m, n, x, y, x', and y'.

ω — Prescribed in Equation (B7) to obtain $P(\omega)$

ω_{mn} — For a plate of given geometry and structural properties, this quantity is computed by hand for a plate with rigid or fixed boundaries using Equation (A7) of Reference 14. For a simply supported plate, use Equation (IV.5.16) of Reference 10.

APPENDIX B3 – PROGRAM IDENTIFICATION

A program is presented for computing mean-square displacement (Subprogram A) of a simply supported rectangular panel excited by a turbulent boundary layer and the modal acoustic-power radiation of the plate in a reverberant field. The program also computes the turbulent pressures on the plate (Subprogram B) and the cross spectral density of the displacement for simple or clamped boundaries without modal cross coupling (Subprogram C) and with modal cross coupling (Subprogram D); see Tables 2 and 3. Computer running times for sample problems are as follows:

Subprogram	Computer	Time
A	IBM 7090 at NSRDC	The Simpson rule of integration 4 modes (m = 1, 3, 5, 7, with n = 1) 1 convection velocity U_c Approximately *28 min*
B	IBM 7090 at NSRDC	48 frequencies 8 spatial separations Approximately *2 min*
C	IBM 360/91 at Applied Physics Laboratory Johns Hopkins University	Gaussian quadrature (9 point) 4 modes (m = 1, 3, 5, 7, with n = 1) 1 U_c Approximately *9 sec*

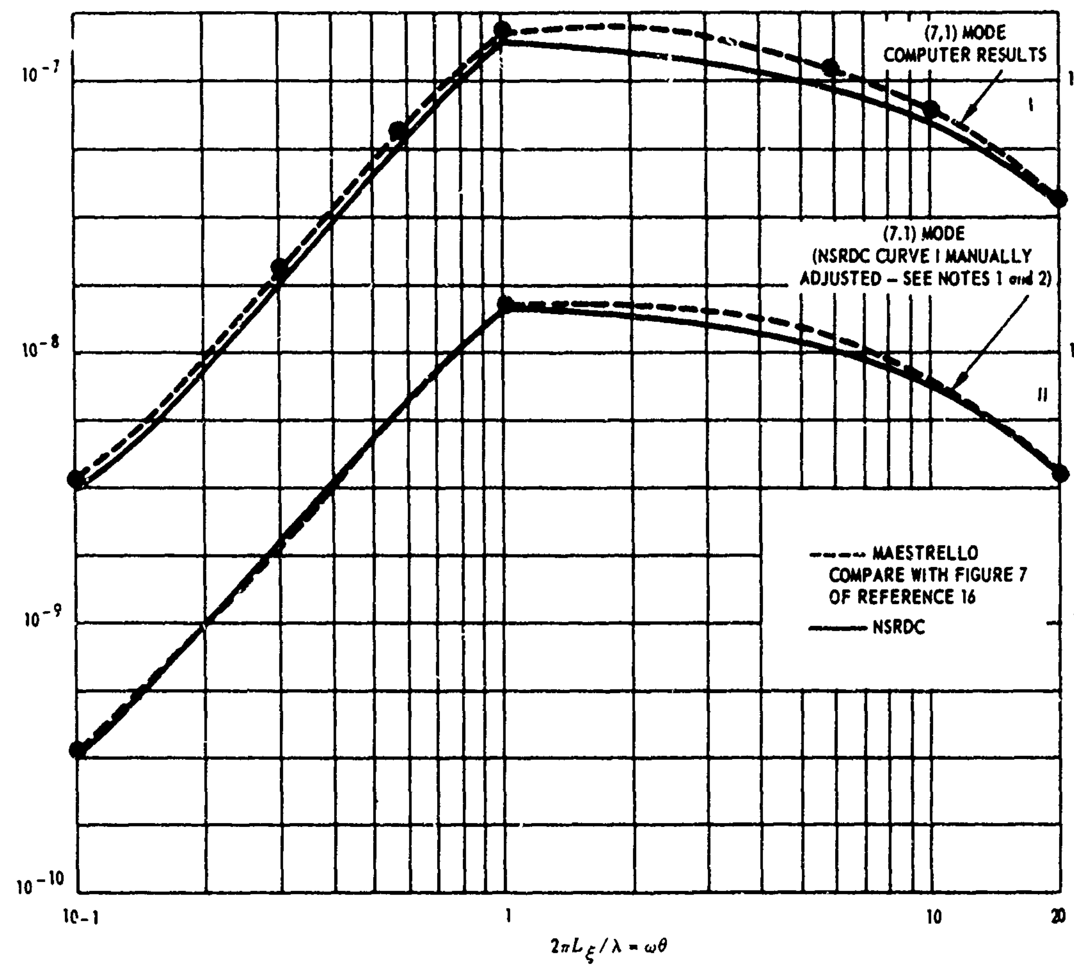

Note 1: For Curves I and II, use ordinate scales to left and right, respectively.

Note 2: NSRDC Curve I was obtained by selection of a value of $\overline{p^2} = 13.72$ lb/in.^{4} which yielded a curve approximating that of Maestrello Curve I. Maestrello's actual value of $\overline{p^2}$ (Figure 7, Reference 16) is unknown. NSRDC Curve I was then manually adjusted to give the same value of $\overline{y^2}$ as that given by Maestrello at $\frac{2\pi L_\xi}{\lambda_{mn}} = 1$. (This should be equivalent to using the same value of $\overline{p^2}$ as Maestrello.) The replot is shown as Curve II. Observe that in view of the scaling errors involved in copying the Maestrello curve, the curves shown in the replot are in good agreement.

Figure 7 – Variation of Modal Mean Square Displacement with Eddy Lifetime for a 36- × 6.5- × 0.04-Inch Panel

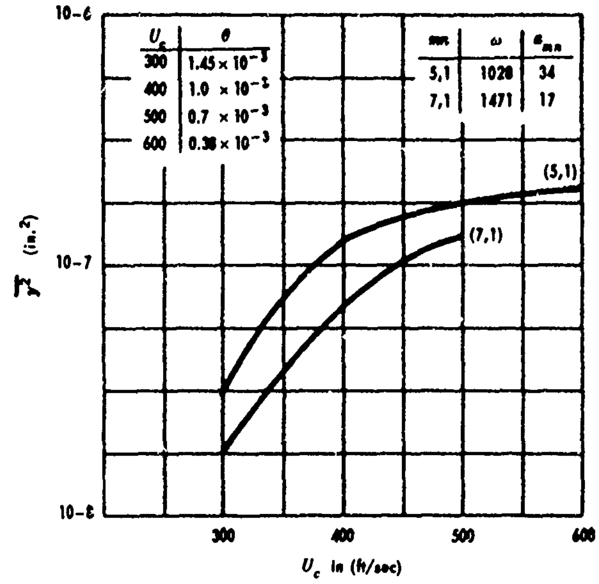

Figure 8 – Computed Modal Mean Square Displacement for a 36- × 6.5- × 0.04-Inch Panel

Compare with Figure 19 of Reference 15. The trend of curves there is similar to curves drawn here, but differences appear to be due either to a normalization factor of $4\pi^2$ or to the use of different values of p^2 than those used here.

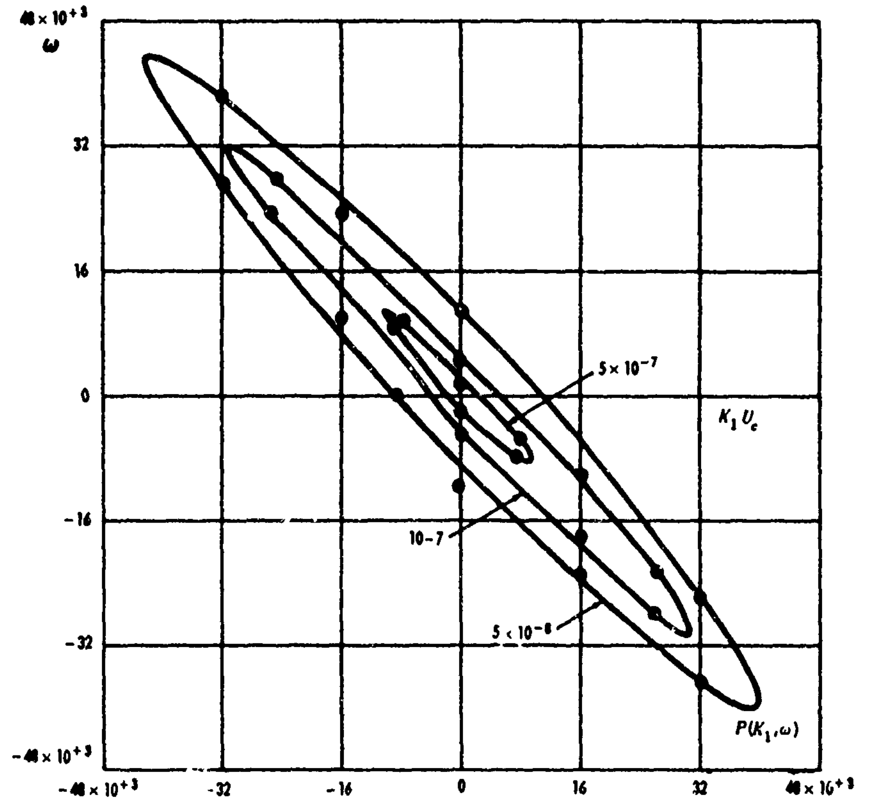

Figure 9 – Contours of Constant Turbulence Pressure Spectrum Level for Convected Semifrozen Pattern

Compare with Figure 5 of Reference 15.

Figure 10 – Computed Displacement Spectral Density for a 12- × 6- × 0.062-Inch Titanium Panel

Compare with Figure 20 of Reference 22.

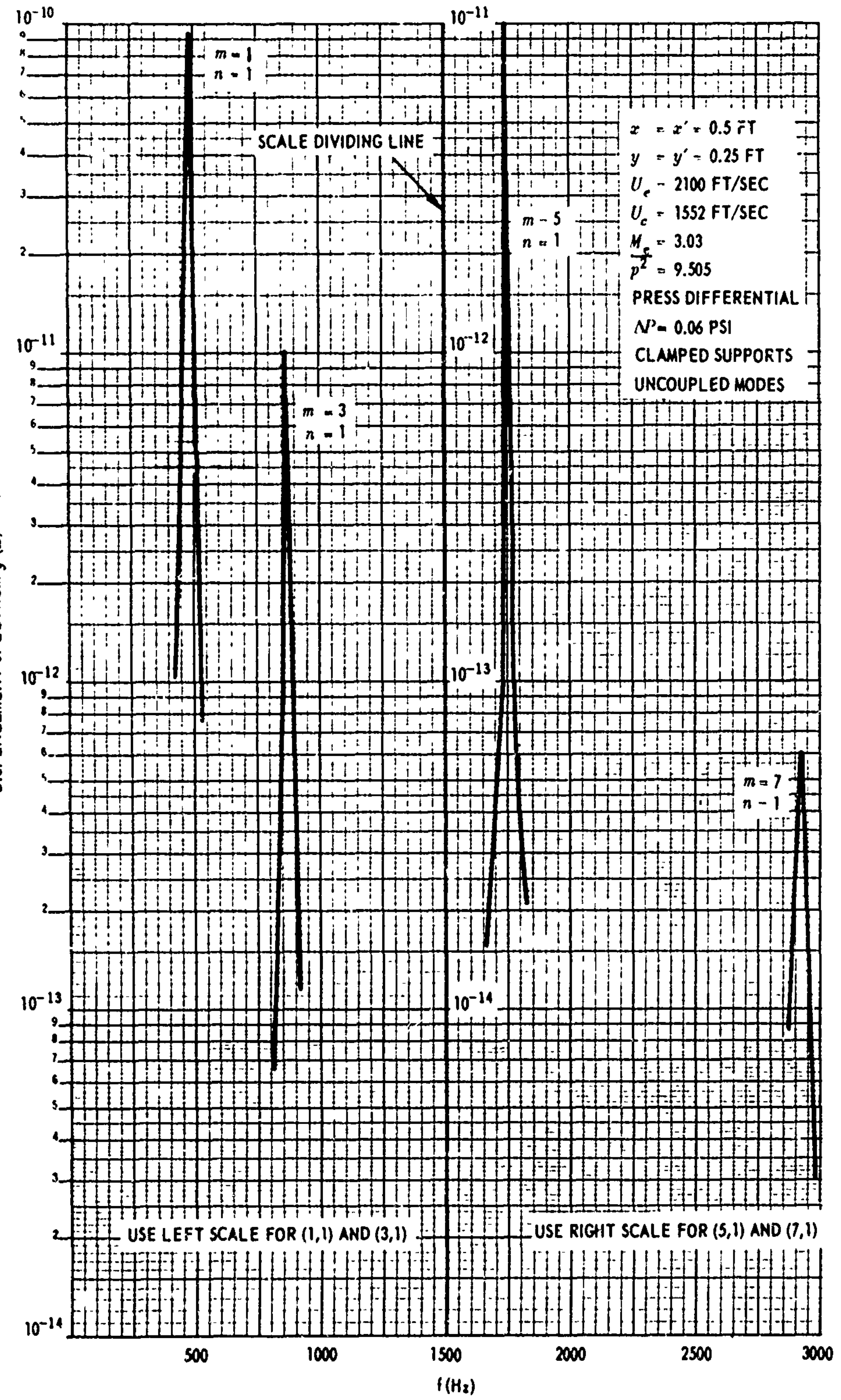

Figure 10a – Result Using Both Parts of Subprogram C

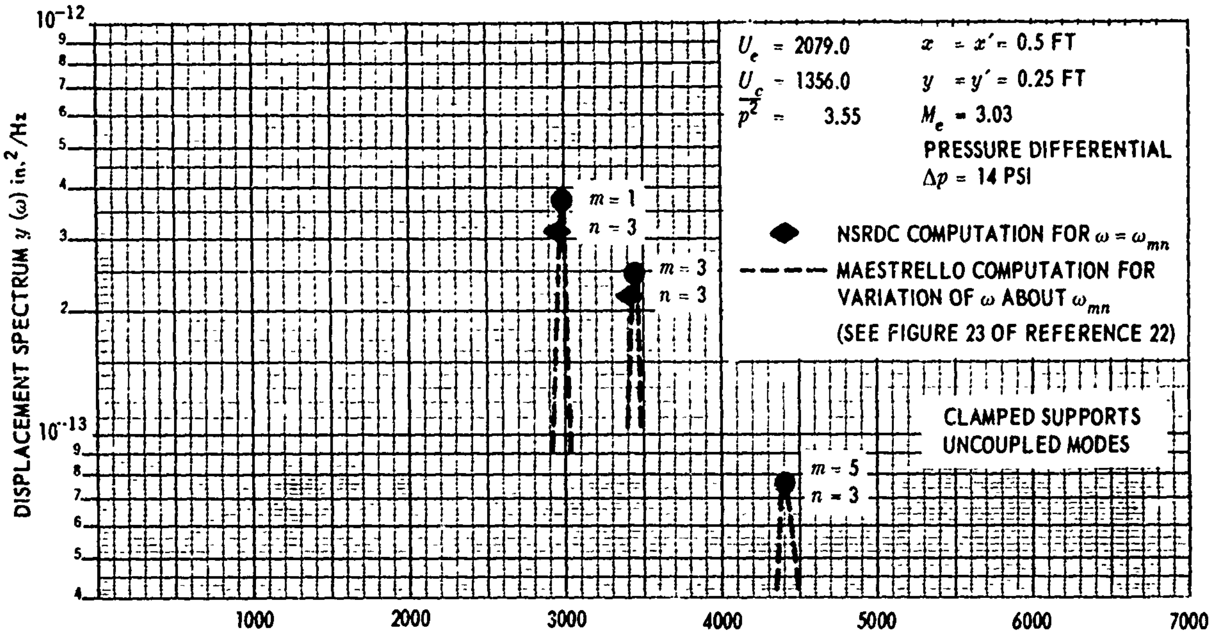

Figure 10b – Results Ignoring the First Part of the Solution

Notes for Figures 10a and 10b:

To compute the power spectrum, without coupling, Subprogram C first uses the Warburton method to determine the eigenfunctions and eigenvalues. Hence the user must submit the coefficients for the boundary conditions he desires. The program comes in two parts: the first solves for the peak response at $\omega = \omega_{mn}$ and the second solves for the spectrum, varying ω around ω_{mn}.

Figure 10a shows a narrow bandwidth for some modes, such as (5.1). This means that if the user were to run the program only for $\omega \neq \omega_{mn}$, (as in Figure 10b which ignores the first part of the solution) he could bypass the peak response. The curve shown in Figure 10a is a *result of both programs,* where DW, the interval used in the computer program, was 100, for the case $\omega \neq \omega_{mn}$. The curve was then extrapolated to its peak value at $\omega = \omega_{mn}$.

Input data for Figures 10a and 10b were obtained from Maestrello, he computed his modal frequencies for $\Delta p = 0.06$ and 14 psi and used experimentally obtained values of damping. The relations $U_c = 0.8\ U_e$ and $\overline{p^2} \approx 12\ \tau_w^2$ were used. Input dimensions of length are in units of feet, whereas by means of a conversion factor in the program, the corresponding output is in inch units.

In Figure 10b the static pressure $\Delta p = 14$ psi is introduced into the program by modifying the value of ω_{res} obtained at $\Delta p = 0.06$ psi ≈ 0 psi from the Warburton equation for clamped boundaries. Since $\omega_{res} \approx \sqrt{\frac{k}{m}}$ and approximately $k \propto E$, then ω_{res} is proportional to the square root of E and therefore the stiffness k. If originally we have $E_{\Delta p = 0} = 0.21 \times 10^8$ psi, then modifying E in proportion to the change in stiffness which was measured with a strain gage on the panel under static loading, we get $E_{\Delta p = 14\text{ psi}} = 0.33 \times 10^8$ psi. We then recompute the value of ω_{res} corresponding to this value of E.

APPENDIX B

TABLE 2

Identification of Subprograms A, B, C, and D – Maestrello

This table includes identification input and output data units (in foot – pound – seconds), flow charts, order of data, and sample data. Computer subprogram listings are given at the end of this appendix as Table 3.

Subprogram A:	Computation of Plate Vibration and Acoustic Response for Model A (Semifrozen Convection)
Subprogram B:	Computation of Cross Spectral Density of Turbulent Pressures for Model A (Semifrozen Convection)
Subprogram C:	Computation of Cross Spectral Density of Displacement
Subprogram D:	Generalization of Subprogram C to Include Modal Cross Coupling

TABLE 2 A

Input Required for *Subprogram A* to Compute the Plate Vibration and Acoustic Response for the Semifrozen Convection (*Model A*) and Corresponding Output

(Units are given in foot-pound-seconds)

Data	Description	Type	Symbol Used in Program
Flow Characteristics	(Subprogram A)		
U_c	Broadband convection velocity	Decimal	UC(I)
$\overline{p^2}$	Mean-square wall-pressure fluctuations, which vary with U_c *	Decimal	PB2*DPB2(I)
$(FU_c)^2$	Quantity $\left(\frac{\delta^* U_c}{U}\right)$ squared where: $\delta^* \equiv$ boundary-layer displacement thickness; $U \equiv$ free stream velocity	Decimal	FUCSQ
K_1,K_2,K_3	Universal constants: $K_1 = 0.470$, $K_2 = 3.0$, $K_3 = 14.0$	Decimal	AK
A_1,A_2,A_2	Universal constants: $A_1 = 1.6$, $A_2 = 7.2$, $A_3 = 12.0$	Decimal	AN

(*PB2 would represent a unique value of $\overline{p^2}$ if $\overline{p^2}$ were independent of U_c. It enters the program (i.e., data cards) once only. Since $\overline{p^2}$ actually varies with U_c, a correction factor DPB2(I) is entered with every value of U_c. Thus $\overline{p^2}$ as a function of U_c is accounted for by the quantity PB2* DPB2(I).

TABLE 2A (Continued)

Data	Description	Type	Symbol Used in Program
Plate Characteristics			
h	Panel thickness	Decimal	H
M^2	Square of plate mass	Decimal	FM2
a, b	Lengths of panel sides	Decimal	ZUP, YUP
$\delta_{m,n}$	Total damping ratio	Decimal	DAMP
$\omega_{m,n}$	Modal frequencies of the plate	Decimal	OMEGA
Additional Quantities			
Range of plate mode numbers for which calculations are desired	First m mode number, last m mode number, interval between m mode number, total number of m's Same information as previously described, with respect to n mode numbers	Integer Integer Integer Integer Integer Integer Integer Integer	MLOW MUP DM MSTEPS NLOW NUP DN NSTEPS
τ	Time delay	Decimal	TAU
Number of values of U_c to be calculated		Integer	KUC
Set of reference points against which mean-square displacement and acoustic power will be tabulated	$\frac{2U_c\theta}{\lambda_{m,n}}$ where θ – eddy lifetime; $\lambda_{m,n}$ – acoustic wave length for mode (m,n)	Decimal	PARAM
Number of values of PARAM specified		Integer	NP
x_0, y_0	Coordinates of a point on plate at which mean-square displacement and acoustic power are calculated	Decimal	XO, YO
x_0', y_0'	any point on plate different from x_0, y_0	Decimal	XOP, YOP

TABLE 2A (Continued)

Data	Description	Type	Symbol Used in Program
Calculated Output in Inch-Pound-Seconds			
$\phi_{m,n}$	Value of eigenfunctions of mean-square displacement A value of EIGEN is computed for each mode (m,n) with three values of total damping; $1/10\ a_{m,n}\ ;a_{m,n}\ ;10a_{m,n}$	Decimal	EIGEN
$a_{m,n}$	Values of total damping associated with each mode (m,n)	Decimal	FA $(m,n,1)$ for computation; A $(m,n,$ DAMP) in output
$\dfrac{\mathrm{Vol}_{m,n}}{\sqrt{2Y}}$	Volume under each eigenfunction	Decimal	VOL
$I(m,n)$	Triple integral of Equation I.13: integral of cross correlation	Decimal	IXY2 I(m,n)
$\overline{Y^2}$	Mean-square displacement for values of $1/10\ a_{m,n};a_{m,n};10a_{m,n}$	Decimal	ANS

Output is printed for a given convection velocity U_c for the modes of interest. The last four columns of the output respectively represent $\overline{Y^2}$ for $1/10\ a_{m,n}$, $\overline{Y^2}$ for a_{mn}, and $\overline{Y^2}$ for $10\,a_{mn}$ for chosen PARAM. Since this program was written, Maestrello has developed methods of computing damping, but here he chooses the magnitude of a_{mn} according to the $\omega\theta$ region of the curve that interests him. For example, Figure 7 plots $\overline{Y^2}$ against $\omega \cdot \theta$. In the region $\omega \cdot \theta = 10^{-1}$ to 1.0 he uses $a_{mn}/10$; however, for $\omega \cdot \theta = 1.0$ to 40, he uses a_{mn}. Also, $\overline{Y^2}$ corresponds to the value of PARAM closest to $\omega\theta$ where θ corresponds to U_c.

TABLE 2A (Continued)

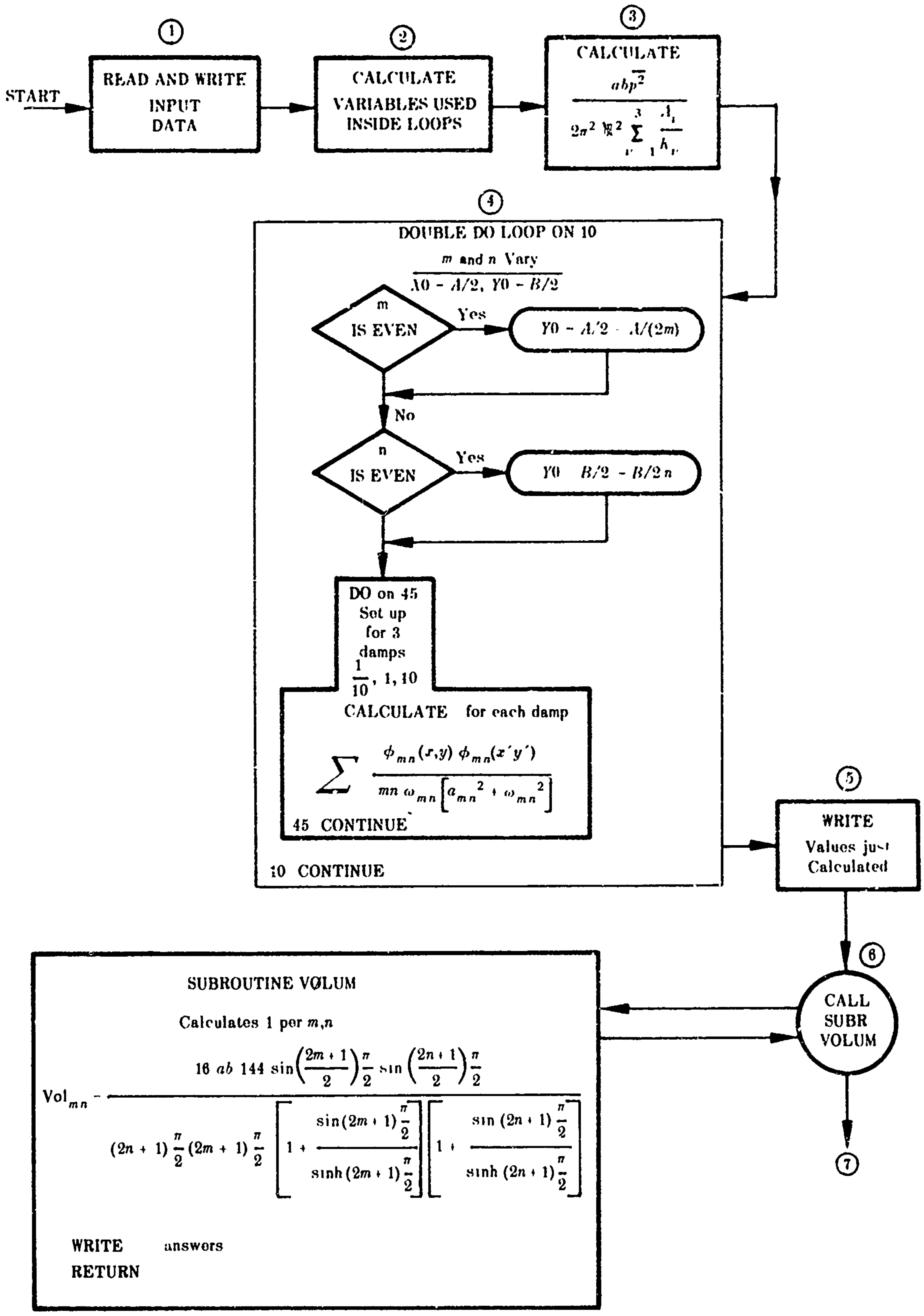

TABLE 2A (Continued)

(7) DO 777 — Vary U_c
CONST (3) - DPB2(KU)
WRITE U_c AND CONST

(8) DO 778 — m Values

(9) DO 779 — Set up θ's
779 θ_i PARAM $(i)/m/U_c$ * A

(10) Set upper and lower limits for x, y, z integrals determine no. of steps for each integral and the step size for each

(11) DO 11
Calculates coefficients for Simpsons Rule

(12) z
Set variable of integration = lower limit on z
Calculates function of z values

$$f_{(z)} = \int_{-a}^{a} \cos\frac{m\pi z}{a} + \frac{1}{m\pi}\left[\sin\left|\frac{m\pi z}{a}\right| - \left|\frac{m\pi z}{a}\right| \cos\left(\frac{m\pi z}{a}\right)\right] dz$$

(13) Y
Set variable of integration = lower limit on y
Calculates function of y values

$$f_{(y)} = \int_{0}^{b} f_{(z)} \left[\cos\frac{n\pi y}{b} + \frac{1}{n\pi}\left[\sin\left(\frac{n\pi y}{b}\right) - \frac{n\pi y}{b}\cos\left(\frac{n\pi y}{b}\right)\right]\right] dy$$

(14) Set up and initialize to zero, the array for summing on outside integral

(15) X
Set variable of integration = lower limit on X
Calculates function of X varying y and z and summing up parts previously calculated

$$f_{(x)} = \int_{0}^{\infty} f_{(y)} \left[mn\frac{4}{ab} e^{-a_{mn}x}\left[\sin\left(\omega_{mn}|x|\right) + \frac{\omega_{mn}}{a_{mn}}\cos\left(\omega_{mn}|x|\right)\right] e^{-|x/\theta|} + \sum_{\nu=1}^{3} \frac{A_\nu K_\nu}{K_\nu^2 + \frac{1}{FU_c}^2 \quad z - U_c(t-x)^2 + y^2} \right] dx$$

(16) WRITE
Answers of triple integral → IXYZ

(17) COMPUTE AND WRITE
ANS = $IXYZ$ * EIGEN AND CONST

778 CONTINUE
777 CONTINUE
↓
STOP

TABLE 2A (Continued)

COLUMN HEADINGS FOR INPUT FORMS ON DATA CARDS

TAU	15	20	30	40	50	60	70
H	10	20	30	40	50	60	70
XO	10	20	30	40	50	60	70
YO	10	20	30	40	50	60	70
XOP	10	20	30	40	50	60	70
YOP	10	20	30	40	50	60	70
FUCSQ	10	20	30	40	50	60	70
PB2	10	20	30	40	50	60	70
FM2	10	20	30	40	50	60	70
AK(1)	10	20	30	40	50	60	70
AK(2)	10	20	30	40	50	60	70
AK(3)	10	20	30	40	50	60	70
AN(1)	10	20	30	40	50	60	70
AN(2)	10	20	30	40	50	60	70

TABLE 2A (Continued)

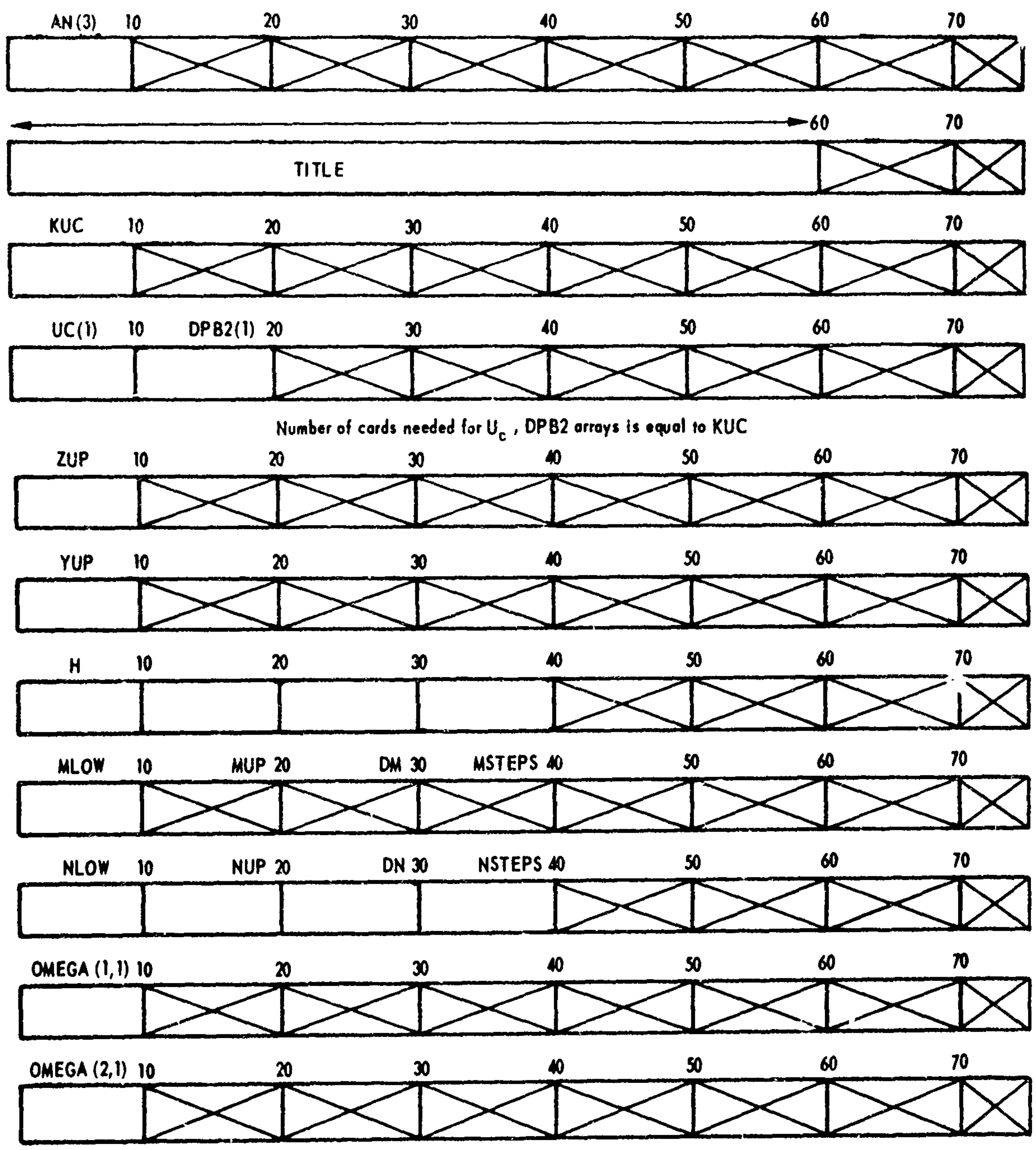

With the order of cards (1,1), (2,1), . . . , (M,1), (1,2), . . . , (M,2), . . . , (1,N), . . . , (m, N) to complete OMEGA (m,n) array.

TABLE 2A (Continued)

DAMP (1,1) 10 20 30 40 50 60 70

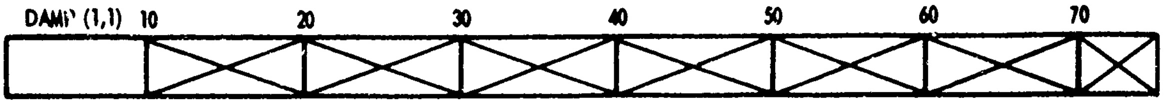

DAMP (2,1) 10 20 30 40 50 60 70

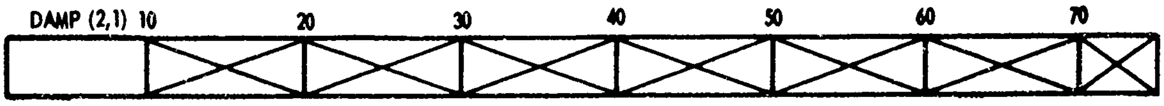

With the order of cards (1,1), (2,1), . . . (m,1), (1,2), . . . (m,2), . . . (1,n), . . . (m,n) to complete the DAMP (m,n) array.

NP 10 20 30 40 50 60 70

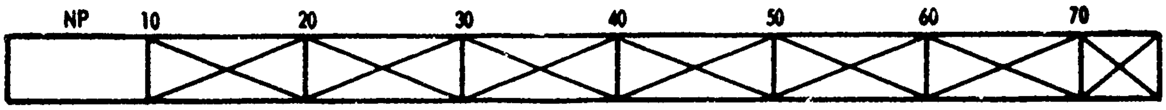

PARAM(1) 10 20 30 40 50 60 70

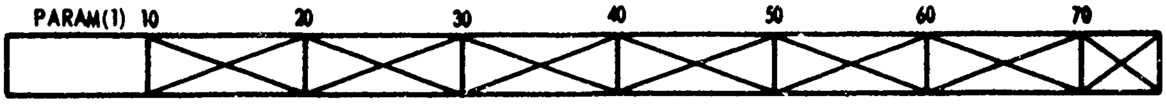

The number of cards needed to complete PARAM array is equal to NP.

TABLE 2B

Input Required for *Subprogram B* to Compute the Cross Spectral Density of Turbulence Pressures for the Semifrozen Convection (*Model A*) and Corresponding Output

(Units are given in foot-pound-seconds)

Data	Description	Type	Symbols Used in Program
Flow Characteristics			
θ	Eddy Lifetime	Decimal	THETA
ξ	$x - x'$ (Plate separation in x direction)	Decimal	SI
τ_w	Wall shear stress	Decimal	TW
ω	Frequency	Decimal	FR
δ^*	Boundary-layer displacement thickness	Decimal	DSTAR
K_1, K_2, K_3	Universal constants: $K_1 = 0.470$, $K_2 = 3.0$, $K_3 = 14.0$	Decimal	D
A_1, A_2, A_3	Universal constants: $A_1 = 1.6$ $A_2 = 7.2$, $A_3 = 12.0$	Decimal	A
U_c	Broadband convection velocity	Decimal	UC
Calculated Output in Foot-Pound-Seconds			
$R(\tau)$	Normalized autocorrelation of the pressure; see Equation (B8)	Decimal	RAUTO
$R(\xi,n,\tau)$	Normalized cross correlation of the pressure; see Equation (B9)	Decimal	RCROSS
$\dfrac{P(\omega)\ U}{\tau_w^2\ \delta^*}$	Dimensionless power spectrum of wall-pressure fluctuations; see Equation (B7)	Decimal	POW
$P(\omega)$	Power spectrum; see Equation (B7)	Decimal	PDW
$P(K_1,\omega)$	Normalized cross-power spectral density, using longitudinal space-time cross correlation of semifrozen model	Decimal	PKW
$P(\omega)$	Power spectrum, corresponding to $P(K_1,\omega)$	Decimal	PW

TABLE 2B (Continued)

AUTOCORRELATION	EQUATION (B8)
CROSS CORRELATION	EQUATION (B9)
POWER SPECTRUM	EQUATION (B7)
$P(K_1, \omega)$	FIGURE 9

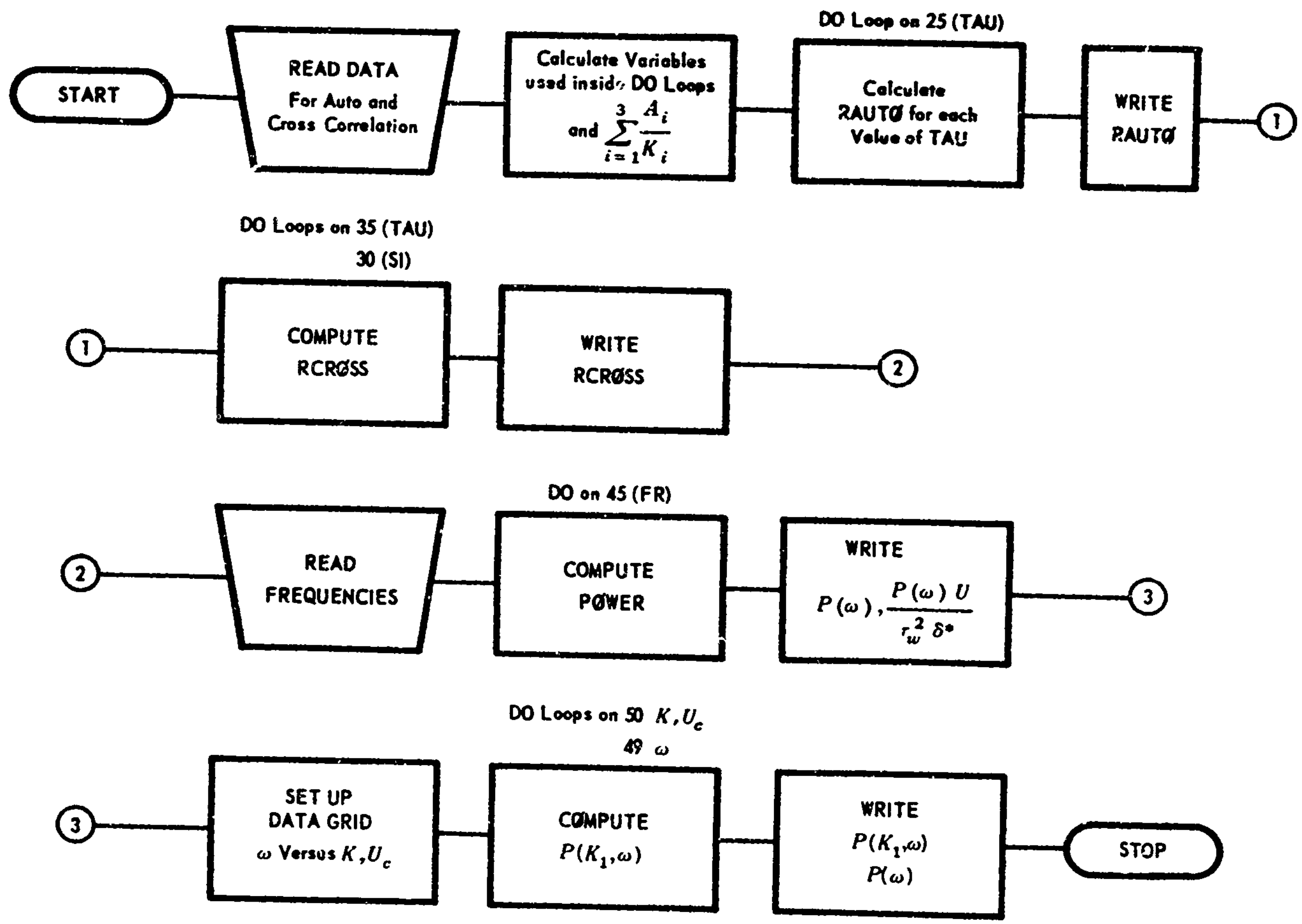

TABLE 2B (Continued)

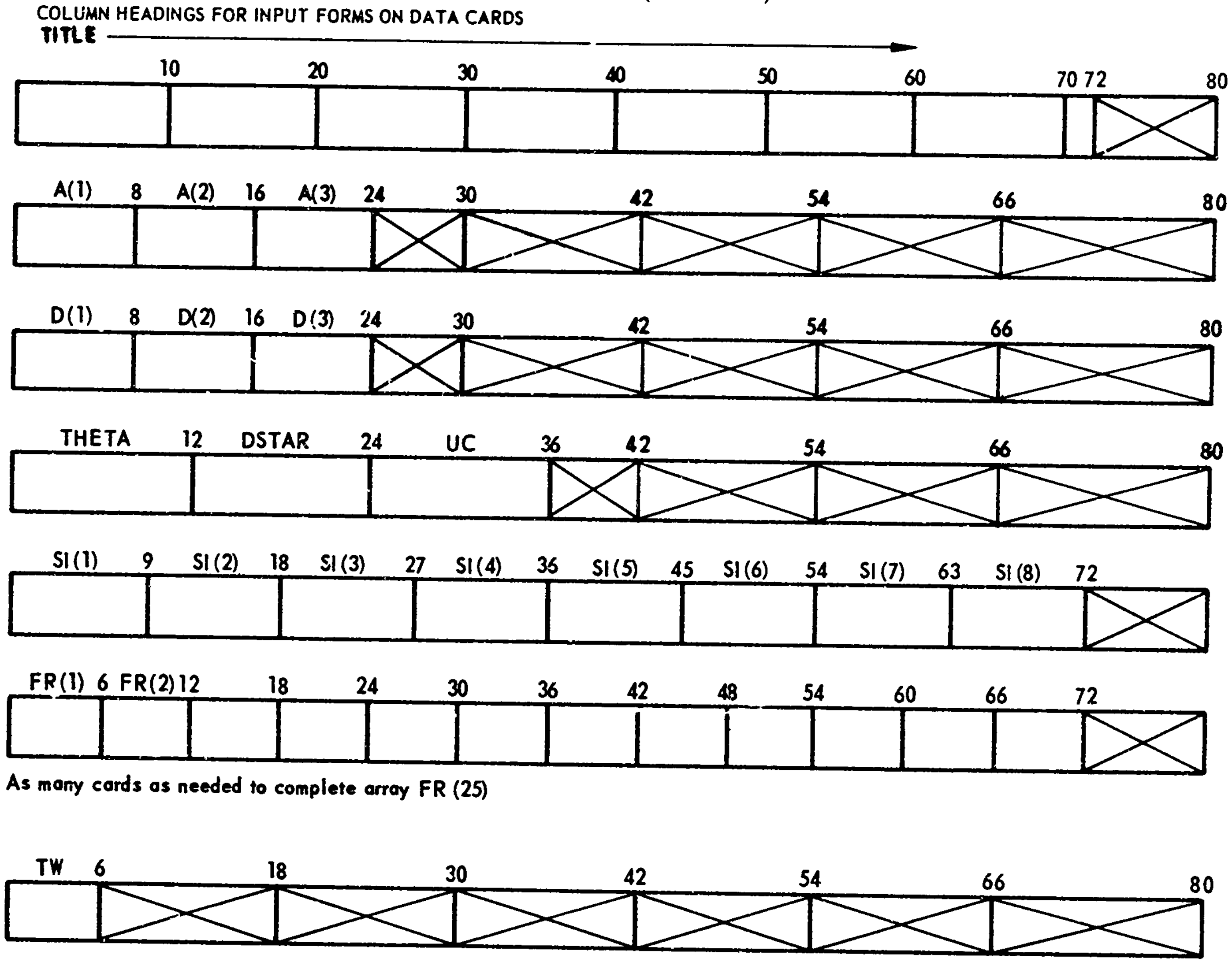

TABLE 2C

Input Required for Subprogram C to Compute Cross Density Displacement and Corresponding Output

(Units are given in foot-pound-seconds)

Symbol	Description	Program Symbol
Flow and Plate Characteristics and Additional Quantities		
ARG(I)	Gaussian quadrature	ARG(I)
WGT(I)	Weights and arguments; NW of them; in this problem 9 points	WGT(I)
NW	Number of points in Gaussian integration	NW
K A	Universal constants; NAK of each; in this case, 4 (supersonic)	AK(I) AN(I)
NAK	Number of A's and K's; 4 (supersonic)	NAK
TITLE	Alphanumeric title -- labels the output; User's choice of words	TITLE(I)
x	x Coordinate position on plate	X
x'	Second x coordinate: $\xi = x - x'$	XP
y	y Coordinate position on plate	Y
y'	Second y coordinate: $\eta = y - y'$	YP
a	Plate size – x direction	A
b	Plate size – y direction	B
U_e	Free-stream velocity	UE
M	Plate mass	FM
δ^*	Boundary layer displacement thickness	DEL
$\widetilde{p^2}$	Mean-square wall pressure fluctuation	PB2
U_c	Convection velocity	UC
θ	Eddy lifetime	TH
MLOW	First mode of interest for m	MLOW
MUP	Last mode of interest for m	MUP
DM	Increment between m modes	DM
NLOW	Same as described but for n modes	NLOW
NUP	Same as described but for n modes	NUP
DN	Same as described but for n modes	DN

TABLE 2C (Continued)

Symbol	Description	Program Symbol
$\left.\begin{matrix}\gamma_m \\ k_m \\ \gamma_n \\ k_n\end{matrix}\right\}$	Warburton $\left.\begin{matrix}\gamma \\ k\end{matrix}\right\}$ for $\theta\ (x)$ to define plates with fixed edges, for m,n modes, respectively.	$\left\{\begin{matrix}\text{GM} \\ \text{KM} \\ \text{GN} \\ \text{KN}\end{matrix}\right.$
ω_{mn}	Plate modal frequencies	WMN (M,N)
a_{mn}	Acoustical damping, obtained experimentally	FA (M,N)
Following Symbols Are Used Only in Program for $\omega \neq \omega_{mn}$		
WI	Lower limit of frequency to vary around a given ω_{mn}	WI
WF	Upper limit for $\omega \neq \omega_{mn}$	WF
DW	Increment size for intervals between WI and WF	DW
Calculated Output in Inch-Pound-Seconds		
$\dfrac{4}{a\,b\,m^2\,n^2\,\phi(x)\,\phi(x')\,\phi(y)\,\phi(y')}$	Plate shapes, by Warburton method	EIGEN (M,N)
$P(\omega)$	Power spectrum: $\sum_i \left(A_i\, e^{(-K_i \omega \delta^*/U_e)}\right) \dfrac{\overline{p^2}\,\delta^*}{U_e}$	POFW*
$Y(x,y\,;x',y',\omega)$	Equation 27 of Reference 21: cross spectral density, assuming panel modes well separated.	ANS*
	Equation 27 $\times\ \omega^4$	PWRSD*
	$(\text{AMN}^2 + (\omega_{mn} - \omega)^2)(\text{AMN}^2 + (\omega_{mn} + \omega)^2)$	DEN

*POFW, ANS PWRSD have real and imaginary parts printed out.

TABLE 2C (Continued)

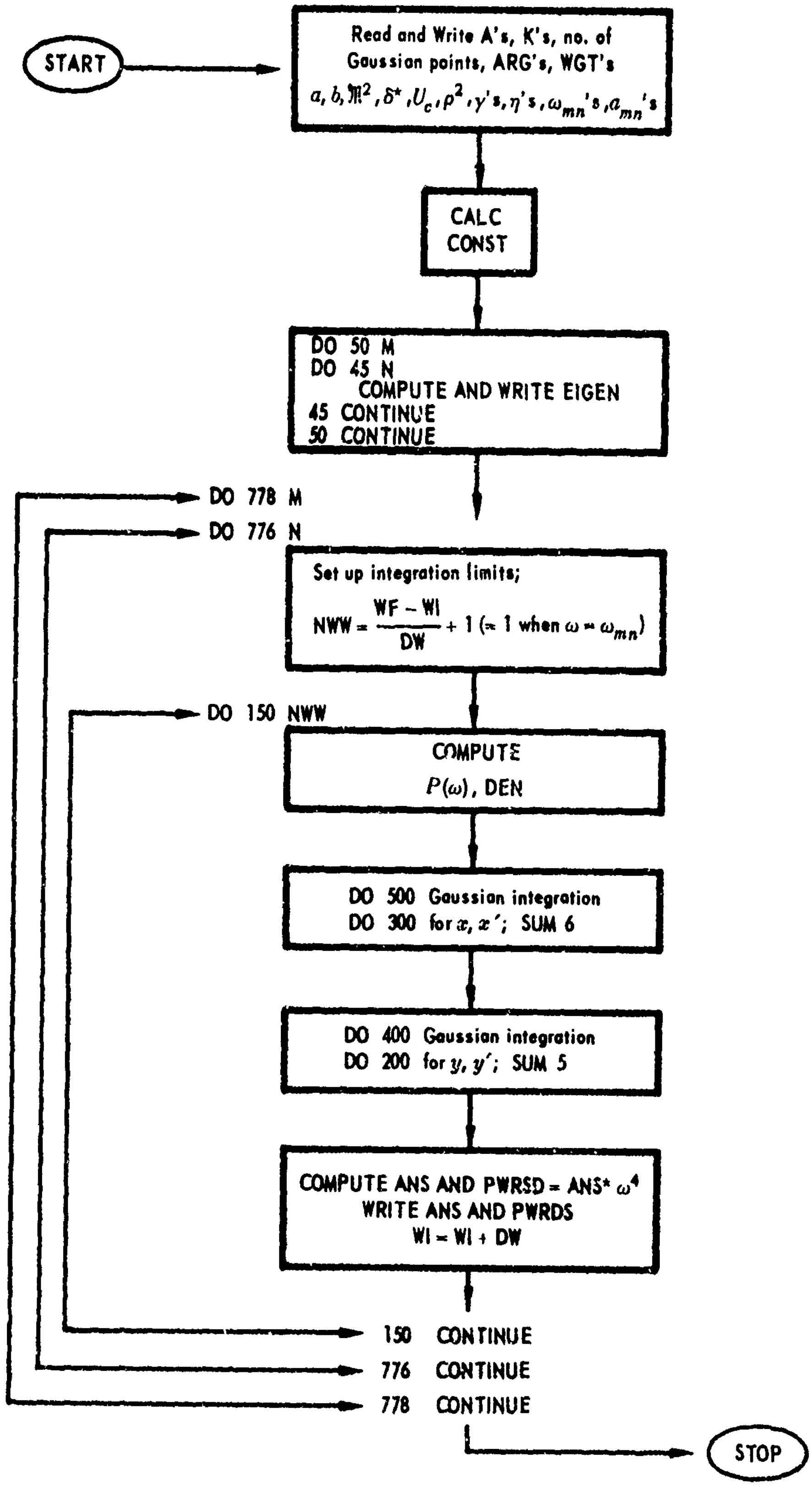

TABLE 2C (Continued)

Column Headings for Input Forms on Data Cards

5	10	30	50	60	80
NW	NAK				

20			80
ARG(1)			

And as many cards as needed to complete the ARG(NW) array (NW cards).

20						80
WGT(1)						

And as many cards as needed to complete the WGT(NW) array (NW cards).

	80
TITLE	(from column 1 through 80)

12	24	36	48	60	72	80
X	XP	Y	YP			

12	24	36	48	60	72	80
AK(1)	...	...	...	...	AK(NAK)	

12	24	36	48	60	72	80
AN(1)	...	...	...	...	AN(NAK)	

12	24	36	48	60	72	80
A	B	FM	UE	DEL	PB2	

12	24					80
UC	TH					

5	10	15	20	25	30				
MLOW	MUP	DM	NLOW	NUP	DN				

TABLE 2C (Continued)

12	24	36 / 48 / 60 / 72	80
GM(1)	GM(2)	. . . and as many cards (6 nos/card) to complete GM(MUP)	X

12	24	36 / 48 / 60 / 72	80
GN(1)	GN(2)	. . . and as many cards (6 nos/card) to complete GN(NUP)	X

12	24	36 / 48 / 60	72	80
KM(1)	KM(2)	. . . as many to complete KM(MUP) $\left(\frac{MUP}{6}\text{ cards}\right)$		X

12	24	36 / 48 / 60	72	80
KN(1)	KN(2)	as many to complete KN (NUP) $\left(\frac{NUP}{6}\text{ cards}\right)$		X

10	36	60	80
WMN(1,1)	X	X	X

10	36	60	80
WMN(2,1)	X	X	X

⋮

10	36	60	80
WMN(MUP)	X	X	X

10	36	60	80
WMN(MUP,1)	X	X	X

WMN(MUP,2), and so on, until MUP x NUP cards are used to complete WMN (MUP, NUP) array

10			
FA(1,1)	X	X	X

10			
FA(MUP, 1)	X	X	X

FA(1,2), and so on, in WMN array, i.e., use MUP x NUP to complete FA(MUP,NUP) array

For case $\omega \neq \omega_{mn}$ only: 1 card for each (M,N): (1,1), (1,2), . . . (1,N), (2,1), . . . so on

12	24	36		
WI	DW	WF	X	X

SUBPROGRAM D

Subprogram D represents a generalization of Subprogram C to include modal-cross coupling. Data descriptions of the subprograms are identical, except that Subprogram D requires a second set of modal input data. These data are:

TABLE 2D

Generalization of Subprogram C to Include Modal Cross Coupling

(Data descriptions of Subprograms C and D are identical except that Subprogram D requires a second set of modal input data as indicated below)

Symbol for Cross-Coupled Modes		Symbols for Uncoupled Modes*
PLOW	for p modes	MLOW
PUP	for p modes	MUP
DP	for p modes	DM
QLOW	for q modes	NLOW
QUP	for q modes	NUP
DQ	for q modes	DN
GP	for p modes	GM
GQ	for q modes	GN
KP	for p modes	KM
KQ	for q modes	KN
WPQ(P,Q)		WMN (M,N)
APQ(P,Q)		FA (M,N).

*Analogous to data in Subprogram C.

Note: The output will now include the additional eigenvalues EIGN (P,Q) for the (P,Q) modes. DENCOM is the denominator of Equation (26), Reference 22.

TABLE 2D (Continued)

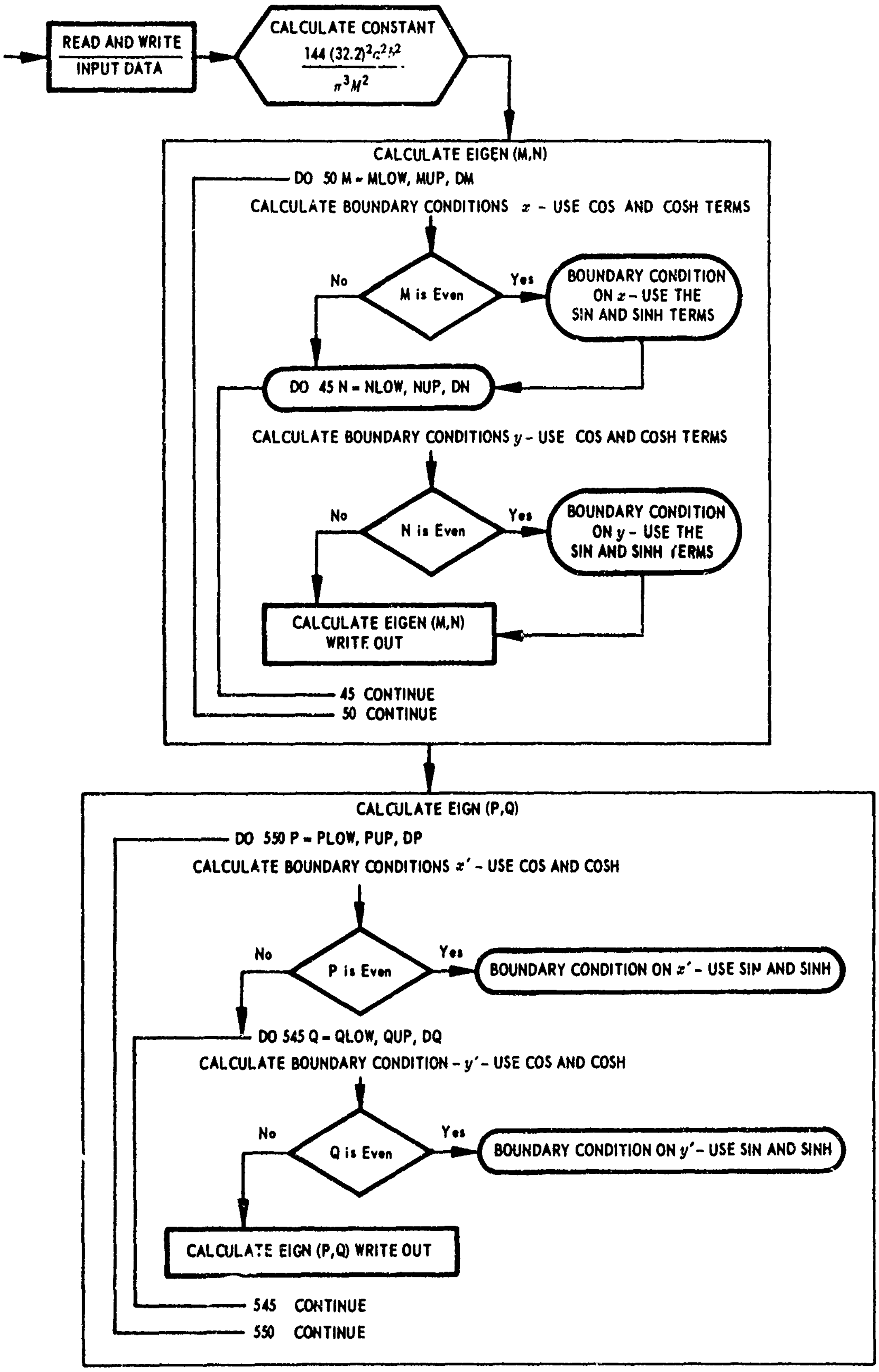

TABLE 2D (Continued)

DO 778 M = MLOW, MUP, DM

DO 7781 P = PLOW, PUP, DP

DO 776 N = NLOW, NUP, DN

DO 7761 Q = QLOW, QUP, DQ

READ $\omega_i, \Delta\omega, \omega_f$ → CALCULATE $n\omega, nx_0, nx_0^1, ny_0, ny_0^1, \omega^2, a^2$ → DO 150 MM1 = 1, NWW
Initialize answer to 0
Calculate DENCOM

$$\left[\frac{(a_{mn}+i\omega)\left[\omega_{mn}\omega_{pq}\left(\frac{a_{mn}+a_{pq}}{2}\right)\right]+\omega_{mn}\omega_{pq}\left\{\left(\frac{a_{mn}+a_{pq}}{2}\right)^2-\left[\left(\frac{\omega_{mn}}{2}\right)^2-\left(\frac{\omega_{pq}}{2}\right)^2\right]\right\}}{(a_{mn}+i\omega)^2+\omega_{mn}^2}\right.$$

$$\left.+\frac{(a_{pq}-i\omega)\left[\omega_{mn}\omega_{pq}\left[\left(\frac{a_{mn}+a_{pq}}{2}\right)\right]+\omega_{pq}\omega_{mn}\left(\frac{a_{mn}+a_{pq}}{2}\right)^2+\left(\frac{\omega_{mn}}{2}\right)^2-\left(\frac{\omega_{pq}}{2}\right)^2\right]}{(a_{pq}-i\omega)^2+\omega_{pq}^2}\right]$$

$$\Big/\ (mnpq)\,\omega_{mn}\omega_{pq}\left\{\left[\left(\frac{a_{mn}+a_{pq}}{2}\right)^2+\left(\frac{\omega_{mn}}{2}\right)^2+\left(\frac{\omega_{pq}}{2}\right)^2\right]^2-\frac{\omega_{mn}^2\omega_{Fi}^2}{4}\right\}$$

$$P(\omega)=\frac{\overline{P^2}\,\delta}{U_e}\sum_{k=1}^{4}A_k\,e^{\frac{-k\omega\delta}{U_e}}$$

TABLE 2D (Continued)

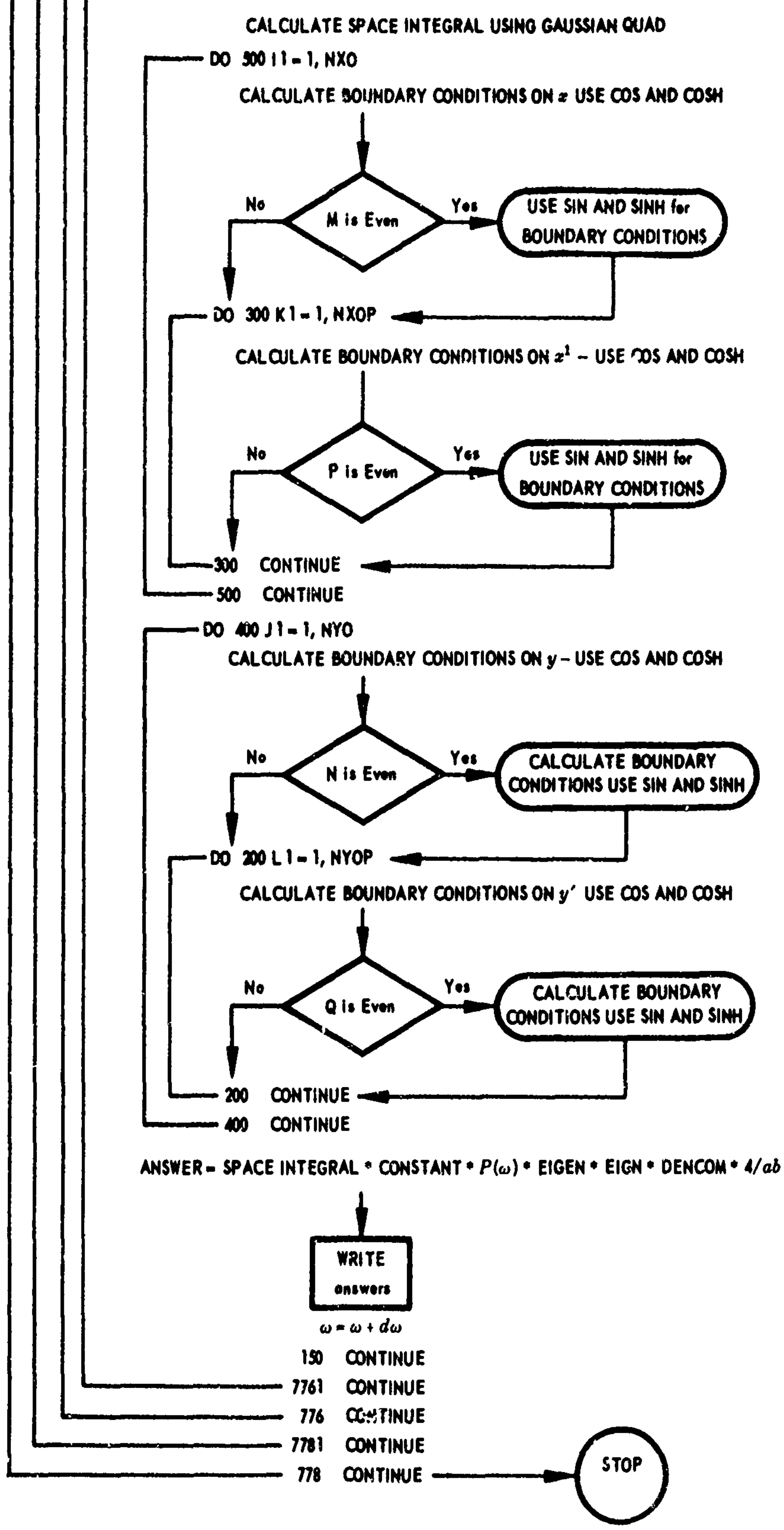

TABLE 2D (Continued)

Column Headings for Input Forms on Data Cards

5	10	30	50	60	80
NW	NAK				

20			80
ARG(1)			

And as many cards as needed to complete the ARG(NW) array (NW cards).

20					80
WGT(1)					

And as many cards as needed to complete the WGT(NW) array (NW cards).

	80
TITLE	(from column 1 through 80)

12	24	36	48	60	72	80
X	XP	Y	YP			

12	24	36	48	60	72	80
AK(1)	...	...	...	...	AK(NAK)	

12	24	36	48	60	72	80
AN(1)	...	...	...	...	AN(NAK)	

12	24	36	48	60	72	80
A	B	FM	UE	DEL	PB2	

12	24					80
UC	TH					

5	10	15	20	25	30				
MLOW	MUP	DM	NLOW	NUP	DN				

TABLE 2D (Continued)

5	10	15	20	25	30	80
PLOW	PUP	DP	QLOW	QUP	DQ	

12	24	36 – 72	80
GM(1)	GM(2)	GM(3) And so on, six numbers per card, to have MUP values of GM.	

12	24	36 – 72	80
GN(1)	GN(2)	And so on, six numbers per card, to have NUP values of GN.	

12	24	36 – 72	80
GQ(1)	GQ(2)	And so on, six numbers per card, to have QUP values of GQ.	

12	24	36 – 60	72	80
KM(1)	KM(2)	And so on, six numbers per card, for MUP values of KM.		

12	24	36 – 60	72	80
KP(1)	KP(2)	And so on, six numbers per card, for PUP values of KP.		

12	24	36 – 60	72	80
KN(1)	KN(2)	And so on, six numbers per card, for NUP values of KN		

12	24	36 – 60	72	80
KQ(1)	KQ(2)	And so on, six numbers per card, for QUP values of KQ.		

12	24	36 – 72	80
GP(1)	GP(2)	And so on, six numbers per card, to have PUP values of GP.	

10	80
WMN(1,1)	

⋮

10	80
WMN(MUP,1)	

⋮

10	80
WMN(1,2)	

TABLE 2D (Continued)

⋮

10			80
WMN(MUP,2)	And so on, one number per card, to have MUP x NUP values of WMN		

10			80
WPQ(1,1)	One number per card, from WPQ(1,1) to WPQ(PUP,1), WPQ(1,2) to WPQ(PUP,2).		

And so on, to WPQ(PUP,QUP), i.e., PUP x QUP cards.

10			80
FA(1,1)	One number per card, MUP x NUP cards. Cycle as for WMN.		

10			80
APQ(1,1)	One number per card, PUP x QUP cards. Cycle as for WPQ.		

12	24	36				80
WI	DW	WF				

One card for each cross mode of interest; cycling for (m, n, p, q).

APPENDIX B4 – TEST RUNS

Results obtained from the computer programs of Table 2 are indicated in Figures 7 – 10. Figures 7 and 8 are obtained from Subprogram A, Figure 9 from Subprogram B, and Figure 10 from Subprogram C. The figures show test runs for modal mean square displacement, turbulence pressure spectrum levels, and displacement spectral density.

TABLE 3

Computer Listings for Subprograms A, B, C, and D – Maestrello

Table 3A – Computer Listing for Subprogram A
(Semifrozen Convection – Model A)

```
$IBFTC TURAD
C       REORGANISED PROGRAM FOR COMPUTING TRIPLE
C       INTEGRAL
C       USING SIMPSONS RULE
        DIMENSION VOL(20,10)
        DIMENSION F3(3),ANS(3)
        DIMENSION IXYZ(10,1,50,3),IYZ(20,1),IY(1),
       1G2(401,20),G3(11,1),YY(11),TEMP1(11),G5(4000)
        DIMENSION PARAM(101),THETA(101)
        DIMENSION AK(3),AN(3),TITLE(20)
        DIMENSION OMEGA(20,10),DAMP(20,10)
        DIMENSION FA(20,10,3),FC(20,10,3),EIGEN(20,10,3),FUDGE(20,10,3)
        DIMENSION UC(20),DPB2(20)
        REAL IXYZ,IYZ,IY
        INTEGER DM,DN
        READ(5,13)   TAU
   13   FORMAT(F10.0)
        WRITE(6,801)  TAU
  801   FORMAT(1H1,/5H TAU=E15.6)
        READ(5,103) H,XO,YO,XOP,YOP,FUCSQ,PB2,FM2,AK,
       1AN,TITLE
  103   FORMAT(14(F10.0/),(10A6))
        WRITE(6,201)  TITLE
  201   FORMAT(20A6)
        WRITE(6,203) FUCSQ,PB2,FM2,AK,AN,XO,YO,
       1XOP,YOP
  203   FORMAT(14H0FUC SQUARED= E16.8,
       X 8H RHO-BAR 9H SQUARED=E16.8,
       1  11H M-SQUARED=E16.8/
       24H0K1=E16.8,4H K2=E16.8,4H K3=E16.8/
       34H A1=E16.6,4H A2=E16.8,4H A3=E16.8/
       44H XO=E16.8,4H YO=E16.8,5H XOP=E16.8,5H YOP=E16.8)
        READ(5,102) KUC,(UC(I),DPB2(I),I = 1,KUC)
  102   FORMAT(I10/(2F10.0))
        WRITE(6,204) (UC(I),DPB2(I),I = 1,KUC)
  204   FORMAT(1H07X2HUC13X4HDPB2/(1H 2E16.8))
   99   READ(5,1) ZUP,YUP,H,MLOW,MUP,DM,MSTEPS,NLOW,NUP,DN,NSTEPS
```

TABLE 3A (Continued)

```
1     FORMAT(3(F10.0/),(4I10))
      WRITE(6,2)MLOW,MUP,DM,MSTEPS,NLOW,NUP,DN,NSTEPS
2     FORMAT(9H0M  FROM I5,4H  TOI5,7H    DM=I5,
     112H  A TOTAL OF I5,7H  STEPS/9H N  FROM I5,
     24H  TOI5,7H    DN=I5,12H  A TOTAL OFI5,7H  STEPS)
      WRITE(6,202) ZUP,YUP,H
202   FORMAT(3H A=E16.8,5H   B=E16.8,5H   H=E16.8)
      READ(5,101) ((OMEGA(M,N),M=1,20),N=1,3)
 101  FORMAT(F10.0)
      WRITE(6,205)((OMEGA(M,N),M=MLOW,MUP,DM),
     1N=NLOW,NUP,DN)
205   FORMAT(7H0OMEGA=/(8E16.8))
      DO 7 N=1,NUP,DN
      DO 7 M=1,MUP,DM
7     DAMP(M,N)=.01
      READ(5,104) ((DAMP(M,N),M=1,20),N=1,3)
 104  FORMAT(F10.0)
      WRITE(6,206) ((DAMP(M,N),M=MLOW,MUP,DM),
     1N=NLOW,NUP,DN)
206   FORMAT(6H0DAMP=/(8E16.8))
      N1=8
      READ(5,207) NP,(PARAM(IP),IP = 1,NP)
 207  FORMAT(I10/(6F10.0))
      A=ZUP
      B=YUP
      B1=AK(1)**2*FUCSQ
      B2=AK(2)**2*FUCSQ
      B3=AK(3)**2*FUCSQ
      B4=AN(1)*AK(1)*FUCSQ
      B5=AN(2)*AK(2)*FUCSQ
      B6=AN(3)*AK(3)*FUCSQ
      B7=AN(1)/AK(1)
      B8=AN(2)/AK(2)
      B9=AN(3)/AK(3)
      C1=4.0/(A*B)
      C2=3.14159265
      C3=1./C2
```

TABLE 3A (Continued)

```
      C4=C2*C2
      C5=(A*B*PB2)/(2.0*C4*FM2*(B7+B8+B9))
      C5=C5*32.2*32.2*12.*12.
      C6=C4/(A*B)
      DO 10 M=MLOW,MUP,DM
      DO 10 N=NLOW,NUP,DN
      XM=M
      XN=N
      XO=A/2.
      YO=B/2.
      IF(M-M/2*2.NE.0)GO TO 43
      XO=A/2.-A/(XM*2.)
43    IF(N-N/2*2.NE.0)GO TO 44
      YO=B/2.-B/(XN*2.)
44    XOP=XO
      YOP=YO
      DAMP(M,N)=DAMP(M,N)/10.
      DO 45 L=1,3
      FA(M,N,L)=DAMP(M,N)/2.*OMEGA(M,N)
      FA(M,N,L)=FA(M,N,L)*0.5
      FC(M,N,L)=OMEGA(M,N)/FA(M,N,L)
      FUDGE(M,N,L)=XM*XN*OMEGA(M,N)*(FA(M,N,L)**2.0+OMEGA(M,N)**2.0)
      EIGEN(M,N,L)=C1/FUDGE(M,N,L)*SIN(XM*C2*XO/A)*SIN(XN*C2*YO/B)*
     1SIN(XM*C2*XOP/A)*SIN(XN*C2*YOP/B)
45    DAMP(M,N)=DAMP(M,N)*10.
10    CONTINUE
      WRITE(6,1003)
1003  FORMAT(33H0XO=XOP,YO=YOP,AND THEY VARY WITH
     117H THE MODE NUMBERS)
      DO 46 L=1,3
      WRITE(6,3)((EIGEN(M,N,L),M=MLOW,MUP,DM),N=NLOW,NUP,DN)
3     FORMAT(7H0EIGEN=/(8E16.8))
46    CONTINUE
      DO 47 L=1,3
      WRITE(6,48)((FA(M,N,L),M=MLOW,MUP,DM),N=NLOW,NUP,DN)
48    FORMAT(13H0A(M,N,DAMP)=/(8E16.8))
47    CONTINUE
```

TABLE 3A (Continued)

```
      CALL VOLUM(A,B,MLOW,MUP,DM,NLOW,NUP,DN,VOL)
      NUPM=NUP-1
      DO 777 KU=1,KUC
      CONST=C5*DPB2(KU)
      WRITE(6,303) UC(KU),CONST
303   FORMAT(4H UC=,E16.8,8H  CONST=,E16.8)
      DO 778 M=MLOW,MUP,DM
      XM=M
      DO 779 IP=1,NP
779   THETA(IP)=PARAM(IP)/XM/UC(KU)*A
      WRITE(6,780)  (THETA(IP),IP = 1,NP)
 780  FORMAT(7H THETA=/(7E16.8))
      IF(THETA(IT).GT.100.)  GO TO 999
      XLOW=0.
      DX=1./(20.*OMEGA(M,NUPM)/2./3.14159265)
      IUP=5./DX*THETA(NP)+1.
      IF(IUP.GT.3599) IUP= 3599
      IF(IUP-IUP/2*2) 501,500,501
500   IUP=IUP+1
501   IUP = IUP +400
 502  DX=(THETA(2)-THETA(1))/2.
      ZLOW=-A
      JUP=20*M+1
      ZJUP=JUP-1
      DZ=2.*A/ZJUP
      YLOW=0.
      KUP = 10* NUPM + 1
      YKUP=KUP-1
      DY=B/YKUP
      DO 11 I=1,IUP
      G5(I)=1.
      IF(I.EQ.401)GO TO 11
      IF(I.NE.1.AND.I.NE.IUP) GO TO 510
      GO TO 511
510   G5(I)=G5(I)*2.
511   IF(I-I/2*2.EQ.0) GO TO 513
      GO TO 11
513   G5(I)=G5(I)*2.
```

TABLE 3A (Continued)

```
11    CONTINUE
      Z=ZLOW
      DO 21 J=1,JUP
      XM=M
      D1=XM*C2*Z/A
      D2=COS(D1)
      G2(J,M)=D2+1./(XM*C2)*(SIN(ABS(D1))-ABS(D1)
     1*D2)
      IF(J.NE.1.AND.J.NE.JUP) GO TO 520
      GO TO 521
520   G2(J,M)=G2(J,M)*2.
 521  IF(J-J/2*2.EQ.0)GO TO 525
      GO TO 21
525   G2(J,M)=G2(M,M)*2.
21    Z=Z+DZ
      Y=YLOW
      DO 31 K=1,KUP
      DO 30 N=NLOW,NUP,DN
      XN=N
      D3=XN*C2*Y/B
      D4=COS(D3)
      G3(K,N)=D4+1./(XN*C2)*(SIN(D3)-D3*D4)
      IF(K.NE.1.AND.K.NE.KUP)  GO TO 530
      GO TO 531
530   G3(K,N)=G3(K,N)*2.
531   IF(K-K/2*2.EQ.0) GO TO 533
      GO TO 30
533   G3(K,N)=G3(K,N)*2.
30    CONTINUE
31    Y=Y+DY
      Y=YLOW
      DO 39 K=1,KUP
      YY(K)=Y*Y
39    Y=Y+DY
      DO 40 L1=1,3
      DO 40 N=NLOW,NUP,DN
      DO 40 IT=1,NP
```

TABLE 3A (Continued)

```
40    IXYZ(M,N,IT,L1)=0.
      KAPPA=0
      X=XLOW
      DO 160 I=1,IUP
      IF(TAU .EQ.0.0)  GO TO 630
      E1 = UC(KU)*(TAU-X)
      GO TO 632
630   E1 = UC(KU)*X
632   CONTINUE
      DO 50 N=NLOW,NUP,DN
50    IYZ(M,N)=0.
      Z=ZLOW
      DO 120 J=1,JUP
      E2=(Z-E1)*(Z-E1)
      E4=B1+E2
      E5=B2+E2
      E6=B3+E2
      DO 60 K=1,KUP
60    TEMP1(K)=B4/(E4+YY(K))+B5/(E5+YY(K))+B6/(E6+YY(K))
      DO 70 N=NLOW,NUP,DN
70    IY(N)=0.
      DO 90 K=1,KUP
      DO 90 N=NLOW,NUP,DN
90    IY(N)=IY(N)+G3(K,N)*TEMP1(K)
      DO 100 N=NLOW,NUP,DN
100   IY(N)=IY(N)*DY/3.
      DO 110 N=NLOW,NUP,DN
      TEMP=IY(N)
110   IYZ(M,N)=IYZ(M,N)+G2(J,M)*TEMP
120   Z=Z+DZ
      DO 130 N=NLOW,NUP,DN
130   IYZ(M,N)=IYZ(M,N)*DZ/3.
1001  CONTINUE
      DO 140 N=NLOW,NUP,DN
      TEMP=IYZ(M,N)
      XM=M
      XN=N
```

TABLE 3A (Continued)

```
      F1=XM*XN*C6
      F2=OMEGA(M,N)*ABS(X)
      DO 140 L1=1,3
      F3(L1)=FA(M,N,L1)*ABS(X)
      IF(F3(L1).GT.5.)GO TO 140
      F6=F1*EXP(-F3(L1))*(SIN(F2)+FC(M,N,L1)*COS(F2))
      DO 137 IT=1,NP
      IF(X.GT.5.*THETA(IT))GO TO 137
      IF(TAU.EQ.0.0) GO TO 634
      G6 = DEXP(-DABS((TAU-X)/THETA(IT)))
      GO TO 636
  634 G6=DEXP(-DABS(X/THETA(IT)))
 636  CONTINUE
      G1=2.*F6*G6*G5(I)
      IXYZ(M,N,IT,L1)=IXYZ(M,N,IT,L1)+G1*TEMP*DX/3.
 137  CONTINUE
 140  CONTINUE
      IF(KAPPA.NE.0)GO TO 160
      IF(I.NE.401)GO TO 160
      KAPPA=1
      DX=1./(20.*OMEGA(M,NUPM)/2./3.14159265)
      GO TO 1001
 160  X=X+DX
      DO 601 N=NLOW,NUP,DN
      IF(THETA(IT).GT.100.)  GO TO 999
      WRITE(6,141) M,N
 141  FORMAT(3H1M=I5,3H N=I5//45X6HI(M,N)38X,18HI(M,N)*EIGEN*CONST//
     12X5HTHETA4X11HOMEGA*THETA6X11HDAMP=1./10.5X7HDAMP=1.9X8HDAMP=10.
     28X11HDAMP=1./10.5X7HDAMP=1.9X8HDAMP=10.7X5HPARAM)
      DO 601 IT=1,NP
      DO 602 L2=1,3
 602  ANS(L2)=IXYZ(M,N,IT,L2)*EIGEN(M,N,L2)*CONST
      T=THETA(IT)*OMEGA(M,N)
      WRITE(6,142)THETA(IT),T,(IXYZ(M,N,IT,L2),L2=1,3),(ANS(L2),L2=1,3),
     1PARAM(IT)
  142 FORMAT(1X,F9.6,E14.6,6E16.8,2X,F10.5)
 601  CONTINUE
```

TABLE 3A (Continued)

```
 778  CONTINUE
 777  CONTINUE
  999 STOP
      END
$IBFTC VOLUME
      SUBROUTINE VOLUM(A,B,MLOW,MUP,DM,NLOW,NUP,DN,VOL)
      INTEGER DM,DN
      DIMENSION VOL(20,10)
      PI=3.14159265
      DO 10 N=NLOW,NUP,DN
      XN=N
      DO 10 M=MLOW,MUP,DM
      XM=M
      VOL(M,N)=0.
      IF(N-N/2*2.EQ.0)GO TO 10
      IF(M-M/2*2.EQ.0)GO TO 10
      GAMMAN=(2.*XN+1.)*PI/2.
      GAMMAM=(2.*XM+1.)*PI/2.
      XKN=SIN(GAMMAN/2.)/SINH(GAMMAN/2.)
      XKM=SIN(GAMMAM/2.)/SINH(GAMMAM/2.)
      VOL(M,N)=16.*A*B/GAMMAM/GAMMAN/(1.+XKM)*144.
     1/(1.+XKN)*SIN(GAMMAM/2.)*SIN(GAMMAN/2.)
 10   CONTINUE
      WRITE(6,20)((VOL(M,N),M=MLOW,MUP,DM),N=NLOW,NUP,DN)
 20   FORMAT(28H0VOLUME UNDER EIGENFUNCTION=//
     1(8E16.8))
      RETURN
      END
```

Table 3B — Computer Listings for Subprogram B
(Semifrozen Convection — Model A)

```
$IBFTC ACCROS
      DIMENSION RAUTO(100),RCROSS(8,100),POW(25),CAK(3)
      DIMENSION  RCRO(8,100),CROSS(8,100)
      DIMENSION  POW(25)
      DIMENSION SI(10),          TAU(100),FR(25),D(3),A(3),AD(3),ADD(3),DA
     X(3),XCORD(25),TITLE(12)
      DIMENSION P(2500)
      DIMENSION  SKNE(500),W(1000)
 1000 FORMAT(12A6)
 1001 FORMAT(3F8.4)
 1002 FORMAT(3F8.4)
 1003 FORMAT(3F12.6)
 1010 FORMAT(8F9.6)
 1012 FORMAT(12F6.0)
 1014 FORMAT(I4)
 1015 FORMAT(6F12.5)
 1016 FORMAT(F6.2)
 2000 FORMAT(1H1,12A6)
 2001 FORMAT(//7H A(1) = F8.4,8H A(2) = F8.4,8H A(3) = F8.4)
 2002 FORMAT(7H D(1) = F8.4,7H D(2) =F8.4,8H D(3) = F8.4)
 2003 FORMAT(8H THETA = F12.6,9H DSTAR = F12.6,8H   UC = F12.6)
 2004 FORMAT(8H1   TAU   ,17H AUTOCORRELATION /(F9.6,2X,F12.8))
 2007 FORMAT(1H1,2X,1HJ,3X,19H CROSS CORRELATION /(3X,I3,2X,8F8.4))
 2010 FORMAT(10X,3H SI/(8F9.6))
 2012 FORMAT(1X,10F6.0)
 2015 FORMAT(1H1,2X,10H K-WAVE NO,2X,10H 2PI*FREQ.,2X,10H K-WAVE NO,2X,
     110H 2PI*FREQ.,2X,10H K-WAVE NO,2X,10H 2PI*FREQ./ (1X,6F12.5)  )
 2016 FORMAT(//6H TW = F6.2)
 2020 FORMAT(1H1,4X,7H XCORD ,18X,5H PSD ,18X,7H POWER )
 2022 FORMAT(4X,F9.6,14X,F9.6,14X,F9.6)
 2030 FORMAT(//2X,3H  I,5X,9H POWER K ,9X,9H POWER W )
 2031 FORMAT(3X,3F12.6)
 2032 FORMAT(3X,I5,4X,F12.9,7X,F12.9)
 2041 FORMAT(I5,4E15.6)
C         LIST OF VARIABLES AND CONSTANTS
C       RAUTO = R(TAU)
C       RCROSS = R(SI,ETA,TAU)
```

TABLE 3B (Continued)

```
C      POW = P(W)U/(TAU**2*DELTA-STAR)
C       DSTAR = DELTA-STAR
C       D(I)  = K(I)
C       FR = FREQUENCY
        PI = 3.1415926
       READ(5,1000)     (TITLE(I),I=1,12)
       WRITE(6,2000) (TITLE(I),I=1,12)
       READ(5,1001)  (A(I),I=1,3)
       READ(5,1002)  (D(I), I=1,3)
       READ(5,1003)  THETA,DSTAR,UC
       WRITE(6,2001)  (A(I),I=1,3)
       WRITE(6,2002)  (D(I),I =1,3)
       WRITE(6,2003)  THETA,DSTAR,UC
       READ(5,1010)  (SI(I,,I=1,8)
       WRITE(6,2010)  (SI(I),I =1,8;
C        COMPUTE AUTOCORRELATION
C     SI = 0, ETA = 0
       AKC = 0.0
       DO 10  I=1,3
       CAK(I) = A(I)/D(I)
   10  AKC = AKC + CAK(I)
       U = UC/0.8
       F = DSTAR/U
       FDUC = (1./(F*UC))**2
       GO TO 400
       TAU(1) =0.0
       DO 25  J=1,100
       RAUT = 0.0
       DO 20  I =1,3
       ADD(I) = (A(I)*D(I))/(D(I)**2+(TAU(J)/F)**2)
   20  RAUT = ADD(I) + RAUT
       RAUTO(J) = RAUT/AKC
       TAU(J+1) = TAU(J) + 0.00001
   25  CONTINUE
       WRITE(6,2004)  (TAU(J),RAUTO(J),J=1,100)
C         COMPUTE CROSS CORRELATION
C      ETA = 0.0
```

```
      DO  16  I = 1, 8
  16   SI(I) = SI(I)/12.
      DO 35  J = 1,100
      DO 33  I = 1,8
      RCRO(I,J) = 0.0
      DO 30  IM = 1,3
      AD(IM) = (A(IM)*D(IM))/(D(IM)**2+FDUC*(SI(I)-UC*TAU(J))**2)
  30  RCRO(I,J) = RCRO(I,J)+AD(IM)
      CROSS(I,J) = RCRO(I,J)*EXP(-ABS(SI(I))/(UC*THETA))
      RCROSS(I,J) = CROSS(I,J)/AKC
      TAU(J+1) = TAU(J) + 0.00001
  33  CONTINUE
  35  CONTINUE
      WRITE(6,2007)  (J,(RCROSS(I,J),I=1,8),J=1,100)
COMMENT   FIG.2  EQTN. 4   SEMI-FRPZEN  CASE
C         COMPUTE POWER
 400  CONTINUE
      READ(5,1012) (FR(I),I=1,25)
      WRITE(6,2012)  (FR(I),I = 1,25)
      READ(5,1016)  TW
      WRITE(6,2016)  TW
      TW = TW**2
      WRITE(6,2020)
      DO 45  J = 1,25
      POW(J) =0.0
      DO 40  I = 1,3
      DA(I) = A(I)*EXP(-D(I)*6.2832*FR(J)*F)
      POW(J) = POW(J) + DA(I)
  40  CONTINUE
      XCORD(J)=(6.2832*FR(J)*DSTAR)/U
      PDW(J) = POW(J)*DSTAR*TW/U
  45  CONTINUE
      WRITE(6,2022)  (XCORD(J),POW(J),PDW(J),J =1,25)
      GO TO 500
COMMENT     COMPUTE P(K1,W)
COMMENT   SKNE IS WAVE NUMBER K-ONE
COMMENT    CORRESPONDS TO GRAPH IN MAESTRELLO, PAGE 415, FIG.5, FOR 2*PI
```

TABLE 3B (Continued)

```
C        *FR  VS P(K-ONE,2*PI*FR)
      WI = -48000.
      SKI = WI
      WF = 48000.
      SKF = WF
      DW = 2000.
      M = (WF-WI)/DW + 1.
      DSK = DW
      N = M
      SK = SKI
      DO 50 I = 1,M
      SKNE(I) = SK
      WW = WI
      DO 49  K = 1,N
      W(K) = WW
      FAC = (THETA*F*UC)/((1.+THETA*THETA*(W(K)+SKNE(I))**2)*2.*PI)
      ARF = 0.0
      DO 55 J = 1,3
      FAR = A(J)*EXP(-ABS(W(K))*D(J)*F)
      ARF = ARF + FAR
   55 CONTINUE
      PKW = FAC*ARF/AKC
      PW = PKW*PI*(1.+THETA*THETA*(W(K)+SKNE(I))**2/THETA)
      WRITE(6,2041)  I,PKW,PW,W(K),SKNE(I)
      WW = WW + DW
   49 CONTINUE
      SK = SK + DSK
   50 CONTINUE
  500 CONTINUE
      STOP
      END
```

Table 3C – Computer Listings for Subprogram C

(Semifrozen Convection – Model A)

```
COMMENT  REMOVE CARD 1030...READ(5,3*)WI,DW,WF   ... FOR CASE W = WMN
COMMENT  NO IBFTC CARD FOR RUN AT APL
COMMENT  NOW RUNNING AT APL ON IBM 360/91
C     MULTIPLE INTEGRAL PROGRAM NO.     FOR LM BY FG
C     USES GAUSSIAN QUADRATURFON FOUR INTEGRALS
C     GENERAL CASE WITH NO COUPLING
C     ANSWER IS IN INCHES SQUARED PER SEC.
C
      IMPLICIT REAL*8(A-H,O-Z)
      INTEGER DM,DN
      REAL KN,KM
      COMPLEX *16 ARGCOM,E2,FV4,SUM4,FV5,SUM5,FV6,SUM6,ANS,ANSINT,PWRSD
      DIMENSION GM(20),GN(10),KN(10),KM(20)
      DIMENSION TITLE(20),AK(4),AN(4),WMN(20,10),FA(20,10),FC(20,10),
     1EIGEN(20,10),WGT(21),ARG(21)
C     READ AND WRITE INPUT DATA
C     NO. OF GAUSSIAN POINTS AND NO OF TERMS IN SUM OF A AND K
      READ(5,9)NW,NAK
      READ(5,33)(ARG(I),I=1,NW)
      READ(5,33)(WGT(I),I=1,NW)
   33 FORMAT(D20.8)
      PI=3.14159265358979323
      PI2=2.*PI
      PI3=PI**3
      READ(5,1)(TITLE(I),I=1,20)
    1 FORMAT(20A4)
      WRITE(6,2)(TITLE(I),I=1,20)
    2 FORMAT(1H1,20A4)
      READ(5,3)X,XP,Y,YP
      READ(5,3)(AK(I),I=1,NAK)
      READ(5,3)(AN(I),I=1,NAK)
      READ(5,3)A,B,FM,UE,DEL,PB2
    3 FORMAT(6F12.6)
      FM2=FM*FM
      READ(5,3)UC,TH
      ALPH1=.02*750./DEL
      ALPH2=3.8/DEL
```

```
      TH=1./(ALPH1*UC*DEL)
      WRITE(6,7)A,B,FM2,UE,DEL,PB2,UC,TH
    7 FORMAT(3H0A=F10.4,5H    B=F10.4,15H  MASS AQUARED= E15.6,
     111H    U SUB E= E15.6/5H DEL=E15.6,17H    P BAR SQUARED= E15.6,
     26H    UC=E15.6,4H TH=E15.6/)
      READ(5,9)MLOW,MUP,DM,NLOW,NUP,DN
    9 FORMAT(16I5)
      READ(5,3)(GM(M),M=1,MUP)
      READ(5,3)(GN(N),N=1,NUP)
      READ(5,3)(KM(M),M=1,MUP)
      READ(5,3)(KN(N),N=1,NUP)
      DO 2000 M=1,MUP
 2000 GM(M)=GM(M)*PI
      DO 2001 N=1,NUP
 2001 GN(N)=GN(N)*PI
      READ(5,12)((WMN(M,N),M=1,MUP),N=1,NUP)
   12 FORMAT(F10.2)
      WRITE(6,13)((WMN(M,N),M=MLOW,MUP,DM),N=NLOW,NUP,DN)
   13 FORMAT(7H0OMEGA=/(1X,8D14.5))
      READ(5,12)((FA(M,N),M=1,MUP),N=1,NUP)
      WRITE(6,18)((FA(M,N),M=1,MUP),N=1,NUP)
   18 FORMAT(8H0A(M,N)= /(8E14.6))
      C1=4./(A*B)
   17 FORMAT(7H CONST= E15.6)
      CONST=144.*32.2*32.2*4.*A*A*B*B/(PI3*FM2)
      WRITE(6,17)CONST
      DO 50 M=MLOW,MUP,DM
      XM=M
      XMPI=XM*PI
      GMXA2=GM(M)*(X/A-.5)
      GMXPA2=GM(M)*(XP/A-.5)
      SXMC2A=DCOS(GMXA2)+KM(M)*DCOSH(GMXA2)
      IF(M-M/2*2.EQ.0)SXMC2A=DSIN(GMXA2)+KM(M)*DSINH(GMXA2)
      SXOPCA=DCOS(GMXPA2)+KM(M)*DCOSH(GMXPA2)
      IF(M-M/2*2.EQ.0)SXOPCA=DSIN(GMXPA2)+KM(M)*DSINH(GMXPA2)
      SINXXP=SXMC2A*SXOPCA
      DO 45 N=NLOW,NUP,DN
```

TABLE 3C (Continued)

```
      XN=N
      XNPI=XN*PI
      OGA=WMN(M,N)
      FC(M,N)=OGA/FA(M,N)
      FUDGE=XM*XM*XN*XN
      GNYB2=GN(N)*(Y/B-.5)
      GNYPB2=GN(N)*(YP/B-.5)
      EIGEN(M,N)=C1/FUDGE*SINXXP*(DCOS(GNYB2)+KN(N)*DCOSH(GNYB2))*
     1(DCOS(GNYPB2)+KN(N)*DCOSH(GNYPB2))
      IF(N-N/2*2.EQ.0)EIGEN(M,N)=C1/FUDGE*SINXXP*
     1(DSIN(GNYB2)+KN(N)*DSINH(GNYB2))*(DSIN(GNYPB2)+KN(N)*DSINH
     2(GNYPB2))
      WRITE(6,16)X,Y,M,N,EIGEN(M,N),FA(M,N)
16    FORMAT(1H02F12.6,2I4,6E13.6)
45    CONTINUE
50    CONTINUE
      WRITE(6,19)
19    FORMAT(1H1,3X,1HM,3X,1HN,14X,1HW,11X,4HPOFW,12X,3HWMN,12X,3HDEN,
     1/18X,8HANSINT R, 7X,8HANSINT I,10X,5HANS R,10X,5HANS I,8X,7HPWRSD
     2R,8X,7HPWRSD I /)
      UCTH=UC*TH
      DO 776 M=MLOW,MUP,DM
      XM=M
      XMPI=XM*PI
      AMPI=A/(XMPI*UCTH)
      DO 776 N=NLOW,NUP,DN
      XN=N
      XNPI=XN*PI
      BNPI=B/(XNPI*UCTH)
      READ(5,3)WI,DW,WF
      NWW=(WF-WI)/DW+1.
      NXO=NW*M
      NYO=NW*N
      NXOP=NW*M
      NYOP=NW*N
      OGA=WMN(M,N)
      OGA2=OGA*OGA
```

TABLE 3C (Continued)

```
      FAL1=FA(M,N)
      FAL12=FAL1*FAL1
      W=WI
      DO 150 MM1=1,NWW
      ANSINT=0.
      W2=W*W
      DEN=(FAL12+(OGA-W)**2)*(FAL12+(OGA+W)**2)
      SUMAK=0.
      DO 120 IS=1,NAK
  120 SUMAK=SUMAK+AN(IS)*DEXP(-AK(IS)*W*DEL/UE)
      POFW=SUMAK*PB2*DEL/UE
      SUM6=0.
      DO 500 I1=1,NXO
      I1Q=(I1-1)/NW
      I1R=I1-NW*I1Q
      XO=PI*(.5+.5*ARG(I1R)+FLOAT(I1Q))
      XOA=GM(M)*(XO/XMPI-.5)
      SFXO=DCOS(XOA)+KM(M)*DCOSH(XOA)
      IF(M-M/2*2.EQ.0)SFXO=DSIN(XOA)+KM(M)*DSINH(XOA)
      SUM4=0.
      DO 300 K1=1,NXOP
      K1 Q=(K1-1)/NW
      K1R=K1-NW*K1Q
      XOP=PI*(.5+.5*ARG(K1R)+FLOAT(K1Q))
      XOXOP=XO-XOP
      E1=DEXP(-A/XMPI*ALPH1*DABS(XOXOP))
      ARGCOM=DCMPLX(0.D0,-W*A/(UC*XMPI)*XOXOP)
      E2=CDEXP(ARGCOM)
      XOPA=GM(M)*(XOP/XMPI-.5)
      SFXOP=DCOS(XOPA)+KM(M)*DCOSH(XOPA)
      IF(M-M/2*2.EQ.0)SFXOP=DSIN(XOPA)+KM(M)*DSINH(XOPA)
      FV4=      SFXOP*E1*E2
      SUM4=SUM4+FV4*WGT(K1R)*PI/2.
  300 CONTINUE
      FV6=SUM4*SFXO
      SUM6=SUM6+FV6*WGT(I1R)*PI/2.
  500 CONTINUE
```

```
      SUM5=0.
      DO 400 J1=1,NYO
      J1Q=(J1-1)/NW
      J1R=J1-NW*J1Q
      YO=PI*(.5+.5*ARG(J1R)+FLOAT(J1Q))
      YOB=GN(N)*(YO/XNPI-.5)
      SFYO=DCOS(YOB)+KN(N)*DCOSH(YOB)
      IF(N-N/2*2.EQ.0)SFYO=DSIN(YOB)+KN(N)*DSINH(YOB)
      SUM3=0.
      DO 200 L1=1,NYOP
      L1Q=(L1-1)/NW
      L1R=L1-NW*L1Q
      YOP=PI*(.5+.5*ARG(L1R)+FLOAT(L1Q))
      YOYOP=YO-YOP
      BNPI=B/(XNPI*UCTH)
      E3=DEXP(-B/XNPI*ALPH2*DABS(YOYOP))
      YOPB=GN(N)*(YOP/XNPI-.5)
      SFYOP=DCOS(YOPB)+KN(N)*DCOSH(YOPB)
      IF(N-N/2*2.EQ.0)SFYOP=DSIN(YOPB)+KN(N)*DSINH(YOPB)
      FV3=SFYOP*E3
      SUM3=SUM3+FV3*WGT(L1R)*PI/2.
  200 CONTINUE
      FV5=SUM3*SFYO
      SUM5=SUM5+FV5*WGT(J1R)*PI/2.
  400 CONTINUE
      ANSINT=SUM6*SUM5
      ANS=ANSINT*CONST*POFW*EIGEN(M,N)/DEN   *C1
      PWRSD=ANS*W**4
      WRITE(6,20)M,N,W,POFW,EIGEN(M,N),DEN
   20 FORMAT(1X,2I4,6E15.6)
      WRITE(6,21)ANSINT,ANS,PWRSD
   21 FORMAT(11X,6E15.6/)
      W=W+DW
  150 CONTINUE
  776 CONTINUE
  778 CONTINUE
      STOP
      END
```

Table 3D – Computer Listings for Subprogram D
(Semifrozen Convection – Model A)

```
C      MULTIPLE INTEGRAL PROGRAM NO.    FOR LM BY FG
C      USES GAUSSIAN QUADRATUREON FOUR INTEGRALS
COMMENT  GENERAL CASE  WMN AND WPQ
C      ANSWER IS IN INCHES SQUARED PER SEC.
C
       IMPLICIT REAL*8(A-H,O-Z)
       INTEGER QLOW,QUP,DQ,PLOW,PUP,DP,P,Q
       INTEGER DM,DN
       REAL KP,KQ
       REAL KN,KM
       COMPLEX*16 DENCOM
       COMPLEX * 16 COM1,COM2,XNMRTR
       COMPLEX *16 ARGCOM,E2,FV4,SUM4,FV5,SUM5,FV6,SUM6,ANS,ANSINT,PWRSD
       DIMENSION EIGN(20,10)
       DIMENSION. APQ(20,10),WPQ(20,10),GP(20),GQ(10),KP(20),KQ(10)
       DIMENSION GM(20),GN(10),KN(10),KM(20)
       DIMENSION TITLE(20),AK(4),AN(4),WMN(20,10),FA(20,10),FC(20,10),
      1EIGEN(20,10),WGT(21),ARG(21)
C      READ AND WRITE INPUT DATA
C      NO. OF GAUSSIAN POINTS AND NO OF TERMS IN SUM OF A AND K
       READ(5,9)NW,NAK
       READ(5,33)(ARG(I),I=1,NW)
       READ(5,33)(WGT(I),I=1,NW)
    33 FORMAT(D20.8)
       PI=3.14159265358979323
       PI2=2.*PI
       PI3=PI**3
       READ(5,1)(TITLE(I),I=1,20)
     1 FORMAT(20A4)
       WRITE(6,2)(TITLE(I),I=1,20)
     2 FORMAT(1H1,20A4)
       READ(5,3)X,XP,Y,YP
       READ(5,3)(AK(I),I=1,NAK)
       READ(5,3)(AN(I),I=1,NAK)
       READ(5,3)A,B,FM,UE,DEL,PB2
     3 FORMAT(6F12.6)
       FM2=FM*FM
```

TABLE 3D (Continued)

```
      READ(5,3)UC,TH
      ALPH1=.02*750./DEL
      ALPH2=3.8/DEL
      TH=1./(ALPH1*UC*DEL)
      WRITE(6,7)A,B,FM2,UE,DEL,PB2,UC,TH
    7 FORMAT(3H0A=F10.4,5H   B=F10.4,15H  MASS AQUARED= E15.6,
     111H   U SUB E= E15.6/5H DEL=E15.6,17H    P BAR SQUARED= E15.6,
     26H   UC=E15.6,4H TH=E15.6/)
      READ(5,9)MLOW,MUP,DM,NLOW,NUP,DN
      READ(5,9)PLOW,PUP,DP,QLOW,QUP,DQ
    9 FORMAT(16I5)
      READ(5,3)(GM(M),M=1,MUP)
      READ(5,3)(GP(P),P=1,PUP)
      READ(5,3)(GN(N),N=1,NUP)
      READ(5,3)(GQ(Q),Q=1,QUP)
      READ(5,3)(KM(M),M=1,MUP)
      READ(5,3)(KP(P),P=1,PUP)
      READ(5,3)(KN(N),N=1,NUP)
      READ(5,3)(KQ(Q),Q=1,QUP)
      DO 2000 M=1,MUP
 2000 GM(M)=GM(M)*PI
      DO 2001 N=1,NUP
 2001 GN(N)=GN(N)*PI
      DO 2002 P=1,PUP
 2002 GP(P)=GP(P)*PI
      DO 2003 Q=1,QUP
 2003 GQ(Q)=GQ(Q)*PI
      READ(5,12)((WMN(M,N),M=1,MUP),N=1,NUP)
      READ(5,12)((WPQ(P,Q),P=1,PUP),Q=1,QUP)
   12 FORMAT(F10.2)
      WRITE(6,13)((WMN(M,N),M=MLOW,MUP,DM),N=NLOW,NUP,DN)
   13 FORMAT(12H0OMEGA(M,N)= /(1X,8D14.5))
      WRITE(6,23)((WPQ(P,Q),P=PLOW,PUP,DP),Q=QLOW,QUP,DQ)
   23 FORMAT(12H0OMEGA(P,Q)= /(1X,8D14.5))
      READ(5,12)((FA(M,N),M=1,MUP),N=1,NUP)
      WRITE(6,18)((FA(M,N),M=1,MUP),N=1,NUP)
   18 FORMAT(8H0A(M,N)= /(8E14.6))
```

```
      READ(5,12)((APQ(P,Q),P=1,PUP),Q=1,QUP)
      WRITE(6,18)((FA(M,N),M=MLOW,MUP,DM),N=NLOW,NUP,DN)
      WRITE(6,28)((APQ(P,Q),P=PLOW,PUP,DP),Q=QLOW,QUP,DP)
   28 FORMAT(8H0A(P,Q)= /(1X,8E14.6))
      C1=2./DSQRT(A*B)
   17 FORMAT(7H CONST= E15.6)
      CONST=144.*32.2*32.2    *A*A*B*B/(PI3*FM2)
      WRITE(6,17)CONST
      DO 50 M=MLOW,MUP,DM
      XM=M
      XMPI=XM*PI
      GMXA2=GM(M)*(X/A-.5)
      SXMC2A=DCOS(GMXA2)+KM(M)*DCOSH(GMXA2)
      IF(M-M/2*2.EQ.0)SXMC2A=DSIN(GMXA2)+KM(M)*DSINH(GMXA2)
      DO 45 N=NLOW,NUP,DN
      XN=N
      XNPI=XN*PI
      OGA=WMN(M,N)
      FC(M,N)=OGA/FA(M,N)
      GNYB2=GN(N)*(Y/B-.5)
      FUDGE=XM*XN
      EIGEN(M,N)=C1/FUDGE*SXMC2A*(DCOS(GNYB2)+KN(N)*DCOSH(GNYB2))
      IF(N-N/2*2.EQ.0)EIGEN(M,N)=C1/FUDGE*SXMC2A*
     1(DSIN(GNYB2)+KN(N)*DSINH(GNYB2))
      WRITE(6,16)X,Y,M,N,EIGEN(M,N),FA(M,N)
   16 FORMAT(1H02F12.6,2I4,6E13.6)
   45 CONTINUE
   50 CONTINUE
      DO 550 P=PLOW,PUP,DP
      XXP=P
      XPPI=XXP*PI
      GMXPA2=GP(P)*(XP/A-.5)
      SXOPCA=DCOS(GMXPA2)+KP(P)*DCOSH(GMXPA2)
      IF(P-P/2*2.EQ.0)SXOPCA=DSIN(GMXPA2)+KP(P)*DSINH(GMXPA2)
      DO 545 Q=QLOW,QUP,DQ
      XQ=Q
      XQPI=XQ*PI
```

```
      OGP=WPQ(P,Q)
      OGP2=OGP*OGP
      FUDGE=XXP*XQ
      GNYPB2=GQ(Q)*(YP/B-.5)
      EIGN(P,Q)=C1/FUDGE*SXOPCA*(DCOS(GNYPB2)+KQ(Q)*DCOSH(GNYPB2))
      IF(Q-Q/2*2.EQ.0)EIGN(P,Q)=C1/FUDGE*SXOPCA*(DSIN(GNYPB2)+KQ(Q)*DSIN
     1H(GNYPB2))
      RITE(6,26)XP,YP,P,Q,EIGN(P,Q),APQ(P,Q)
   26 FORMAT(1H 2F12.6,2I4,6E13.6)
  545 CONTINUE
  550 CONTINUE
      WRITE(6,19)
   19 FORMAT(1H1,3X,1HM,3X,1HN,14X,1HW,11X,4HPOFW,12X,3HWMN,12X,3HDEN,
     1/18X,8HANSINT R, 7X,8HANSINT I,10X,5HANS R,10X,5HANS I,8X,7HPWRSD
     2R,8X,7HPWRSD I /)
      UCTH=UC*TH
      DO 778 M=MLOW,MUP,DM
      XM=M
      XMPI=XM*PI
      AMPI=A/(XMPI*UCTH)
      DO 7781 P=PLOW,PUP,DP
      XXP=P
      XPPI=XXP*PI
      DO 776 N=NLOW,NUP,DN
      XN=N
      XNPI=XN*PI
      BNPI=B/(XNPI*UCTH)
      DO 7761 Q=QLOW,QUP,DQ
      XQ=Q
      XQPI=XQ*PI
      READ(5,3)WI,DW,WF
      NWW=(WF-WI)/DW+1.
      MXO=NW*M
      NYO=NW*N
      NXOP=NW*P
      NYOP=NW*Q
      OGA=WMN(M,N)
```

TABLE 3D (Continued)

```
      OGA2=OGA*OGA
      FAL1=FA(M,N)
      FAL12=FAL1*FAL1
      OGP=WPQ(P,Q)
      OGP2=OGP*OGP
      FAL2=APQ(P,Q)
      FAL22=FAL2*FAL2
      W=WI
      DO 150 MM1=1,NWW
      ANSINT=0.
      W2=W*W
      DEN=((((FAL1+FAL2)/2.)**2+OGA2/4.+OGP2/4.)**2
     1-CGA2*OGP2/4.)*OGA*OGP
      COM1=FAL1+DCMPLX(0.D0,W)
      COM2=FAL2-DCMPLX(0.D0,W)
      FALL12=(FAL1+FAL2)/2.
      XNMRTR=(COM1*(OGA*OGP*FALL12)+OGA*OGP*(FALL12*FALL12-
     1(OGA2/4.        -OGP2/4.)  ))/(COM1*COM1+OGA2)+(COM2*
     2(OGA*OGP*FALL12)+OGA*OGP*(FALL12*FALL12+OGA2/4.-OGP2/4.))/(COM2*CO
     3M2+OGP2)
      DENCOM=XNMRTR/DEN
      SUMAK=0.
      DO 120 IS=1,NAK
  120 SUMAK=SUMAK+AN(IS)*DEXP(-AK(IS)*W*DEL/UE)
      POFW=SUMAK*PB2*DEL/UE
      SUM6=0.
      DO 500 I1=1,NXO
      I1Q=(I1-1)/NW
      I1R=I1-NW*I1Q
      XO=PI*(.5+.5*ARG(I1R)+FLOAT(I1Q))
      XOA=GM(M)*(XO/XMPI-.5)
      SFXO=DCOS(XOA)+KM(M)*DCOSH(XOA)
      IF(M-M/2*2.EQ.0)SFXO=DSIN(XOA)+KM(M)*DSINH(XOA)
      SUM4=0.
      DO 300 K1=1,NXOP
      K1Q=(K1-1)/NW
      K1R=K1-NW*K1Q
```

TABLE 3D (Continued)

```
      XOP=PI*(.5+.5*ARG(K1R)+FLOAT(K1Q))
      XOXOP=XO-XOP
      E1=DEXP(-A/ PI*ALPH1 *DABS(XO/XM-XOP/XXP))
      ARGCOM=DCMPLX(0.D0,-W*A/(UC*PI)*(XO/XM-XOP/XXP))
      E2=CDEXP(ARGCOM)
      XOPA=GP(P)*(XOP/XPPI-.5)
      SFXOP=DCOS(XOPA)+KP(P)*DCOSH(XOPA)
      IF(P-P/2*2.EQ.0)SFXOP=DSIN(XOPA)+KP(P)*DSINH(XOPA)
      FV4=      SFXOP*E1*E2
      SUM4=SUM4+FV4*WGT(K1R)*PI/2.
  300 CONTINUE
      FV6=SUM4*SFXO
      SUM6=SUM6+FV6*WGT(I1R)*PI/2.
  500 CONTINUE
      SUM5=0.
      DO 400 J1=1,NYO
      J1Q=(J1-1)/NW
      J1R=J1-NW*J1Q
      YO=PI*(.5+.5*ARG(J1R)+FLOAT(J1Q))
      YOB=GN(N)*(YO/XNPI-.5)
      SFYO=DCOS(YOB)+KN(N)*DCOSH(YOB)
      IF(N-N/2*2.EQ.0)SFYO=DSIN(YOB)+KN(N)*DSINH(YOB)
      SUM3=0.
      DO 200 L1=1,NYOP
      L1Q=(L1-1)/NW
      L1R=L1-NW*L1Q
      YOP=PI*(.5+.5*ARG(L1R)+FLOAT(L1Q))
      YOYOP=YO-YOP
      BNPI=B/(XNPI*UCTH)
      E3=DEXP(-B/PI * ALPH2*DABS(YO/XN-YOP/XQ))
      YOPB=GQ(Q)*(YOP/XQPI-.5)
      SFYOP=DCOS(YOPB)+KQ(Q)*DCOSH(YOPB)
      IF(Q-Q/2*2.EQ.0)SFYOP=DSIN(YOPB)+KQ(Q)*DSINH(YOPB)
      FV3=SFYOP*E3
      SUM3=SUM3+FV3*WGT(L1R)*PI/2.
  200 CONTINUE
      FV5=SUM3*SFYO
```

TABLE 3D (Continued)

```
      SUM5=SUM5+FV5*WGT(J1R)*PI/2.
  400 CONTINUE
      ANSINT=SUM5*SUM5
      ANS=ANSINT*CONST*POFW*EIGEN(M,N)*EIGN(P,Q)*DENCOM*C1*C1
      PWRSD=ANS*W**4
      WRITE(6,20)M,N,W,POFW,EIGEN(M,N),DEN
      WRITE(6,20)P,Q,XNMRTR,EIGN(P,Q),DENCOM
   20 FORMAT(1X,2I4,6E15.6)
      WRITE(6,21)ANSINT,ANS,PWRSD
   21 FORMAT(11X,6E15.6/)
      W=W+DW
  150 CONTINUE
 7761 CONTINUE
  776 CONTINUE
 7781 CONTINUE
  778 CONTINUE
      STOP
      END
```

APPENDIX C

ELECTRIC BOAT PROGRAM (IZZO)

NOTATION

A	Correlation area of turbulence over which the mean square pressure $\overline{p^2}$ is constant
A_{mn}, A_{rs}	Coefficient used in series representation of deflection
A_n, A_n'	Normal acceleration of plate
a_i	Speed of sound in water
a_m, b_m, c_m, d_m	
a_n, b_n, c_n, d_n	Constants
a_{mn}	Modal damping function
B	Equal to $\eta / 2$
b	Bending stiffness
C_{mn}, D_{mn}	Constants defined in Equation (C27)
C_{mn}^{rs}	Coefficient in Equation (C34)
$g(\ )$	Greens function (impulse response of plate at point r_0 due to forcing function P at r_0) defined by Equation (C10)
h	Plate thickness
I, i	Refers to properties on the side of the plate where the fluid is in motion (i.e., turbulent) and where the fluid is stagnant, respectively, as shown in Figure 11.
$I_{mn}(\tau)$	Time correlation integral defined by Equation (C24)
K	Constant
$K'(\omega_{mn})$	Modal amplitude factor
$\overline{K}_{mn}$, K_{mn}	Constants defined in Equation (C27) and (C28), respectively
$L(\ )$	Linear differential operator defined in Equation (C12)
L_x, L_y	Lateral dimensions of plate along the x and y axes, respectively
M	Mass per unit area of plate
m, n; p, q; r, s	Mode numbers
P_i	Acoustic pressure
$\overline{P^2}$	Mean square pressure at surface beneath turbulent boundary layer

$p(r, t)$	Surface pressure beneath turbulent boundary layer
$R_A(\ )$	Space-time correlation of plate accelerations
$R_p(r, r', \tau)$	Space-time correlation of acoustic pressures
$R_p(r_0, r_0', \tau)$	Space-time correlation of turbulence pressures
$R_v(\ )$	Space-time correlation of plate velocities
$R_z(\ )$	Space-time correlation of plate displacements
r, r', r_0, r_0'	Radius vectors defined in Figure 11
$\vec{r}_0(\bar{x}_0, \bar{y}_0, \bar{z}_0), \vec{t}_0$ or $\vec{r}_0', \vec{t}_0'$	Space-time coordinates of the forcing function p
S, S_0, S_0'	Surface area of plate ($dS_0 = dx_0\, dy_0$ etc)
$S_p(r, r', \omega)$	Cross-spectral density of acoustic pressures
$S_p(r, \omega)$	Power spectrum of acoustic pressures at a point r along the normal through the center of the plate
$S_z(r, r', \omega)$	Cross-spectral density of plate displacements
T	Kinetic energy of plate
$t, t', t_0, t_0', \overline{t_0}, \overline{t_0'}$	Time variables
$U(t-\overline{t_0})$	Unit step function
U_c	Average convective speed of turbulent pressure field (or pattern)
U_0	Ship speed; free stream velocity
u	Velocity component, at any point y in the boundary layer, parallel to the x axis; see Figure 11
V	Potential energy of plate
V_n, V_n'	Normal velocity of plate
w	Plate displacement
$X_m(x), Y_n(y)$	Mode shapes of the plate along x and y, respectively
x, x', x_0, x_0' y, y', y_0, y_0'	Space coordinates defined in Figure 11
Z_n, Z_n', z, z'	Normal displacement of plate

α	Equal to $m\pi U_c/L_x$
β_0	Plate viscous damping (resistance coefficient)
β_1	Radiation damping coefficient
γ, μ	Functions of the time variables as defined by Equation (C 22)
δ, δ^*	Boundary layer thickness and boundary layer displacement thickness, respectively
$\delta(\ )$	Dirac delta function
δ_{mn}, δ_{pq}	Kronecker delta equal to $\begin{matrix} 1 \text{ for } m = n \text{ or } p = q \\ 0 \text{ for } m \neq n \text{ or } p \neq q \end{matrix}$
δ_{mn}	Kronecker delta equal to $\begin{matrix} 1 \text{ for } mn = rs \\ 0 \text{ for } mn \neq rs \end{matrix}$
η	Loss factor (plate hysteretic damping)
θ	Temporal decay factor of turbulent boundary layer associated with eddy decay
κ	Measure of the inverse radius of the turbulence eddy
λ_{mn}	Eigenvalue
μ	Poisson's ratio
ρ	Density of plate material
ρ_i	Fluid density
τ, τ', τ_0	Delay times equal to $t' - t$, $t' - t + \dfrac{r_0 - r_0'}{a_i}$, and $\overline{t_0} - \overline{t_0'}$, respectively
$\Phi\left(\dfrac{\omega}{\omega_{mn}}\right)$	Spectrum shape factor
ϕ_{mn}, ϕ_{pq}	Eigenfunction
ω	Circular frequency, equal to $2\pi f$
ω_{mn}	Undamped natural modal frequency
$*$	Symbol representing the complex conjugate
$\langle\ \rangle$	Symbol representing cross (space-time) correlation function

APPENDIX C1 – MATHEMATICAL ANALYSIS

Equations are now derived for the space-time correlation and spectral density of the acoustic pressure in the near and far field on both sides of a turbulence excited vibrating plate.[26]

The Rayleigh formulation[27] of the velocity potential in the acoustic field resulting from a vibrating plane is

$$\phi(r,t) = -\frac{1}{2\pi}\iint \frac{dS_0}{r} V_n\left(r_0, t-\frac{r_0}{a_i}\right) \tag{C1a}$$

The corresponding acoustic pressure is

$$P_i(r,t) = -\rho_i \frac{\partial \phi}{\partial t} = \frac{\rho_i}{2\pi}\int \frac{dS_0}{r_0} \frac{\partial V_n}{\partial t}\left(r_0, t-\frac{r_0}{a_i}\right) \tag{C1b}$$

Figure 11 shows the coordinate system used for this formulation. The space-time correlation of the acoustic pressures are

$$<P_i(r,t)\, P_i(r',t')> = R_p(r,r',\tau) = <\frac{\rho_i}{2\pi}\int_S \frac{dS_0}{r_0} \frac{\partial V_n}{\partial t}\left(r_0, t-\frac{r_0}{a_i}\right)\cdot$$

$$\frac{\rho_i}{2\pi}\int_S \frac{dS_0'}{r_0'} \frac{\partial V_n}{\partial t}\left(r_0', t'-\frac{r_0'}{a_i}\right)> \tag{C2}$$

where $t' = t + \tau$.

The integration and ensemble averaging processes may be interchanged to give

$$R_p(r,r',\tau) = \frac{\rho_i^2}{4\pi^2}\int_S\int_S \frac{dS_0}{r_0}\frac{dS_0'}{r_0'} < \frac{\partial V_n}{\partial t}\left(r_0, t-\frac{r_0}{a_i}\right)\frac{\partial V_n}{\partial t}\left(r_0', t'-\frac{r_0'}{a_i}\right)> \tag{C3}$$

Now

$$<\frac{\partial^2 Z_n}{\partial t^2}\frac{\partial^2 Z_n'}{\partial t'^2}> = <\frac{\partial V_n}{\partial t}\frac{\partial V_n'}{\partial t'}> = <A \quad A'>$$

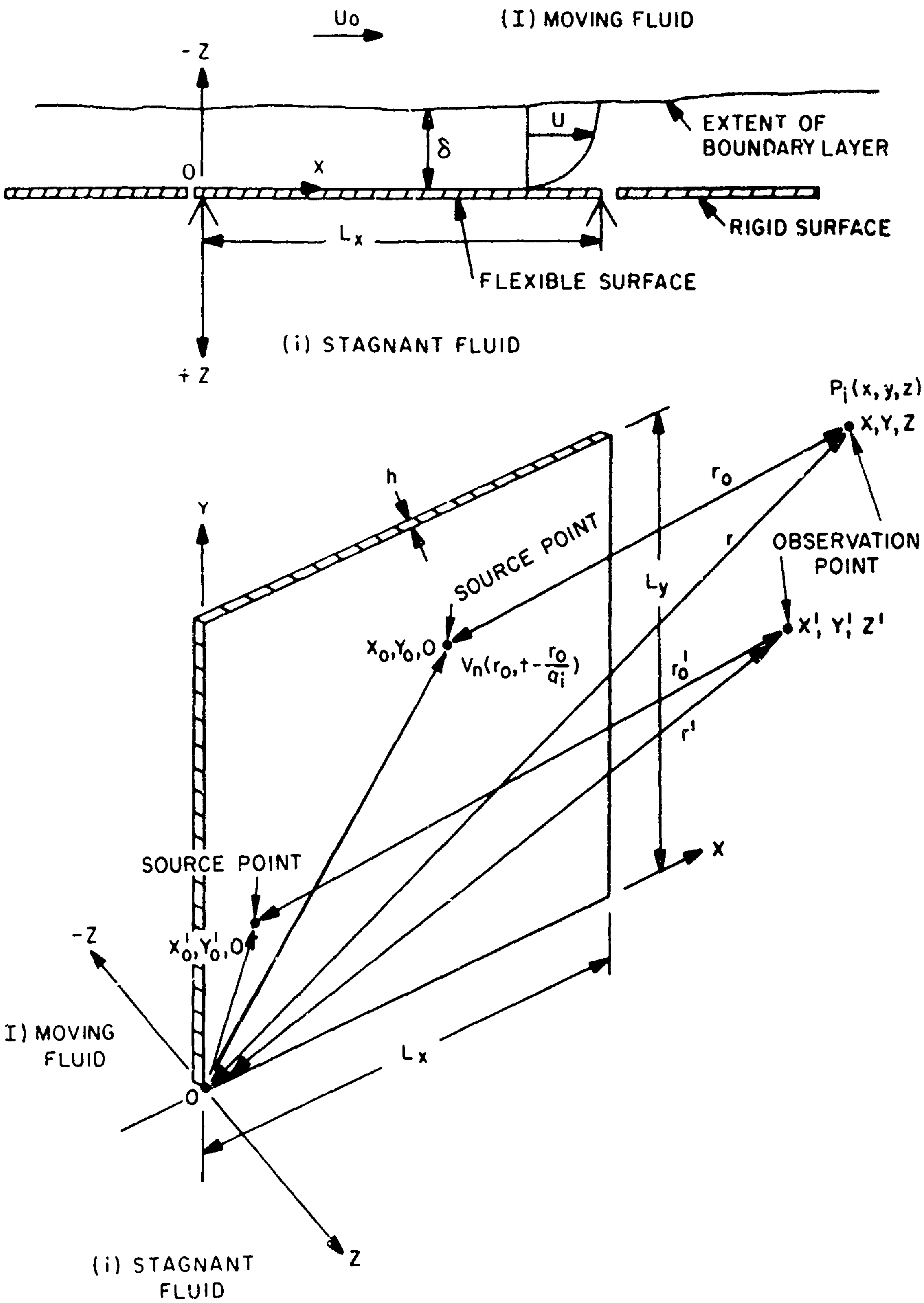

Figure 11 – Coordinate System

may be written as [28]

$$\frac{\partial^4}{\partial\tau^4} R_z \left(r_0, t - \frac{r_0}{a_i} ; r_0', t' - \frac{r_0'}{a_i}\right) = \frac{\partial^2 R_v}{\partial\tau^2} \left(r_0, t - \frac{r_0}{a_i}; r_0', t' - \frac{r_0'}{a_i}\right)$$

$$= R_A \left(r_0, t - \frac{r_0}{a_i}; r_0', t' - \frac{r_0'}{a_i}\right) \quad \text{(C4)}$$

Hence

$$R_p(r, r', \tau) = \frac{\rho_i^2}{4\pi^2} \iint_{S\,S} \frac{dS_0}{r_0} \frac{dS_0'}{r_0'} \frac{\partial^4}{\partial\tau^4} R_z \left(r_0, t - \frac{r_0}{a_i}; r_0', t - \frac{r_0'}{a_i}\right) \quad \text{(C5)}$$

Assuming a stationary random process, we can shift the time origin by an amount r_0 / a_i without changing the results of averaging. We get

$$R_p(r, r', \tau) = \frac{\rho_i^2}{4\pi^2} \iint_{S\,S} \frac{dS_0}{r_0} \frac{dS_0'}{r_0'} \frac{\partial^4}{\partial\tau^4} R_z(r_0, t; r_0', t + \tau') \quad \text{(C6)}$$

where $\tau' = \tau + \frac{r_0 - r_0'}{a_i}$.

The Wiener-Khintchine relations between the cross-correlation and cross-spectral density of the acoustic pressures are

$$S_p(r, r', \omega) = \frac{1}{2\pi}\int_{-\infty}^{\infty} d\tau \; R_p(r, r', \tau) \; e^{-i\omega\tau} \quad \text{(C7a)}$$

$$R_p(r, r', \tau) = \int_{-\infty}^{\infty} d\omega \; S_p(r, r', \omega) \; e^{i\omega\tau} \quad \text{(C7b)}$$

Substituting Equation (C5) in (C7a), we obtain*

$$S_p(r, r', \omega) = \frac{\omega^4 \rho_t^2}{4\pi^2} \int_S \int_S \frac{dS_0}{r_0} \frac{dS_0'}{r_0'} S_z(r, r', \omega) \qquad \text{(C8)}$$

Equation (C6), (C7), and (C8) describe the acoustic pressure resulting from the vibration of a plane surface in a semi-infinite medium. The equations are a function of R_z only and are applicable to any type of plate with any type of boundaries.

The method for determining plate response to turbulence excitation is *identical* to that of Dyer except that more general boundary conditions are included here. However, because the notation is somewhat different, the relevant equations are outlined for the benefit of the computer program user. The reader is referred to Appendix A1 for a more detailed development. The differential equation of motion of the linear system $Lz = -p$ has the solution

$$Z(r_0, t) = \int_{-\infty}^{t} d\overline{t_0} \int_S dS_0\, g(r_0, t; \overline{r_0}, \overline{t_0})\, p(\overline{r_0}, \overline{t_0}) \qquad \text{(C9)}$$

where

$$Lg = -\delta(r - \overline{r_0})\, \delta(t_0 - \overline{t_0}) = -\delta(x_0 - \overline{x_0})\, \delta(y_0 - \overline{y_0})\, \delta(t_0 - \overline{t_0}) \qquad \text{(C10)}$$

For turbulence excitation (random pressures), the ensemble average or cross correlation of the plate displacements can then be expressed in terms of the correlation of the turbulent pressure forces by

$$< z(r_0, t)\, Z^*(r_0', t') > = R_z(r_0, r_0', \tau) = \int_{-\infty}^{t} d\overline{t_0} \int_{-\infty}^{t} d\overline{t_0'} \int_{S_0} dS_0 \int_{S_0'} dS_0' \,\cdot$$

$$< g(r_0, t; \overline{r_0}, \overline{t_0})\, g^*(r_0', t'; \overline{r_0'}, \overline{t_0'}) > < p(\overline{r_0}, \overline{t_0})\, p^*(\overline{r_0'}, \overline{t_0'}) >$$

$$= \int_{-\infty}^{t} d\overline{t_0} \int_{-\infty}^{t'} d\overline{t_0'} \int_S dS_0 \int_S dS_0'\, g(r_0, t; \overline{r_0}, \overline{t_0})\, g^*(r_0', t'; \overline{r_0'}, \overline{t_0'})$$

$$\cdot R_{tp}(r_0, r_0', \tau) \qquad \text{(C11)}$$

---

* $$\mathcal{F}\left(\frac{\partial^4 R_z}{\partial \tau^4}\right) = \omega^4 S_z$$

For thin plate vibration

$$b(1 - i\eta)\nabla^4 (\ ) + M \frac{\partial^2(\ )}{\partial t^2} + \beta_0 \frac{\partial(\ )}{\partial t} = L(\ ) \tag{C12}$$

The Green function satisfying Equation (C12) has been shown to be represented by

$$\mathcal{G}(\vec{r}_0, t; \vec{r}_0, t_0) = \sum_{mn} \frac{\phi_{mn}(\vec{r}_0)\,\phi_{mn}(\vec{r}_0)}{\omega_{mn} M} e^{-a_{mn}(t - \vec{t}_0)} \sin \omega_{mn}(t - \vec{t}_0)\, U(t - \vec{t}_0) \tag{C13}$$

where $\phi_{mn}(\ )$, the orthonormal set of eigenfunctions, satisfies the conditions:

$$L\,\phi_{mn} = 0 \tag{C14}$$

and

$$\int_S \phi_{mn}\,\phi_{pq}\, dS = \delta_{mn}\ \delta_{pq} \tag{C15}$$

and where*

$$a_{mn} = \frac{\omega_{mn}}{\eta} \left[\left(1 + \frac{\eta\beta}{\omega_{mn} M} + \eta^2 \right)^{1/2} - 1 \right] \tag{C16}$$

$$\omega_{mn} = \left(\frac{b}{M} \right)^{1/2} \lambda_{mn}^2 \tag{C17}$$

---

*Equation (A7) of Appendix A can be written in the present notation as

$$a_{mn} = \frac{\omega_{mn}}{\eta} \left\{ \left[\left(\frac{\beta\eta}{2M\omega_{mn}} + \frac{\lambda_{mn}^4 b\eta^2}{2M\omega_{mn}^2} + 1 \right)^2 \right] - 1 \right\}$$

Expanding this equation and assuming, with Dyer (Equation (12) of Reference 2), that $\eta \leq 1/3$ and $\frac{\beta}{2\omega_{mn} M} \leq 1/3$ as well as using Equation (A8) in the expansion, we obtain Equation (C16).

When radiation damping is also included, we write

$$a_{mn} = \frac{\beta_0}{2M} + \frac{\eta}{2}\omega_{mn} + \frac{\beta_1}{2M} \tag{C18}$$

In this analysis, it is assumed that β_0 and β_1 are negligible* so that

$$a_{mn} = \frac{\eta}{2}\omega_{mn} = B\omega_{mn} \tag{C19}$$

Using Dyer's equation for the pressure correlation

$$R_{tp}(r, \tau) = \overline{p^2} A \delta[(x_0 - x_0') - U_c\tau]\delta(y_0 - y_0')\, e^{-\frac{|\tau|}{\theta}} \tag{C20}$$

Using Equations (C12), (C13), and (C20), we obtain the working expression for the displacement correlation function for a plate excited by a turbulent boundary layer. It is applicable to arbitrary boundary conditions provided expressions can be obtained for the eigenvalues and normalized eigenfunctions.

$$R_z(r_0, r_0', \tau) = \sum_{pq}\sum_{mn} \frac{A\overline{p^2}\,\phi_{pq}(r_0)}{\omega_{mn}\omega_{pq}M^2}\,\phi_{mn}(r_0')\int_{-\infty}^{t} d\overline{t_0}\int_{-\infty}^{t'} d\overline{t_0'}\int_S d\overline{S_0}$$

$$\cdot\int_S d\overline{S_0'}\,\phi_{mn}(\overline{r_0})\,\phi_{pq}(\overline{r_0'})\, e^{\left[-a_{mn}(t-\overline{t_0}) - a_{pq}(t'-\overline{t_0'}) - \frac{|\tau_0|}{\theta}\right]}$$

$$\cdot \sin\omega_{mn}(t-\overline{t_0})\sin\omega_{pq}(t'-\overline{t_0'})\,\delta[(x_0 - x_0') - U_c\tau]\,\delta(y_0 - y_0') \tag{C21}$$

Performing a spatial integration of Equation (C21), then introducing the transformation used by Dyer

$$\gamma = (t' - \overline{t_0'}) - (t - \overline{t_0}) = \tau_0 - \tau$$

$$\mu = (t' - \overline{t_0'}) + (t - \overline{t_0}) \tag{C22}$$

---

*If values or relations for β_0, β_1 are known, we can include these terms in the analysis and program.

followed by a temporal integration yields

$$R_z(\tau_0, \tau_0', \tau) = \sum_m \sum_n \frac{A\overline{p^2}}{4\omega_{mn}^2 M^2} \phi_{mn}(\tau_0)\, \phi_{mn}(\tau_0')\, I_{mn}(\tau) \tag{C23}$$

where

$$I_{mn}(\tau) = \int_0^\infty d\mu \int_{-\mu}^{\mu} dy\, e^{\left[-a_{mn}\mu - \frac{|\gamma+\tau|}{\theta}\right]} \cos \alpha(\gamma+\tau)[\cos\omega_{mn}\gamma - \cos\omega_{mn}\mu], \quad \tau \geq 0 \tag{C24}$$

where $\alpha = m\pi U_c / L_x$.

Since θ is small, then for $|\tau_0| > 0$, $e^{-\frac{|\tau_0|}{\theta}} \to 0$ so that from Equation (C21) $R_z(\tau_0, \tau_0', \tau') \to 0$. Hence, with small error, we need consider only the value $\tau_0 = (\overline{t_0} - \overline{t_0'}) = 0$. With this approximation we perform the integration in Equation (C21) to obtain the displacement correlation below coincidence. To render the analysis tractable for the integration, it is also assumed that $U_c \theta << L_x$, $\frac{m\pi U_c}{L_x} << \omega_{mn}$, i.e. the correlation length of the pressure field is much smaller than the length of the plate and the convection speed of the turbulence is small compared to the modal wavelength, and $a_{mn}\theta << 1$ (low damping); see (A22), (A23), (A36), and (A36b) of Appendix A1. The result for the displacement correlation function, which is independent of plate boundary conditions, is*

---

*It is important to note that although the same symbols $\phi_{mn}(\tau_0)$ and $\phi_{mn}(\tau_0')$ are used,

$$\phi_{mn}(\tau_0)\Big|_{\text{Eq (C25)}} = \frac{\left(L_x L_y\right)^{1/2}}{2}\, \phi_{mn}(\tau_0)\Big|_{\text{Eq (C21)}} \quad ; \quad \phi_{mn}(\tau_0')\Big|_{\text{Eq (C25)}} = \frac{\left(L_x L_y\right)^{1/2}}{2}\, \phi_{mn}(\tau_0')\Big|_{\text{Eq (C21)}}$$

The value of the normalized eigenfunction ϕ_{mn} used in Equation (C21) agrees with that used by Dyer That the value of ϕ_{mn} used in Equation (C25) differs from Dyer's results by a factor $\frac{(L_x L_y)^{1/2}}{2}$ can be seen by comparing Equations (C35) and (A20) for the case of a simply supported plate. Thus, we see that Equations (C25) and Equation (A27), where $I_{mn}(\tau)$ is given by Equation (A36), are in agreement.

$$R_z(r_0, r_0', \tau) = \sum_m \sum_n \frac{2A\theta\overline{p^2}}{L_x L_y \omega_{mn}^2 a_{mn} M^2 (1 + \omega_{mn}^2 \theta^2)} \cdot$$

$$\cdot \phi_{mn}(r_0)\, \phi_{mn}(r_0')\, e^{-[a_{mn}|\tau|]} \cos \omega_{mn}\tau \qquad \text{(C25)}$$

For the plate mode shape, assume that

$$\phi_{mn}(r) = X_m(x)\, Y_n(y) \qquad \text{(C26)}$$

where

$$X_m(x) = a_m \cos \alpha_m x + b_m \sin \alpha_m x + c_m \cosh \alpha_m x + d_m \sinh \alpha_m x$$

$$Y_n(y) = a_n \cos \alpha_n y + b_n \sin \alpha_n y + c_n \cosh \alpha_n y + d_n \sinh \alpha_n y \qquad \text{(C26a)}$$

From Equations (C4) and (C6), we see that $R_p(r, r', \tau)$ is a function of

$$\frac{\partial^4}{\partial \tau^4} R_z(r_0, r_0', \tau) = R_A(r_0, r_0', \tau) \; .$$

Page 99 of Reference 28 shows that the correlation of the plate acceleration for $\tau > 0$ can be expressed as*

$$R_A(r_0, r_0', \tau) = \sum_{m\,m} \overline{K}_{mn} \phi_{mn}(r_0)\, \phi_{mn}(r_0')\, e^{-a_{mn}\tau} [C_{mn} \cos \omega_{mn}\tau + D_{mn} \sin \omega_{mn}\tau]$$

$$; \tau > 0 \qquad \text{(C27)}$$

where

$$\overline{K}_{mn} = \frac{2A\theta\overline{p^2}}{L_x L_y \omega_{mn}^2 M^2 (1 + \omega_{mn}^2 \theta^2)}$$

$$C_{mn} = \omega_{mn}^4 - 6\, \omega_{mn} a_{mn}^2 + a_{mn}^4$$

$$D_{mn} = 4 a_{mn}\, \omega_{mn} (a_{mn}^2 - \omega_{mn}^2)$$

---

*Footnote on following page.

*Footnote to preceding page. Using Equation (C25) and the relationship between R_A and R_z we have

$$R_A = \frac{\partial^4}{\partial \tau^4} R_z = K \frac{\partial^4}{\partial \tau^4}\left[e^{-a_{mn}|\tau|}\right] \cos \omega_{mn}\tau$$

where

$$K = \sum_m \sum_n \frac{2A\theta \overline{p^2}}{L_x L_y \omega_{mn}^2 a_{mn} M^2 (1 + \omega_{mn}^2 \theta^2)} \phi_{mn}(r_0)\phi_{mn}(r_0')$$

Let $a_{mn} = a$, $\omega_{mn} = b$. Then

$$f(\tau) = e^{-a|\tau|} \cos b\tau = e^{a\tau} \cos b\tau \text{ for } \tau < 0$$
$$= e^{-a\tau} \cos b\tau \text{ for } \tau > 0$$

or

$$= e^{-\alpha\tau} \cos b\tau = u \cdot v \text{ where } \alpha = -a \text{ for } \tau < 0$$
$$\alpha = a \text{ for } \tau > 0$$
$$u(\tau) = e^{-\alpha\tau} \text{ and } v(\tau) = \cos b\tau$$

The Leibriz theorem is obtained by differentiating uv, with respect to τ, n times. When $n = 4$, corresponding to the fourth derivative, the theorem gives

$$f''''(\tau) = u''''v + 4u'''v' + 6u''v'' + 4u'v''' + uv''''$$
$$= \alpha^4 e^{-\alpha\tau} \cos b\tau + 4(-\alpha^3) e^{-\alpha\tau}(-b \sin b\tau) + 6\alpha^2 e^{-\alpha\tau}(-b^2) \cos b\tau$$
$$+ 4(-\alpha) e^{-\alpha\tau} b^3 \sin b\tau + b^4 e^{-\alpha\tau} \cos b\tau$$
$$= (\alpha^4 - 6\alpha^2 b^2 + b^2) f(\tau) + 4\alpha b(\alpha^2 - b^2) g(\tau)$$
$$= (a^4 - 6a^2 b^2 + b^4) f(\tau) + 4ab(a^2 - b^2) g(\tau) \text{ for } \tau > 0$$
$$= (a^4 - 6a^2 b^2 + b^4) f(\tau) - 4ab(a^2 - b^2) g(\tau) \text{ for } \tau < 0$$

where $f(\tau) = e^{-\alpha\tau} \cos b\tau$ and $g(\tau) = e^{-\alpha\tau} \sin b\tau = e^{-a|\tau|} \sin b\tau$.

The results agree with those in Appendix II of Reference 29 determined there by use of Heaveside functions. We note that the first derivative of $f(\tau)$ has a finite discontinuity at the origin so that the second and higher order derivatives will have infinite discontinuities at this point.

Reference 29 also shows that Equation (C27) satisfies the Wiener-Khintchine relations, Equations (C7a) and (C7b), thereby establishing the derived expression for $R_A(r_0, r_0', \tau)$ as a valid correlation function.*

*To show that $\frac{\partial^4 f(\tau)}{\partial \tau^4}$ and therefore R_a satisfies the Wiener-Khintchine relations, consider the Fourier cosine transform of $\frac{\partial^4 f(\tau)}{\partial \tau^4}$. Because $\frac{\partial^4 f(\tau)}{\partial \tau^4}$ is an even function, the Fourier sine transform of this function vanishes. Since the fourth derivative is a continuous function, we integrate by parts to find

$$\int_0^\infty \frac{\partial^4 f(\tau)}{\partial \tau^4} \cos \omega\tau \, d\tau = \left[\frac{\partial^3 f(\tau)}{\partial \tau^4} \cos \omega\tau \, d\tau + \omega \frac{\partial^2 f(\tau)}{\partial \tau^2} \sin \omega\tau - \omega^2 \frac{\partial f(\tau)}{\partial \tau} \cos \omega\tau \right]_0^\infty$$

$$-\omega^3 \int_0^\infty \frac{\partial f(\tau)}{\partial \tau} \sin \omega\tau \, d\tau$$

$f(\tau)$ and all of its derivatives are zero at $\tau = \infty$. Also, odd derivatives of $f(\tau)$ over the range $-\infty \leq \tau \leq \infty$ are odd functions of τ so that the value of these derivatives at the point of discontinuity (i.e., origin $\tau = 0$) is zero. Hence, this equation reduces to

$$\int_0^\infty \frac{\partial^4 f(\tau)}{\partial \tau^4} \cos \omega\tau \, d\tau = -\omega^3 \int_0^\infty \frac{\partial f(\tau)}{\partial \tau} \sin \omega\tau \, d\tau \quad -\omega^4 \int_0^\infty f(\tau) \cos \omega\tau \, d\tau$$

after integration by parts of the bracketed integral. Substituting $f(\tau) = e^{-a|\tau|} \cos b\tau$ in the last integral we obtain

$$\int_0^\infty \frac{\partial^4 f(\tau)}{\partial \tau^4} \cos \omega\tau \, d\tau = \frac{a}{2} \left[\frac{\omega^4}{a^2 + (b+\omega)^2} + \frac{\omega^4}{a^2 + (b-\omega)^2} \right]$$

The inverse Fourier cosine transform of this expression is

$$\frac{1}{2\pi} \int_0^\infty \frac{a}{2} \left[\frac{\omega^4}{a^2 + (b+\omega)^2} + \frac{\omega^4}{a^2 + (b-\omega)^2} \right] \cos \omega\tau \, d\tau$$

$$= (a^4 - 6a^2 b^2 + b^4) f(\tau) + 4ab(a^2 - b^2) g(\tau)$$

which we have previously shown to be $\frac{d^4 f(\tau)}{d\tau^4}$ for $\tau > 0$. Thus, the terms $\frac{d^4 f(\tau)}{d\tau^4}$ and $\frac{a}{2}\left[\frac{\omega^4}{a^2 + (b+\omega)^2} + \frac{\omega^4}{a^2 + (b-\omega)^2} \right]$ are Fourier pairs. These results are obtained with somewhat more rigor in Reference 29.

Substitution of Equation (C27) in (C6) yields the following expression for the cross correlation of acoustic pressures*

$$R_p(r, r', \tau) = \sum_{mn} K_{mn} \iint_{S\,S} \frac{dS_0}{r_0} \frac{dS_0'}{r_0'} \phi_{mn}(r_0)\, \phi_{mn}(r_0')\, e^{-a_{mn}\tau'}$$

$$\cdot \left[C_{mn} \cos \omega_{mn}\tau' + D_{mn} \sin \omega_{mn}\tau'\right] \qquad \text{(C28)}$$

where

$$K_{mn} = \frac{\rho_i^2}{4\pi^2} \breve{K}_{mn}$$

and

$$\tau' = \tau + \frac{(r_0 - r_0')}{a_i}$$

Equations (C28) and (C7) represent working expressions for determining anywhere in the field the desired statistical properties of the acoustic pressure resulting from the vibrations of a turbulence-excited finite plate of arbitrary boundary conditions. The mode shapes of the plate $\phi_{mn}(r)$ in these equations implicitly represent the dependence of the acoustic field on the boundary conditions.

The method of analysis used by Young[30] (the Ritz method) is used to determine the eigenfunctions and eigenvalues of vibrating rectangular plates with continuous spring-type boundary conditions. This treatment allows for various combinations of clamped and free boundaries.

The Ritz method consists of equating the maximum potential energy of the plate

$$V = \frac{b}{2} \iint_{\substack{\text{plate}\\ \text{area}}} \left[\left(\frac{\partial^2 w}{\partial x^2}\right)^2 + \left(\frac{\partial^2 w}{\partial y^2}\right)^2 + 2\mu \frac{\partial^2 w}{\partial x^2} \frac{\partial^2 w}{\partial y^2} + 2(1-\mu)\left(\frac{\partial^2 w}{\partial x \partial y}\right)^2\right] dx dy \quad \text{(C29)}$$

*Note that whereas in the statement below Equation (C26a) the term $\frac{r_0 - r_0'}{a_i}$ was implicitly included in the variables r_0, r_0' of the function $R_A(r_0, r_0', \tau)$, in Equation (C27) the term $\frac{r_0 - r_0'}{a_i}$ is linked with τ to form τ'.

to the maximum kinetic energy of the plate

$$T = \omega^2 \frac{\rho h}{2} \iint\limits_{\substack{\text{plate}\\ \text{area}}} w^2 \, dxdy \tag{C30}$$

to obtain an expression for the frequency of the vibrating system

$$\omega^2 = \frac{2}{\rho h} \frac{V}{\iint\limits_{\substack{\text{plate}\\ \text{area}}} w^2 \, dxdy} \tag{C31}$$

The natural frequencies are determined by finding expressions for w that satisfy the boundary conditions and minimize Equation (C31). The Ritz method consists of assuming the deflection $w(x, y)$ as a linear series of "admissible" functions (see Reference 30) and adjusting the coefficients in the series so as to minimize Equation (C31).

For a rectangular plate with edges parallel to the x- and y-axes, the series approximation for the displacement function is taken in the form

$$w(x, y) = \sum_{m=1}^{p} \sum_{n=1}^{q} A_{mn} X_m(x) \, Y_n(y) \tag{C32}$$

and substituted in Equation (C31). We get

$$\omega^2 = \frac{2}{\rho h} \frac{V}{\iint\limits_{\text{plate}} \Sigma \, \Sigma \, A_{mn} X_m(x) \, Y_n(y) \, dxdy}$$

or

$$V = \frac{\omega^2 \rho h}{2} \iint\limits_{\text{plate}} \sum \sum A_{mn} X_m(x) \, Y_n(y) \, dxdy$$

This expression is minimized by setting the partial derivative with respect to each coefficient equal to zero. This yields

$$\frac{\partial V}{\partial A_{rs}} - \frac{\omega^2 \rho h}{2} \frac{\partial}{\partial A_{rs}} \iint\limits_{\text{plate}} w^2 \, dxdy = 0 \tag{C33}$$

where A_{rs} is any of the coefficients A_{mn}. Equation (C33) represents a system of linear homogeneous equations in the unknowns A_{mn}. The approximate natural frequencies of the plate $\omega_1, \omega_2, \ldots$ are obtained from Equation (C33) by setting the determinant of the system equal to zero.

The functions $X_m(x)$ and $Y_n(y)$ inserted in Equation (C33) are the mode shapes of a beam supported by torsional and transverse linear springs along its boundaries. The characteristics of the springs along each side are constant. These spring-type edge conditions allow the effects of edge rotational and edge translational constraints to be analyzed on a quantative basis. Once the mode shapes are known or determined – *for the clamped-clamped plate, we use the functions given by Equation (C26) and (C26a) as the mode shapes $X(x)$ and $Y(y)$ of a beam with its ends clamped in the Ritz method* --all of the integrals in Equation (C33) can be calculated. Then as explained in Reference (30), the set of integral Equations (C33) can be reduced to a set of linear algebraic equations of the form*

$$\sum_{m=1}^{p}\sum_{n=1}^{q}\left[C_{mn}^{rs} - \lambda\delta_{mn}^{rs}\right]A_{mn} = 0 \qquad \text{(C34)}$$

where

$$\delta_{mn}^{rs} = \begin{cases} 1 \text{ for } mn = rs \\ 0 \text{ for } mn \neq rs \end{cases}$$

$$\lambda = \omega^2 \rho h L_x^3 L_y / b \quad \text{(proportional to } \omega^2\text{)}$$

In Equation (C34), r assumes all values between 1 and p and s assumes all values between 1 and q. The eigenvalues and therefore the natural frequencies ω_{rs} are found from the condition that the determinant of the system of Equation (C34) must vanish for nontrivial solutions A_{mn}. Once the eigenmatrices of Equation (C34) have been determined, the mode shapes of the plate are obtained from Equation (C32).

Reference 29 compares the spectrum of the sound pressure level for a clamped-clamped plate with that of a simply supported plate. The comparison suggests that a *simplified and realistic approach to the investigation of plates with nonsimple supports would be to calculate the modal frequencies considering the true (clamped-clamped) end conditions but to use the mode shapes considering the end conditions as simple supports.* Comparison runs using this approach, which requires much less computation, and the exact approach (clamped-clamped

*The general functional form for C_{mn}^{rs} is given in Reference 30.

frequencies and mode shapes) produced results in very good agreement.[29] In connection with this aspect of the problem, the following equations were developed to obtain the sound radiated from *simply supported* plates.

For a simply supported plate of dimensions L_x, L_y and thickness h, the normalized eigenfunctions (mode shapes) and corresponding modal frequencies are [2] (see footnote for paragraph preceding equation (C25))

$$\phi_{mn} = \sin \frac{m\pi x}{L_x} \sin \frac{n\pi y}{L_y} \tag{C35}$$

$$\omega_{mn}^2 = \left(\frac{b}{M}\right)^{1/2} \lambda_{mn}^2 \tag{C36}$$

where

$$\lambda_{mn}^2 = \left(\frac{m\pi}{L_x}\right)^2 + \left(\frac{n\pi}{L_y}\right)^2$$

Substituting Equation (C35) in (C28), we obtain for *locations in the far field* on a *normal through the center of the plate* ($r_0 - r_0' \approx 0$; more generally $r_0 \approx r_0' \approx r$, see Figure C1, and consequently $r' \approx r$)

$$R_p = \sum_m \sum_n \frac{K_{mn}}{r^2} e^{-a_{mn}\tau} \left[C_{mn} \cos \omega_{mn}\tau + D_{mn} \sin \omega_{mn}\tau\right] \cdot$$

$$\cdot \int_0^{L_x} \sin \frac{m\pi x}{L_x} dx \int_0^{L_x} \sin \frac{m\pi x}{L_x} dx \int_0^{L_y} \sin \frac{n\pi y}{L_y} dy \int_0^{L_y} \sin \frac{n\pi y}{L_y} dy$$

Now

$$\int_0^{L_x} \sin \frac{m\pi x}{L_x} dx = \frac{L_x}{m\pi} \left[-\cos m\pi - 1\right] = \frac{L_x}{m\pi} [-1(-1)^m - 1]$$

and similarly for the other three integrals. Hence, the product of the four integrals yields the term $\frac{L_x^2}{m^2\pi^2}[-1(-1)^m-1]^2 \cdot \frac{L_y^2}{n^2\pi^2}[-1(-1)^n-1]^2$ and the auto correlation of the acoustic pressure at r is

$$R_p(r,\tau) = \sum_m \sum_n \frac{K_{mn}}{r^2} [C_{mn} \cos \omega_{mn}\tau + D_{mn} \sin \omega_{mn}\tau] \cdot$$

$$\cdot\, e^{-a_{mn}\tau} \frac{L_x^2 L_y^2}{\pi^4 m^2 n^2} [(-1)^m - 1]^2 [(-1)^n - 1]^2 \qquad \text{(C37)}$$

The power spectrum of the pressure at r is

$$S_p(r,\omega) = \frac{1}{2\pi}\int_{-\infty}^{\infty} R_p(r,\tau)\, e^{-i\omega\tau} = \frac{L_x^2 L_y^2}{r^2 \pi^4} \sum_m \sum_n \frac{K_{mn}}{m^2 n^2} [(-1)^m - 1]^2 [(-1)^n - 1]^2 \frac{1}{2\pi} \cdot$$

$$\cdot \int_{-\infty}^{\infty} e^{-a_{mn}|\tau|} [C_{mn} \cos \omega_{mn}\tau + D_{mn} \sin \omega_{mn}|\tau|]\, e^{-i\omega\tau} d\tau$$

Note that Equation (C27) and what followed held for $\tau > 0$. To obtain S_p here, we treat τ in the infinite range $(-\infty, \infty)$ hence $\tau \rightarrow |\tau|$ above. Using Table 3.3 of Reference 31 we obtain directly the *value of the integral* as*

$$= \left[\frac{a_{mn} c_{mn} + d_{mn}(\omega + \omega_{mn})}{a_{mn}^2 + (\omega + \omega_{mn})^2} + \frac{a_{mn} c_{mn} - d_{mn}(\omega - \omega_{mn})}{a_{mn}^2 + (\omega - \omega_{mn})^2} \right]$$

and from Equations (C19) and (C27)

$$a_{mn} = B\,\omega_{mn}$$

$$C_{mn} = \omega_{mn}^4 - 6\omega_{mn}^2 a_{mn}^2 + a_{mn}^4 = \omega_{mn}^4 - 6B\omega_{mn}^4 + B^4 \omega_{mn}^4 = \omega_{mn}^4 (1 - 6B^2 + B^4)$$

$$D_{mn} = 4a_{mn}\, \omega_{mn} (a_{mn}^2 - \omega_{mn}^2) = 4B\omega_{mn}^2 (B^2 \omega_{mn}^2 - \omega_{mn}^2)$$

Substituting the values of a_{mn}, C_{mn}, and D_{mn} in the equation directly above and dropping terms of higher order in B, i.e., $0(B^5)$ and $0(B^3)$ reduces this equation to

---

*We take one-half the value given in this table since we use $-\infty \leq \omega < \infty$ here whereas Reference 31 gives the one-sided power spectral density function.

$$\omega_{mn}^3 B\left[\frac{4\dfrac{\omega}{\omega_{mn}}-3}{B^2+\left(1+\dfrac{\omega}{\omega_{mn}}\right)^2}-\frac{3+4\dfrac{\omega}{\omega_{mn}}}{B^2+\left(1-\dfrac{\omega}{\omega_{mn}}\right)^2}\right]$$

Using this value and the value of K_{mn}, $\overleftarrow{K}_{mn}$ given by Equations (C28) and (C27), respectively, we get

$$S_p(r,\omega) = \frac{1}{4\pi^7}\left(\frac{L_xL_y}{r^2}\right)\frac{\rho_i^{\,2}A\theta\overline{p^2}}{M^2}\sum_m\sum_n[1-(-1)^m]^2[1-(-1)^n]^2 \; .$$

$$\cdot\frac{1}{(1+\omega_{mn}^2\theta^2)\,m^2n^2}\left[\frac{4\dfrac{\omega}{\omega_{mn}}-3}{B^2+\left(1-\dfrac{\omega}{\omega_{mn}}\right)^2}-\frac{3+4\dfrac{\omega}{\omega_{mn}}}{B^2+\left(1+\dfrac{\omega}{\omega_{mn}}\right)^2}\right]$$

In accordance with Reference 2, we take

$$A=\frac{2\pi}{\kappa^2}=\frac{2\pi}{(2/\delta^*)^2}=\frac{\pi(\delta^*)^2}{2}\;,\;\theta=\frac{30\,\delta^*}{U_0}\;,\;\overline{p^2}=(3\times10^{-3})^2\,\rho_i^{\,2}\,U_0^4$$

Substituting these values in the equation for $S_p(r,\omega)$, the nondimensional power spectrum at r is then represented by*

$$\frac{S_p(r,\omega)}{\rho_i^2\,U_0^3\,\delta^*}=\underbrace{\frac{33.75\times10^{-6}}{\pi^6}}_{=\,\mathrm{K}}\left(\frac{L_xL_y}{r^2}\right)\left(\frac{\rho_i\,\delta^*}{M}\right)^2\sum_m\sum_n[1-(-1)^m]^2[1-(-1)^n]^2$$

$$\cdot\frac{1}{(1+\omega_{mn}^2\,\theta)\,m^2n^2}\left[\frac{4\dfrac{\omega}{\omega_{mn}}-3}{B^2+\left(1-\dfrac{\omega}{\omega_{mn}}\right)^2}-\frac{3+4\dfrac{\omega}{\omega_{mn}}}{B^2+\left(1+\dfrac{\omega}{\omega_{mn}}\right)^2}\right] \qquad \text{(C38)}$$

---

*Note that Equation (C38) does not agree with Equation (6-38) of Reference 26 which appears to contain a typrographical error.

or

$$\overline{S}_p(r, \omega) = \sum_m \sum_n K'(\omega_{mn}) \, \Phi\left(\frac{\omega}{\omega_{mn}}\right) \qquad \text{(C39)}$$

Thus $\overline{S}_p(r, \omega)$ is the product of a modal amplitude factor $K'(\omega_{mn})$ and a spectrum shape factor $\Phi\left(\frac{\omega}{\omega_{mn}}\right)$.

APPENDIX C2 – METHOD FOR DETERMINING INPUT DATA

The method for determining input data for the Electric Boat Computer Program is the same as the Dyer method (Appendix A), and the system of units is consistent with Dyer.

APPENDIX C3 – PROGRAM IDENTIFICATION

This program computes the space-time cross correlation and cross-spectral density of the acoustic pressures resulting from the vibration of a turbulence-excited finite plate of arbitrary boundary conditions.

APPENDIX C

TABLE 4

Identification for Electric Boat Program – IZZO

This table includes input and output data identification, flow chart, order of input data, and computer running times. Computer program listings are given in Table 5.

Table 4A: Input Data

Table 4B: Output Data

Table 4C: Flow Chart (Electric Boat) for Turbulence – Excited Clamped and Simply Supported Plate Problem

Table 4D: Input Formats

TABLE 4A

Input Data

Input Data	Description	Type	Program Symbol
Description for Main Program			
M	Order of m-mode numbers	Integer	MM
N	Order of n-mode numbers	Integer	NN
IM	= 1: m's and n's are read as a vector = MM: m's and n's are read as a matrix such as A(1,1), A(1,2) A(1,3), A(2,1), A(2,2), A(2,3)	Integer	IM
IN	NN	Integer	IN
NXYZ	Number of cases in autocorrelation	Integer	NXYZ
KXYZ	Number of cases in CROSS1-correlation	Integer	KXYZ
LXYZ	Number of cases in CROSS2-correlation	Integer	LXYZ
NAUTO	1: Access to autocorrelation 0: No	Integer	NAUTO
NCROSS	1: Access to CROSS1-correlation 0: No	Integer	NCROSS
NCROST	1: Access to CROSS2-correlation 0: No	Integer	NCROST
XL1	Upper-first-integration limit (plate dimension x)	Decimal	XL1
XL0	Lower-first-integration limit	Decimal	XL0
YL1	Upper-second-integration limit (plate dimension y)	Decimal	YL1
YL0	Lower-second-integration limit	Decimal	YL0
AI	Speed of sound in fluid	Decimal	AI
B	$\beta\omega_{mn}$ = damping coefficient $- \alpha_{mn}$	Decimal	B
C	Constant a) simply supported plate b) nonsimply supported	Decimal	C
θ	Decay constant = δ^* / U_∞	Decimal	THETA
p^{2*}	(rms press.)^2 $(lb/ft^2)^2 = (6 \times 10^{-3} \cdot 1/2 \rho U_\infty^2)^2$ where ρ = mass density of fluid	Decimal	P2
$\omega_{m,n}$	Frequencies for (m,n) modes (radians)	Decimal	W
MAM	m-mode shape numbers	Integer	MAM
NAN	n-mode shape numbers (MAX-50)	Integer	NAN
α_m	Normalized eigenfunction	Decimal	ALMM
a_m	parameters; used only	Decimal	AMM
b_m	in the general	Decimal	BMM
c_m	(i.e., clamped) case;	Decimal	CMM
d_m	for m-mode	Decimal	DMM
α_n		Decimal	ALNN
a_n	Same as above,	Decimal	ANN
b_n	only for n-node	Decimal	BNN
c_n		Decimal	CNN
d_n		Decimal	DNN

*Force → lb, hence mass = $\frac{\text{force}}{\text{acceleration}} \rightarrow \frac{\text{lb}}{\text{ft/sec}^2}$; also length → ft and time → sec.
This system of units is consistent with that of Dyer.

TABLE 4A (Continued)

Input Data	Description	Type	Program Symbol
Description for Subroutine Autocorrelation (Time and Frequency Dependent)			
x	Coordinates of point	Decimal	X
y	for correlation	Decimal	Y
z	measurement	Decimal	Z
τ_0	Initial value of τ	Decimal	TAU
$\Delta\tau$	Increment of τ	Decimal	DTAU
NTAU	Number of τ's	Integer	NTAU
EPS	Convergence constant (test value)	Decimal	EPS
NMAX	Maximum number of iterations	Integer	NMAX
NWA	Number of specified frequencies	Integer	NWA
WA	Specified frequencies (radians) chosen by user according to his boundary specifications	Decimal	WA
Comment: There are NXYZ sets of data cards for this subroutine.			
Description for Subroutine Cross Correlation Space Dependent			
x		Decimal	XX
y	Coordinates of fixed point	Decimal	YY
z		Decimal	ZZ
MXP	Number of variable points	Integer	MXP
MTAU	Number of τ's	Integer	MTAU
EPS	Convergence constant	Decimal	EPS
NMAX	Maximum number of iterations	Integer	NMAX
τ	Value of τ	Decimal	TAU
x'		Decimal	XP(I)
y'	Coordinates of variable points	Decimal	YP(I)
z'		Decimal	ZP(I)
NOR	= 0	Integer	NOR
Comment There are KXYZ sets of input cards for this subroutine.			
Description for CROSS 2 Correlation (Time and Frequency Dependent)			
x		Decimal	XX
y	Coordinate of fixed point	Decimal	YY
z		Decimal	ZZ
MXP	Number of variable points	Integer	MXP
TAU	Initial value of τ	Decimal	TAU
DTAU	Increment of $\Delta\tau$	Decimal	DTAU
NTAU	Number of τ's	Integer	NTAU
EPS	Convergence constant	Decimal	EPS
NMAX	Maximum number of iterations	Integer	NMAX
NWA	Number of frequencies	Integer	NWA
x'		Decimal	XP(I)
y'	Coordinate of variable point	Decimal	YP(I)
z'		Decimal	ZP(I)
NOR	= 0		NOR
WA	Different frequencies (radians) chosen by user		
Comment: There must be LXYZ sets of input cards.			

TABLE 4B

Output Data

Description	Program Label	Output Label
Description for AUTO 1 Autocorrelation with Two Options (1. NTAU - no. points of time; 2. NWS - no. frequencies)		
Number of time increments	K	NTAU
Point of time at which auto-correlation taken	ATAU	TAU
Normalized autocorrelation of acoustic pressure over time, i.e., $RP(x_1 - x_2, \tau) / RP(x_1 - x_2, 0)$	RPBAR(K)	NORM. COR. OF ACC. PRES.
Autocorrelation normalized by rms pressure	PRP(K)	RP(K)/P2
Normalized factor RP(1) for RPBAR(K), i.e., $RP(x_1 - x_2, 0)$ or $R_{11}(0,0)$	RP(1)	NORM. FACTOR
Comment: Above not printed out if NTAU - 0		
Number of frequency	K	K
Specified frequencies	WA(K)	FREQ
WA(K)/2π	RAD	RAD/SEC
Cross spectral density	FI(K)	CROSS SPEC. DENS.
10 LOG(FI(K)) + 127.6	PHI	DB(RE0.0002)
Comment: Above not printed out if NWA 0		
Description for CROSS 1 (for Various Times in Space)		
Indicates time	I	I
Point of time at which cross-correlation computed	TAU(I)	TAU
Indicates space	J	J
Space coordinates	XP(J) YP(J) ZP(J)	XP(J) YP(J) ZP(J)
Normalized cross-correlation	CRPBAR(I,J)	CRPBAR(I,J)
Normalization factor - CRPBAR(1,1)	CNORM	CNORM
Description for CROSS 2 (Time Variable)		
Number of time point	K	NTAU
Point of time	TAU	TAU
Normalized correlation of acoustic pressure, by $RP(x_1 - x_2, 0)$ or $R_{12}(0,0)$	RPBAR(K)	NORM. CORR. OF ACC. PRESS.
Correlation normalized by rms pressure	RP(K)/P2	PRP(K)
Normalization factor $RP(x_1 - x_2, 0)$	RP(1)	NORM. FACTOR
Number of frequency	K	K
Specified frequency	WA(K)	FREQ
Frequency /2π	RAD	RAD/SEC
Cross spectral density	FI(K)	CROSS SPEC. DENS.
10 LOG(FI(K) + 127.6	PHI	DB(RE0.0002)

Interpretation of Data Output and Computer Running Times

The following information is useful in interpreting the program.

The program generally yields results normalized by p^2 or by the correlation of two points at $\tau = 0$.

The Electric Boat program consists of two parts which represent the simple case and the general case. The simple case, Equation (C(35)), uses only simply supported boundaries for the plate modal function although frequencies for clamped boundaries may be used. This procedure yielded Figure 12 (see page 154). The general case uses mode shapes represented by Equation (C(26)). In addition the program requires either of the following values for C

$$C = \frac{P_0^2 A p^2}{2\pi^2 M^2 L_x L_y} \qquad \text{(simply supported boundaries)}$$

$$C = \frac{P_0^2 A p^2}{8\pi^2 M^2} \qquad \text{(clamped-clamped boundaries)}$$

Figure 12 (Figure 17 in Reference 26), is normalized by $R_{11}(0,0)$, that is, the autocorrelation function of the fixed point x_1 at $\tau = 0$. Therefore, the nonnormalized correlation for each $\Delta x, \tau$ desired was abstracted from the program and divided by $R_{11}(0,0)$ to yield this curve. Similarly, calculations were necessary to obtain the data in the form used in Figure 13 (Figure 15 in Reference 26); see page 207 of this report. The program yields a normalized answer in CROSS2, which is not in suitable form for representing the curve as shown. Therefore, the normalized program result is manually multiplied by the NORM FACTOR to give a non-normalized quantity $R_{12}(\Delta X, \tau)$; see equation below. More precisely, this is accomplished by first multiplying the number in the upper right corner labeled "NORM FACTOR =". by the corresponding quantity in the column labeled "NORM. CORR. OF. ACC. PRESS,". Only $\tau = 0$ was used for this curve so that the corresponding quantity would appear in the line for TAU = 0. The second step is to get the normalization factors from AUTO 1, which must have as many cases as there are variable points in CROSS2. $R_{11}(0,0)$ refers to $R(x_1 - x_1, \tau = 0)$ for all cases where 11 is a fixed reference point in the longitudinal direction, but $R_{22}(0,0)$ refers to $R(x_2 - x_2, \tau = 0)$ where 22 is any other point in the longitudinal direction. The corresponding cross points are denoted by 12 in the correlation function, i.e., $R_{12}(\Delta x, \tau)$. The quantity to be used from AUTO 1 is labeled "NORM.FACTOR =".

The total function plotted then becomes

$$\frac{\text{NORM.CORR. OF ACC.PRESS. (from (CROSS2))} \times \text{NORM.FACTOR (CROSS2)}}{\sqrt{\text{NORM.FACTOR (AUTO1 with } X_1) \times \text{NORM.FACTOR (AUTO1 with } X_2)}}.$$

The major subroutines results and running times on the IBM 7090 are:

AUTO 1	CROSS 1	CROSS 2
1. Autocorrelation	1. Cross correlation keeping time constant	1. Cross correlation, varying time and/or space
2. Auto power spectrum	2. Not Applicable	2. Power spectrum for first point
Approximately 3 min per case (i.e., point)	Approximately 3 min for 1 point, 1 time (see CROSS2)	Approximately 1.5 min per variable point over 120 time increments

The printout yields intermediate results, such as integration sums and nonnormalized, noncumulative results for each mode. For example, 37 modes would imply 37 sets of these results, followed by the normalized answers for each of the major subroutines. For the auto-spectrum final results, the labels FREQ. and RAD/SEC should be interchanged.

TABLE 4C

Flow-Chart (Electric Boat) Turbulence-Excited, Clamped and Simply Supported Plate Problem

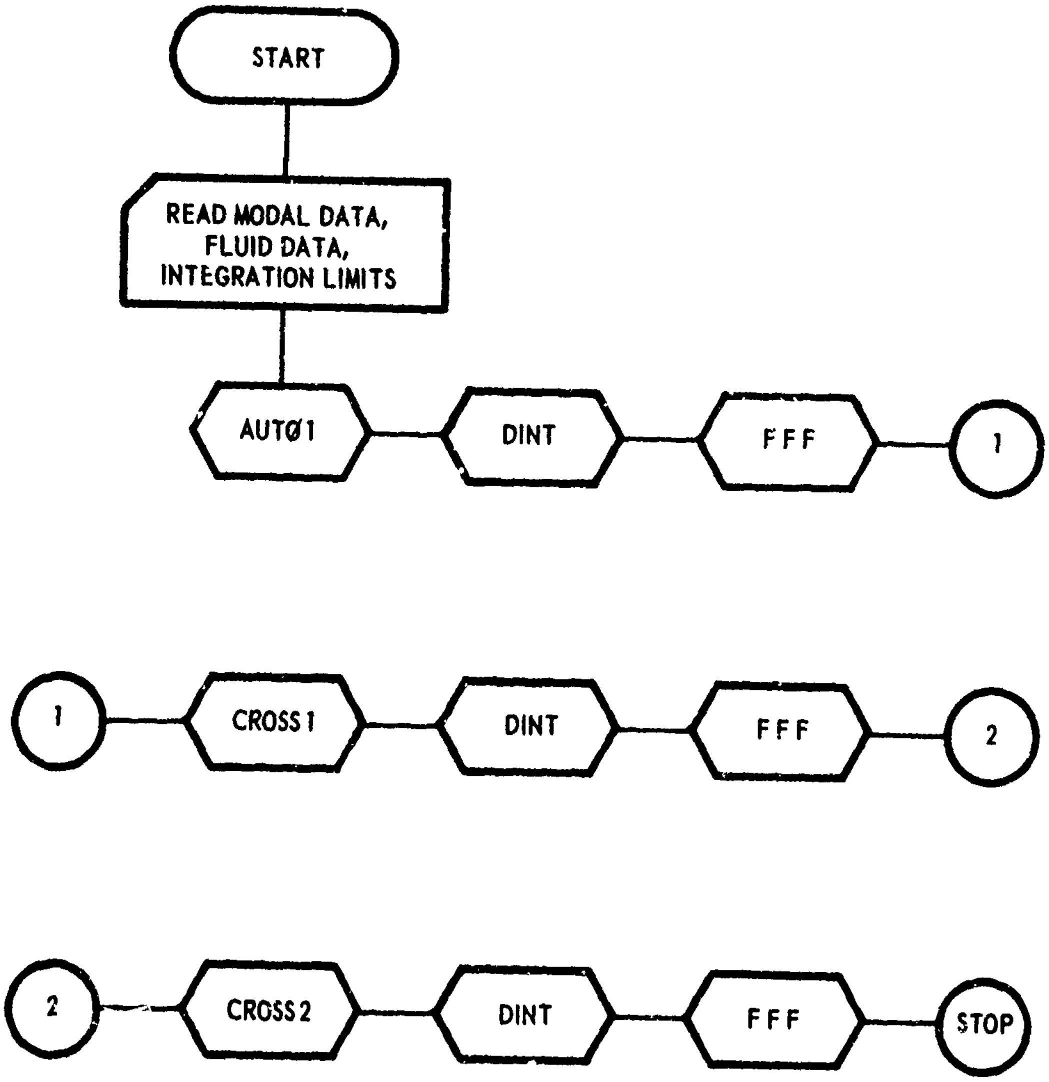

TABLE 4C (Continued)

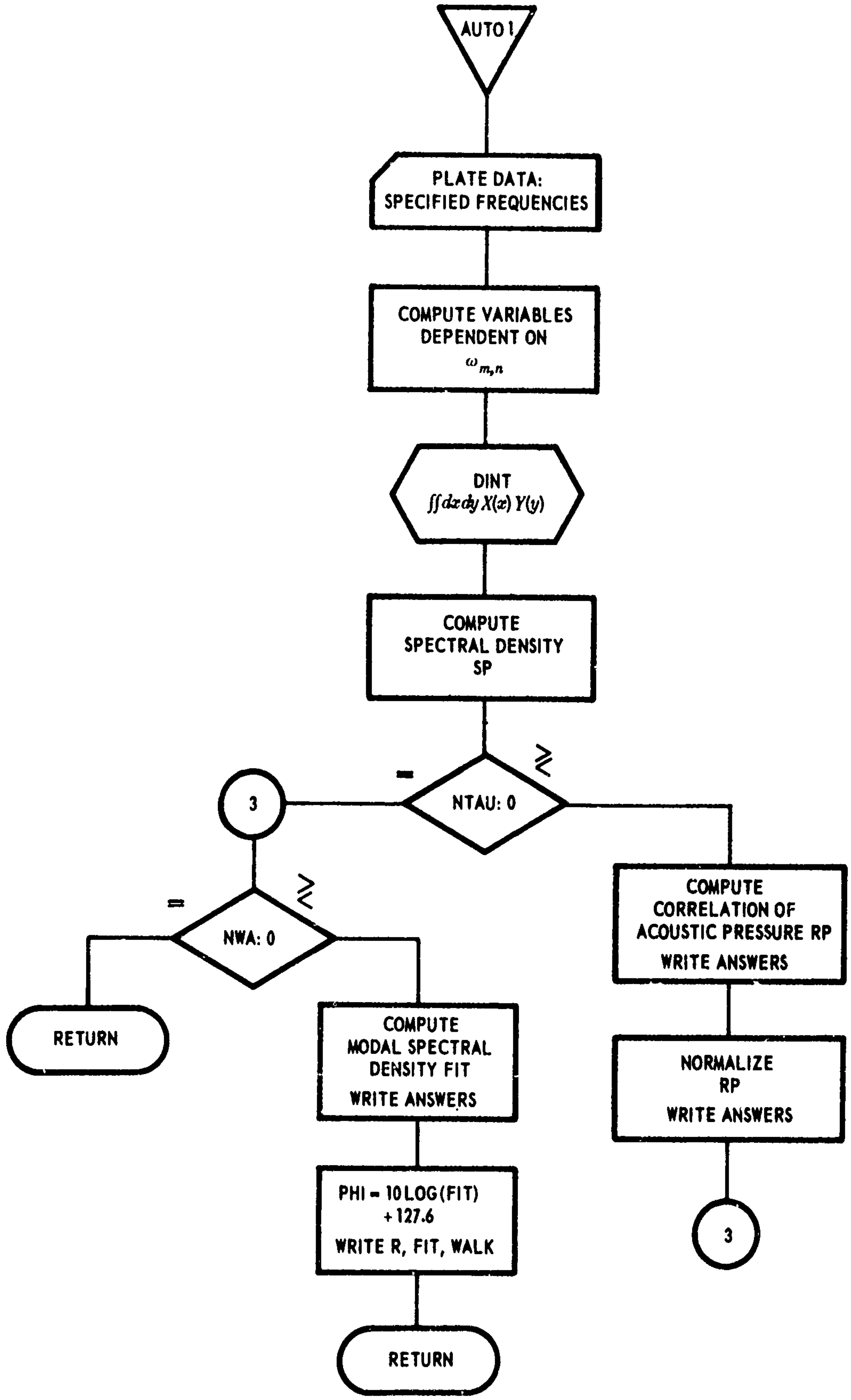

TABLE 4C (Continued)

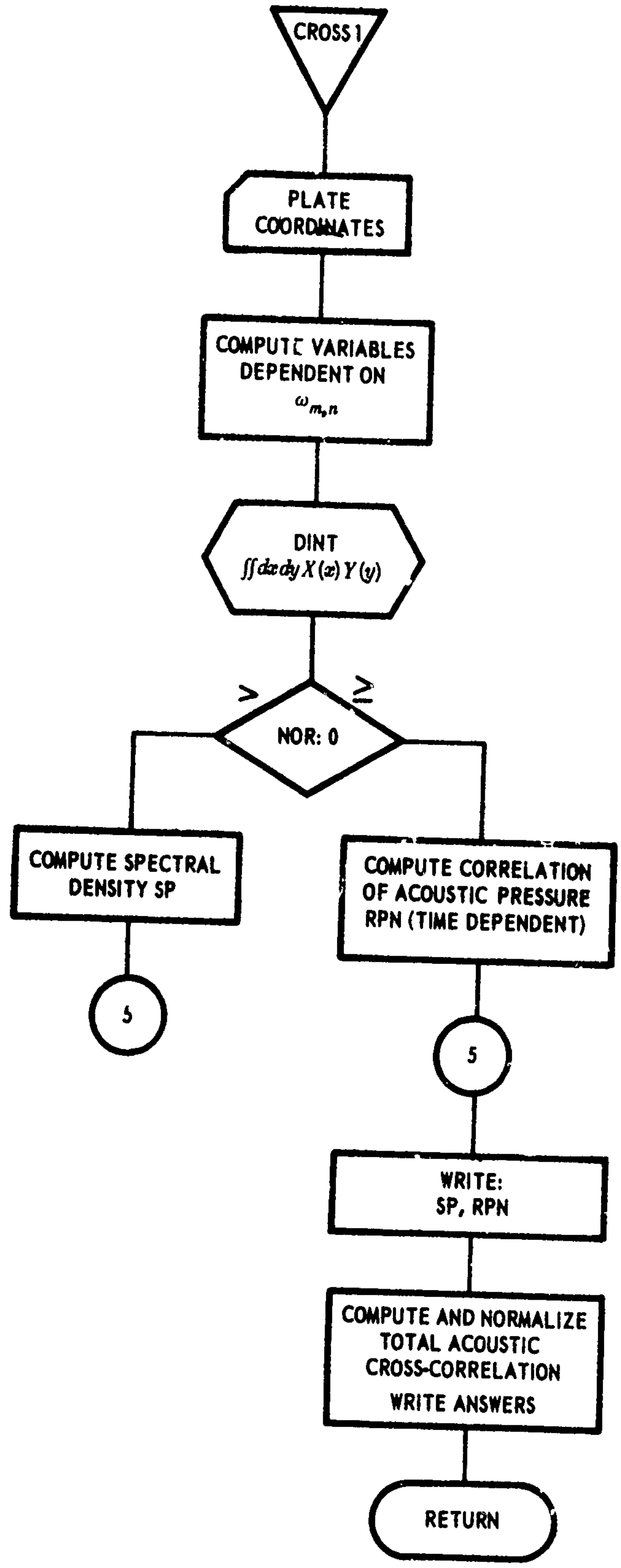

TABLE 4C (Continued)

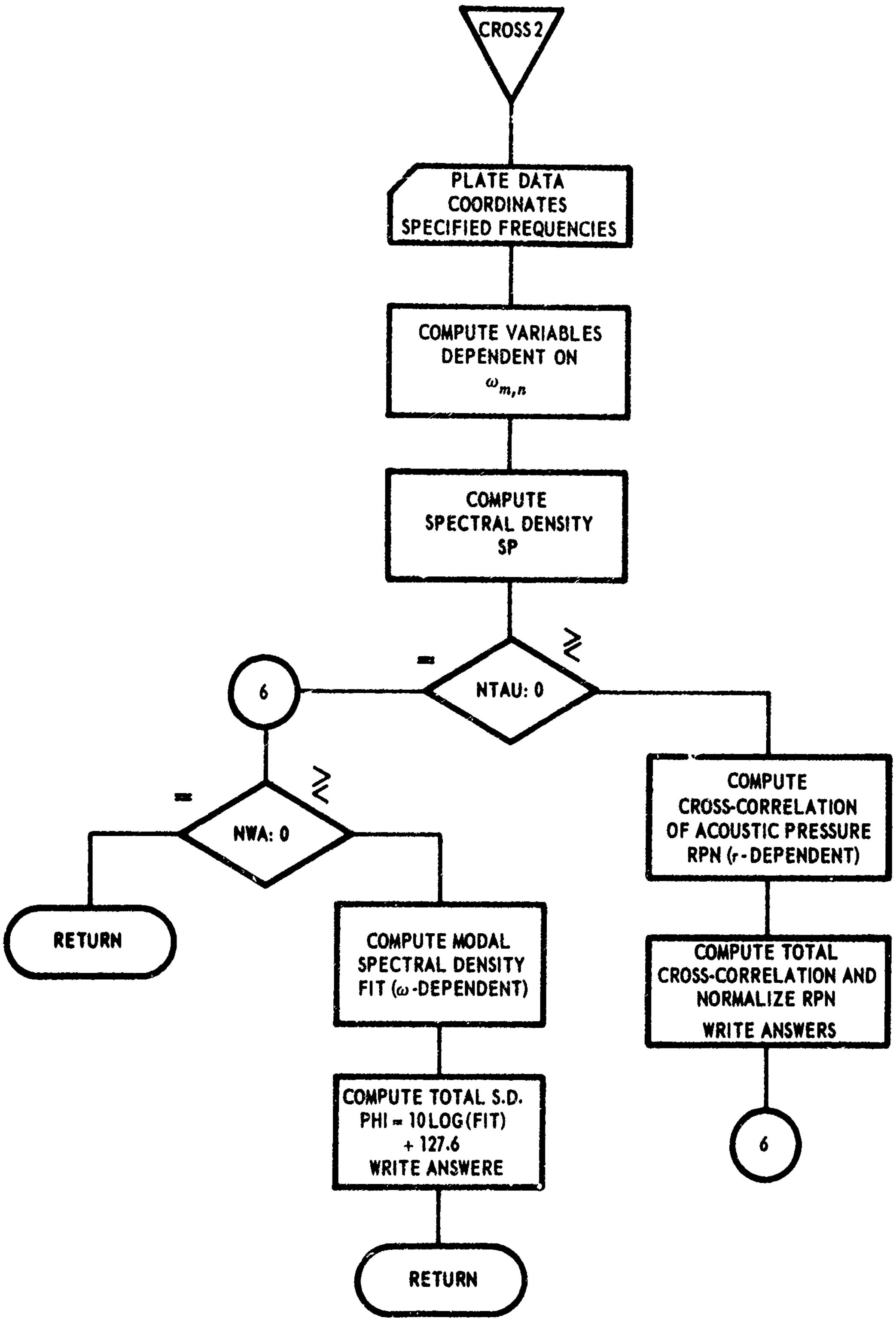

TABLE 4C (Continued)

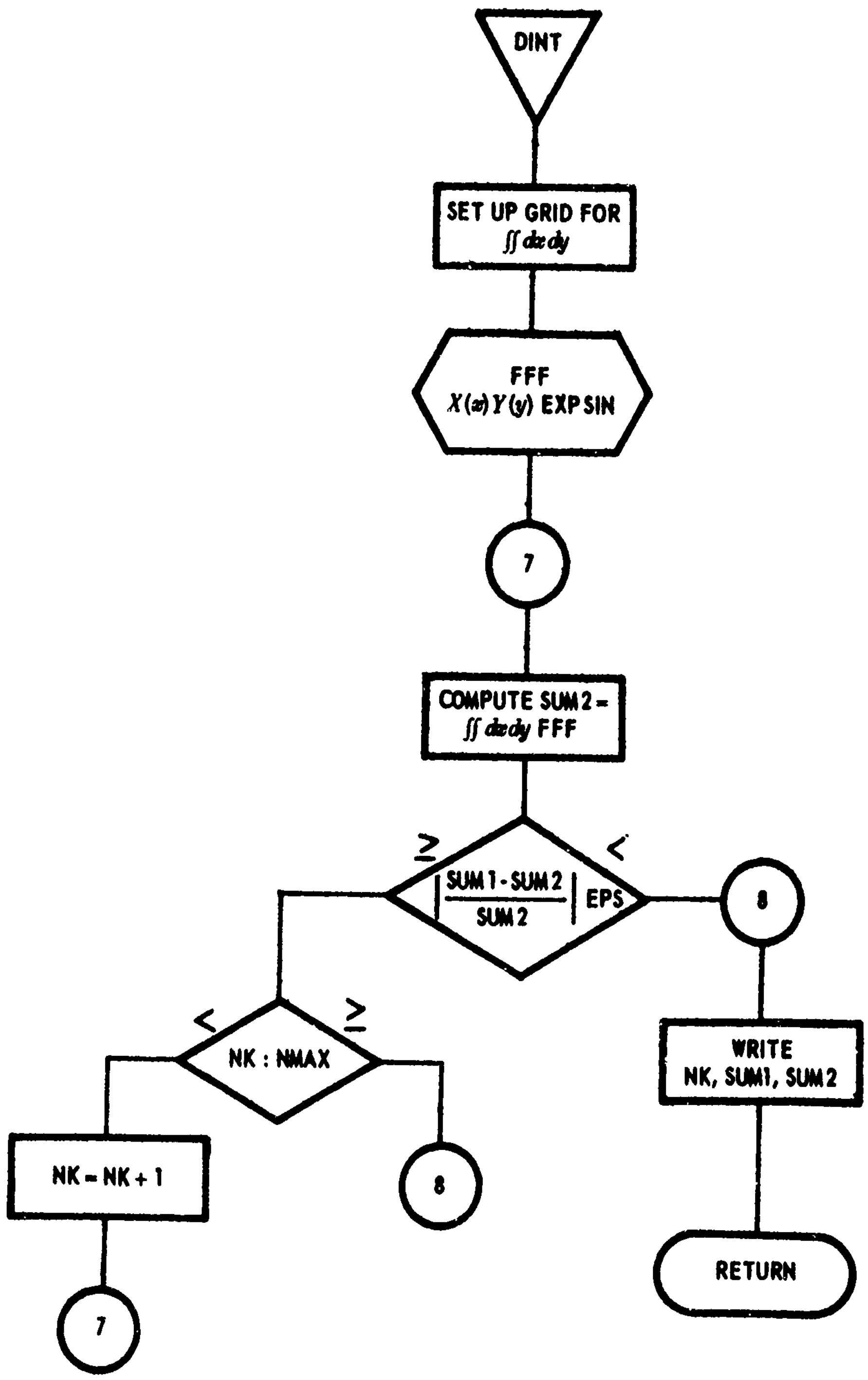

TABLE 4D

Input Format for Main Program, General Case

TITLE

10 20 30 40 50 60 70 80

TITLE

10 20 30 40 50 60 70 80

Columns 1–40, below, contain respectively, in 4-column blocks: MM; NN; IM; IN; NXYZ; KXYZ, LXYZ; NAUTO; NCROSS: NCROST

4 8 12 16 20 24 28 32 36 40 60 80

XL1 12 XL0 24 YL1 36 YL0 48 60 80

AI 15 B 30 C 45 THETA 60 P2 75 80

IM x IN sets of 6-column blocks are needed for the W(IM,IN) array: w(1,1); w(1,2); . . . ; w(1,IN); w(2,1); . . . , w(2,IN); . . . , w(IM,IN)

W array 6 12 18 24 30 36 42 48 54 60 66 72 80

(MM + NN) /20 cards are needed to complete arrays MAM(MM) and NAN(NN): MAM(1); MAM(2); . . . ; MAM(MM); NAN(1); NAN(2); . . . ; NAN(NN)

4 8 12 16 20 24 28 32 36 40 44 48 52 56 60 64 68 72 76 80

MM cards are needed to complete the following arrays: (used in general case only)

ALMM(1) 15 AMM(1) 30 BMM(1) 45 CMM(1) 60 DMM(1) 75 80

ALMM(MM) 15 AMM(MM) 30 BMM(MM) 45 CMM(MM) 60 DMM(MM) 75 80

NN cards are needed to complete the following arrays: (used in general case only)

ALNN(1) 15 ANN(1) 30 BNN(2) 45 CNN(1) 60 DNN(1) 75 80

ALNN(NN) 15 ANN(NN) 30 BNN(NN) 45 CNN(NN) 60 DNN(NN) 75 80

TABLE 4D (Continued)

INPUT FORMAT FOR SUBROUTINE AUTO 1

X	Y	Z	TAU	DTAU	NTAU	EPS	NMAX	NWA	
12	24	36	48	60	64	70	74	78	80

NWA/12 cards are needed to complete the WA(NWA) array:

WA(1)	WA(2)	. . .		. . .							WA(12)	
6	12	18	24	30	36	42	48	54	60	66	72	80

INPUT FORMAT FOR SUBROUTINE CROSS 1

XX	YY	ZZ	MXP	MTAU	EPS	NMAX		
12	24	36	42	48	60	66	72	80

MTAU/6 cards are needed to complete the TAU(MTAU) array:

TAU(1)	TAU(2)	. . .	. . .	. . .	TAU(6)	
12	24	36	48	60	72	80

MXP/2 cards are needed to complete the following arrays:

XP(1)	YP(1)	ZP(1)	NOR(1)	XP(2)	YP(2)	ZP(2)	NOR(2)
12	24	36	40	52	64	76	80

TABLE 4D (Continued)

INPUT FORMAT FOR SUBROUTINE CROSS 2

XX	12	YY	24	ZZ	36	MXP	39	TAU	51	DTAU	63	NTAU	66	EPS	72	NMAX	75	NWA	78		80

MXP/2 cards are needed to complete the following arrays:

XP(1)	12	YP(1)	24	ZP(1)	36	NOR(1)	40	XP(2)	52	YP(2)	64	ZP(2)	76	NOR(2)	80

NWA/12 cards are needed to complete the WA(NWA) array:

WA(1)	WA(2)	...	...	...	...	...	...	...	...	...	WA(12)	
6	12	18	24	30	36	42	48	54	60	66	72	80

APPENDIX C4 – TEST RUNS

Test runs for the power spectrum, longitudinal correlation function, and longitudinal space-time correlation function of the acoustic pressures are plotted in Figures 12, 13, and 14. The computer programs used to obtain these results have been given in Table 4, and the computer listings are presented in Table 5.

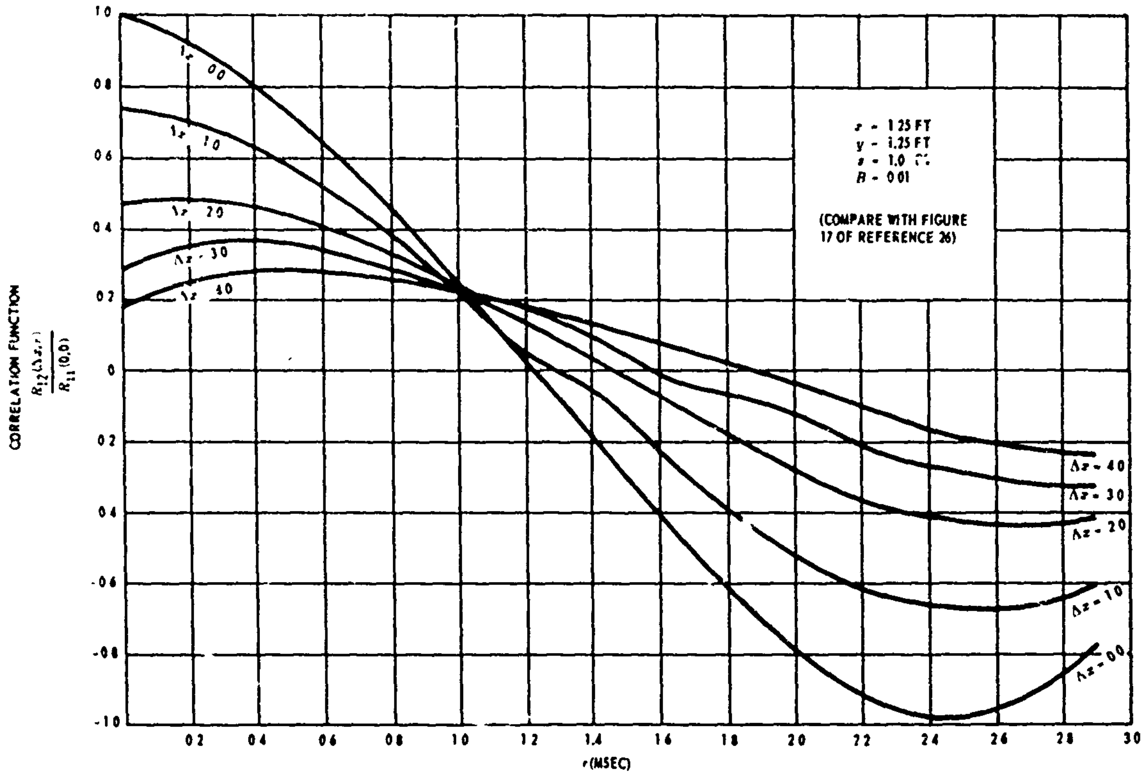

Figure 12a – Clamped-Clamped Steel Plate

This subfigure is based on the use of frequencies obtained for a clamped-clamped plate but modes obtained for a simply supported plate. (see statement following Equation (C34))

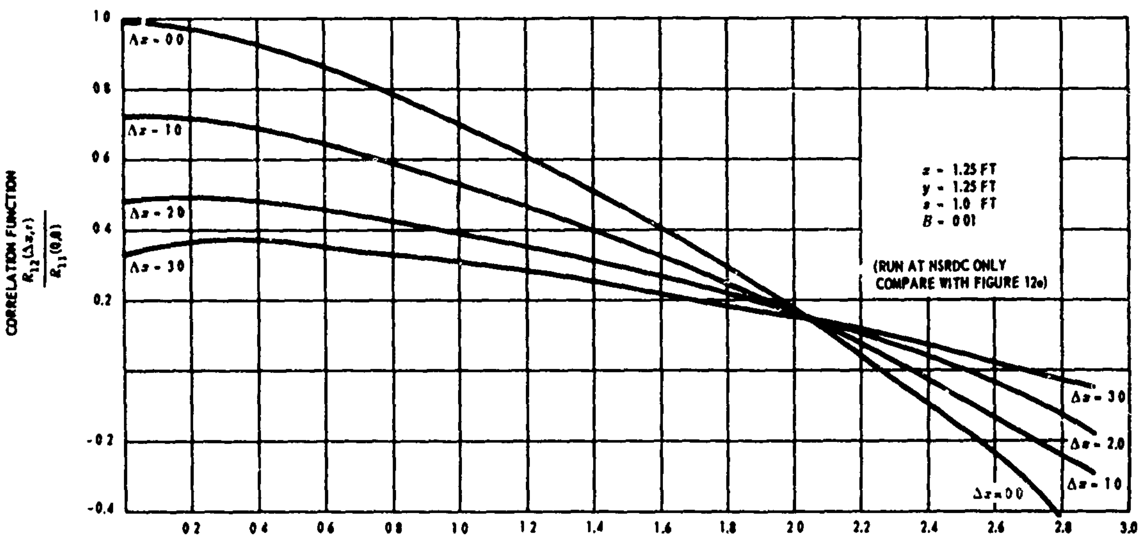

Figure 12b – Simply Supported Steel Plate

This subfigure is based on the use of frequencies and mode shapes obtained for a simply supported plate.

Figure 12 – Longitudinal Space-Time Correlation Function for a 2-Foot × 2.33-Foot × 3/8-Inch Steel Plate

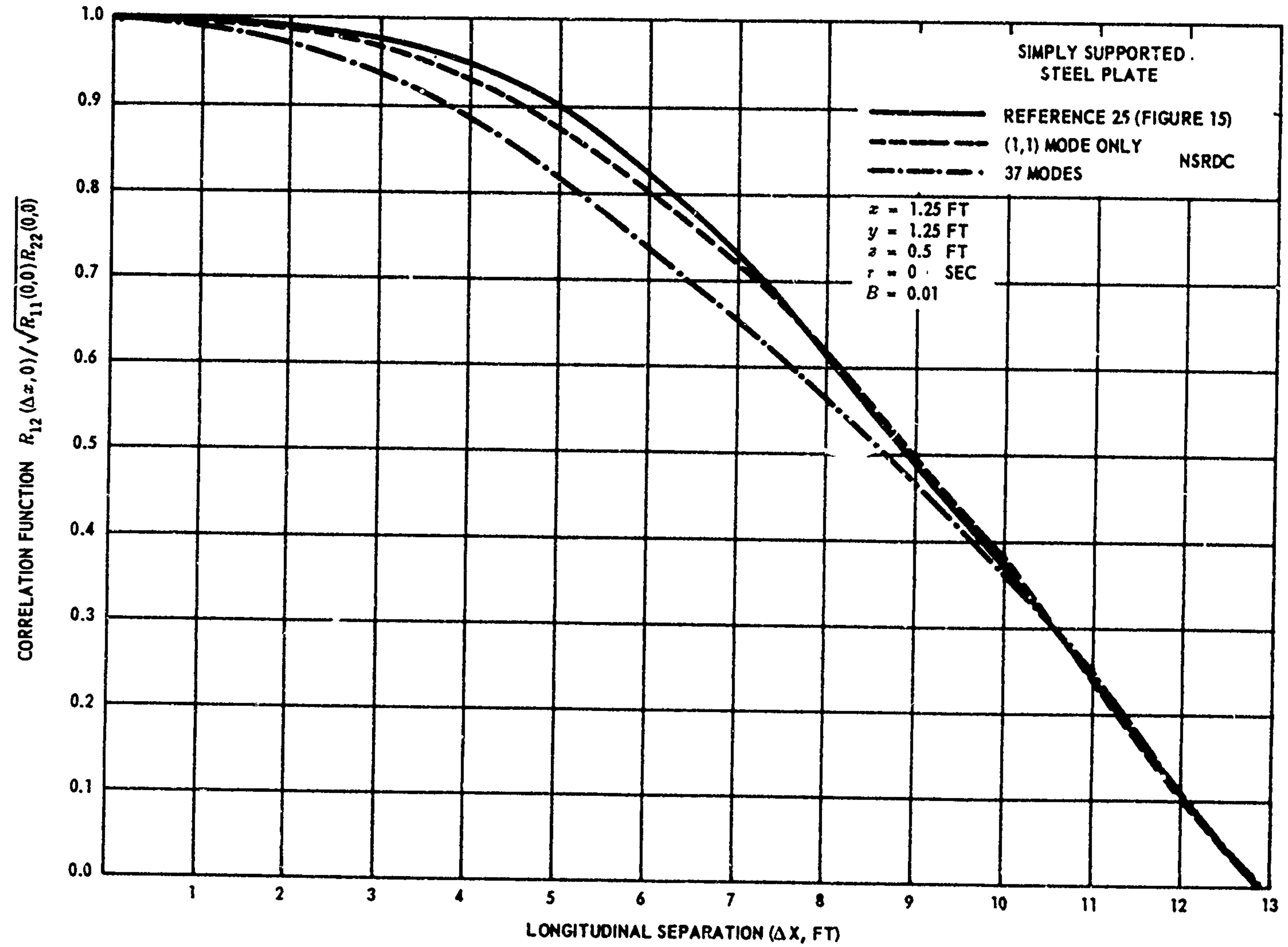

Figure 13 – Longitudinal Correlation Function for a 2-Foot × 2.33-Foot × 3/8-Inch Steel Plate

Comparison of the results obtained using the (1,1) mode only and using 37 modes shows the error involved, over the longitudinal range, in neglecting the contributions of the higher modes to the correlation.

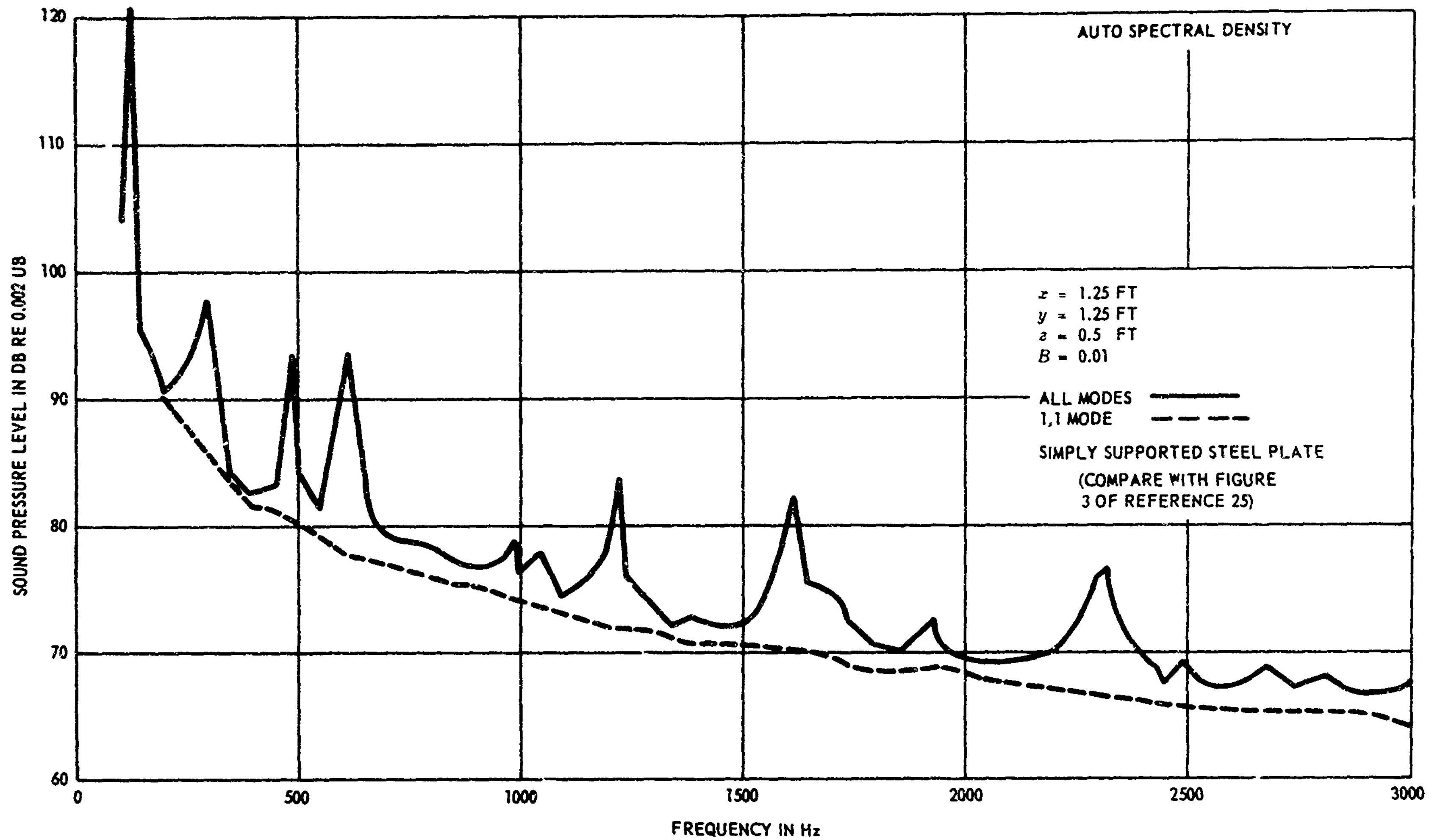

Figure 14 – Computed Power Spectrum for a 2-Foot × 2.33-Foot × 3/8-Inch Steel Plate

TABLE 5

Computer Listings for Electric Boat Program – Izzo

Table 5A – Simply Supported Boundaries

```
$IBFTC TURAD2
C
C
 1000 FORMAT(12A6)
 1001 FORMAT(10I4)
 1002 FORMAT(4E12.6/5E15.8)
 1003 FORMAT(12F6.0)
 1004 FORMAT(20I4)
 1005 FORMAT(5E15.8)
C
 2000 FORMAT(1H1,10X,6HF.P.S.,15X,12A6/22X,12A6////)
 2001 FORMAT (1H0,29X,45HORDER OF M (MODE NUMBERS) .............. MM =,I
     16/30X,45HORDER OF N (MODE NUMBERS) .............. NN =,I6/30X,
     245HNUMBER OF CASES  (XYZ) IN AUTO CORR... NXYZ =,I6/30X,45HNUMBER
     3OF CASES  (XYZ) IN CROSS CORR.. KXYZ =,I6 /       30X,45HAUTO CO
     4RRELATION CONSTANT ..........  NAUTO =,I6/30X,45HCROSS CORRELATION
     5CONSTANT .......... NCROSS =,I6/30X,45HLIMITS OF THE 1-ST INTEGRAL
     6 ........... XL1 =,F11.4/30X,45H
     7      XL0 =,F11.4/30X,45HLIMITS OF THE 2-ND INTEGRAL ........... Y
     8L1 =,F11.4/30X,45H                                        YL0 =,F1
     91.4/30X,45HSPEED OF SOUND IN WATER ................ AI =,F13.6/30X
     A,45HDAMPING CONSTANT ........................ B =,F13.6/30X,45HC
     BCONSTANT ............................ C =,F13.6/30X,45HTEMPORAL D
     CECAY FACTOR OF TURBULENCE   THETA =,F11.4/30X,45HR.M.S. PRESSURE .
     D...................... P2 =,F13.6//30X,2I10)
 2002 FORMAT(1H0,40X,35HUNDAMPED NATURAL FREQUENCIES W(M,N)//(10X,10F8.0
     X))
 2003 FORMAT(1H0,50X,12HMODE NUMBERS//(40X,10I5))
 2005 FORMAT(1H0,40X,35HNORMALIZED EIGENFUNCTION PARAMETERS //(15X,5E18.
     18) )
 2006 FORMAT(1H0,29X,45HNUMBER OF CASES IN CROSS CORR. (TIME).. LXYZ=,
     1I6/30X,45HCROSS CORR. (TIME) CONSTANT ......... NCROST=,I6//
     230X,2I10)
C
C
      COMMON /AAA/A(4000)
C
```

```
      EQUIVALENCE (A(1),MM),(A(2),NN),(A(3),IM),(A(4),IN),(A(5),NXYZ),
     1(A(6),KXYZ),(A(7),NAUTO),(A(8),NCROSS),(A(9),M),(A(10),N) ,
     2(A(11),LXYZ),(A(12),NCROST,
C
      EQUIVALENCE (A(21),XL1),(A(22),XLO),(A(23),YL1),(A(24),YLO),
     1(A(25),AI),(A(26),B),(A(27),C),(A(28),THETA),(A(29),P2),(A(30),PI)
     2,(A(31),X),(A(32),Y),(A(33),Z),(A(34),EPS),(A(35),NMAX),
     3(A(36),WMN),(A(37),AMN),(A(38),SUM1),(A(39),SUM2)
C
      EQUIVALENCE (A(101),MAM),(A(151),NAN),(A(1001),W)
C
C
      DIMENSION TITLE(24),W(20,50),MAM(50),NAN(50)
C
      REAL KMN
C
C  READ AND PRINT TITLE
C
      READ (5,1000) (TITLE(I),I=1,24)
      WRITE(6,2000) (TITLE(I),I=1,24)
C
C  READ AND PRINT GENERAL INPUT CONSTANTS
C
      READ (5,1001) MM,NN,IM,IN,NXYZ,KXYZ,LXYZ,NAUTO,NCROSS,NCROST
      READ(5,1002) XL1,XLO,YL1,YLO,AI,B,C,THETA,P2
      READ (5,1003) ((W(I,J),J=1,IN),I=1,IM)
      READ (5,1004) (MAM(I),I=1,MM),(NAN(I),I=1,NN)
C
      WRITE(6,2001) MM,NN,NXYZ,KXYZ,NAUTO,NCROSS,XL1,XLO,YL1,YLO,AI,B,
     1C,THETA,P2
      WRITE(6,2006) LXYZ,NCROST,IM,IN
      WRITE(6,2002) ((W(I,J),J=1,IN),I=1,IM)
      WRITE(6,2003) (MAM(I),I=1,MM),(NAN(I),I=1,NN)
C
C
      PI=3.14159
C
```

TABLE 5A (Continued)

```
C  AUTO CORRELATION
C
      IF (NAUTO.EQ.1) CALL AUTO1
C
C
C  CROSS CORRELATION
C
      IF (NCROSS.EQ.1) CALL CROSS1
C
C
C  CROSS CORRELATION (TIME)
C
      IF (NCROST.EQ.1) CALL CROSS2
C
C
      STOP
      END
$IBFTC XAUTO1
      SUBROUTINE AUTO1
C
C
C
C
C  AUTO CORRELATION)  X=XP , Y=YP , Z=ZP
C
C
 3000 FORMAT(5E12.6,I4,E6.2,2I4)
 3001 FORMAT(12F6.0)
C
 4000 FORMAT(1H1,50X,16HAUTO CORRELATION///30X,1HX,30X,1HY,30X,1HZ//
     122X,E14.8,17X,E14.8,17X,E14.8//10X,5HTAU =,E14.8,5X,6HDTAU =,E14.8
     2,5X,6HNTAU =,I4,5X,5HEPS =,E14.8,5X,6HNMAX =,I4 ,5X,5HNWA =,I4 /)
 4002 FORMAT(1H1,8H PNT CNT,12X,1HX,12X,1HY,12X,1HZ,12X,1HM,4X,1HN,5X,
     1 4HFREQ,5X,21HM.S. SPECTRAL DENSITY,4X,20H   DB(RE.0002)      //
     2I6,10X,F9.4,4X,F9.4,4X,F9.4,I10,I5,3X,F6.0,5X,E16.8,6X,E16.8////
     X40X
     3,1HK,8X,3HTAU,15X,9HRPMN(TAU) //)
```

TABLE 5A (Continued)

```
4003 FORMAT(1H ,30X,I10,E16.8,E20.8)
4004 FORMAT(1H0,50X,12HINTEGRATIONS // 33X,9HINT. NUM.,5X, 8H  MESH  ,
    15X,6HM     N,10X, 4HSUM2,16X, 4HSUM1)
4005 FORMAT(1H1,30X,44HNORMALIZED CORRELATION OF ACCOUSTIC PRESSURE///
    110X, 4HNTAU,10X, 3HTAU,10X,25HNORM. CORR. OF ACC. PRES.,10X,
    28HRP(K)/P2,12X,14HNORM. FACTOR =,E14.8//)
4006 FORMAT(1H , 8X,I4,8X,F8.6,10X,E16.8,11X,E16.8)
4010 FORMAT(1H1,7E16.8)
4011 FORMAT(1H1,30X,23HAUTO SPECTRAL DENSITY   ///12X,1HK,10X, 4HFREQ,
    110X, 7HRAD/SEC,10X,17HCROSS SPEC. DENS.,10X,11HDB(RE.0002)//)
4012 FORMAT(1H ,8X,I4, 8X,F6.0,8X,F9.4,2(10X,E14.8))
4013 FORMAT(1H0,30X,18HCHOSEN FREQUENCIES //(10X,10F10.0))
4014 FORMAT(1H1,30X,1HK,10X,4HFREQ,10X,7HRAD/SEC,10X,17HMODAL SPEC. DEN
    1S.,10X,11HDB(RE.0002) //)
4015 FORMAT(1H ,21X,I10,8X,F6.0,8X,F9.4,2(8X,E16.8))
C
C
      COMMON /AAA/A(4000)
C
      EQUIVALENCE (A(1),MM),(A(2),NN),(A(3),IM),(A(4),IN),(A(5),NXYZ),
     1(A(6),KXYZ),(A(7),NAUTO),(A(8),NCROSS),(A(9),M),(A(10),N)
      EQUIVALENCE (A(21),XL1),(A(22),XL0),(A(23),YL1),(A(24),YL0),
     1(A(25),AI),(A(26),B),(A(27),C),(A(28),THETA),(A(29),P2),(A(30),PI)
     2,(A(31),X),(A(32),Y),(A(33),Z),(A(34),EPS),(A(35),NMAX),
     3(A(36),WMN),(A(37),AMN),(A(38),SUM1),(A(39),SUM2),
     4(A(40),JA),(A(41),JB)
      EQUIVALENCE (A(101),MAM),(A(151),NAN),(A(1001),W)
C
      DIMENSION MAM(50),NAN(50),W(20,50),RP(110),RPBAR(110),PRP(110) ,
     1WA(110),FI(110)
C
      REAL KMN
C
      CONVT = 60000.
C
C
      DO  5 II=1,NXYZ
```

TABLE 5A (Continued)

```
C
      READ (5,3000) X,Y,Z,TAU,DTAU,NTAU,EPS,NMAX,NWA
C
      WRITE(6,4000) X,Y,Z,TAU,DTAU,NTAU,EPS,NMAX,NWA
C
      IF (NWA)  2,1,2
C
    2 READ (5,3001) (WA(K),K=1,NWA)
      WRITE(6,4013)  (WA(K),K=1,NWA)
C
C
    1 ATAU = TAU
C
      DO  6 IA=1,NTAU
    6 RP(IA) = 0.
C
      DO 7 IA=1,NWA
    7 FI(IA) = 0.
C
      DO 10 I=1,IM
      DO 10 J=1,IN
      JA = J
      JB=J
      IF (IM.EQ.MM) JA=I
      M=MAM(JA)
      N = NAN(J)
C
      WMN = W(I,J)
C
      KMN = C*THETA / (B*(1.+W(I,J)**2*THETA**2))
      AMN = B*W(I,J)
      CMN = W(I,J)*(1.-6.*B**2 + B**4)
      DMN = 4.*B*W(I,J)*(B**2-1.)
C
      WBAR1=(B**2+2.) /(B*W(I,J)*(B**2+4.))
      WBAR2 = B*WBAR1 / (B**2+2. )
      CBAR = KMN*W(I,J)*P2
```

TABLE 5A (Continued)

```
C
      WRITE(6,4010) KMN,AMN,CMN,DMN,WBAR1,WBAR2,CBAR
      WRITE(6,4004)
C
      PHASE=1.5708
      KKK=2
      CALL DINT (AMN,PHASE,KKK)
      CAP2=SUM2
C
      KKK=1
      AMN=-AMN
      CALL DINT (AMN,PHASE,KKK)
      CAP1=SUM2
C
      KKK=5
      PHASE=0.
      CALL DINT (AMN,PHASE,KKK)
      CAP5=SUM2
C
      KKK=4
      AMN=-AMN
      CALL DINT (AMN,PHASE,KKK)
      CAP4=SUM2
C
C
      SP = CBAR* (WBAR1*CAP1*CAP2 + WBAR2*CAP1*CAP4 - WBAR2*CAP5*CAP2 +
     1WBAR1*CAP5*CAP4 )
C
      IF  (SP)  11,11,12
   11 PHI = 0.
      GO TO 13
   12 PHI = 10.* ALOG10(SP) + 127.6
   13 WRITE(6,4002)II,X,Y,Z,M,N,W(I,J),SP,PHI
      IF (NTAU) 22,21,22
   22 TAU = ATAU
C
      DO 15 K=1,NTAU
```

```
C
      TH1 = CMN*COS(W(I,J)*TAU) + DMN * SIN(W(I,J)*TAU)
      TH2=CMN*SIN(W(I,J)*TAU)-DMN*COS(W(I,J)*TAU)
C
C
      RPN=KMN*EXP(-AMN*TAU) * (TH1*CAP1*CAP2 + TH2*CAP1*CAP4 - TH2
     1*CAP5*CAP2 + TH1*CAP5*CAP4)
      RP(K)=RP(K)+RPN
C
      WRITE(6,4003) K,TAU,RPN
C
   15 TAU = TAU + DTAU
C
  21  IF (NWA)  14,10,14
  14  WRITE(6,4014)
C
      DO 20 K=1,NWA
      RAD = WA(K)/(2.*PI)
      DD = (B**2*W(I,J)**2 + (W(I,J)-WA(K))**2)* (B**2*W(I,J)**2 +
     1(W(I,J) + WA(K))**2)
C
      AAMN = (B*W(I,J)*(B**2*W(I,J)**2 + W(I,J)**2 + WA(K)**2)) / DD
      BBMN = (W(I,J)*(B**2*W(I,J)**2 + W(I,J)**2 - WA(K)**2)) / DD
C
      TW1 = CMN*AAMN + DMN*BBMN
      TW2 = CMN*BBMN - DMN*AAMN
C
      FIT = KMN * (TW1*CAP1*CAP2 + TW2*CAP1*CAP4 - TW2*CAP5*CAP2 +
     1TW1*CAP5*CAP4)
C
      FAT = FIT
      IF (FIT) 19,19,17
  19  PHI = 0.
      FIT = 0.
      GO TO 18
   17 PHI = 10.*ALOG10(FIT) + 127.6
   18 WRITE(6,4015) K,WA(K),RAD,FAT,PHI
```

```
C
   20 FI(K) = FI(K) + FIT
C
   10 CONTINUE
C
      IF (NTAU)  52,51,52
C
  52  WRITE(6,4005) RP(1)
C
      DO 30 K=1,NTAU
      RPBAR(K)=RP(K)/RP(1)
      PRP(K) = RP(K)/P2
      WRITE(6,4006) K,ATAU,RPBAR(K),PRP(K)
   30 ATAU=ATAU+DTAU
C
  51  IF (NWA) 61,5,61
  61  WRITE(6,4011)
C
      DO 40 K=1,NWA
      RAD = WA(K)/(2.*PI)
      IF (FI(K))  71,71,41
  71  PHI = 0.
      GO TO 40
C
   41 PHI = 10.* ALOG10(FI(K)) + 127.6
   40 WRITE(6,4012) K,WA(K),RAD,FI(K),PHI
    5 CONTINUE
C
C
      RETURN
      END
$IBFTC XCROS1
      SUBROUTINE CROSS1
C
C
C
C  CROSS CORRELATION)  TIME = CONSTANT
```

TABLE 5A (Continued)

```
C
C
C
 1000 FORMAT(3E12.6,2I6,E12.6,I6/(6E12.8))
 1001 FORMAT(2(3E12.6,I4))
C
 2000 FORMAT(1H1,50X,17HCROSS CORRELATION///20X,1HX,20X,1HY,20X,1HZ,20X,
     13HMXP,10X,4HMTAU,10X, 3HEPS,10X, 4HNMAX //12X,E14.8,2(7X,E14.8),
     214X,I4,9X,I4, 5X,E12.6,7X,I3// 5X,7HTAU(I)=,5E16.8//12X,5E16.8//)
 2001 FORMAT(1H0,30X,2HXP,20X,2HYP,20X,2HZP,10X,3HNOR//(23X,E14.8,8X,E14
     1.8,8X,E14.8,5X,I3 ))
 2002 FORMAT(1H0,1HI ,4X,3HTAU,4X, 7HPNT CNT,5X,2HXP,10X,2HYP,10X,2HZP,
     110X, 6HM    N,4X,4HFREQ , 5X,17HCROSS SPEC. DENS.,5X,11HDB(RE.0002
     2),5X, 9HRPMN(TAU)//I2,E11.5,I4,E14.6,E12.6,E12.6,2X,2I5,2X,F6.0,
     36X,E14.8,4X,2E14.8 )
 2004 FORMAT(1H1,4X,1HI,8X, 3HTAU,12X,1HJ,10X,5HXP(J),9X,5HYP(J), 9X,
     15HZP(J),12X,11HCRPBAR(I,J),10X,12HNORM. FACTOR/// I6,5X,E10.5,
     24X,I5,3X,3E14.6,E20.8,E22.8/(25X,I5,3X,3E14.6,E20.8,E22.8))
 2005 FORMAT(1H0,50X,12HINTEGRATIONS // 33X,9HINT. NUM.,5X, 8H  MESH  ,
     15X,6HM    N,10X, 4HSUM2,16X, 4HSUM1)
 2010 FORMAT(1H1,7E16.8)
C
C
      COMMON /AAA/A(4000)
C
      EQUIVALENCE (A(1),MM),(A(2),NN),(A(3),IM),(A(4),IN),(A(5),NXYZ),
     1(A(6),KXYZ),(A(7),NAUTO),(A(8),NCROSS),(A(9),M),(A(10),N)
      EQUIVALENCE (A(21),XL1),(A(22),XLO),(A(23),YL1),(A(24),YLO),
     1(A(25),AI),(A(26),B),(A(27),C),(A(28),THETA),(A(29),P2),(A(30),PI)
     2,(A(31),X),(A(32),Y),(A(33),Z),(A(34),EPS),(A(35),NMAX),
     3(A(36),WMN),(A(37),AMN),(A(38),SUM1),(A(39),SUM2),
     4(A(40),JA),(A(41),JB)
      EQUIVALENCE (A(101),MAM),(A(151),NAN),(A(1001),W),(A(2001),DIX1),
     1(A(3001),DIX5)
C
      DIMENSION  TAV(110),XP(50),YP(50),ZP(50),NOR(50),MAM(50),
     1NAN(50),W(20,50),DIX1(20,50),DIX5(20,50),CRPBAR(50)
```

TABLE 5A (Continued)

```
C
      REAL KMN
C
C
C
      CONVT = 60000.
C
C
      DO 5 II=1,KXYZ
C
      READ (5,1000)XX,YY,ZZ,MXP,MTAV,EPS,NMAX,(TAV(I),I=1,MTAV)
      WRITE(6,2000)XX,YY,ZZ,MXP,MTAV,EPS,NMAX,(TAV(I),I=1,MTAV)
C
      READ (5,1001)(XP(I),YP(I),ZP(I),NOR(I),  I=1,MXP)
      WRITE(6,2001)(XP(I),YP(I),ZP(I),NOR(I),  I=1,MXP)
C
      DO 10 I=1, MTAV
C
      DO 20 J=1,MXP
      CRP = 0.
C
C
      DO 30 K=1,IM
      DO 30 L=1,IN
      JA=L
      JB=L
      IF (IM.EQ.MM) JA=K
      M=MAM(JA)
      N=NAN(L)
      WMN= W(K,L)
C
      KMN = C*THETA / (B*(1.+W(K,L)**2*THETA**2))
      AMN = B*W(K,L)
      CMN = W(K,L)*(1.-6.*B**2 + B**4)
      DMN = 4.*B*W(K,L)*(B**2-1.)
      WBAR1=(B**2+2.)/(B*W(K,L)*(B**2+4.))
      WBAR2= B* WBAR1 / (B**2+2.)
```

TABLE 5A (Continued)

```
      CBAR = KMN * W(K,L) * P2
C
      WRITE(6,2010) KMN,AMN,CMN,DMN,WBAR1,WBAR2,CBAR
      WRITE(6,2005)
C
      IF (J.NE.1) GO TO 31
C
      X=XX
      Y=YY
      Z=ZZ
C
      PHASE =1.5708
      KKK=1
      AMN =-AMN
      CALL DINT(AMN,PHASE,KKK)
      DIX1(K,L) = SUM2
C
      PHASE = 0.
      KKK= 5
      CALL DINT(AMN,PHASE,KKK)
      DIX5(K,L) = SUM2
C
      AMN = -AMN
C
   31 X=XP(J)
      Y=YP(J)
      Z=ZP(J)
C
      PHASE =1.5708
      KKK = 2
      CALL DINT(AMN,PHASE,KKK)
      CAP2 = SUM2
C
      PHASE = 0.
      KKK = 4
      CALL DINT(AMN,PHASE,KKK)
      CAP4 = SUM2
```

```
C
      SP = .5E+20
      PHI = .5E+20
C
      IF (NOR(J))  39,32,32
   39 SP = CBAR * (WBAR1*DIX1(K,L)*CAP2 + WBAR2*DIX1(K,L)*CAP4 -WBAR2*
     1DIX5(K,L)*CAP2 + WBAR1*DIX5(K,L)*CAP4 )
C
      IF (SP)  37,37,33
   37 PHI = 0.
      GO TO 32
C
   33 PHI = 10.* ALOG10(SP) + 127.6
C
   32 TH1 = CMN*COS(W(K,L)*TAV(I)) + DMN*SIN(W(K,L)*TAV(I))
      TH2 = CMN*SIN(W(K,L)*TAV(I)) - DMN*COS(W(K,L)*TAV(I))
C
      RPN = KMN*EXP(-AMN*TAV(I))*(TH1*DIX1(K,L)*CAP2 + TH2*DIX1(K,L)*
     1CAP4 - TH2*DIX5(K,L)*CAP2 + TH1*DIX5(K,L)*CAP4)
C
      CRP = CRP + RPN
C
   34 WRITE(6,2002) I,TAV(I),J,XP(J),YP(J),ZP(J),M,N,W(K,L),SP,PHI,RPN
C
   30 CONTINUE
C
      IF ((I+J).EQ.2) CNORM =CRP
      CRPBAR(J)    = CRP / CNORM
   20 CONTINUE
C
      WRITE(6,2004) I,TAV(I),(J,XP(J),YP(J),ZP(J),CRPBAR(J),CNORM,
     1J=1,MXP)
C
   10 CONTINUE
C
    5 CONTINUE
C
```

TABLE 5A (Continued)

```
C
C
C
      RETURN
      END
$IBFTC XCROS2
      SUBROUTINE CROSS2
C
C
C
C  CROSS CORRELATION (TIME)  (AUTO CORRELATION INCLUDED FOR THE FIRST POINT)
C
 1000 FORMAT(3E12.6,I3,2E12.8,I3,E6.2,2I3)
 1001 FORMAT(2(3E12.6,I4))
 1002 FORMAT(12F6.0)
C
 2000 FORMAT(1H1,50X,24HCROSS CORRELATION (TIME)///30X,1HX,30X,1HY,30X,
     11HZ,//4X,3E31.8///4X, 5HMXP =,I4,4X, 5HTAU =,E14.8,4X, 6HDTAU =,
     2E14.8,4X, 6HNTAU =,I4,4X, 5HEPS =,E14.8,4X, 6HNMAX =,I4,4X,5HNWA =
     3,I4 /)
 2001 FORMAT(1H0,30X,2HXP,20X,2HYP,20X,2HZP,10X,3HNOR//(23X,E14.8,8X,E14
     1.8,8X,E14.8,5X,I3 ))
 2002 FORMAT(1H0, 9HCASE NUM.,5X,11HINTEG. PNT., 5X,2HXP,10X,2HYP,10X,
     12HZP,10X, 6HM    N,5X,4HFREQ ,5X,21HM.S. SPECTRAL DENSITY,5X,
     211HDB(RE.0002)//I5,10X,I5,3X,3(3X,F9.4),4X,2I5,3X,F6.0,3X,2E20.8
     3////40X,1HK,8X,3HTAU,15X, 9HRPMN(TAU)//)
 2003 FORMAT(1H0, 9HCASE NUM.,5X,11HINTEG. PNT., 5X,2HXP,10X,2HYP,10X,
     12HZP,10X, 6HM    N,5X,4HFREQ //I5,10X,I5, 3X,3(3X,F9.4);4X,2I5,3X,
     2F6.0,////40X,1HK,8X,3HTAU,15X,9HRPMN(TAU)//)
 2004 FORMAT(1H ,30X,I10,E16.8,E20.8)
 2005 FORMAT(1H1,50X,12HINTEGRATIONS // 33X,9HINT. NUM.,5X, 8H  MESH  ,
     15X,6HM    N,10X, 4HSUM2,16X, 4HSUM1)
 2007 FORMAT(1H1,30X,44HNORMALIZED CORRELATION OF ACCOUSTIC PRESSURE///
     110X, 4HNTAU,10X, 3HTAU,10X,25HNORM. CORR. OF ACC. PRES.,10X,
     28HRP(K)/P2,12X,14HNORM. FACTOR =,E14.8//)
 2008 FORMAT(1H , 8X,I4,8X,F8.6,10X,E16.8,11X,E16.8)
 2010 FORMAT(1H0,30X,18HCHOSEN FREQUENCIES //(10X,10F10.0))
```

```
 2011 FORMAT(1H1,30X,23HCROSS SPECTRAL DENSITY  ///12X,1HK,10X, 4HFREQ,
     110X, 7HRAD/SEC,10X,17HCROSS SPEC. DENS.,10X,11HDB(RE.0002)//)
 2012 FORMAT(1H ,8X,I4,8X,F6.0,8X,F9.4,2(10X,E14.8))
 2013 FORMAT(1H1,30X,1HK,10X,4HFREQ,10X,7HRAD/SEC,10X,17HMODAL SPEC. DEN
     1S.,10X,11HDB(RE.0002) //)
 2014 FORMAT(1H ,21X,I10, 8X,F6.0,8X,F9.4,2(8X,E16.8))
C
      COMMON /AAA/A(4000)
C
      EQUIVALENCE (A(1),MM),(A(2),NN),(A(3),IM),(A(4),IN),(A(5),NXYZ),
     1(A(6),KXYZ),(A(7),NAUTO),(A(8),NCROSS),(A(9),M),(A(10),N) ,
     2(A(11),LXYZ),(A(12),NCROST)
      EQUIVALENCE (A(21),XL1),(A(22),XL0),(A(23),YL1),(A(24),YL0),
     1(A(25),AI),(A(26),B),(A(27),C),(A(28),THETA),(A(29),P2),(A(30),PI)
     2,(A(31),X),(A(32),Y),(A(33),Z),(A(34),EPS),(A(35),NMAX),
     3(A(36),WMN),(A(37),AMN),(A(38),SUM1),(A(39),SUM2),
     4(A(40),JA),(A(41),JB)
      EQUIVALENCE (A(101),MAM),(A(151),NAN),(A(1001),W),(A(2001),DIX1),
     1(A(3001),DIX5)
C
      DIMENSION MAM(50),NAN(50),W(20,50),RP(110),RPBAR(110),PRP(110),
     1WA(110),FI(110)
      DIMENSION XP(50),YP(50),ZP(50),DIX1(20,50),DIX5(20,50),NOR(50)
C
      REAL KMN
C
C
C
      CONVT = 60000.
C
C
      DO 5 II=1,LXYZ
C
      READ (5,1000) XX,YY,ZZ,MXP,TAU,DTAU,NTAU,EPS,NMAX,NWA
C
      WRITE(6,2000) XX,YY,ZZ,MXP,TAU,DTAU,NTAU,EPS,NMAX,NWA
C
```

```
C
      ATAU = TAU
C
      READ (5,1001) (XP(I),YP(I),ZP(I),NOR(I), I=1,MXP)
      WRITE(6,2001) (XP(I),YP(I),ZP(I),NOR(I), I=1,MXP)
C
      IF (NWA) 8,1,8
    8 READ (5,1002) (WA(K),K=1,NWA)
      WRITE(6,2010) (WA(K),K=1,NWA)
C
    1 DO 10 JJ=1,MXP
C
      DO  6 IA=1,NTAU
    6 RP(IA) = 0.
C
      DO 7 IA=1,NWA
    7 FI(IA) = 0.
C
      DO 20 I=1,IM
      DO 20 J=1,IN
      JA = J
      JB=J
      IF (IM.EQ.MM) JA=I
      M=MAM(JA)
      N = NAN(J)
C
      WMN = W(I,J)
C
      KMN = C*THETA / (B*(1.+W(I,J)**2*THETA**2))
      AMN = B*W(I,J)
      CMN = W(I,J)*(1.-6.*B**2 + B**4)
      DMN = 4.*B*W(I,J)*(B**2-1.)
C
C
      WRITE(6,2005)
      IF (JJ.NE.1) GO TO 21
C
```

TABLE 5A (Continued)

```
      X=XX
      Y=YY
      Z=ZZ
C
      PHASE =1.5708
      KKK=1
      AMN =-AMN
      CALL DINT(AMN,PHASE,KKK)
      DIX1(I,J) = SUM2
C
      PHASE = 0.
      KKK= 5
      CALL DINT(AMN,PHASE,KKK)
      DIX5(I,J) = SUM2
C
      AMN = -AMN
C
   21 X=XP(JJ)
      Y=YP(JJ)
      Z=ZP(JJ)
C
      PHASE =1.5708
      KKK = 2
      CALL DINT(AMN,PHASE,KKK)
      CAP2 = SUM2
C
      PHASE = 0.
      KKK = 4
      CALL DINT(AMN,PHASE,KKK)
      CAP4 = SUM2
C
      IF (JJ.NE.1) GO TO 24
      WBAR1=(B**2+2.) /(B*W(I,J)*(B**2+4.))
      WBAR2 = B*WBAR1 / (B**2+2. )
      CBAR = KMN*W(I,J)*P2
C
      SP = CBAR * (WBAR1*DIX1(I,J)*CAP2 + WBAR2*DIX1(I,J)*CAP4 -WBAR2*
```

TABLE 5A (Continued)

```
     1DIX5(I,J)*CAP2 + WBAR1*DIX5(I,J)*CAP4
      IF (SP) 28,28,22
 28   PHI = 0.
      GO TO 23
   22 PHI = 10.* ALOG10(SP) + 127.6
   23 WRITE(6,2002) II,JJ,XP(JJ),YP(JJ),ZP(JJ),M,N,W(I,J),SP,PHI
      GO TO 25
   24 WRITE(6,2003) II,JJ,XP(JJ),YP(JJ),ZP(JJ),M,N,W(I,J)
  25  IF (NTAU)  39,31,39
  39  TAU = ATAU
C
      DO 30 K=1,NTAU
C
      TH1 = CMN*COS(W(I,J)*TAU) + DMN * SIN(W(I,J)*TAU)
      TH2=CMN*SIN(W(I,J)*TAU)-DMN*COS(W(I,J)*TAU)
C
      RPN=KMN*EXP(-AMN*TAU)*(TH1*DIX1(I,J)*CAP2+TH2*DIX1(I,J)*CAP4-TH2*
     1DIX5(I,J)*CAP2 + TH1*DIX5(I,J)*CAP4)
      RP(K)=RP(K)+RPN
C
      WRITE(6,2004) K,TAU,RPN
C
   30 TAU = TAU + DTAU
C
  31  IF (NWA)  29,20,29
  29  WRITE(6,2013)
C
      DO 19 K=1,NWA
      RAD = WA(K)/(2.*PI)
      DD = (B**2*W(I,J)**2 + (W(I,J)-WA(K))**2)* (B**2*W(I,J)**2 +
     1(W(I,J) + WA(K))**2)
C
      AAMN = (B*W(I,J)*(B**2*W(I,J)**2 + W(I,J)**2 + WA(K)**2)) / DD
      BBMN = (W(I,J)*(B**2*W(I,J)**2 + W(I,J)**2 - WA(K)**2)) / DD
C
      TW1 = CMN*AAMN + DMN*BBMN
      TW2 = CMN*BBMN - DMN*AAMN
```

TABLE 5A (Continued)

```
C
      FIT = KMN * (TW1*DIX1(I,J)*CAP2 + TW2*DIX1(I,J)*CAP4 - TW2*DIX5(I,
     1J)*CAP2 + TW1*DIX5(I,J)*CAP4)
C
      FAT = FIT
      IF (FIT)  71,71,17
   71 PHI = 0.
      FIT = 0.
      GO TO 18
   17 PHI = 10.*ALOG10(FIT) + 127.6
   18 WRITE(6,2014) K,WA(K),RAD,FAT,PHI
C
   19 FI(K) = FI(K) + FIT
C
   20 CONTINUE
C
      IF (NTAU) 47,45,47
   47 WRITE(6,2007) RP(1)
      TAU = ATAU
C
      DO 40 K=1,NTAU
      RPBAR(K)=RP(K)/ RP(1)
      PRP(K) = RP(K)/P2
C
      WRITE(6,2008) K, TAU,RPBAR(K),PRP(K)
   40 TAU = TAU + DTAU
C
   45 IF (NWA)  74,10,74
   74 WRITE(6,2011)
C
      DO 50 K=1,NWA
      RAD = WA(K)/(2.*PI)
      IF (FI(K)) 75,75,51
   75 PHI = 0.
      GO TO 50
C
   51 PHI = 10.* ALOG10(FI(K)) + 127.6
```

```
   50 WRITE(6,2012) K,WA(K),RAD,FI(K),PHI
C
C
   10 CONTINUE
C
C
    5 CONTINUE
C
C
C
      RETURN
      END
$IBFTC XDINT
      SUBROUTINE DINT (SAMN,SPHASE,KKS)
C
C
C  DOUBLE INTEGRATION SUBROUTINE
C
C
      COMMON /AAA/A(4000)
C
      EQUIVALENCE (A(9),M),(A(10),N),(A(21),XL1),(A(22),XL0),(A(23),YL1)
     1,(A(24),YL0),(A(34),EPS),(A(35),NMAX),(A(38),SUM1),(A(39),SUM2)
C
C
      DIMENSION P(5),WW(5)
C
      DATA (P(I),I=1,5),(WW(I),I=1,5) /.453089923,-.453089923,.269234655
     1,-.269234655,0.0,2*.118463443,2*.239314335,.284444444 /
C
 2000 FORMAT(1H0,28H  ***** NO CONVERGENCE *****,5X,I4,10X,I4,5X,I4,I5,
     12E18.8)
 2002 FORMAT(1H0,33X,I4,10X,I4,4X,I5,I5,2E18.8)
C
C
C
      NK=2
```

```
      BINC1=XL1-XL0
      BINC2=YL1-YL0
C
      DO 25 K=1,NMAX
      SUM1=SUM2
      SUM2=0.0
      CNK = NK
      DINC1 = BINC1/CNK
      DINC2 = BINC2/CNK
      H1 = XL0 + DINC1/2.
C
      DO 26 I=1,NK
      H2 = YL0 + DINC2/2.
C
      DO 27 J=1,NK
      DO 28 II=1,5
      ABS1=DINC1*P(II)+H1
      DO 29 JJ=1,5
      ABS2=DINC2*P(JJ)+H2
   29 SUM2=SUM2+WW(II)*WW(JJ)*FFF(ABS1,ABS2,SAMN,SPHASE)
   28 CONTINUE
   27 H2=H2+DINC2
   26 H1=H1+DINC1
      SUM2=SUM2*DINC1*DINC2
C
C
      IF (K.EQ.1) GO TO 30
      IF (ABS((SUM1-SUM2)/SUM2)-EPS) 31,31,30
   30 NK=NK + 1
   25 CONTINUE
C
      WRITE(6,2000) KKS,NK,M,N,SUM2,SUM1
      SUM2 = 0.
C
      GO TO 32
C
C
```

TABLE 5A (Continued)

```
   31 WRITE(6,2002) KKS,NK,M,N,SUM2,SUM1
C
   32 RETURN
      END
$IBFTC XFFF
      FUNCTION FFF(X0,Y0,FAMN,FPHASE)
C
C
C   DOUBLE INTEGRATION FUNCTION
C
C
C
      COMMON /AAA/A(4000)
C
      EQUIVALENCE (A(7),NAUTO),(A(8),NCROSS),(A(9),M),(A(10),N),
     1(A(21),XL1),(A(22),XL0),(A(23),YL1),(A(24),YL0),(A(25),AI),
     2(A(30),PI),(A(31),X),(A(32),Y),(A(33),Z),(A(36),WMN),(A(40),JA),
     3(A(41),JB)
C
C
C     INTEGER W,WMN
C
C
      R0=SQRT((X-X0)**2+(Y-Y0)**2 + Z**2)
C
      CM = M
      CN = N
      PHX = SIN(CM*PI*X0/XL1)
      PHY = SIN(CN*PI*Y0/YL1)
C
      FFF = PHX * PHY * EXP((FAMN/AI)*R0) * SIN((WMN/AI)*R0+FPHASE)/ R0
C
      RETURN
      END
```

Table 5B – Clamped-Clamped Boundaries

```
$IBFTC TURGEN
C
C
 1000 FORMAT(12A6)
 1001 FORMAT(10I4)
 1002 FORMAT(4E12.6/5E15.8)
 1003 FORMAT(12F6.0)
 1004 FORMAT(20I4)
 1005 FORMAT(5E15.8)
C
 2000 FORMAT(1H1,10X,6HF.P.S.,15X,12A6/22X,12A6////)
 2001 FORMAT (1H0,29X,45HORDER OF M (MODE NUMBERS) .............. MM =,I
     16/30X,45HORDER OF N (MODE NUMBERS) ............. NN =,I6/30X,
     245HNUMBER OF CASES  (XYZ) IN AUTO CORR... NXYZ =,I6/30X,45HNUMBER
     3OF CASES  (XYZ) IN CROSS CORR.. KXYZ =,I6 /          30X,45HAUTO CO
     4RRELATION CONSTANT ..........  NAUTO =,I6/30X,45HCROSS CORRELATION
     5CONSTANT .......... NCROSS =,I6/30X,45HLIMITS OF THE 1-ST INTEGRAL
     6 ........... XL1 =,F11.4/30X,45H
     7      XL0 =,F11.4/30X,45HLIMITS OF THE 2-ND INTEGRAL ........... Y
     8L1 =,F11.4/30X,45H                                     YL0 =,F1
     91.4/30X,45HSPEED OF SOUND IN WATER ................ AI =,F13.6/30X
     A,45HDAMPING CONSTANT ...................... B =,F13.6/30X,45HC
     BCONSTANT .......................... C =,F13.6/30X,45HTEMPORAL D
     CECAY FACTOR OF TURBULENCE   THETA =,F11.4/30X,45HR.M.S. PRESSURE .
     D..................... P2 =,F13.6//30X,2I10)
 2002 FORMAT(1H0,40X,35HUNDAMPED NATURAL FREQUENCIES W(M,N)//(10X,10F8.0
     X))
 2003 FORMAT(1H0,50X,12HMODE NUMBERS//(40X,10I5))
 2005 FORMAT(1H0,40X,35HNORMALIZED EIGENFUNCTION PARAMETERS //(15X,5E18.
     18) )
 2006 FORMAT(1H0,29X,45HNUMBER OF CASES IN CROSS CORR. (TIME).. LXYZ=,
     1I6/30X,45HCROSS CORR. (TIME) CONSTANT ......... NCROST=,I6//
     230X,2I10)
C
C
      COMMON /AAA/A(4000)
C
```

```
      EQUIVALENCE (A(1),MM),(A(2),NN),(A(3),IM),(A(4),IN),(A(5),NXYZ),
     1(A(6),KXYZ),(A(7),NAUTO),(A(8),NCROSS),(A(9),M),(A(10),N) ,
     2(A(11),LXYZ),(A(12),NCROST)
C
      EQUIVALENCE (A(21),XL1),(A(22),XLO),(A(23),YL1),(A(24),YLO),
     1(A(25),AI),(A(26),B),(A(27),C),(A(28),THETA),(A(29),P2),(A(30),PI)
     2,(A(31),X),(A(32),Y),(A(33),Z),(A(34),EPS),(A(35),NMAX),
     3'A(36),WMN),(A(37),AMN),(A(38),SUM1),(A(39),SUM2)
C
      EQUIVALENCE (A(101),MAM),(A(151),NAN),(A(1001),W)
C
      EQUIVALENCE (A(201),AMM),(A(251), ANN),(A(301),BMM),(A(351),BNN),
     1(A(401),CMM),(A(451),CNN),(A(501),DMM),(A(551),DNN),(A(601),ALMM),
     2(A(651),ALNN)
C
C
      DIMENSION TITLE(24),W(20,50),MAM(50),NAN(50)
      DIMENSION AMM(50),ANN(50),BMM(50),BNN(50),CMM(50),CNN(50),DMM(50),
     1DNN(50),ALMM(50),ALNN(50)
C
      REAL KMN
C     INTEGER W
C
C
C
C     CALL STARTR
C     IF ACCUMULATOR OVERFLOW ,
C
C  READ AND PRINT TITLE
C
      READ(5,1000)  (TITLE(I),I=1,24)
      WRITE(6,2000) (TITLE(I),I=1,24)
C
C  READ AND PRINT GENERAL INPUT CONSTANTS
C
      READ (5,1001) MM,NN,IM,IN,NXYZ,KXYZ,LXYZ,NAUTO,NCROSS,NCROST
      READ (5,1002) XL1,XLO,YL1,YLO,AI,B,C,THETA,P2
```

```
      READ (5,1003) ((W(I,J),J=1,IN),I=1,IM)
      READ (5,1004) (MAM(I),I=1,MM),(NAN(I),I=1,NN)
C
      WRITE(6,2001) MM,NN,NXYZ,KXYZ,NAUTO,NCROSS,XL1,XLO,YL1,YLO,AI,B,
     1C,THETA,P2
      WRITE(6,2006) LXYZ,NCROST,IM,IN
      WRITE(6,2002) ((W(I,J),J=1,IN),I=1,IM)
      WRITE(6,2003) (MAM(I),I=1,MM),(NAN(I),I=1,NN)
C
C
      PI=3.14159
C
C  AUTO CORRELATION
C
      IF  (NAUTO)  13,3,13
C
   13 READ (5,1005) (ALMM(I),AMM(I),BMM(I),CMM(I),DMM(I),I=1,MM),
     1(ALNN(I),ANN(I),BNN(I),CNN(I),DNN(I),I=1,NN)
      WRITE(6,2005) (ALMM(I),AMM(I),BMM(I),CMM(I),DMM(I),I=1,MM),
     1(ALNN(I),ANN(I),BNN(I),CNN(I),DNN(I),I=1,NN)
C
      CALL AUTO1
C
C  CROSS CORRELATION (SPACE)
C
    3 IF (NCROSS)  10,6,10
   10 IF (NAUTO.EQ. 1) GO TO 5
C
      READ (5,1005) (ALMM(I),AMM(I),BMM(I),CMM(I),DMM(I),I=1,MM),
     1(ALNN(I),ANN(I),BNN(I),CNN(I),DNN(I),I=1,NN)
      WRITE(6,2005) (ALMM(I),AMM(I),BMM(I),CMM(I),DMM(I),I=1,MM),
     1(ALNN(I),ANN(I),BNN(I),CNN(I),DNN(I),I=1,NN)
C
    5 CALL CROSS1
C
C
C   CROSS CORRELATION (TIME)
```

```
C
   6  IF (NCROST)  18,8,18
  18  IF ((NAUTO.EQ.1).OR.(NCROSS.EQ.1)) GO TO 7
      READ (5,1005) (ALMM(I),AMM(I),BMM(I),CMM(I),DMM(I),I=1,MM),
     1(ALNN(I),ANN(I),BNN(I),CNN(I),DNN(I),I=1,NN)
      WRITE(6,2005) (ALMM(I),AMM(I),BMM(I),CMM(I),DMM(I),I=1,MM),
     1(ALNN(I),ANN(I),BNN(I),CNN(I),DNN(I),I=1,NN)
C
    7 CALL CROSS2
C

   8  STOP
      END
$IBFTC XAUTO1
      SUBROUTINE AUTO1
C
C
C
C
C  AUTO CORRELATION)  X=XP , Y=YP , Z=ZP
C
C
 3000 FORMAT(5E12.6,I4,E6.2,2I4)
 3001 FORMAT(12F6.0)
C
 4000 FORMAT(1H1,50X,16HAUTO CORRELATION///30X,1HX,30X,1HY,30X,1HZ//
     122X,E14.8,17X,E14.8,17X,E14.8//10X,5HTAU =,E14.8,5X,6HDTAU =,E14.8
     2,5X,6HNTAU =,I4,5X,5HEPS =,E14.8,5X,6HNMAX =,I4 ,5X,5HNWA =,I4 /)
 4002 FORMAT(1H1,8H PNT CNT,12X,1HX,12X,1HY,12X,1HZ,12X,1HM,4X,1HN,5X,
     1 4HFREQ,5X,21HM.S. SPECTRAL DENSITY,4X,20H   DB(RE.0002)      //
     2I6,10X,F9.4,4X,F9.4,4X,F9.4,I10,I5,3X,F6.0,5X,E16.8,6X,E16.8////
     X40X
     3,1HK,8X,3HTAU,15X,9HRPMN(TAU) //)
 4003 FORMAT(1H ,30X,I10,E16.8,E20.8)
 4004 FORMAT(1H0,50X,12HINTEGRATIONS // 33X,9HINT. NUM.,5X, 8H  MESH  ,
     15X,6HM    N,10X, 4HSUM2,16X, 4HSUM1)
 4005 FORMAT(1H1,30X,44HNORMALIZED CORRELATION OF ACCOUSTIC PRESSURE///
```

```
     110X, 4HNTAU,10X, 3HTAU,10X,25HNORM. CORR. OF ACC. PRES.,10X,
     28HRP(K)/P2,12X,14HNORM. FACTOR =,E14.5//)
 4006 FORMAT(1H , 8X,I4,8X,F8.6,10X,E16.8,11X,E16.8)
 4007 FORMAT(1H1,40X,40HTIME ELAPSED IN AUTO CORRELATION  (MIN.),F10.4)
 4010 FORMAT(1H1,7E16.8)
 4011 FORMAT(1H1,30X,23HAUTO SPECTRAL DENSITY   ///12X,1HK,10X, 4HFREQ,
     110X, 7HRAD/SEC,10X,17HCROSS SPEC. DENS.,10X,11HDB(RE.0002)//)
 4012 FORMAT(1H ,8X,I4, 8X,I6,8X,F9.4,2(10X,E14.8))
 4013 FORMAT(1H0,30X,18HCHOSEN FREQUENCIES //(10X,10F10.0))
 4014 FORMAT(1H1,30X,1HK,10X,4HFREQ,10X,7HRAD/SEC,10X,17HMODAL SPEC. DEN
     1S.,10X,11HDB(RE.0002) //)
 4015 FORMAT(1H ,21X,I10,8X,F6.0,8X,F9.4,2(8X,E16.8))
C
C
      COMMON /AAA/A(4000)
C
      EQUIVALENCE (A(1),MM),(A(2),NN),(A(3),IM),(A(4),IN),(A(5),NXYZ),
     1(A(6),KXYZ),(A(7),NAUTO),(A(8),NCROSS),(A(9),M),(A(10),N)
      EQUIVALENCE (A(21),XL1),(A(22),XLO),(A(23),YL1),(A(24),YLO),
     1(A(25),AI),(A(26),B),(A(27),C),(A(28),THETA),(A(29),P2),(A(30),PI)
     2,(A(31),X),(A(32),Y),(A(33),Z),(A(34),EPS),(A(35),NMAX),
     3(A(36),WMN),(A(37),AMN),(A(38),SUM1),(A(39),SUM2),
     4(A(40),JA),(A(41),JB)
      EQUIVALENCE (A(101),MAM),(A(151),NAN),(A(1001),W)
C
      DIMENSION MAM(50),NAN(50),W(20,50),RP(110),RPBAR(110),PRP(110) ,
     1WA(110),FI(110)
C
C     INTEGER W,WMN,WA
      REAL KMN
C
      CONVT = 60000.
C
C     CALL CLOCK(MTIME)
C
      DO  5 II=1,NXYZ
C
```

TABLE 5B (Continued)

```
      READ (5,3000) X,Y,Z,TAU,DTAU,NTAU,EPS,NMAX,NWA
C
      WRITE(6,4000) X,Y,Z,TAU,DTAU,NTAU,EPS,NMAX,NWA
C
      IF (NWA)  11,1,11
C
   11 READ (5,3001) (WA(K),K=1,NWA)
      WRITE(6,4013)  (WA(K),K=1,NWA)
C
C
    1 ATAU = TAU
C
      DO  6 IA=1,NTAU
    6 RP(IA) = 0.
C
      DO 7 IA=1,NWA
    7 FI(IA) = 0.
C
      DO 10 I=1,IM
      DO 10 J=1,IN
      JA = J
      JB=J
      IF (IM.EQ.MM) JA=I
      M=MAM(JA)
      N = NAN(J)
C
      WMN = W(I,J)
C
      KMN = C*THETA / (B*(1.+W(I,J)**2*THETA**2))
      AMN = B*W(I,J)
      CMN = W(I,J)*(1.-6.*B**2 + B**4)
      DMN = 4.*B*W(I,J)*(B**2-1.)
C
      WBAR1=(B**2+2.) /(B*W(I,J)*(B**2+4.))
      WBAR2 = B*WBAR1 / (B**2+2. )
      CBAR = KMN*W(I,J)*P2
C
```

```
      WRITE(6,4010) KMN,AMN,CMN,DMN,WBAR1,WBAR2,CBAR
      WRITE(6,4004)
C
C
      PHASE=1.5708
      KKK=2
      CALL DINT (AMN,PHASE,KKK)
      CAP2=SUM2
C
      KKK=1
      AMN=-AMN
      CALL DINT (AMN,PHASE,KKK)
      CAP1=SUM2
C
      KKK=5
      PHASE=0.
      CALL DINT (AMN,PHASE,KKK)
      CAP5=SUM2
C
      KKK=4
      AMN=-AMN
      CALL DINT (AMN,PHASE,KKK)
      CAP4=SUM2
C
C
      SP = CBAR* (WBAR1*CAP1*CAP2 + WBAR2*CAP1*CAP4 - WBAR2*CAP5*CAP2 +
     1WBAR1*CAP5*CAP4 )
C
      IF (SP) 9,9,12
    9 PHI = 0.
      GO TO 13
   12 PHI = 10.* ALOG10(SP) + 127.6
C
C
C
   13 WRITE(6,4002)II,X,Y,Z,M,N,W(I,J),SP,PHI
      IF  (NTAU)  22,21,22
```

TABLE 5B (Continued)

```
 22   TAU = ATAU
C
      DO 15 K=1,NTAU
C
      TH1 = CMN*COS(W(I,J)*TAU) + DMN * SIN(W(I,J)*TAU)
      TH2=CMN*SIN(W(I,J)*TAU)-DMN*COS(W(I,J)*TAU)
C
C
      RPN=KMN*EXP(-AMN*TAU) * (TH1*CAP1*CAP2 + TH2*CAP1*CAP4 - TH2
     1*CAP5*CAP2 + TH1*CAP5*CAP4)
      RP(K)=RP(K)+RPN
C
      WRITE(6,4003) K,TAU,RPN
C
   15 TAU = TAU + DTAU
C
 21   IF(NWA)  25,10,25
 25   WRITF(6,4014)
C
      DO 20 K=1,NWA
      RAD = WA(K)/(2.*PI)
      DD = (B**2*W(I,J)**2 + (W(I,J)-WA(K))**2)* (B**2*W(I,J)**2 +
     1(W(I,J) + WA(K))**2)
C
      AAMN = (B*W(I,J)*(B**2*W(I,J)**2 + W(I,J)**2 + WA(K)**2)) / DD
      BBMN = (W(I,J)*(B**2*W(I,J)**2 + W(I,J)**2 - WA(K)**2)) / DD
C
      TW1 = CMN*AAMN + DMN*BBMN
      TW2 = CMN*BBMN - DMN*AAMN
C
      FIT = KMN * (TW1*CAP1*CAP2 + TW2*CAP1*CAP4 - TW2*CAP5*CAP2 +
     1TW1*CAP5*CAP4)
C
      FAT = FIT
      IF (FIT)  19,19,17
 19   PHI = 0.
      FIT = 0.
```

TABLE 5B (Continued)

```
      GO TO 18
   17 PHI = 10.*ALOG10(FIT) + 127.6
   18 WRITE(6,4015) K,WA(K),RAD,FAT,PHI
C
   20 FI(K) = FI(K) + FIT
C
   10 CONTINUE
C
      IF (NTAU)  52,51,52
C
  52  WRITE(6,4005) RP(1)
C
      DO 30 K=1,NTAU
      RPBAR(K)=RP(K)/RP(1)
      PRP(K) = RP(K)/P2
      WRITE(6,4006) K,ATAU,RPBAR(K),PRP(K)
   30 ATAU=ATAU+DTAU
C
C
  51  IF (NWA)  27,5,27
  27  WRITE(6,4011)
C
      DO 40 K=1,NWA
      RAD = WA(K)/(2.*PI)
      IF (FI(K)) 45,45,41
  45  PHI = 0.
      GO TO 40
C
   41 PHI = 10.* ALOG10(FI(K)) + 127.6
   40 WRITE(6,4012) K,WA(K),RAD,FI(K),PHI
    5 CONTINUE
C
C     CALL CLOCK(NTIME)
C     TIME = (NTIME-MTIME)/CONVT
C
C     WRITE(6,4002)  TIME
C
```

```
      RETURN
      END
$IBFTC XCROS1
      SUBROUTINE CROSS1
C
C
C
C  CROSS CORRELATION)  TIME = CONSTANT
C
C
C
 1000 FORMAT(3E12.6,2I6,E12.6,I6/(6E12.8))
 1001 FORMAT(2(3E12.6,I4))
C
 2000 FORMAT(1H1,50X,17HCROSS CORRELATION///20X,1HX,20X,1HY,20X,1HZ,20X,
     13HMXP,10X,4HMTAU,10X, 3HEPS,10X, 4HNMAX //12X,E14.8,2(7X,E14.8),
     214X,I4,9X,I4, 5X,E12.6,7X,I3// 5X,7HTAU(I)=,5E16.8//12X,5E16.8//)
 2001 FORMAT(1H0,30X,2HXP,20X,2HYP,20X,2HZP,10X,3HNOR//(23X,E14.8,8X,E14
     1.8,8X,E14.8,5X,I3 ))
 2002 FORMAT(1H0,1HI ,4X,3HTAU,4X, 7HPNT CNT,5X,2HXP,10X,2HYP,10X,2HZP,
     110X, 6HM    N,4X,4HFREQ , 5X,17HCROSS SPEC. DENS.,5X,11HDB(RE.0002
     2),5X, 9HRPMN(TAU)//I2,E11.5,I4,E14.6,E12.6,E12.6,2X,2I5,2X,F6.0,
     36X,E14.8,4X,2E14.8 )
 2004 FORMAT(1H1,4X,1HI,8X, 3HTAU,12X,1HJ,10X,5HXP(J),9X,5HYP(J), 9X,
     15HZP(J),12X,11HCRPBAR(I,J),10X,12HNORM. FACTOR/// I6,5X,E10.5,
     24X,I5,3X,3E14.6,E20.8,E22.8/(25X,I5,3X,3E14.6,E20.8,E22.8))
 2005 FORMAT(1H0,50X,12HINTEGRATIONS // 33X,9HINT. NUM.,5X, 8H  MESH  ,
     15X,6HM    N,10X, 4HSUM2,16X, 4HSUM1)
 2010 FORMAT(1H1,7E16.8)
 2100 FORMAT(1H1,40X,41HTIME ELAPSED IN CROSS CORRELATION  (MIN.),F10.4)
C
C
      COMMON /AAA/A(4000)
C
      EQUIVALENCE (A(1),MM),(A(2),NN),(A(3),IM),(A(4),IN),(A(5),NXYZ),
     1(A(6),KXYZ),(A(7),NAUTO),(A(8),NCROSS),(A(9),M),(A(10),N)
      EQUIVALENCE (A(21),XL1),(A(22),XL0),(A(23),YL1),(A(24),YL0),
```

```
     1(A(25),AI),(A(26),B),(A(27),C),(A(28),THETA),(A(29),P2),(A(30),PI)
     2,(A(31),X),(A(32),Y),(A(33),Z),(A(34),EPS),(A(35),NMAX),
     3(A(36),WMN),(A(37),AMN),(A(38),SUM1),(A(39),SUM2),
     4(A(40),JA),(A(41),JB)
      EQUIVALENCE (A(101),MAM),(A(151),NAN),(A(1001),W),(A(2001),DIX1),
     1(A(3001),DIX5)
C
      DIMENSION  TAV(110),XP(50),YP(50),ZP(50),NOR(50),MAM(50),
     1NAN(50),W(20,50),DIX1(20,50),DIX5(20,50),CRPBAR(50)
C
C     INTEGER W,WMN
      REAL KMN
C
C     CALL CLOCK(MTIME)
C
C
      CONVT = 60000.
C
C
      DO 5 II=1,KXYZ
C
      READ (5,1000)XX,YY,ZZ,MXP,MTAV,EPS,NMAX,(TAV(I),I=1,MTAV)
      WRITE(6,2000)XX,YY,ZZ,MXP,MTAV,EPS,NMAX,(TAV(I),I=1,MTAV)
C
      READ (5,1001)(XP(I),YP(I),ZP(I),NOR(I),  I=1,MXP)
      WRITE(6,2001)(XP(I),YP(I),ZP(I),NOR(I),  I=1,MXP)
C
      DO 10 I=1, MTAV
C
      DO 20 J=1,MXP
      CRP = 0.
C
      DO 30 K=1,IM
      DO 30 L=1,IN
      JA=L
      JB=L
      IF (IM.EQ.MM) JA=K
```

TABLE 5B (Continued)

```
      M=MAM(JA)
      N=NAN(L)
      WMN= W(K,L)
C
      KMN = C*THETA / (B*(1.+W(K,L)**2*THETA**2))
      AMN = B*W(K,L)
      CMN = W(K,L)*(1.-6.*B**2 + B**4)
      DMN = 4.*B*W(K,L)*(B**2-1.)
      WBAR1=(B**2+2.)/(B*W(K,L)*(B**2+4.))
      WBAR2= B* WBAR1 / (B**2+2.)
      CBAR = KMN * W(K,L) * P2
C
      WRITE(6,2010) KMN,AMN,CMN,DMN,WBAR1,WBAR2,CBAR
      WRITE(6,2005)
C
      IF (J.NE.1) GO TO 31
C
      X=XX
      Y=YY
      Z=ZZ
C
      PHASE =1.5708
      KKK=1
      AMN =-AMN
      CALL DINT(AMN,PHASE,KKK)
      DIX1(K,L) = SUM2
C
      PHASE = 0.
      KKK= 5
      CALL DINT(AMN,PHASE,KKK)
      DIX5(K,L) = SUM2
C
      AMN = -AMN
C
   31 X=XP(J)
      Y=YP(J)
      Z=ZP(J)
```

```
C
      PHASE =1.5708
      KKK = 2
      CALL DINT(AMN,PHASE,KKK)
      CAP2 = SUM2
C
      PHASE = 0.
      KKK = 4
      CALL DINT(AMN,PHASE,KKK)
      CAP4 = SUM2
C
      SP = .5E+20
      PHI = .5E+20
C
      IF (NOR(J))  39,32,32
C
   39 SP = CBAR * (WBAR1*DIX1(K,L)*CAP2 + WBAR2*DIX1(K,L)*CAP4 -WBAR2*
     1DIX5(K,L)*CAP2 + WBAR1*DIX5(K,L)*CAP4 )
C
      IF (SP)  38,38,33
C
   38 PHI = 0.
      GO TO 32
C
   33 PHI = 10.* ALOG10(SP) + 127.6
C
   32 TH1 = CMN*COS(W(K,L)*TAV(I)) + DMN*SIN(W(K,L)*TAV(I))
      TH2 = CMN*SIN(W(K,L)*TAV(I)) - DMN*COS(W(K,L)*TAV(I))
C
      RPN = KMN*EXP(-AMN*TAV(I))*(TH1*DIX1(K,L)*CAP2 + TH2*DIX1(K,L)*
     1CAP4 - TH2*DIX5(K,L)*CAP2 + TH1*DIX5(K,L)*CAP4)
C
      CRP = CRP + RPN
C
   34 WRITE(6,2002)  I,TAV(I),J,XP(J),YP(J),ZP(J),M,N,W(K,L),SP,PHI,RPN
C
   30 CONTINUE
```

TABLE 5B (Continued)

```
C
      IF ((I+J).EQ.2) CNORM =CRP
      CRPBAR(J)    = CRP / CNORM
   20 CONTINUE
C
      WRITE(6,2004) I,TAV(I),(J,XP(J),YP(J),ZP(J),CRPBAR(J),CNORM,
     1J=1,MXP)
C
   10 CONTINUE
C
    5 CONTINUE
C
C
C     CALL CLOCK(NTIME)
C     TIME = (NTIME -MTIME)/ CONVT
C     WRITE(6,2100) TIME
C
C
      RETURN
      END
$IBFTC XCROS2
      SUBROUTINE CROSS2
C
C
C
C  CROSS CORRELATION (TIME)  (AUTO CORRELATION INCLUDED FOR THE FIRST POINT)
C
 1000 FORMAT(3E12.6,I3,2E12.8,I3,E6.2,2I3)
 1001 FORMAT(2(3E12.6,I4))
 1002 FORMAT(12F6.0)
C
 2000 FORMAT(1H1,50X,24HCROSS CORRELATION (TIME)///30X,1HX,30X,1HY,30X,
     11HZ,//4X,3E31.8///4X, 5HMXP =,I4,4X, 5HTAU =,E14.8,4X, 6HDTAU =,
     2E14.8,4X, 6HNTAU =,I4,4X, 5HEPS =,E14.8,4X, 6HNMAX =,I4,4X,5HNWA =
     3,I4 /)
 2001 FORMAT(1H0,30X,2HXP,20X,2HYP,20X,2HZP,10X,3HNOR//(23X,E14.8,8X,E14
     1.8,8X,E14.8,5X,I3 ))
```

```
2002 FORMAT(1H0, 9HCASE NUM.,5X,11HINTEG. PNT., 5X,2HXP,10X,2HYP,10X,
    12HZP,10X, 6HM    N,5X,4HFREQ ,5X,21HM.S. SPECTRAL DENSITY,5X,
    211HDB(RE.0002)//I5,10X,I5, 3X,3(3X,F9.4),4X,2I5,3X,F6.0,3X,2E20.8
    3////40X,1HK,8X,3HTAU,15X, 9HRPMN(TAU)//)
2003 FORMAT(1H0, 9HCASE NUM.,5X,11HINTEG. PNT., 5X,2HXP,10X,2HYP,10X,
    12HZP,10X, 6HM    N,5X,4HFREQ //I5,10X,I5, 3X,3(3X,F9.4),4X,2I5,3X,
    2I6 ////40X,1HK,8X,3HTAU,15X, 9HRPMN(TAU)//)
2004 FORMAT(1H ,30X,I10,E16.8,E20.8)
2005 FORMAT(1H1,50X,12HINTEGRATIONS // 33X,9HINT. NUM.,5X, 8H  MESH
    15X,6HM    N,10X, 4HSUM2,16X, 4HSUM1)
2007 FORMAT(1H1,30X,44HNORMALIZED CORRELATION OF ACCOUSTIC PRESSURE///
    110X, 4HNTAU,10X, 3HTAU,10X,25HNORM. CORR. OF ACC. PRES.,10X,
    28HRP(K)/P2,12X,14HNORM. FACTOR =,E14.8//)
2008 FORMAT(1H , 8X,I4,8X,F8.6,10X,E16.8,11X,E16.8)
2009 FORMAT(1H1,40X,40HTIME ELAPSED IN CROSS CORR.(TIME) (MIN.),F10.4)
2010 FORMAT(1H0,30X,18HCHOSEN FREQUENCIES //(10X,10F10.0))
2011 FORMAT(1H1,30X,23HCROSS SPECTRAL DENSITY  ///12X,1HK,10X, 4HFREQ,
    110X, 7HRAD/SEC,10X,17HCROSS SPEC. DENS.,10X,11HDB(RE.0002)//)
2012 FORMAT(1H ,8X,I4, 8X,I6,8X,F9.4,2(10X,E14.8))
2013 FORMAT(1H1,30X,1HK,10X,4HFREQ,10X,7HRAD/SEC,10X,17HMODAL SPEC. DEN
    1S.,10X,11HDB(RE.0002) //)
2014 FORMAT(1H ,21X,I10,8X,F6.0,8X,F9.4,2(3X,E16.8))
C
     COMMON /AAA/A(4000)
C
     EQUIVALENCE (A(1),MM),(A(2),NN),(A(3),IM),(A(4),IN),(A(5),NXYZ),
    1(A(6),KXYZ),(A(7),NAUTO),(A(8),NCROSS),(A(9),M),(A(10),N) ,
    2(A(11),LXYZ),(A(12),NCROST)
     EQUIVALENCE (A(21),XL1),(A(22),XL0),(A(23),YL1),(A(24),YL0),
    1(A(25),AI),(A(26),B),(A(27),C),(A(28),THETA),(A(29),P2),(A(30),PI)
    2,(A(31),X),(A(32),Y),(A(33),Z),(A(34),EPS),(A(35),NMAX),
    3(A(36),WMN),(A(37),AMN),(A(38),SUM1),(A(39),SUM2),
    4(A(40),JA),(A(41),JB)
     EQUIVALENCE (A(101),MAM),(A(151),NAN),(A(1001),W),(A(2001),DIX1),
    1(A(3001),DIX5)
C
     DIMENSION MAM(50),NAN(50),W(20,50),RP(110),RPBAR(110),PRP(110),
```

TABLE 5B (Continued)

```
     1WA(110),FI(110)
      DIMENSION XP(50),YP(50),ZP(50),DIX1(20,50),DIX5(20,50),NOR(50)
C
C     INTEGER W,WMN,WA
      REAL KMN
C
C     CALL CLOCK(MTIME)
C
C
      CONVT = 60000.
C
C
      DO 5 II=1,LXYZ
C
      READ (5,1000) XX,YY,ZZ,MXP,TAU,DTAU,NTAU,EPS,NMAX,NWA
C
      WRITE(6,2000) XX,YY,ZZ,MXP,TAU,DTAU,NTAU,EPS,NMAX,NWA
C
C
      ATAU = TAU
C
      READ (5,1001) (XP(I),YP(I),ZP(I),NOR(I), I=1,MXP.
      WRITE(6,2001) (XP(I),YP(I),ZP(I),NOR(I), I=1,MXP)
C
      IF (NWA) 2,1,2
C
  2   READ (5,1002) (WA(K),K=1,NWA)
      WRITE(6,2010) (WA(K),K=1,NWA)
C
    1 DO 10 JJ=1,MXP
C
      DO  6 IA=1,NTAU
    6 RP(IA) = 0.
C
      DO 7 IA=1,NWA
    7 FI(IA) = 0.
C
```

TABLE 5B (Continued)

```
      DO 20 I=1,IM
      DO 20 J=1,IN
      JA = J
      JB=J
      IF (IM.EQ.MM) JA=I
      M=MAM(JA)
      N = NAN(J)

      WMN = W(I,J)

      KMN = C*THETA / (B*(1.+W(I,J)**2*THETA**2))
      AMN = B*W(I,J)
      CMN = W(I,J)*(1.-6.*B**2 + B**4)
      DMN = 4.*B*W(I,J)*(B**2-1.)


      WRITE(6,2005)
      IF (JJ.NE.1) GO TO 21

      X=XX
      Y=YY
      Z=ZZ

      PHASE =1.5708
      KKK=1
      AMN =-AMN
      CALL DINT(AMN,PHASE,KKK)
      DIX1(I,J) = SUM2

      PHASE = 0.
      KKK= 5
      CALL DINT(AMN,PHASE,KKK)
      DIX5(I,J) = SUM2

      AMN = -AMN

   21 X=XP(JJ)
```

```
      Y=YP(JJ)
      Z=ZP(JJ)
C
      PHASE =1.5708
      KKK = 2
      CALL DINT(AMN,PHASE,KKK)
      CAP2 = SUM2
C
      PHASE = 0.
      KKK = 4
      CALL DINT(AMN,PHASE,KKK)
      CAP4 = SUM2
C
      IF (JJ.NE.1) GO TO 24
      WBAR1=(B**2+2.) /(B*W(I,J)*(B**2+4.))
      WBAR2 = B*WBAR1 / (B**2+2. )
      CBAR = KMN*W(I,J)*P2
C
      SP = CBAR * (WBAR1*DIX1(I,J)*CAP2 + WBAR2*DIX1(I,J)*CAP4 -WBAR2*
     1DIX5(I,J)*CAP2 + WBAR1*DIX5(I,J)*CAP4 )
      IF (SP) 11,11,22
   11 PHI = 0.
C
      GO TO 23
C
   22 PHI = 10.* ALOG10(SP) + 127.6
C
   23 WRITE(6,2002) II,JJ,XP(JJ),YP(JJ),ZP(JJ),M,N,W(I,J),SP,PHI
      GO TO 25
C
   24 WRITE(6,2003) II,JJ,XP(JJ),YP(JJ),ZP(JJ),M,N,W(I,J)
C
   25 IF (NTAU)  32,31,32
   32 TAU = ATAU
C
      DO 20 K=1,NTAU
C
```

TABLE 5B (Continued)

```
      TH1 = CMN*COS(W(I,J)*TAU) + DMN * SIN(W(I,J)*TAU)
      TH2=CMN*SIN(W(I,J)*TAU)-DMN*COS(W(I,J)*TAU)
C
      RPN=KMN*EXP(-AMN*TAU)*(TH1*DIX1(I,J)*CAP2+TH2*DIX1(I,J)*CAP4-TH2*
     1DIX5(I,J)*CAP2 + TH1*DIX5(I,J)*CAP4)
      RP(K)=RP(K)+RPN
C
      WRITE(6,2004) K,TAU,RPN
C
   30 TAU = TAU + DTAU
C
   31 IF (KWA) 33,20,33
C
   33 WRITE(6,2013)
C
      DO 19 K=1,NWA
      RAD = WA(K)/(2.*PI)
      DD = (B**2*W(I,J)**2 + (W(I,J)-WA(K))**2)* (B**2*W(I,J)**2 +
     1(W(I,J) + WA(K))**2)
C
      AAMN = (B*W(I,J)*(B**2*W(I,J)**2 + W(I,J)**2 + WA(K)**2)) / DD
      BBMN = (W(I,J)*(B**2*W(I,J)**2 + W(I,J)**2 - WA(K)**2)) / DD
C
      TW1 = CMN*AAMN + DMN*BBMN
      TW2 = CMN*BBMN - DMN*AAMN
C
      FIT = KMN * (TW1*DIX1(I,J)*CAP2 + TW2*DIX1(I,J)*CAP4 - TW2*DIX5(I,
     1J)*CAP2 + TW1*DIX5(I,J)*CAP4)
C
      FAT = FIT
      IF (FIT ) 77,77,17
   77 PHI = 0.
      FIT = 0.
      GO TO 18
   17 PHI = 10.*ALOG10(FIT) + 127.6
   18 WRITE(6,2014) K,WA(K),RAD,FAT,PHI
   19 FI(K) = FI(K) + FIT
```

TABLE 5B (Continued)

```
   20 CONTINUE
      IF (NTAU) 47,45,47
C
   47 WRITE(6,2007) RP(1)
      TAU = ATAU
C
      DO 40 K=1,NTAU
      RPBAR(K)=RP(K)/ RP(1)
      PRP(K) = RP(K)/P2
C
      WRITE(6,2008) K, TAU,RPBAR(K),PRP(K)
   40 TAU = TAU + DTAU
C
   45 IF (NWA)  49,10,49
   49 WRITE(6,2011)
C
      DO 50 K=1,NWA
      RAD = WA(K)/(2.*PI)
      IF (FI(K)) 53,53,51
   53 PHI = 0.
      GO TO 50
C
   51 PHI = 10.* ALOG10(FI(K)) + 127.6
   50 WRITE(6,2012) K,WA(K),RAD,FI(K),PHI
C
C
   10 CONTINUE
C
C
    5 CONTINUE
C
C     CALL CLOCK(NTIME)
C     TIME = (NTIME-MTIME)/CONVT
C
C     WRITE(6,2009)  TIME
C
      RETURN
```

```
      END
$IBFTC XDINT
      SUBROUTINE DINT (SAMN,SPHASE,KKS)
C
C
C  DOUBLE INTEGRATION SUBROUTINE
C
C
      COMMON /AAA/A(4000)
C
      EQUIVALENCE (A(9),M),(A(10),N),(A(21),XL1),(A(22),XL0),(A(23),YL1)
     1,(A(24),YL0),(A(34),EPS),(A(35),NMAX),(A(38),SUM1),(A(39),SUM2)
C
C
      DIMENSION P(5),WW(5)
C
      DATA (P(I),I=1,5),(WW(I),I=1,5) /.453089923,-.453089923,.269234655
     1,-.269234655,0.0,2*.118463443,2*.239314335,.284444444 /
C
 2000 FORMAT(1H0,28H  ***** NO CONVERGENCE *****,5X,I4,10X,I4,5X,I4,I5,
     12E18.8)
 2002 FORMAT(1H0,35X,I4,10X,I4,4X,I5,I5,2E18.8)
C
C
C
      NK=2
      BINC1=XL1-XL0
      BINC2=YL1-YL0
C
      DO 25 K=1,NMAX
      SUM1=SUM2
      SUM2=0.0
      CNK = NK
      DINC1 = BINC1/CNK
      DINC2 = BINC2/CNK
      H1 = XL0 + DINC1/2.
C
```

```
      DO 26 I=1,NK
      H2 = YLO + DINC2/2.
C
      DO 27 J=1,NK
      DO 28 II=1,5
      ABS1=DINC1*P(II)+H1
      DO 29 JJ=1,5
      ABS2=DINC2*P(JJ)+H2
   29 SUM2=SUM2+WW(II)*WW(JJ)*FFF(ABS1,ABS2,SAMN,SPHASE)
   28 CONTINUE
   27 H2=H2+DINC2
   26 H1=H1+DINC1
      SUM2=SUM2*DINC1*DINC2
C
C
      IF (K.EQ.1) GO TO 30
      IF (ABS((SUM1-SUM2)/SUM2)-EPS) 31,31,30
   30 NK=NK + 1
   25 CONTINUE
C
      WRITE(6,2000) KKS,NK,M,N,SUM2,SUM1
      SUM2 = 0.
C
      GO TO 32
C
C
   31 WRITE(6,2002) KKS,NK,M,N,SUM2,SUM1
C
   32 RETURN
      END
$IBFTC XFFF
      FUNCTION FFF(X0,Y0,FAMN,FPHASE)
C
C
C     DOUBLE INTEGRATION FUNCTION
C
C
```

```
C
      COMMON /AAA/A(4000)
C
      EQUIVALENCE (A(7),NAUTO),(A(8),NCROSS),(A(9),M),(A(10),N),
     1(A(21),XL1),(A(22),XL0),(A(23),YL1),(A(24),YL0),(A(25),AI),
     2(A(30),PI),(A(31),X),(A(32),Y),(A(33),Z),(A(36),WMN),(A(40),JA),
     3(A(41),JB)
C
      EQUIVALENCE (A(201),AMM),(A(251), ANN),(A(301),BMM),(A(351),BNN),
     1(A(401),CMM),(A(451),CNN),(A(501),DMM),(A(551),DNN),(A(601),ALMM),
     2(A(651),ALNN)
C
      DIMENSION AMM(50),ANN(50),BMM(50),BNN(50),CMM(50),CNN(50),DMM(50),
     1DNN(50),ALMM(50),ALNN(50)
C
C     INTEGER W,WMN
C
C
      R0=SQRT((X-X0)**2+(Y-Y0)**2 + Z**2)
C
      PHX = AMM(JA)*SIN(ALMM(JA)*X0)+ BMM(JA)*COS(ALMM(JA)*X0) +
     1CMM(JA)*SINH(ALMM(JA)*X0) + DMM(JA)*COSH(ALMM(JA)*X0)
C
      PHY=  ANN(JB)*SIN(ALNN(JB)*Y0)+ BNN(JB)*COS(ALNN(JB)*Y0) +
     1CNN(JB)*SINH(ALNN(JB)*Y0) + DNN(JB)*COSH(ALNN(JB)*Y0)
C
      FFF = PHX * PHY * EXP((FAMN/AI)*R0) * SIN((WMN/AI)*R0+FPHASE)/ R0
C
      RETURN
      END
```

APPENDIX D

UNDERWATER SOUND LABORATORY PROGRAM (STRAWDERMAN)

NOTATION

A	Equal to $0.75 \times 10^{-5}\ a^2 \rho_f^2 U_0^3 \delta^*$
a	Plate and acoustic cavity dimension in x-coordinate (longitudinal) direction
b	Plate and acoustic cavity dimension in y-coordinate (lateral) direction
b^+	Dimensionless plate and acoustic cavity dimension defined in Equation (D68)
C_j	Arbitrary constants
c	Speed of sound in acoustic medium
c^+	Dimensionless speed of sound defined in Equation (D77)
D	Plate flexural rigidity
D^+	Dimensionless plate flexural rigidity
d	Acoustic cavity dimension in z-coordinate (depth) direction
d^+	Dimensionless cavity dimension defined in Equation (D77)
$E[\ ]$	Denotes ensemble average
$F_{qrst}(x_1, x_2, y_1, y_2)$	Defined by Equation (D51)
$f_{qrst}(\Omega)$	Defined by Equation (D52)
G_{ns}	Defined subsequent to Equation (D21b)
$G^+_{mn}(\omega^+)$	Defined by Equation (D72)
$G_{jkmn}(x_1, x_2, y_1, y_2)$	Defined by Equation (D54)
$g_{jkmn}(z_1, z_2, \omega)$	Defined by Equation (D55)
$H(x, x', y, y', \omega)$	Complex frequency response of plate
$h(x, x', y, y', \theta)$	Plate displacement response to a unit impulsive force
i	Square root of -1
$K_{jkmnqrst}$	Defined by Equation (D60)
k	Acoustic wave number defined in Equation (D33)
k_x	Acoustic wave number in the x-coordinate direction
k_y	Acoustic wave number in the y-coordinate direction
$k_z, k_{z_{jk}}(\omega)$	Acoustic wave number in the z-coordinate direction

$k^{+}_{z_{jk}}(\omega^{+})$	Dimensionless acoustic wave number in the z-coordinate direction
M	Dimensionless fluid mass defined by Equation (D68)
m, n, etc.	Mode numbers
P_n	Defined subsequent to Equation (D21b)
$P^{+}_{n}(\omega^{+})$	Defined by Equation (D73)
P_t	Turbulent boundary layer wall pressure
p_a	Cavity acoustic pressure
$Q_{aa}(x_1, x_2, y_1, y_2, z_1, z_2$ $t_1, t_2)$	Cavity acoustic pressure cross correlation
$Q_{pp}(x_1, x_2, y_1, y_2, t)$	Plate pressure cross correlation
$Q_{\phi\phi}(x_1, x_2, y_1, y_2, t_1, t_2)$	Plate velocity cross correlation
R_m	Defined subsequent to Equation (D21b)
$R^{+}_{m}(\omega^{+})$	Defined by Equation (D69)
r	Effective plate damping coefficient per unit area
$r_{c_{mn}}$	Critical plate damping coefficient for the m-n^{th} mode
r^{+}	Dimensionless plate damping coefficient defined in Equation (D68)
$r^{+}_{c_{mn}}$	Dimensionless critical plate damping coefficient for the m-n^{th} mode
$S_{aa}(x_1, x_2, y_1, y_2, z_1,$ $z_2, \omega)$	Cavity acoustic pressure cross spectral density
$S_{pp}(\xi, \eta, \omega)$	Turbulent wall pressure cross spectral density
$S_{\phi\phi}(x_1, x_2, y_1, y_2, \omega)$	Plate velocity cross spectral density
T_{mn}	Defined subsequent to Equation (D21b)
$T^{+}_{mn}(\omega^{+})$	Defined by Equation (D74)
t	Time coordinate
t'	Time at which impulsive force occurs
U_0	Free stream velocity of flowing fluid in x-coordinate direction

U_c	Mean convection velocity of turbulent boundary layer
U^+	Dimensionless free stream velocity defined by Equation (D68)
$U^+_{jkmn}(\omega^+)$	Defined by Equation (D78)
$\vec{u}$	Acoustic phase velocity vector
u_x	Acoustic phase velocity in the x-coordinate direction
u_y	Acoustic phase velocity in the y-coordinate direction
u_z	Acoustic phase velocity in the z-coordinate direction
V_{mnqs}	Defined subsequent to Equation (D21b)
W_{mnqs}	Defined by Equation (D23)
$W^+_{mnqs}(\omega^+)$	Defined by Equation (D75)
w	Plate displacement in the z-coordinate direction
$X_{j\ell}(\omega)$	Defined by Equation (D40)
x	Longitudinal spacial coordinate
x^+	Dimensionless longitudinal spacial coordinate defined by Equation (D68)
y	Lateral spacial coordinate
y^+	Dimensionless lateral spacial coordinate defined by Equation (D68)
z	Spacial coordinate normal to the plate
z^+	Dimensionless spacial coordinate defined by Equation (D77)
α	A dimensionless constant
$\alpha_{mn}(x,y)$	Plate normalized natural mode shapes
$\delta_{j\ell}$	Kronecker delta
$\delta(\omega-\Omega)$	Dirac delta function
δ^*	Turbulent boundary layer displacement thickness
δ^+	Dimensionless turbulent boundary layer displacement thickness defined by Equation (D68)
$\xi(x,x',y,y',\theta)$	Plate velocity response to a suit inpulsive force
η	Relative lateral coordinate $(y-y')$
θ	Relative time coordinate $(t-t')$

λ_{mn}	Phase angle defined subsequent to Equation (D21b)
μ	Effective mass of plate per unit area
ν_m	Phase angle defined subsequent to Equation (D21b)
ξ	Relative longitudinal coordinate $(x - x')$
ρ_f	Mass density of flowing fluid
ρ_{a_0}	Time average mass density of acoustic medium
ρ_a	Instantaneous mass density of acoustic medium
τ	Time difference $(t_2 - t_1)$
$\Phi(\omega)$	Turbulent wall pressure spectral density
$\phi^+(\omega)$	Dimensionless turbulent wall pressure spectral density
$\Phi_{\phi}(x, y, \omega)$ or $\Phi(x^+, y^+, \omega^+)$	Plate velocity spectral density
$\Phi_{\phi}^+(x^+, y^+, \omega^+)$	Dimensionless plate velocity spectral density
$\Phi_a(x, y, z, \omega)$ or $\Phi_a(x^+, y^+, z^+, \omega^+)$	Cavity acoustic pressure spectral density
$\Phi_a^+(x^+, y^+, z^+, \omega^+)$	Dimensionless cavity acoustic pressure spectral density
ϕ	Plate velocity
ψ	Acoustic velocity potential
ω	Radial frequency
ω^+	Dimensionless radial frequency
ω_{mn}	Natural frequency of *m-n* mode of plate
ω_{mn}^+	Dimensionless natural frequency of *m-n* mode of plate
∇^4	Biharmonic operator
$X(\omega)$	Defined by Equation (D53)
Ω	Radial frequency

APPENDIX D1 – MATHEMATICAL ANALYSIS

The equations for the plate velocity and cavity acoustic pressure spectral densities and cross correlations are now derived[32] for a plate (Figure 15) subject to turbulence excitation.

The differential equation governing the displacement of the plate due to turbulent boundary layer pressure excitation on the plate surface is

$$D\nabla^4 w + r\frac{\partial w}{\partial t} + \mu\frac{\partial^2 w}{\partial t^2} = p_t(x, y, z) \qquad \text{(D1)}$$

Following Dyer (see Appendix A), the equation for the free undamped plate

$$D\nabla^4 w + \mu\frac{\partial^2 w}{\partial t^2} = 0 \qquad \text{(D2)}$$

has the normal mode solution, satisfying the simply supported edge conditions (Figure 15), given by

$$w(x, y, t) = a_{mn}(x, y)\sin\omega_{mn} t \qquad \text{(D3)}$$

where

$$a_{mn}(x, y) = \frac{2}{\sqrt{ab}}\sin\frac{m\pi y}{a}\sin\frac{n\pi x}{a} \qquad \text{(D4)}$$

$$\omega_{mn} = \sqrt{\frac{D}{\mu}}\left[\left(\frac{m\pi}{a}\right)^2 + \left(\frac{n\pi}{b}\right)^2\right] \qquad \text{(D5)}$$

and

$$\int_0^b\int_0^a a_{mn}(x, y)\, a_{qr}(x,y)\, dx\, dy = \delta_{mq}\,\delta_{nr} \qquad \text{(D6)}$$

The solution to Equation (D1) for any *deterministic* pressure is then assumed to be

$$w(x, y, t) = \sum_{\substack{m=1\\n=1}}^{\substack{\infty\\\infty}} a_{mn}(x, y)\, T_{mn}(t) \qquad \text{(D7)}$$

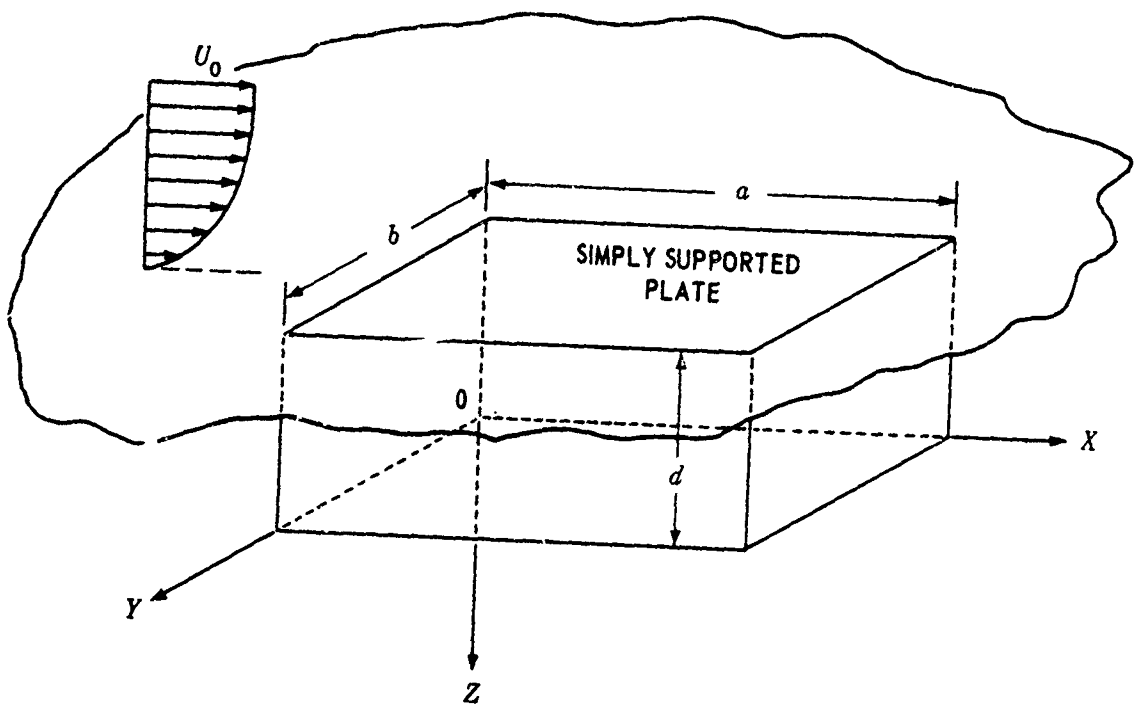

Figure 15 – Illustration of the Theoretical Model

Substituting Equation (D7) in (D1) and using Equation (D6), we find $T_{mn}(t)$ must satisfy

$$\frac{d^2 T_{mn}}{dt^2} + \frac{r}{\mu}\frac{dT_{mn}}{dt} + \omega_{mn}^2 T_{mn} = \frac{1}{\mu}\int_0^b \int_0^a p_t(x,y,t)\, a_{mn}(x,y)\, dx\, dy \, . \quad \text{(D8)}$$

For later use, we consider the following two cases.

CASE I: Concentrated load applied at $(x'y')$ varying sinusoidally in time

$$p_t(x,y,t) = \delta(x-x')\,\delta(y-y')\, e^{i\omega t} \qquad \text{(D9)}$$

Substituting Equation (D9) in (D8) results in the following solution for Equation (D7):

$$w(x,y,t) = \sum_{\substack{m=1\\ n=1}}^{\substack{\infty\\ \infty}} \frac{a_{mn}(x,y)a_{mn}(x',y')}{\mu\left[\left(\omega_{mn}^2 - \omega^2\right) + \frac{ir\omega}{\mu}\right]} e^{i\omega t} = H(x,x',y,y',\omega)\, e^{i\omega t} \qquad \text{(D10)}$$

where $H(x,x',y,y',\omega)$, the complex frequency response,[32] is

$$H(x,x',y,y',\omega) = \frac{1}{\mu} \sum_{\substack{m=1\\ n=1}}^{\substack{\infty\\ \infty}} \frac{a_{mn}(x,y)\, a_{mn}(x',y')}{\left[\left(\omega_{mn}^2 - \omega^2\right) + \frac{ir\omega}{\mu}\right]} \qquad \text{(D11)}$$

CASE II: Inpulsive loading at time t' applied at (x', y')

$$p_t(x,y,t) = \delta(x-x')\,\delta(y-y')\,\delta(t-t') \qquad \text{(D12)}$$

Define

$$\theta = t - t'$$

$$h(x,x',y,y',\theta) = \begin{cases} w(x,y,t) & \theta > 0 \\ 0 & \theta \le 0 \end{cases}$$

Substituting Equation (D12) in (D8) results in the following solution for Equation (D7):

$$h(x,x',y,y',\theta) = w(x,y,t) = \frac{e^{\frac{-r\theta}{2\mu}}}{\mu} \sum_{\substack{m=1\\n=1}}^{\infty}\sum^{\infty} \frac{a_{mn}(x,y)\, a_{mn}(x',y')}{\sqrt{\omega_{mn}^2 - \left(\frac{r}{2\mu}\right)^2}} \sin\sqrt{\omega_{mn}^2 - \left(\frac{r}{2\mu}\right)^2}\,\theta \qquad \theta \geq 0$$

(D13)

By superposition, the response for any deterministic pressure field may be written

$$w(x,y,t) = \int_{-\infty}^{t}\int_0^b\int_0^a p_t(x',y',t')\,h(x,x',y,y',\theta)\,dx'\,dy'\,dt' =$$

$$\int_0^{\infty}\int_0^b\int_0^a p_t(x',y',t-\theta)\,h(x,x',y,y'\theta)\,dx'\,dy'\,d\theta \qquad \text{(D14)}$$

Since the velocity of the plate, rather than displacement, is required for the boundary value in the *acoustic* problem, we define the velocity *response* of the plate to impulse loading thus

$$\zeta(x,x',y,y',\theta) = \frac{\partial h(x,x',y,y',\theta)}{\partial t} = \frac{e^{\frac{-r\theta}{2\mu}}}{\mu} \sum_{\substack{m=1\\n=1}}^{\infty}\sum^{\infty} \frac{a_{mn}(x,y)\, a_{mn}(x',y')}{\sqrt{\omega_{mn}^2 - \left(\frac{r}{2\mu}\right)^2}} \cdot$$

$$\cdot\left\{\sqrt{\omega_{mn}^2 - \left(\frac{r}{2\mu}\right)^2}\cos\sqrt{\omega_{mn}^2 - \left(\frac{r}{2\mu}\right)^2}\,\theta - \frac{r}{2\mu}\sin\sqrt{\omega_{mn}^2 - \left(\frac{r}{2\mu}\right)^2}\,\theta\right\} \qquad \theta \geq 0$$

(D15)

And we define the *velocity field* of the plate as

$$\phi(x,y,t) = \frac{\partial w(x,y,t)}{\partial t} = \int_0^{\infty}\int_0^b\int_0^a p_t(x',y',t-\theta)\,\delta(x,x',y,y',\theta)\,dx'\,dy'\,d\theta$$

(D16)

We define the turbulent *wall pressure cross correlation* by (E denotes the ensemble average):

$$Q_{pp}(x_1,x_2,y_1,y_2,t) = E\left[p_t(x_1,y_1,t)\,p_t(x_2,y_2,t)\right] \qquad \text{(D17)}$$

The *plate velocity cross correlation* is then

$$Q_{\phi\phi}(x_1, x_2, y_1, y_2, t_1, t_2) = E[\,\phi(x_1, y_1, t_1)\,\phi(x_2, y_2, t_2)] = E\left[\int_0^b \int_0^a \int_0^b \int_0^a \int_0^\infty \int_0^\infty \cdot\right.$$

$$\cdot\, p_t(x_1', y_1', t_1 - \theta_1)\, p_t(x_2', y_2', t_2 - \theta_2)\, \delta(x_1, x_1', y_1, y_1', \theta_1)\,\cdot$$

$$\left.\cdot\, \zeta(x_2, x_2', y_2, y_2', \theta_2)\, d\theta_1\, d\theta_2\, dx_1'\, dy_1'\, dx_2'\, dy_2'\right]$$

$$= \int_0^b \int_0^a \int_0^b \int_0^a \int_0^\infty \int_0^\infty Q_{pp}(x_1', x_2', y_1', y_2', t_1 - \theta_1, t_2 - \theta_2)\, \zeta(x_1, x_1', y_1, y_1', \theta_1)$$

$$\cdot\, \zeta(x_2, x_2', y_2, y_2', \theta_2)\, d\theta_1\, d\theta_2\, dx_1'\, dy_1'\, dx_2'\, dy_2'$$

$$= \int_0^b \int_0^a \int_0^b \int_0^a \int_0^\infty \int_0^\infty Q_{pp}(\zeta', \eta', \tau + \theta_1 - \theta_2)\, \zeta(x_1, x_1', y_1, y_1', \theta_1)$$

$$\zeta(x_2, x_2', y_2, y_2', \theta_2)\, d\theta_1\, d\theta_2\, dx_1'\, dy_1'\, dx_2'\, dy_2' \qquad \text{(D18)}$$

In obtaining Equation (D18), we took account of the fact that since the plate velocity impulse function is not a random quantity, the ensemble average applied only to the turbulent pressure field. Also, since the turbulent boundary layer pressure is assumed to be a homogeneous stationary process, Q_{pp} is a function of the difference between the spatial and temporal coordinates rather than the coordinates themselves[33].

The *plate velocity cross spectral density* is then (multiplying and dividing Equation (D18) by $e^{-i\omega(\theta_1 - \theta_2)}$ to obtain the third member below):

$$S_{\phi\phi}(x_1, x_2, y_1, y_2, \omega) = \frac{1}{\sqrt{2\pi}} \int_{-\infty}^{\infty} Q_{\phi\phi}(x_1, x_2, y_1, y_2, \tau)\, e^{-i\omega\tau}\, d\tau =$$

$$\int_0^b \int_0^a \int_0^b \int_0^a \int_0^\infty \int_0^\infty \left\{ \frac{1}{\sqrt{2\pi}} \int_{-\infty}^{\infty} Q_{pp}(\xi', \eta', \tau + \theta_1 - \theta_2)\, e^{-i\omega(\tau+\theta_1-\theta_2)} \cdot \right.$$

$$\left. \cdot\, d(\tau + \theta_1 - \theta_2) \right\} \zeta(x_1, x_1', y_1, y_1'\, \theta_1)\, e^{i\omega\theta_1}\, \zeta(x_2, x_2', y_2, y_2', \theta_2) \cdot$$

$$\cdot\, e^{-i\omega\theta_2}\, d\theta_1\, d\theta_2 dx_1', dy_1', dx_2'\, dy_2'$$

$$= \int_0^b \int_0^a \int_0^b \int_0^a S_{pp}(\xi', \eta', \omega) \int_{0}^{\infty} \zeta\, (x_1, x_1', y_1, y_1'\, \theta_1) e^{i\omega\theta_1}\, d\theta_1 \cdot$$

$$\cdot \int_0^\infty \zeta(x_2, x_2', y_2, y_2', \theta_2)\, e^{-i\omega\theta_2}\, d\theta_2\, dx_1'\, dy_1'\, dx_2'\, dy_2'$$

$$= \int_0^b \int_0^a \int_0^b \int_0^a \omega^2 S_{pp}(\xi', \eta', \omega)\, H(x_1, x_1', y_1, y_1' - \omega)\, H(x_2, x_2', y_2, y_2' - \omega)\, dx_1'\, dy_1'\, dx_2'\, dy_2'$$

(D19)

where, since $\zeta(x, x', y, y', \omega)$ is zero for $\theta \leq 0$, the semi-infinite limits in θ_1 and θ_2 have been replaced by infinite limits and as can be shown (see Equation 2.11 of Reference 33)

$$\int_{\infty}^{\infty} \zeta(x_2, x_2', y_2, y_2', \theta_2)\, e^{-i\omega\theta_2}\, d\theta_2 = i\omega\, H(x_2, x_2', y_2, y_2' - \omega)$$

$$\int_{-\infty}^{\infty} \zeta(x_1, x_1', y_1, y_1', \theta_1)\, e^{i\omega\theta_1}\, d\theta_1 = -i\omega H(x_1, x_1', y_1, y_1' - \omega)$$

(D20)

The mathematical model for S_{pp} used by Strawderman and discussed in detail in Reference 32 is*

$$S_{pp}(\xi,\eta,\omega) = 0.75\times 10^{-5}\ a^2\rho_f^2 U_0^3\,\delta^*\left[e^{-0.115\left|\frac{\omega\xi}{U_c}\right|}\right]\left[e^{-0.7\left|\frac{\omega\eta}{U_c}\right|}\right]e^{-i\left(\frac{\omega\xi}{U_c}\right)}\ ;\ \omega\le 1.256\,\frac{U_0}{\delta^*}$$

$$= 1.5\times 10^{-5}\ a^2\,\frac{\rho_f^2 U_0^6}{\omega^3\delta^{*2}}\left[e^{-0.115\left|\frac{\omega\xi}{U_c}\right|}\right]\left[e^{-0.7\left|\frac{\omega\eta}{U_c}\right|}\right]e^{-i\left(\frac{\omega\xi}{U_c}\right)}\ ;\ \omega > 1.256\,\frac{U_0}{\delta^*}$$

(D21a)

where $a = 1.0$ for water and $a = 3.0$ for air.

Substituting Equation (D21a) in (D19) and using Equations (D11) and (D4), we obtain after extensive, but routine, simplification (see Reference 32 for details):

$$S_{\phi\phi}(x_1; x_2, y_1, y_2) = \frac{16A\omega^2}{\mu^2a^2b^2}\sum_{\substack{m=1\\n=1}}^{\infty}\sum_{\substack{q=1\\s=1}}^{\infty}\frac{\sin\frac{m\pi x_1}{a}\sin\frac{n\pi y_1}{b}\sin\frac{q\pi x_2}{a}\sin\frac{s\pi y_2}{b}}{T_{mn}T_{qs}P_nP_sR_mR_q}\,.$$

$$\cdot\, G_{ns}\,V_{mnqs}\ ;\ \omega\le 1.256\,\frac{U_0}{\delta^*}$$

$$S_{\phi\phi}(x_1, x_2, y_1, y_2) = \frac{32A\omega^2}{\mu^2a^2b^2}\left(\frac{\omega\delta^*}{U_0}\right)^{-3}\sum_{\substack{m=1\\n=1}}^{\infty}\sum_{\substack{q=1\\s=1}}^{\infty}\frac{\sin\frac{m\pi x_1}{a}\sin\frac{n\pi y_1}{b}\sin\frac{q\pi x_2}{a}\sin\frac{s\pi y_2}{b}}{T_{mn}T_{qs}P_nP_sR_mR_q}\,.$$

$$\cdot\, G_{ns}\,V_{mnqs}\ ;\ \omega > 1.256\,\frac{U_0}{\delta^*} \qquad \text{(D21b)}$$

---

*Equation (D21a) represents a mathematical fit to the Corcos model which is based on experimental data. The Skudryzk and Haddle expression for the turbulent wall pressure spectral density $\phi(\omega)$ is incorporated in this model. See Equation (3.1) of Reference 32.

where

$$A = 0.75 \times 10^{-5}\; a^2 \rho_f^2\, U_0^3\, \delta^*$$

$$T_{mn} = \sqrt{(\omega_{mn}^2 - \omega^2)^2 + \left(\frac{r\omega}{\mu}\right)^2} \quad ; \text{ similarly for } T_{qs}$$

$$P_n = \left(0.7\,\frac{\omega}{U_c}\right)^2 + \left(\frac{n\pi}{b}\right)^2 \quad ; \text{ similarly for } P_s$$

$$R_m = \sqrt{\left(\frac{m\pi}{a}\right)^2 - 0.987\left(\frac{\omega}{U_c}\right)^{2\quad 2} + 0.0529\left(\frac{\omega}{U_c}\right)^4} \quad ; \text{ similarly for } R_q$$

$$G_{ns} = 0.35\,\frac{\omega b}{U_c}\;\delta_{ns}\left[2\left(0.7\,\frac{\omega}{U_c}\right)^2 + \left(\frac{n\pi}{b}\right)^2 + \left(\frac{s\pi}{b}\right)^2\right]$$

$$+\;\frac{ns\pi^2}{b^2}\left[1 - \delta_{ns}\right]\left[(-1)^n\,(-1)^s - 1\right]$$

$$+\;\frac{ns\pi^2}{b^2}\left\{2 - \left[(-1)^n + (-1)^s\right] e^{-0.7\left(\frac{\omega b}{U_c}\right)}\right\}$$

$$V_{mnqs} = \left\{\delta_{mq}\; 1.0066\,\frac{\omega a}{U_c}\, R_m\,(\nu_m - 0.463\,\pi)\right.$$

$$+\;(1-\delta_{mq})\,\frac{mq\pi^2\,[(-1)^m(-1)^q - 1]}{a^2\left[\left(\frac{m\pi}{a}\right)^2 - \left(\frac{q\pi}{a}\right)^2\right]}\left[R_m\, e^{i\nu_q} - R_q\, e^{-i\nu_m}\right] + \frac{2mq\pi^2}{a^2}\cdot\cos(\nu_q + \nu_m)$$

$$\left. -\;\frac{mq\pi^2}{a^2}\, e^{-0.115\left(\frac{\omega a}{U_c}\right)}\left[(-1)^m\, e^{i\left(\frac{\omega a}{U_c} + \nu_q + \nu_m\right)} + (-1)^q\, e^{-i\left(\frac{\omega a}{U_c} + \nu_q + \nu_m\right)}\right]\right\} e^{i\left(\lambda_{mn} - \lambda_{qs}\right)}$$

$$\nu_m = \tan^{-1}\frac{0.23\left(\frac{\omega}{U_c}\right)^2}{\left[\left(\frac{m\pi}{a}\right)^2 - 0.987\left(\frac{\omega}{U_c}\right)^2\right]} \quad ; \text{ similarly for } \nu_q$$

$$\lambda_{mn} = \tan^{-1} \frac{\frac{r\omega}{\mu}}{\omega_{mn}^2 - \omega^2}; \text{ similarly for } \lambda_{qs}$$

The power spectrum of the plate velocity $\Phi_{\phi}(x,y,\omega)$ is found as follows. First let $x_1 = x_2 = x$, $y_1 = y_2 = y$ in Equations (D21b); since $\Phi(x,y,\omega)$ must be a real, even function then the summations in the resultant equations must be real if they are to be considered as valid solutions for $\Phi_{\phi}(x,y,\omega)$. Then substitute V_{mnqs} from Equation (D21b) in the equation for $\Phi_{\phi}(x,y,\omega)$. After rearranging this equation and taking $G_{ns} = G_{sn}$, since G_{ns} is a symmetrical matrix, we find (see Reference 32 for details):

$$\Phi_{\phi}(x,y,\omega) = S_{\phi}(x_1, x_1, y_1, y_1; \omega) = \frac{16A\omega^2}{\mu^2 a^2 b^2} \sum_{\substack{m=1 \\ n=1}}^{\infty\ \infty} \sum_{\substack{q=1 \\ s=1}}^{\infty\ \infty}$$

$$\cdot \frac{\sin\frac{m\pi x}{a} \sin\frac{n\pi y}{b} \sin\frac{q\pi x}{a} \sin\frac{s\pi y}{b}}{T_{mn} T_{qs} P_n P_s R_m R_q} G_{ns} W_{mnqs} \;; \omega \leq 1.256 \frac{U_0}{\delta *}$$

$$= \frac{32A\omega^2}{\mu^2 a^2 b^2} \left(\frac{\omega\delta *}{U_0}\right)^{-3} \sum_{\substack{m=1 \\ n=1}}^{\infty\ \infty} \sum_{\substack{q=1 \\ s=1}}^{\infty\ \infty} \frac{\sin\frac{m\pi x}{a} \sin\frac{n\pi y}{b} \sin\frac{q\pi x}{a} \sin\frac{s\pi y}{b}}{T_{mn} T_{qs} P_n P_s R_m R_q} G_{ns} W_{mnqs} \;; \omega > 1.256 \frac{U_0}{\delta *}$$

(D22)

where

$$W_{mnqs} = 1.0066 \frac{\omega a}{U_e} \delta_{mq} R_m \cos(\nu_m - 0.463\pi) \cos(\lambda_{mn} - \lambda_{qs})$$

$$+ \frac{2mq\pi^2}{a^2} \cos(\nu_m + \nu_q)(\cos\lambda_{mn} - \lambda_{qs}) + (1 - \delta_{mq}) \frac{mq\pi^2}{a^2} \frac{[(-1)^m(-1)^q - 1]}{\left[\left(\frac{m\pi}{a}\right)^2 - \left(\frac{q\pi}{a}\right)^2\right]}$$

$$+ [R_m \cos(\lambda_q + \lambda_{mn} - \lambda_{qs}) - R_q \cos(\nu_m + \lambda_{qs} - \lambda_{mn})]$$

$$-\frac{mq\pi^2}{a^2} e^{-0.115 \frac{\omega a}{U_c}} \left[(-1)^m \cos\left(\frac{\omega a}{U_c} + \nu_q + \nu_m + \lambda_{mn} - \lambda_{qs}\right)\right.$$

$$\left. + (-1)^q \cos\left(\frac{\omega a}{U_c} + \nu_q + \nu_m + \lambda_{qs} - \lambda_{mn}\right)\right] \tag{D23}$$

We now find the cavity acoustic pressure due to an arbitrary plate velocity distribution. From this we will obtain the cavity acoustic pressure cross correlation and spectral density.

We start with the equations governing acoustic phenomena and the boundary conditions for Figure 12.

Momentum equation: $$\rho_a \frac{\partial \overline{u}}{\partial t} + \nabla p_a = 0 \tag{D24}$$

Continuity equation: $$\frac{\partial \rho_a}{\partial t} + \rho_{a_0} \nabla \cdot \overline{u} = 0 \tag{D25}$$

Equation of state: $$p_a = c^2 \rho_a \tag{D26}$$

Boundary conditions: $$u_x(0,y,z,t) = 0 \tag{D27a}$$

$$u_x(a,y,z,t) = 0 \tag{D27b}$$

$$u_y(x,0,z,t) = 0 \tag{D27c}$$

$$u_y(x,b,z,t) = 0 \tag{D27d}$$

$$u_z(x,y,0,t) = 0 \tag{D27e}$$

$$u_z(x,y,-d,t) = \phi(x,y,t) \tag{D27f}$$

Since Equation (D24) was derived for an inviscid fluid, the acoustic field may be assumed to be irrotational. Hence the acoustic phase velocity may be defined in terms of the velocity potential

$$\overline{u}(x,y,z,t) = \nabla \psi (x,y,z,t) \tag{D28}$$

Equation (D28 specifies ψ to within an arbitrary function of time. To uniquely specify ψ define, in addition

$$p_a(x,y,z,t) = -\rho_{a_0} \frac{\partial \psi (x,y,z,t)}{\partial t} \tag{D29}$$

Substitution of Equations (D28) and (D29) into (D24) satisfies the latter equation. To satisfy Equations (D25) and (D26), we proceed as follows:

Substitute Equation (D26) into (D25) to obtain

$$\frac{1}{c^2}\frac{\partial p_a}{\partial t} + \rho_{a_0} \nabla \cdot \overline{u} = 0 \qquad \text{(D30)}$$

Substitute Equations (D28) and (D29) into (D30) to obtain the scalar wave equation in ψ

$$\nabla^2\psi - \frac{1}{c^2}\frac{\partial^2\psi}{\partial t^2} = 0 \qquad \text{(D31)}$$

which, by virtue of the separation of variables technique, has the solution

$$\psi(x,y,z,t) = [C_1 \sin k_x x + C_2 \cos k_x x]\,[C_3 \sin k_y y + C_4 \cos k_y y]$$

$$[C_5 \sin k_z z + C_6 k_z z]\; C_7\, e^{ikct} \qquad \text{(D32)}$$

where

$$k_x^2 + k_y^2 + k_z^2 = k^2 \qquad \text{(D33)}$$

Substituting the boundary conditions, Equations (D27a–e), into Equation (D32), using Equation (D28), we obtain

$$C_1 = C_3 = C_5 = 0 \qquad \text{(D34)}$$

$$k_x = \frac{j\pi}{a} \qquad j = \text{integer} \qquad \text{(D35)}$$

$$k_y = \frac{\ell\pi}{b} \qquad \ell = \text{integer} \qquad \text{(D36)}$$

Defining $\omega = k\ C$ (D37)

and using Equations (D34), (D35), and (D36), we have

$$\psi(x,y,z,t) = \sum_{\substack{j=0\\ \ell=0}}^{\substack{\infty\\ \infty}} C_{2_j} \cos\frac{j\pi x}{a}\, C_{4_\ell} \cos\frac{\ell\pi y}{b} C_6 \cos(k_{z_{j\ell}} z)\, C_7\, e^{i\omega t} \qquad \text{(D38a)}$$

Combining the constants, we assume that the solution for $\psi(x,y,z,t)$ has the form

$$\psi(x,y,z,t) = \sum_{\substack{j=0 \\ \ell=0}}^{\infty\ \infty} \cos\frac{j\pi x}{a} \cos\frac{\ell\pi y}{b} \int_{-\infty}^{\infty} Y_{j\ell}(\omega) \cos(k_{z_{j\ell}} z)\, e^{i\omega t} \frac{d\omega}{\sqrt{2\pi}} \tag{D38b}$$

Equation (D38b) satisfies the wave Equation (D31) as can be seen by substituting Equation (D38b) in (D31). Also, by applying the above arguments, Equations (D27a – e) are satisfied. It remains only to satisfy the boundary condition (D27f), $u_z(x,y,-d,t) = \phi(x,y,t)$ $= \left.\frac{\partial\psi(x,y,z,t)}{\partial z}\right|_{z=-d}$.

Hence

$$\phi(x,y,t) = \sum_{\substack{j=0 \\ \ell=0}}^{\infty\ \infty} \cos\frac{j\pi x}{a} \cos\frac{\ell\pi y}{b} \int_{-\infty}^{\infty} Y_{j\ell}(\omega) \left\{-k_{z_{j\ell}} \sin\left[k_{z_{j\ell}}(-d)\right]\right\} e^{i\omega t} \frac{d\omega}{\sqrt{2\pi}}$$

$$= \sum_{\substack{j=0 \\ \ell=0}}^{\infty\ \infty} \cos\frac{j\pi x}{a} \cos\frac{\ell\pi y}{b} \int_{-\infty}^{\infty} X_{j\ell}(\omega)\, e^{i\omega t} \frac{d\omega}{\sqrt{2\pi}} \tag{D39}$$

where

$$X_{j\ell}(\omega) = K_{z_{j\ell}}(\omega)\, Y_{j\ell}(\omega) \sin(k_{z_{j\ell}} d) \tag{D40}$$

Multiplying both sides of Equation (D39) by $\cos\frac{j\pi x}{a} \cos\frac{\ell\pi y}{b}$ and integrating over the area of the plate, we find by virtue of the orthogonality principle that*

$$\int_{-\infty}^{\infty} X_{j\ell}(\omega)\, e^{i\omega t} \frac{d\omega}{\sqrt{2\pi}} = \frac{4}{ab(1+\delta_{0j})(1+\delta_{0\ell})} \int_0^b \int_0^a \phi(x,y,t) \cos\frac{j\pi x}{a} \cos\frac{\ell\pi y}{b}\, dx\, dy \tag{D41a}$$

*By L' Hôpital's rule, $\lim_{j\to 0} \frac{\sin 2j\pi}{2j\pi} = \frac{2\pi}{2\pi} = 1$, hence $\frac{\sin 2j\pi}{2j\pi} = \delta_{0j}$. Similarly for $\delta_{0\ell}$.

Transformation of Equation (D41a) yields

$$X_{j\ell}(\omega) = \frac{4}{ab(1+\delta_{0j})\,(1+\delta_{0\ell})}\int_{-\infty}^{\infty}\int_{0}^{b}\int_{0}^{a} \phi(x,y,t)\cos\frac{j\pi x}{a}\cos\frac{\ell\pi y}{b}\cdot e^{-i\omega t}\,dx\,dy\,\frac{dt}{\sqrt{2\pi}} \tag{D41b}$$

Thus, from Equation (D40)

$$Y_{j\ell}(\omega) = \frac{4}{ab(1+\delta_{0j})(1+\delta_{0\ell})k_{z_{j\ell}}\sin k_{z_{j\ell}}d}\int_{-\infty}^{\infty}\int_{0}^{b}\int_{0}^{a}$$

$$\cdot\,\phi(x,y,t)\cos\frac{j\pi x}{a}\cos\frac{\ell\pi y}{b}e^{-i\omega t}\,dx\,dy\,\frac{dt}{\sqrt{2\pi}} \tag{D42}$$

Substitution of Equation (D42) in (D38b) yields

$$\psi(x,y,z,t) = \frac{2}{\pi ab}\sum_{\substack{j=0\\ \ell=0}}^{\substack{\infty\\ \infty}}\cos\frac{j\pi x}{a}\cos\frac{\ell\pi y}{b}\int_{-\infty}^{\infty}\frac{\cos k_{z_{j\ell}}z}{(1+\delta_{0j})\,(1+\delta_{0\ell})k_{z_{j\ell}}\sin k_{z_{j\ell}}d}$$

$$\left\{\int_{-\infty}^{\infty}\int_{0}^{b}\int_{0}^{a}\phi(x,y,t)\cos\frac{j\pi x}{a}\cos\frac{\ell\pi y}{b}e^{-i\omega t}\,dx\,dy\,dt\right\}e^{i\omega t}\,d\omega \tag{D43}$$

Substitution of Equation (D43) in (D29) yields the cavity acoustic pressure for an arbitrary, deterministic plate velocity

$$p_a(x,y,z,t) = \frac{-2i\rho_{a_0}}{\pi ab}\sum_{\substack{j=0\\ \ell=0}}^{\substack{\infty\\ \infty}}\cos\frac{j\pi x}{a}\cos\frac{\ell\pi y}{b}\int_{-\infty}^{\infty}\frac{\omega\cos k_{z_{j\ell}}z}{(1+\delta_{0j})(1+\delta_{0\ell})k_{z_{j\ell}}\sin k_{z_{j\ell}}d}$$

$$\left\{\int_{-\infty}^{\infty}\int_{0}^{b}\int_{0}^{a}\phi(x,y,t)\cos\frac{j\pi x}{a}\cos\frac{\ell\pi y}{b}e^{-i\omega t}\,dx\,dy\,dt\right\}e^{-i\omega t}\,d\omega \tag{D44}$$

If now $\phi(x,y,t)$ is considered to be the only random quantity in p_a, then the *cavity acoustic pressure cross correlation* is

$$Q_{aa}(x_1,x_2,y_1,y_2,z_1,z_2,t_1,t_2) = E[\,p_a(x_1,y_1,z_1,t_1)\,p_a(x_2,y_2,z_2,t_2)\,]$$

$$= \frac{-4\rho^2_{a_0}}{\pi^2 a^2 b^2} \sum_{\substack{j=0\\ \ell=0}}^{\infty}{}^{\infty} \sum_{\substack{r=0\\ t=0}}^{\infty}{}^{\infty} \cos\frac{j\pi x_1}{a}\cos\frac{\ell\pi y_1}{b}\cos\frac{r\pi x_2}{a}\cos\frac{t\pi y_2}{b}$$

$$\Bigg\{\int_{-\infty}^{\infty}\int_{-\infty}^{\infty} \frac{\omega\,\Omega\,\cos k_{z_{j\ell}} z_1 \cos k_{z_{rt}} z_2}{(1+\delta_{0j})(1+\delta_{0\ell})(1+\delta_{0r})(1+\delta_{0t})\,k_{z_{rt}}(\Omega)\sin k_{z_{j\ell}} d\,\sin k_{z_{rt}} d}$$

$$\Bigg[\int_{-\infty}^{\infty}\int_{-\infty}^{\infty}\int_0^b\int_0^a\int_0^b\int_0^a E\Big[\phi(x_1,y_1,t_1)\,\phi(x_2,y_2,t_2)\Big]\cos\frac{j\pi x_1}{a}\cos\frac{\ell\pi y_1}{b}\cos\frac{r\pi x_2}{a}$$

$$\cos\frac{t\pi y_2}{b}\, e^{-i\omega t_1}\, e^{-i\Omega t_1}\, dx_1\, dy_1\, dx_2\, dy_2\, dt_1\, dt_2\Bigg] e^{i\omega t_1}\, e^{i\Omega t_2}\, d\omega d\Omega\Bigg\}$$

(D45)

In Equation (D45), we note that from Equation (D18)

$$E[\phi(x_1,y_1,t_1)\,\phi(x_2,y_2,t_2)\,] = Q_{\phi\phi}(x_1,x_2,y_1,y_2,\tau) \qquad \text{(D46)}$$

Also, since $\tau = t_2 - t_1$, then using Equation (D19) and noting that $\int_{-\infty}^{\infty} e^{-i(\omega+\Omega)t_1}\, dt_1$ $= 2\pi\,\delta(\omega+\Omega)$

$$\int_{-\infty}^{\infty}\int_{-\infty}^{\infty} Q_{\phi\phi}(x_1,x_2,y_1,y_2,\tau)\, e^{-i\omega t_1}\, e^{-i\Omega t_2}\, dt_1\, dt_2$$

$$= \int_{-\infty}^{\infty} Q_{\phi\phi}(x_1,x_2,y_1,y_2,\tau)\, e^{-i\Omega\tau}\int_{-\infty}^{\infty} e^{-i(\omega+\Omega)t_1}\, dt_1$$

$$= \sqrt{2\pi}\, S_{\phi\phi}(x_1,x_2,y_1,y_2,\omega)\int_{-\infty}^{\infty} e^{-i(\omega+\Omega)t_1}\, dt_1 = (2\pi)^{3/2}\, S_{\phi\phi}(x_1,x_2,y_1,y_2,\Omega)\;\delta(\omega+\Omega)$$

(D47)

Substituting Equation (D47) in (D45), integrating over ω, and using the identity $\tau = t_2 - t_1$ yields

$$Q_{aa}(x_1,x_2,y_1,y_2,z_1,z_2,\tau) = \frac{-8\sqrt{2}\rho_{a_0}^2}{\sqrt{\pi}a^2b^2} \sum_{\substack{j=0\\ \ell=0}}^{\infty\ \infty} \sum_{\substack{r=0\\ t=0}}^{\infty\ \infty} \cos\frac{j\pi x_1}{a} \cos\frac{\ell\pi y_1}{b} \cos\frac{r\pi x_2}{a} \cos\frac{t\pi y_2}{b}$$

$$\int_{-\infty}^{\infty} \frac{\Omega^2 \cos k_{z_{j\ell}} z_1 \cos k_{z_{rt}} z_2}{(1+\delta_{0j})(1+\delta_{0\ell})(1+\delta_{0r})(1+\delta_{0t}) k_{z_{j\ell}}(-\Omega) k_{z_{rt}}(\Omega) \sin k_{z_{j\ell}} d \sin k_{z_{rt}} d}$$

$$\left\{ \int_0^b \int_0^a \int_0^b \int_0^a S_{\phi\phi}(x_1,x_2,y_1,y_2,\Omega) \cos\frac{j\pi x_1}{a} \cos\frac{\ell\pi y_1}{b} \cos\frac{r\pi x_2}{a} \cos\frac{t\pi y_2}{b} \right.$$

$$\left. dx_1\, dy_1\, dx_2\, dy_2 \right\} e^{i\Omega\tau}\, d\Omega \qquad \text{(D48a)}$$

where from Equations (D33), (D35), (D36), and (D37)

$$k_{z_{j\ell}}(\omega) = \left[\frac{\omega^2}{c^2} - \left(\frac{j\pi}{a}\right)^2 - \left(\frac{\ell\pi}{b}\right)^2\right]^{1/2} \qquad \text{(D48b)}$$

Hence

$$k_{z_{j\ell}}(\omega) = k_{z_{j\ell}}(-\omega) \qquad \text{(D48c)}$$

The cavity acoustic pressure cross spectral density is

$$S_{aa}(x_1,x_2,y_1,y_2,z_1,z_2,\omega) = \frac{1}{\sqrt{2\pi}} \int_{-\infty}^{\infty} Q_{aa}(x_1,x_2,y_1,y_2,z_1,z_2,\tau)\, e^{-i\omega\tau}\, d\tau \qquad \text{(D49)}$$

Substitution of Equation (D48a) in (D49) with $S_{\phi\phi}$ given by Equation (D21b) yields (after reassigning the subscripts such that j,k,m,n apply to the acoustics problem and q,r,s and t to the plate)

$$
S_{aa}(x_1,x_2,y_1,y_2,z_1,z_2,\omega) = \frac{8\rho_{a_0}^2}{\pi a^2 b^2} \sum_{\substack{j=0\\k=0}}^{\substack{\infty\\\infty}} \sum_{\substack{m=0\\n=0}}^{\substack{\infty\\\infty}} G_{jkmn}(x_1,x_2,y_1,y_2)
$$

$$
\int_{-\infty}^{\infty} \left\{ \int_{-\infty}^{\infty} \frac{g_{jkmn}(z_1,z_2,\Omega)}{(1+\delta_{0j})\,(1+\delta_{0k})\,(1+\delta_{0m})\,(1+\delta_{0n})}\, X(\Omega) \right.
$$

$$
\sum_{\substack{q=1\\r=1}}^{\substack{\infty\\\infty}} \sum_{\substack{s=1\\t=1}}^{\substack{\infty\\\infty}} \left[\int_0^b \int_0^a \int_0^b \int_0^a F_{qrst}(x_1,x_2,y_1,y_2)\, f_{qrst}(\Omega)\, G_{jkmn}(x_1,x_2,y_1,y_2) \right.
$$

$$
\left. dx_1\, dy_1\, dx_2\, dy_2 \right] e^{i\Omega\tau}\, d\Omega \Bigg\}\, e^{-i\omega\tau}\, d\tau
$$

$$
= \frac{8\rho_{a_0}^2}{\pi a^2 b^2} \sum_{\substack{j=0\\k=0}}^{\substack{\infty\\\infty}} \sum_{\substack{m=0\\n=0}}^{\substack{\infty\\\infty}} \sum_{\substack{q=1\\r=1}}^{\substack{\infty\\\infty}} \sum_{\substack{s=1\\t=1}}^{\substack{\infty\\\infty}} \frac{G_{jkmn}(x_1,x_2,y_1,y_2)}{(1+\delta_{0j})\,(1+\delta_{0k})\,(1+\delta_{0m})\,(1+\delta_{0n})}
$$

$$
\left[\int_0^b \int_0^a \int_0^b \int_0^a F_{qrst}(x_1,x_2,y_1,y_2)\, G_{jkmn}(x_1,x_2,y_1,y_2)\, dx_1\, dy_1\, dx_2\, dy_2 \right]
$$

$$
\int_{-\infty}^{\infty} \left\{ \int_{-\infty}^{\infty} g_{jkmn}(z_1,z_2,\Omega)\, X(\Omega)\, f_{qrst}(\Omega)\, e^{i\Omega\tau}\, d\Omega \right\} e^{-i\omega\tau}\, d\tau \qquad \text{(D50)}
$$

where

$$
F_{qrst}(x_1,x_2,y_1,y_2) = \sin\frac{q\pi x_1}{a}\, \sin\frac{r\pi y_1}{b}\, \sin\frac{s\pi x_2}{a}\, \sin\frac{t\pi y_2}{b} \qquad \text{(D51)}
$$

$$
f_{qrst}(\Omega) = \frac{G_{rt}(\Omega)\, V_{qrst}(\Omega)}{T_{qr}(\Omega)\, T_{st}(\Omega)\, P_r(\Omega)\, P_t(\Omega)\, R_q(\Omega)\, R_s(\Omega)} \qquad \text{(D52)}
$$

$$X(\Omega) = \begin{cases} \dfrac{16A\Omega^2}{\mu^2 a^2 b^2} & \Omega \le 1.256 \dfrac{U_0}{\delta^*} \\ \\ \dfrac{32A\Omega^2}{\mu^2 a^2 b^2} \left(\dfrac{\Omega\delta^*}{U_0}\right)^{-3} & \Omega > 1.256 \dfrac{U_0}{\delta^*} \end{cases} \tag{D53}$$

$$G_{jkmn}(x_1,x_2,y_1,y_2) = \cos\frac{j\pi x_1}{a}\cos\frac{k\pi y_1}{b}\cos\frac{m\pi x_2}{a}\cos\frac{n\pi y_2}{b} \tag{D54}$$

$$g_{jkmn}(z_1,z_2,\Omega) = \frac{\Omega^2 \cos k_{z_{jk}} z_1 \cos k_{z_{mn}} z_2}{k_{z_{jk}}(\Omega)\, k_{z_{mn}}(\Omega) \sin k_{z_{jk}} d \sin k_{z_{mn}} d} \tag{D55}$$

Integration over frequency Ω of the bracketed term in the right member of Equation (D50) results in

$$\sqrt{2\pi}\; g_{jkmn}(z_1, z_2, \tau)\, X(\tau)\, f_{qrst}(\tau) \tag{D56}$$

where

$$f(\tau) = \frac{1}{\sqrt{2\pi}} \int_{-\infty}^{\infty} F(\omega)\, e^{i\omega\tau}\, d\omega \tag{D57}$$

Substitution of Equation (D56) in (D50) and integration over τ yields the final expression for the cavity acoustic cross spectral density:

$$S_{aa}(x_1,x_2,y_1,y_2,z_1,z_2,\omega) = \frac{16\rho_{a_0}^2}{a^2 b^2} \sum_{\substack{j=0\\k=0}}^{\infty\;\infty} \sum_{\substack{m=0\\n=0}}^{\infty\;\infty} \sum_{\substack{q=1\\r=1}}^{\infty\;\infty} \sum_{\substack{s=1\\t=1}}^{\infty\;\infty}$$

$$G_{jkmn}(x_1,x_2,y_1,y_2)\, g_{jkmn}(z_1,z_2,\omega)\, X(\omega)\, f_{qrst}(\omega) \cdot$$

$$\cdot \left[\frac{1}{(1+\delta_{0j})(1+\delta_{0k})(1+\delta_{0m})(1+\delta_{0n})} \int_0^b \int_0^a \int_0^b \int_0^a F_{qrst}(x_1,x_2,y_1,y_2) \right.$$

$$\left. G_{jkmn}(x_1,x_2,y_1,y_2)\, dx_1\, dy_1\, dx_2\, dy_2 \right] \tag{D58}$$

Integrating over the spatial coordinates, using Equations (D51) and (D54), we obtain by means of standard integration techniques

$$S_{aa}(x_1,x_2,y_1,y_2,z_1,z_2,\omega) = \frac{16\rho_{a_0}^2}{\pi^4} X(\omega) \sum_{\substack{j=0\\k=0}}^{\substack{\infty\\\infty}} \sum_{\substack{m=0\\n=0}}^{\substack{\infty\\\infty}} \sum_{\substack{q=1\\r=1}}^{\substack{\infty\\\infty}} \sum_{\substack{s=1\\t=1}}^{\substack{\infty\\\infty}}$$

$$G_{jkmn}(x_1,x_2,y_1,y_2)\, g_{jkmn}(z_1,z_2,\omega)\, f_{qrst}(\omega)\, K_{jkmnqrst} \tag{D59}$$

where G_{jkmn}, g_{jkmn}, f_{qrst}, and $X(\omega)$ are defined in Equations (D54), (D55), (D52), and (D53), respectively, and where

$$K_{jkmnqrst} = \frac{(1-\delta_{qj})(1-\delta_{rk})(1-\delta_{sm})(1-\delta_{tn})\, qrst \left[1-(-1)^q(-1)^j\right]\left[1-(-1)^r(-1)^k\right]}{(1+\delta_{0j})(1+\delta_{0k})(1+\delta_{0m})(1+\delta_{0n})(q^2-j^2)(r^2-k^2)}$$

$$\cdot \frac{\left[1-(-1)^s(-1)^m\right]\left[1-(-1)^t(-1)^n\right]}{(s^2-m^2)(t^2-n^2)} \tag{D60}$$

The *cavity acoustic pressure spectral density* obtained from Equation (D58) is

$$\Phi_a(x_1,y_1,z_1,\omega) = S_{aa}(x_1,x_1,y_1,y_1,z_1,z_1,\omega) = \frac{16\rho_{a_0}^2}{\pi^4} X(\omega) \cdot$$

$$\sum_{\substack{j=0\\k=0}}^{\substack{\infty\\\infty}} \sum_{\substack{m=0\\n=0}}^{\substack{\infty\\\infty}} \sum_{\substack{q=1\\r=1}}^{\substack{\infty\\\infty}} \sum_{\substack{s=1\\t=1}}^{\substack{\infty\\\infty}} G_{jkmn}(x_1,x_1,y_1,y_1)\, g_{jkmn}(z_1,z_1,\omega) f_{qrst}(\omega) K_{jkmnqrst} \tag{D61}$$

Setting $x_1 = x_2$, $y_1 = y_2$ in Equation (D54) and $z_1 = z_2$ in Equation (D55), we have

$$G_{jkmn}(x_1,x_1,y_1,y_1) = G_{mnjk}(x_1,x_1,y_1,y_1) = G_{jkmn}(x_1,y_1) \qquad \text{(D62)}$$

$$g_{jkmn}(z_1,z_1,\omega) = g_{mnjk}(z_1,z_1\omega) = g_{jkmn}(z_1,\omega) \qquad \text{(D63)}$$

Also

$$K_{jkmnqrst} = K_{mnjkstqr} \qquad \text{(D64)}$$

Hence using (D52), (D53), (D62), and (D63) in Equation (D61) and dropping the subscripts on spatial coordinates , we obtain

$$\Phi_a(x,y,z,\omega) = \frac{256A\rho_{a_0}^2\omega^2}{\pi^4\mu^2a^2b^2} \sum_{\substack{j=0\\k=0}}^{\infty\,\infty} \sum_{\substack{m=0\\n=0}}^{\infty\,\infty} \sum_{\substack{q=1\\r=1}}^{\infty\,\infty} \sum_{\substack{s=1\\t=1}}^{\infty\,\infty} \frac{G_{jkmn}(x,y)g_{jkmn}(z,\omega)G_{rt}(\omega)}{T_{qr}(\omega)\,T_{st}(\omega)\,P_r(\omega)\,P_t(\omega)R_q(\omega)R_s(\omega)}$$

$$\cdot\, K_{jkmnqrst}\,V_{qrst}(\omega); \qquad \omega \le 1.256\frac{U_0}{\delta*}$$

$$= \frac{512A\rho_{a_0}^2\omega^2}{\pi^4\mu^2a^2b^2}\left(\frac{\omega\delta*}{U_0}\right)^{-3} \sum_{\substack{j=0\\k=0}}^{\infty\,\infty} \sum_{\substack{m=0\\n=0}}^{\infty\,\infty} \sum_{\substack{q=1\\r=1}}^{\infty\,\infty} \sum_{\substack{s=1\\t=1}}^{\infty\,\infty} \frac{G_{jkmn}(x,y)\,g_{jkmn}(z,\omega)G_{rt}(\omega)}{T_{qr}(\omega)\,T_{st}(\omega)\,P_r(\omega)\,P_t(\omega)\,R_q(\omega)\,R_s(\omega)}\,\cdot$$

$$\cdot\, K_{jkmnqrst}\,V_{qrst}(\omega) \qquad \omega > 1.256\,\frac{U_0}{\delta*} \qquad \text{(D65)}$$

As for the case of the plate velocity spectral density, the cavity acoustic pressure spectral density must be a real, even function of frequency. Thus by substituting V_{qrst} (as given below Equation (D21b)) in Equation (D65), rearranging Equation (D65) first for the frequency range $\omega \le 1.256\,\frac{U_0}{\delta*}$, (see Reference 32 for details) and then for $\omega > 1.256\,\frac{U_0}{\delta*}$, and using Equations (D62), (D63), and (D64), we finally obtain

$$\Phi_a(x,y,z,\omega) = \frac{256 A\rho_{a_0}^2\,\omega^2}{\pi^4\mu^2 a^2 b^2} \sum_{\substack{j=0\\k=0}}^{\infty\,\infty} \sum_{\substack{m=0\\n=0}}^{\infty\,\infty} \sum_{\substack{q=1\\r=1}}^{\infty\,\infty} \sum_{\substack{s=1\\t=1}}^{\infty\,\infty} \frac{G_{jkmn}(x,y)\, g_{jkmn}(z,\omega) G_{rt}(\omega)}{T_{qr}(\omega)\, T_{st}(\omega)\, P_r(\omega)\, P_t(\omega)\, R_q(\omega)\, R_s(\omega)} \,.$$

$$\cdot\, W_{qrst}(\omega)\, K_{jkmnqrst}; \qquad \omega \leq 1.256\,\frac{U_0}{\delta^*}$$

$$\Phi_a(x,y,z,\omega) = \frac{512 A\rho_{a_0}^2\,\omega^2}{\pi^4\mu^2 a^2 b^2} \cdot \left(\frac{\omega\delta^*}{U_0}\right)^{-3} \sum_{\substack{j=0\\k=0}}^{\infty\,\infty} \sum_{\substack{m=0\\n=0}}^{\infty\,\infty} \sum_{\substack{q=1\\r=1}}^{\infty\,\infty} \sum_{\substack{s=1\\t=1}}^{\infty\,\infty} \frac{G_{jkmn}(x,y) g_{jkmn}(z,\omega) G_{rt}(\omega)}{T_{qr}(\omega)\, T_{st}(\omega)\, P_r(\omega)\, P_t(\omega) R_q(\omega) R_s(\omega)}$$

$$\cdot\, W_{qrst}(\omega)\, K_{jkmnqrst} \qquad \omega > 1.256\,\frac{U_0}{\delta^*} \tag{D66}$$

For practical utility, the plate velocities and cavity acoustic pressures are expressed in nondimensional form. *The nondimensional expressions given below are the working expressions used in the computer program.*

The *nondimensional form of the plate spectral velocity* is defined as

$$\Phi_\phi^+ (x^+, y^+, \omega^+) = \frac{\Phi_\phi (x^+, y^+, \omega^+)}{a^2\, U_c\, a} = 4.38 \times 10^{-4} M^2 \delta^+ \omega^{+^{-2}} \,.$$

$$\sum_{\substack{m=1\\n=1}}^{\infty\,\infty} \sum_{\substack{q=1\\s=1}}^{\infty\,\infty} \frac{\sin m\pi x^+ \sin q\pi x^+ \sin \frac{n\pi y^+}{b^+} \sin \frac{s\pi y^+}{b^+}\, G_{ns}^+ (\omega^+) W_{mnqs}^+(\omega^+)}{T_{mn}^+(\omega^+)\, T_{qs}^+(\omega^+)\, P_n^+(\omega^+) P_s^+(\omega^+)\, R_m^+(\omega^+)\, R_q^+(\omega^+)}; \quad \omega^+ \delta^+ \leq 1.932$$

$$= 3.2 \times 10^{-3} M^2 \delta^{+^{-2}} \omega^{+^{-5}} \sum_{\substack{m=1\\n=1}}^{\infty\,\infty} \sum_{\substack{q=1\\s=1}}^{\infty\,\infty}$$

$$\frac{\sin m\pi x^+ \sin q\pi x^+ \sin \frac{n\pi y^+}{b^+} \sin \frac{s\pi y^+}{b^+}\, G_{ns}^+ (\omega^+) W_{mnqs}^+ (\omega^+)}{T_{mn}^+(\omega^+)\, T_{qs}^+(\omega^+)\, P_n^+(\omega^+)\, P_s^+(\omega^+)\, R_m^+(\omega^+)\, R_q^+(\omega^+)}; \quad \omega^+ \delta^+ > 1.932 \tag{D67}$$

where the dimensionless input parameters and spatial and frequency variables are defined as follows

$$M = \frac{\rho_f a}{\mu} \qquad x^+ = \frac{x}{a}$$

$$U^+ = \frac{U_0}{U_c} \qquad y^+ = \frac{y}{a}$$

$$\delta^+ = \frac{\delta^*}{a} \qquad \omega^+ = \frac{\omega a}{U_c}$$

$$b^+ = \frac{b}{a}$$

$$\omega^+_{mn} = \frac{\omega_{mn} a}{U_c}$$

$$r^+ = \frac{r a}{\mu U_c}$$

$$r^+_{c_{mn}} = \frac{r_{c_{mn}} a}{\mu U_c} = \frac{2\omega_{mn} a}{U_c}$$

$$D^+ = \frac{D}{\mu U_c^2 a^2} \tag{D68}$$

The quantities defined below Equation (D21) for R_m, R_q, ν_m, ν_q, λ_{mn}, λ_{qs}, G_{ns}, P_n, P_s, T_{mn}, T_{qs}, and Equation (D23) have been rewritten in dimensionless terms as follows:

$$R_m^+(\omega^+) = \left\{\left[(m\pi)^2 - 0.987\,\omega^{+2}\right]^2 + 0.0529\,\omega^{+4}\right\}^{1/2} \tag{D69}$$

$$\nu_m = \tan^{-1}\left[\frac{0.23\,\omega^{+2}}{(m\pi)^2 - 0.987\,\omega^{+2}}\right] \tag{D70}$$

$$\lambda_{mn} = \tan^{-1}\left[\frac{r^+\omega^+}{(\omega^+_{mn})^2 - (\omega^+)^2}\right] \tag{D71}$$

$$G^+_{mn}(\omega^+) = 0.35\,\omega^+ b^+ \delta_{mn}\left[2(0.7\,\omega^+ b^+)^2 + (m\pi)^2 + (n\pi)^2\right]$$

$$+\, mn\pi^2\left[(-1)^m(-1)^n - 1\right]\left[1-\delta_{mn}\right] + mn\pi^2\left\{2 - \left[(-1)^m + (-1)^n\right]e^{-0.7\,\omega^+ b^+}\right\}$$

(D72)

$$P^+_m(\omega^+) = (m\pi)^2 + (0.7\,\omega^+ b^+)^2 \qquad \text{(D73)}$$

$$T^+_{mn}(\omega^+) = \left\{\left[\left(\frac{\omega^+_{mn}}{\omega^+}\right)^2 - 1\right]^2 + \left[2\,\frac{r^+}{r^+_{c_{mn}}}\,\frac{\omega^+_{mn}}{\omega^+}\right]^2\right\}^{1/2} \qquad \text{(D74)}$$

$$W^+_{jkmn}(\omega^+) = 1.0066\,\omega + \delta_{jm}\,R^+_m\cos(\nu_j - 0.463\pi)\cos(\lambda_{jk} - \lambda_{mn})$$

$$+\, 2jm\pi^2\cos(\nu_j + \nu_m)\cos(\lambda_{jk} - \lambda_{mn}) + (1-\delta_{jm})\cdot\frac{jm\pi^2\left[(-1)^j(-1)^m - 1\right]}{\left[(j\pi)^2 - (m\pi)^2\right]}$$

$$\cdot\left[R^+_j\cos(\nu_m + \lambda_{jk} - \lambda_{mn}) - R^+_m\cos(\nu_j + \lambda_{mn} - \lambda_{jk})\right] - jm\pi^2 e^{-0.115\,\omega^+}$$

$$\cdot\left[(-1)^j\cos(\omega^+ + \nu_j + \nu_m + \lambda_{jk} - \lambda_{mn}) + (-1)^m\cos(\omega^+ + \nu_j + \nu_m + \lambda_{mn} - \lambda_{jk})\right]$$

(D75)

The nondimensional *form of the cavity acoustic pressure spectral density* is defined as

$$\Phi^+_a(x^+, y^+, z^+, \omega^+) = \frac{\Phi_a(x^+, y^+, z^+, \omega^+)\,a}{a^2\mu^2U_c^3} = \frac{7.008\times 10^{-3}}{\pi^4}\,\rho^{+2}M^2\delta^+\,\cdot$$

$$\cdot\sum_{\substack{j=0\\k=0}}^{\infty\,\infty}\;\sum_{\substack{m=0\\n=0}}^{\infty\,\infty}\;\sum_{\substack{q=1\\r=1}}^{\infty\,\infty}\;\sum_{\substack{s=1\\t=1}}^{\infty\,\infty}\left\{\frac{G^+_{rt}(\omega^+)W^+_{qrst}(\omega^+)K_{jkmnqrst}}{U^+_{jkmn}(\omega^+)}\right\}\,.$$

$$
\cdot \frac{\cos j\pi x^{+} \cos m\pi x^{+} \cos \dfrac{k\pi y^{+}}{b^{+}} \cos \dfrac{n\pi y^{+}}{b^{+}} \cos k^{+}_{z_{jk}} z^{+} \cos k^{+}_{z_{mn}} z^{+}}{T^{+}_{qr}(\omega^{+})\, T^{+}_{st}(\omega^{+})\, P^{+}_{r}(\omega^{+})\, P^{+}_{t}(\omega^{+})\, R^{+}_{q}(\omega^{+})\, R^{+}_{s}(\omega^{+})} \;;\; \omega^{+}\delta^{+} \leq 1.932
$$

$$
= \frac{5.112 \times 10^{-2}}{\pi^{4}} \rho^{+2} M^{2} \delta^{+-2} \omega^{+-3} \sum_{\substack{j=0 \\ k=0}}^{\infty\ \infty} \sum_{\substack{m=0 \\ n=0}}^{\infty\ \infty} \sum_{\substack{q=1 \\ r=1}}^{\infty\ \infty} \sum_{\substack{s=1 \\ t=1}}^{\infty\ \infty}
$$

$$
\cdot \left\{ \frac{G^{+}_{rt}(\omega^{+})\, W^{+}_{qrst}(\omega^{+})\, K_{jkmnqrst}}{U^{+}_{jkmn}(\omega^{+})} \right\} \cdot
$$

$$
\cdot \frac{\cos j\pi x^{+} \cos m\pi x^{+} \cos \dfrac{k\pi y^{+}}{b^{+}} \cos \dfrac{n\pi y^{+}}{b^{+}} \cos k^{+}_{z_{jk}} z^{+} \cos k^{+}_{z_{mn}} z^{+}}{T^{+}_{qr}(\omega^{+})\, T^{+}_{st}(\omega^{+})\, P^{+}_{r}(\omega^{+})\, P^{+}_{t}(\omega^{+})\, R^{+}_{q}(\omega^{+})\, R^{+}_{s}(\omega^{+})} \;;\; \omega^{+}\delta^{+} > 1.932
$$

(D76)

Equation (D76) is obtained from Equations (D66), (D69) through (D75), and the following definitions for the dimensionless input parameters and spatial variable:

$$
c^{+} = \frac{c}{U_c} \qquad \rho^{+} = \frac{\rho_{a_0} a}{\mu}
$$

$$
d^{+} = \frac{d}{a} \qquad z^{+} = \frac{z}{a} \tag{D77}
$$

which are used to form the following dimensionless quantities

$$
k^{+}_{z_{jk}}(\omega^{+}) = \left[\left(\frac{\omega^{+}}{c^{+}} \right)^{2} - (j\pi)^{2} - \left(\frac{k\pi}{b^{+}} \right)^{2} \right]^{1/2}
$$

$$
U^{+}_{jkmn}(\omega^{+}) = k^{+}_{z_{jk}}(\omega^{+})\, k^{+}_{z_{mn}}(\omega^{+}) \sin k^{+}_{z_{jk}} d^{+} \sin k^{+}_{z_{mn}} d^{+} \tag{D78}
$$

APPENDIX D2 – METHOD FOR DETERMINING INPUT DATA

The following data are furnished to the computer:

1. Dimensionless input parameters to determine the dimensionless plate velocity sprectral density:

$$M = \frac{\rho_f a}{\mu}$$

$$U^+ = \frac{U_0}{U_c}$$ (See Figure 4 of Reference 32; U^+ was taken to be constant, equal to 1.54 in Reference 32.)

$$\delta^+ = \frac{\delta^*}{\mu}$$

$$b^+ = \frac{b}{a}$$

$$D^+ = \frac{D}{\mu U_c{}^2 a^2}$$

$$r^+ = \frac{ra}{\mu U_c}$$

The values for the data used in determining the input parameters may be either arbitrarily prescribed or measured by methods similar to those presented in Appendix C.*

The range must also be specified for the spacial and frequency variables $x^+ = \frac{x}{a}$, $y^+ = \frac{y}{a}$, and $\omega^+ = \omega a / U_c$

2. Dimensionless input parameters to determine the dimensionless cavity acoustic pressure spectral density.

In addition to the foregoing parameters, it is necessary to specify the following additions:

$$c^+ = \frac{c}{U_c}$$

---

*Additional input parameters $\omega^+_{mn} = \frac{\omega_{mn} a}{U_c}$ and $r^+_{c_{mn}} = \frac{r_{c_{mn}} a}{\mu U_c} = \frac{2\omega_{mn} a}{U_c}$ are functions of D^+ and b^+ only, hence need not be independently specified.

$$d^{+} = \frac{d}{a}$$

$$\rho^{+} = \frac{\rho_{a_0} a}{\mu}$$

and the range for $z^{+} = \frac{z}{a}$.

The values for these data are either known from the geometry and properties of the actual structure and fluid or are arbitrarily specified.

Reference 32 gives dimensionless input parameters which fall in the range of interest for submarine sonar applications.

APPENDIX D3 – PROGRAM IDENTIFICATION

This program computes the plate velocity power spectrum and cavity acoustic pressure power spectrum resulting from the vibrations of a turbulence excited finite plate with simply supported boundaries. The program is designated as TURB3. It consists of two subprograms, I and II. Subprogram I computes the plate velocity power spectrum and Subprogram II the cavity acoustic pressure power spectrum. Both use similar notation. There are slight differences in their inputs and in the interpretation of their output. See identification below. A time estimate of the computer running times on the IBM 7090 is given below.

Figure No.	Subprogram	Frequency Range	Running Time min
16	I	$1 \leq \omega^+ \leq 1000$	9.13
17	I	$1 \leq \omega^+ \leq 1000$	12.0
18	II	$1 \leq \omega^+ \leq 1500$	442.0

APPENDIX D

TABLE 6

Identification for Subprograms I and II – Strawderman

This table includes input and output data identification, flow chart, and order of input data. Computer running times have been given on the previous page. Computer program listings are presented in Table 7.

TABLE 6A: Input Data

TABLE 6B: Output Data

TABLE 6C: Flow Charts

TABLE 6D: Input Format

TABLE 6A

Input Data

(Dimensionless Units)

Symbol	Identification	Program
x^+	Dimensionless longitudinal spacial coordinate x/a	X
y^+	Dimensionless lateral spacial coordinate y/a	Y
z^+	Dimensionless spatial coordinate z/a	ZP
b^+	Dimensionless plate and acoustic cavity dimension b/a	BP
d^+	Dimensionless cavity dimension d/a where d is acoustic cavity dimension in z-direction	DEPTH
$\dfrac{r^+}{r^+_{c_{m,n}}}$	Dimensionless plate damping coefficient divided by dimensionless critical plate damping for the *m-nth* mode	DAMP
ω^+	Dimensionless radial frequency	OMEGA
$c^+ = \dfrac{c}{U_c} = \dfrac{cU^+}{U_0}$	Dimensionless speed of sound	CP
D^+	Dimensionless plate flexural rigidity	DP
M	Dimensionless fluid mass	CAPM
δ^+	Dimensionless turbulent boundary layer displacement thickness	DELTA
a	Constant mult. factor; changes for different fluids; $a = 1.0$ for water $a = 3.0$ for air (See Interpretation of Data Output)	ALFA
	Largest frequency of interest, i.e., cutoff frequency at which program is to stop	TIP
	Convergence criterion in Equation (D76) with TOLH > 1.0 (Case I only)	TOLH
	Convergence criterion in Equation (D76) with TOLL < 1.0 (Case I only)	TOLL
ρ^+	Dimensionless fluid density equal to $\rho_{a_0} a / \mu$	RHO

TABLE 6B

Output Data

Symbol	Identification	Program
ω_{mn}	Modal natural frequencies $\omega_{mn} = \sqrt{\frac{D}{\mu}\left[\left(\frac{m\pi}{a}\right)^2 + \left(\frac{n\pi}{b}\right)^2\right]}$	PNOME (I,J)
$\phi_a^+(x^+, y^+, z^+, \omega^+)$	Subprogram II: Equation (D76) Dimensionless form of the cavity acoustic spectral density. NOTE: PHIP was multiplied by $(\rho^+)^2 = \left(\frac{\rho_{a_0} a}{\mu}\right)^2$ to agree with (D76); see Interpretation of Data Output below	
	10.0 LOG_e(PHIP)/2.302589	PHIDB
	Corresponding frequency to PHIP and PHIDB	OMEGA
	Subprogram I. Equation (D67) Dimensionless plate velocity spectral density	PHIP
	10.0 LOG_e (PHIP)/2.3025859	PHIDB
	Number of terms needed for convergence for each PHIP	ITOP
	Subscript indicating how many times summation gone through before convergence.	MU

Interpretation of Data Output

Comment: Subprogram I involves eight nested do-loops which means that the inner operations are done a minimum of 2^8 times; the next index on the loop would be 4^8, 6^8, . . . etc. until convergence. Case I involves only four nested loops.

Special Instruction: Sense Switch 4 is turned *on* by operator at beginning of program.

Curves – Three Examples

Example 1 (Figure 16): Subprogram I, Equation (D67) is used for this curve. The computer results for the plate velocity spectrum were then changed to dimensional form and finally converted to the ratio of displacement spectral density to turbulent pressure spectral

density. The subprogram uses Bull data. The form of the final response is 10 Log_{10} $[(\Phi_d(\omega) / \Phi_t(\omega))]$ plotted against f. The following conversions were made manually.

a. Use the program to compute $\phi_{\phi}^{+}(\omega)$ Equation (D67) multiplied by a^2

b. Convert $\phi_{\phi}^{+}(\omega) = \dfrac{\phi_{\phi}(\omega)}{U_c a}$, where $a^2 \phi_{\phi}^{+}(\omega)$ is the quantity appearing in the program. This quantity is then multiplied by $U_c a$ to yield $\phi_{\phi}(\omega)$.

c. $\Phi_d(\omega) = \dfrac{\phi_{\phi}(\omega)}{\omega^2}$ (from velocity to displacement).

d. $\Phi_t(\omega) = \phi_p$, Equations 3.1 of Reference 32. Use first of Equations 3.1 of Reference 32 since the Bull data yield maximum frequency $\omega = 12{,}566$ cps but $\omega = \dfrac{1.258 U_0}{\delta^*} =$ 47,272 is cutoff point in this equation.

e. Other unit conversions:

(1) ω^+ to f by $\omega^+ = \dfrac{2\pi f a}{U_c}$

(2) $\delta^* = a\delta^+$

(3) $U_c = \dfrac{U_0}{U^+}$

f. $$\frac{\Phi_d(\omega)}{\Phi_t(\omega)} = \frac{\phi_{\phi}(\omega)}{\omega^2 \phi_p(\omega)} \Rightarrow 10 \text{ Log } \frac{\Phi_d(\omega)}{\Phi_t(\omega)} = 10 \text{ Log } \frac{\phi_{\phi}(\omega)}{\omega^2 \phi_p(\omega)} =$$

$$10 \text{ Log } (\phi_{\phi}(\omega)) - 10 \text{ Log } (\omega^2 \phi_p(\omega)) =$$

$$10 \text{ Log } (U_c a \phi_{\phi}^{+}(\omega)) - 10 \text{ Log}(\omega^2 \phi_p(\omega)) =$$

$$[10 \text{ Log } (U_c a) + 10 \text{ Log } (\phi_{\phi}^{+}(\omega)) - 10 \text{ Log } (\omega^2 \phi_p(\omega))]$$

$$[10 \text{ Log } (U_c a) + 10 \text{ Log } (\phi_{\phi}^{+}(\omega)) - 20 \text{ Log}\,\omega - 10 \text{ Log } \phi_p(\omega)] .$$

Plot this versus f.

As an alternative, the foregoing results may be obtained by a simplified procedure. This option eliminates most but not all of the manual computations.

For subprogram use, the Bull data are nondimensionalized (see Figure 16). Note that for this frequency range in the figure, the value of ϕ_p is a constant. This makes the correction simpler. The following FORTRAN lines, in which the constants are dependent on the Bull data, are inserted into the Strawderman program to yield direct results for plotting Figure 16. These lines are inserted immediately after Statement 212 in the program. The curve was plotted with RESP (PHISUBD/PHISUBT) against FREQ. It should be noted that the curve is about 6 dB lower than Strawderman's, since he originally used 116 (an arithmetic error which he corrected following publication of Reference 32) instead of 110.392; see subroutine above.

```
      Col. 7

      PHIC=PHIDB+110.392
      OF=OMEGA*190.986
      OFW=OF*6.2318
      WRITE(6,240)PHIC,OF,OFW
240   FORMAT(1X,6HΔPHIC=E17.8,6HΔFREO=E17.8,10HΔ20LOG(W)=E17.8)
      RESP=PHIC-OFW
      WRITE(6,241)RESP
241   FORMAT(1X,17HPHISUBD/PHISUBT=E17.8)
```

Example 2 (Figure 17): Subprogram I is used. Computer result PHIDB is plotted against OMEGA. This gives representation of Equation (D67) directly, i.e., PHIDB represents the dimensionless plate velocity spectral density corresponding to values of ω^+.

Example 3 (Figure 18): Subprogram I is used. Computer result PHIDB is plotted against OMEGA. Note: for agreement with Equation (D76) (cavity acoustic spectral density), the result PHIP must be multiplied by $(\rho^{+2}) = (\rho_{a_0} a/\mu)^2$ or $20 \operatorname{Log}_{10} \rho^+$ must be added to $10.0 \operatorname{Log}_e (\text{PHIP}) / 2.302589$ = PHIDB.* In Figure D4 the convergence criterion was a tolerance of 20 percent, with TOLL = 0.8 and TOLH = 1.2.

It is important to note that the original subprograms gave the following results: $a^2\Phi_\phi^+(x^+, y^+, \omega^+)$ and $a^2\Phi_a^+(x^+, y^+, z^+, \omega^+)$ rather than $\Phi_\phi^+(x^+, y^+, \omega^+)$ and $\Phi_a^+(x^+, y^+, z^+, \omega^+)$. By setting $a = 1$, the subprograms have now been modified to yield the *normalized results* $\Phi_\phi^+(x^+, y^+, \omega^+)$ and $\Phi_a^+(x^+, y^+, z^+, \omega^+)$. The *unnormalized results* $\Phi_\phi(x^+, y^+, \omega^+) = a^2 U_c a \Phi_\phi^+(x^+, y^+, \omega^+)$ and $\Phi_a(x^+, y^+, z^+, \omega^+) = a^2 \mu^2 U_c^3 \Phi_a^+(x^+, y^+, z^+, \omega^+)$ are then obtained *manually* for water ($a = 1$) or air ($a = 3$), i.e, set $a = 1$ or 3, accordingly.

*This operation was performed in order to manually compensate for the inadvertant omission of $(\rho^+)^2$ from the program. Subsequent to the computation of Figure 18, the program was corrected to include $(\rho^+)^2$. Hence manual compensation is no longer necessary since the true results are obtained directly from the computer.

Flow Chart for Subprogram I – Plate Velocity Power Spectrum

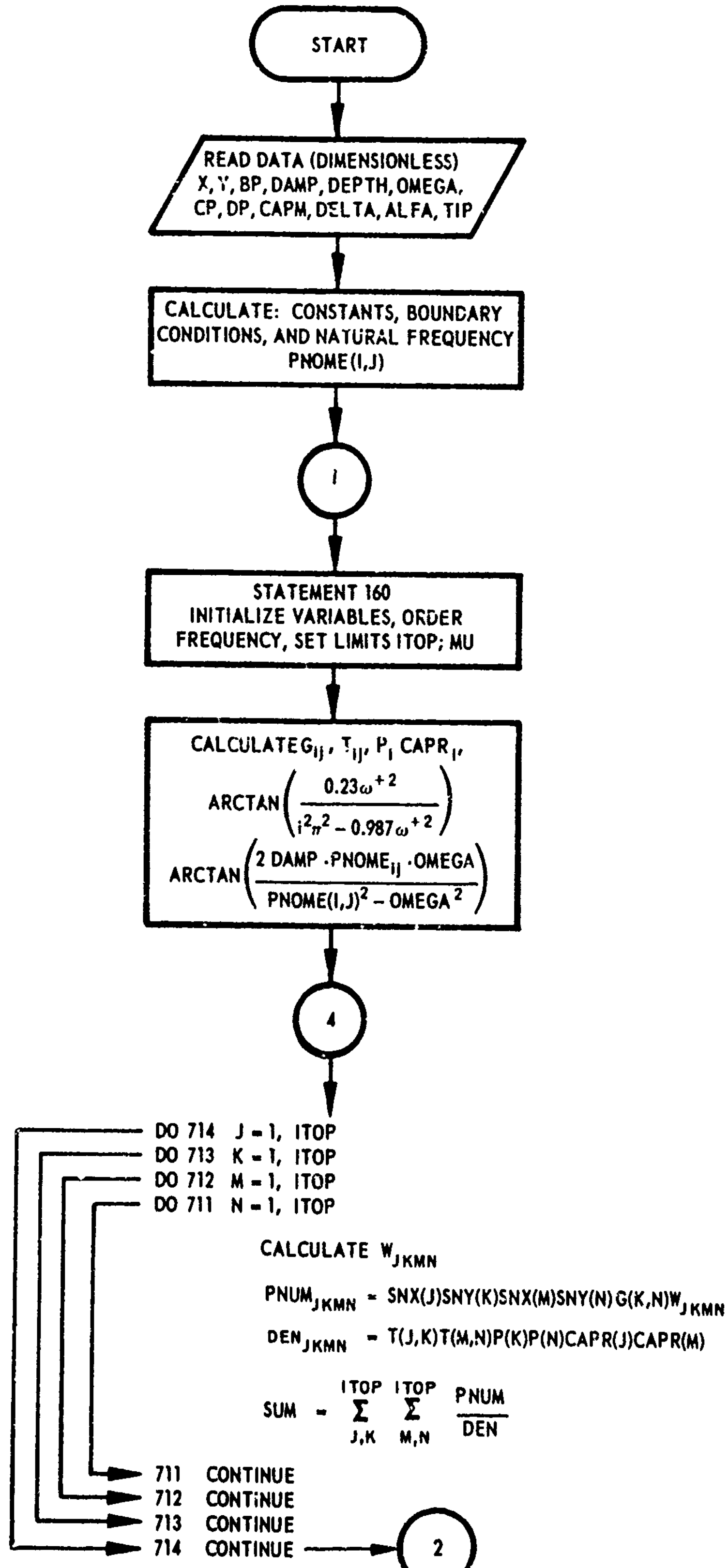

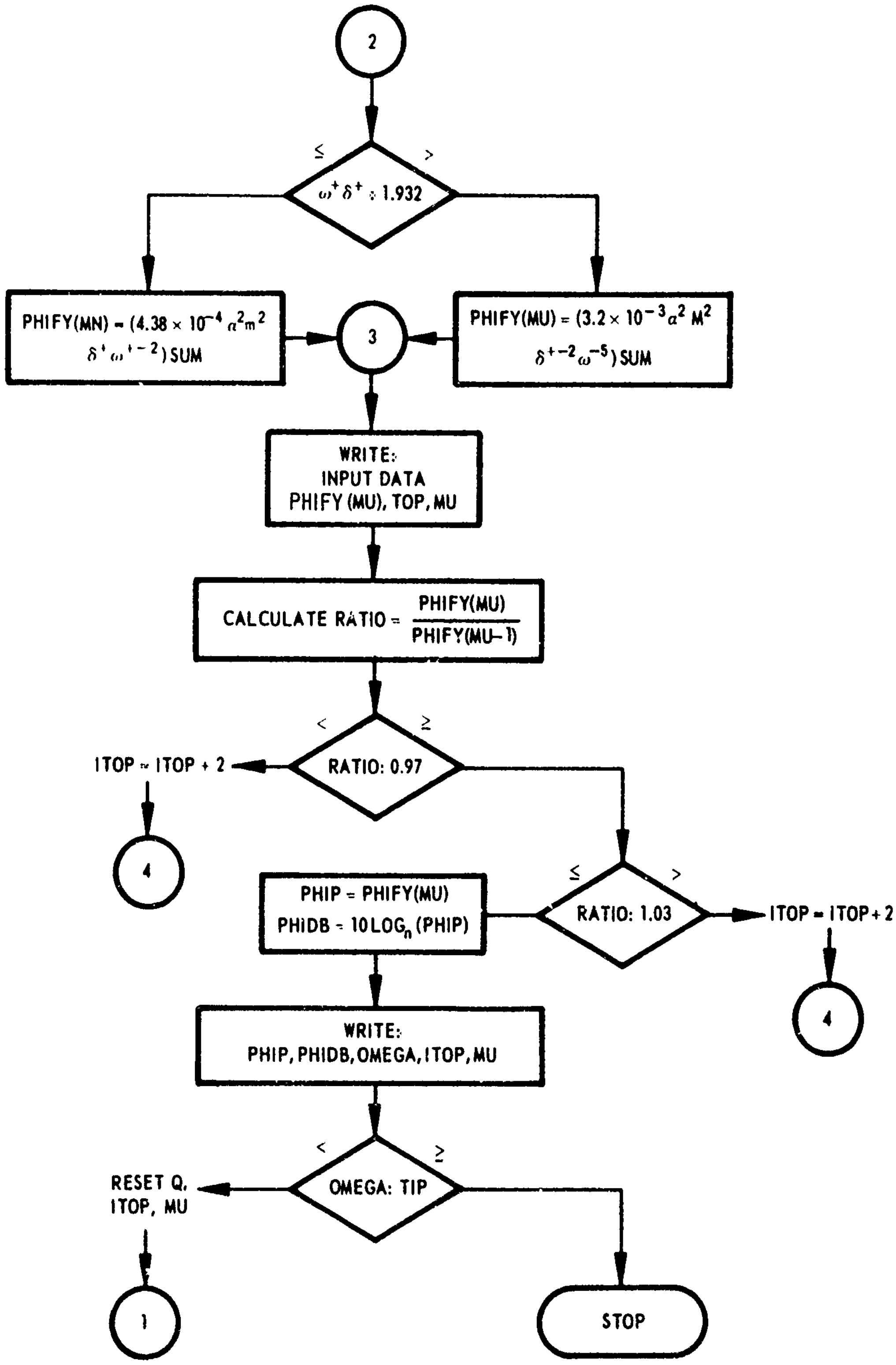
2
≤
>
ω⁺δ⁺ : 1.932
PHIFY(MN) = (4.38 × 10⁻⁴ a²m² δ⁺ω⁺⁻²) SUM
3
PHIFY(MU) = (3.2 × 10⁻³ a² M² δ⁺⁻² ω⁻⁵) SUM
WRITE:
INPUT DATA
PHIFY (MU), TOP, MU
CALCULATE RATIO = PHIFY(MU) / PHIFY(MU-1)
<
≥
RATIO: 0.97
ITOP = ITOP + 2
4
PHIP = PHIFY(MU)
PHIDB = 10LOGn (PHIP)
≤
>
RATIO: 1.03
ITOP = ITOP + 2
4
WRITE:
PHIP, PHIDB, OMEGA, ITOP, MU
<
≥
OMEGA: TIP
RESET Q,
ITOP, MU
1
STOP

Flow Chart for Subprogram II – Cavity Acoustic Pressure Spectrum

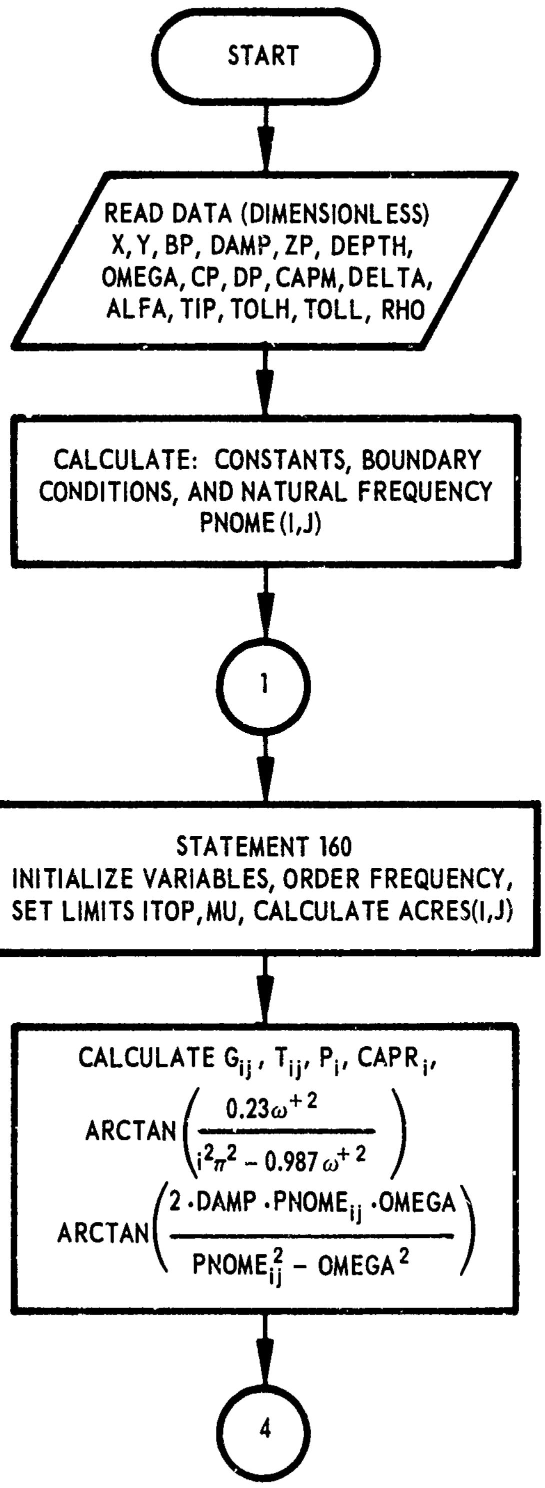

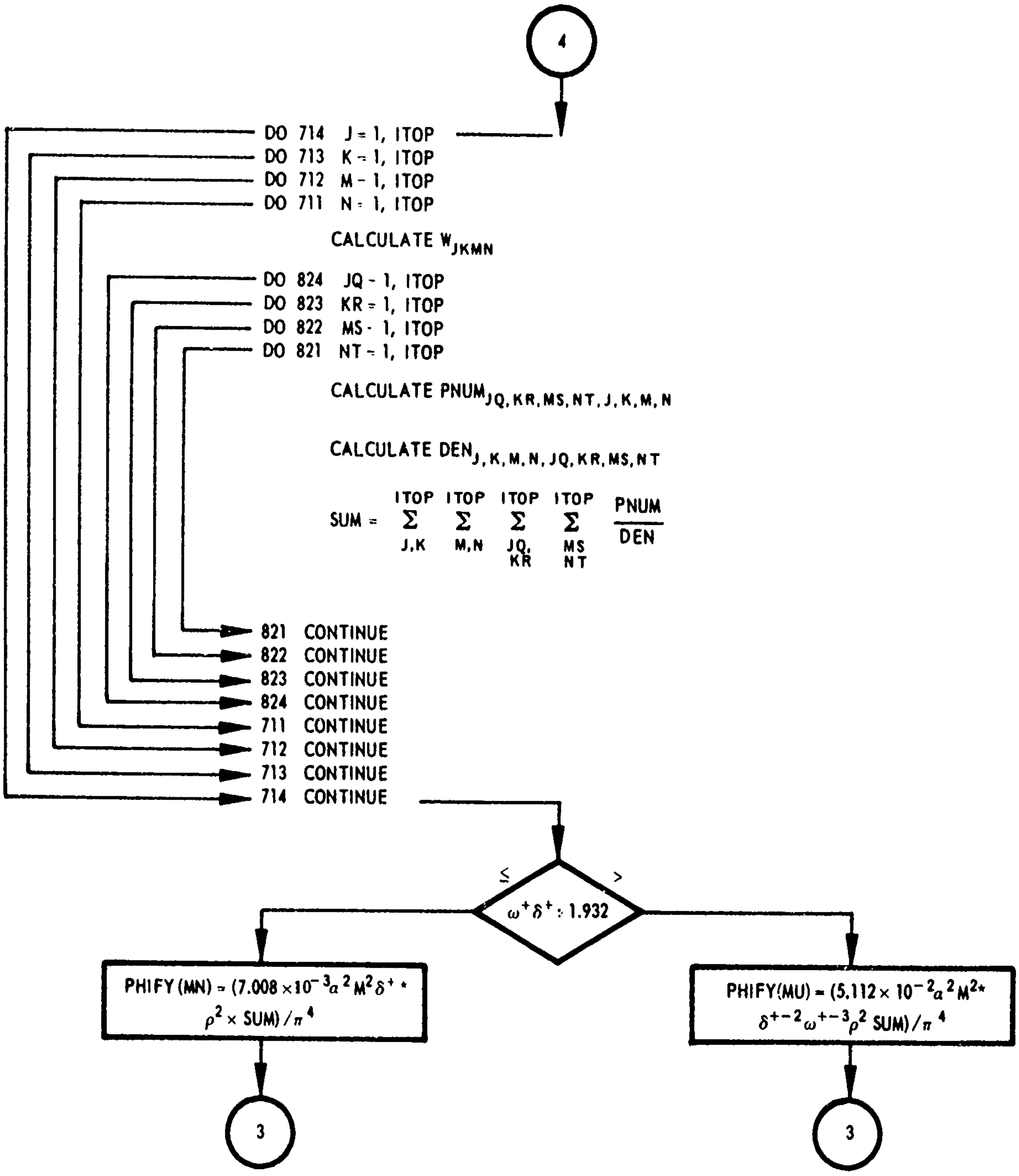
4
DO 714 J = 1, ITOP
DO 713 K = 1, ITOP
DO 712 M - 1, ITOP
DO 711 N = 1, ITOP
CALCULATE W_{JKMN}
DO 824 JQ - 1, ITOP
DO 823 KR = 1, ITOP
DO 822 MS - 1, ITOP
DO 821 NT = 1, ITOP
CALCULATE $PNUM_{JQ,KR,MS,NT,J,K,M,N}$
CALCULATE $DEN_{J,K,M,N,JQ,KR,MS,NT}$
$SUM = \sum_{J,K}^{ITOP} \sum_{M,N}^{ITOP} \sum_{JQ,KR}^{ITOP} \sum_{MS,NT}^{ITOP} \frac{PNUM}{DEN}$
821 CONTINUE
822 CONTINUE
823 CONTINUE
824 CONTINUE
711 CONTINUE
712 CONTINUE
713 CONTINUE
714 CONTINUE
$\leq$
$>$
$\omega^+\delta^+ : 1.932$
PHIFY (MN) = $(7.008 \times 10^{-3} a^2 M^2 \delta^{+*} \rho^2 \times SUM)/\pi^4$
PHIFY(MU) = $(5.112 \times 10^{-2} a^2 M^{2*} \delta^{+-2} \omega^{+-3} \rho^2 SUM)/\pi^4$
3
3

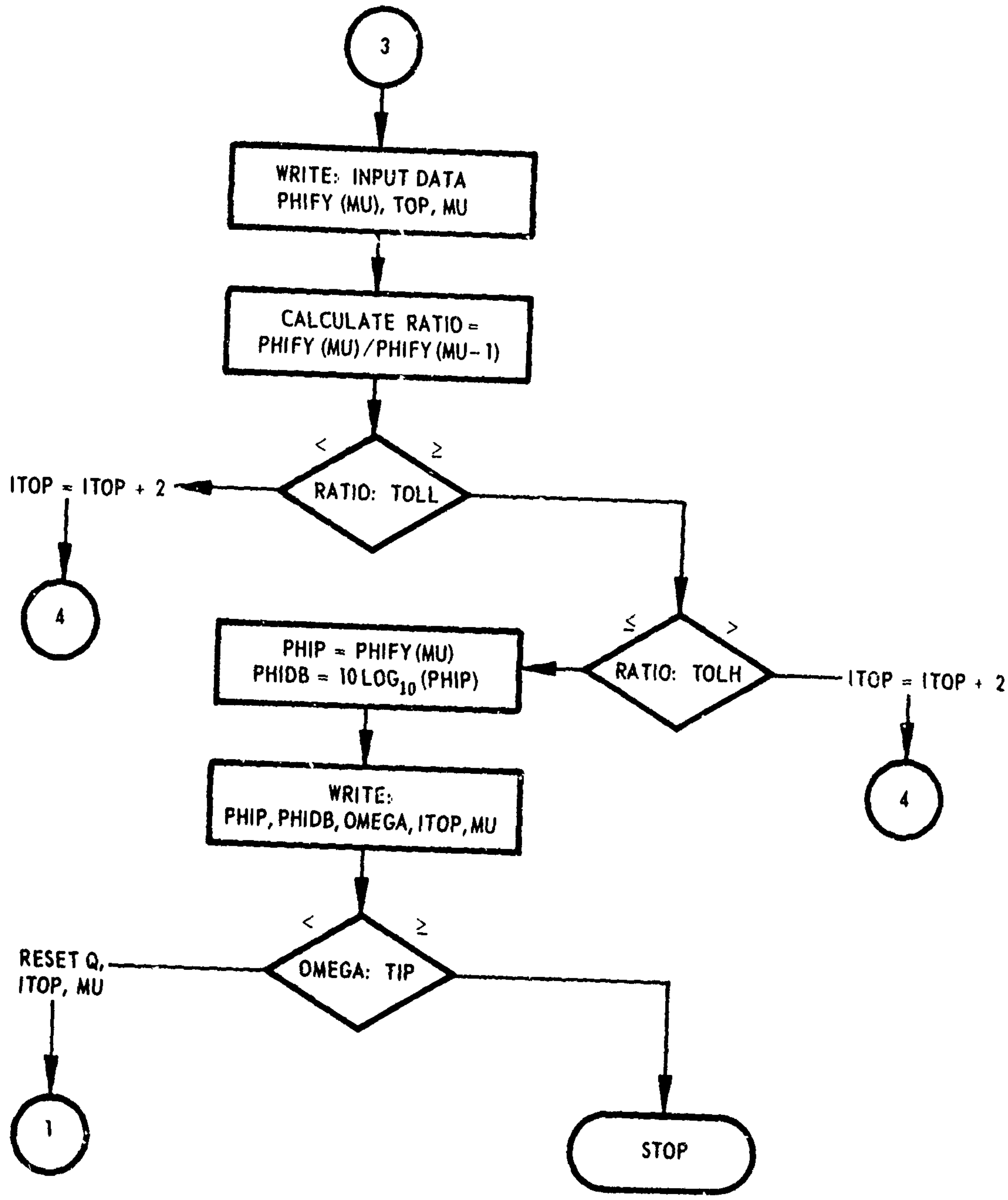
3
WRITE: INPUT DATA
PHIFY (MU), TOP, MU
CALCULATE RATIO =
PHIFY (MU)/PHIFY (MU-1)
<
≥
RATIO: TOLL
ITOP = ITOP + 2
4
≤
>
RATIO: TOLH
PHIP = PHIFY (MU)
PHIDB = 10 LOG10 (PHIP)
ITOP = ITOP + 2
4
WRITE:
PHIP, PHIDB, OMEGA, ITOP, MU
<
≥
OMEGA: TIP
RESET Q,
ITOP, MU
1
STOP

TABLE 6D

Input Format

CASE 1

	X 10	Y 20	ZP 30	BP 40	DEPTH 50	60	70	80
10.8								

	DAMP 10	OMEGA 20	CP 30	DP 40	CAPM 50	60	70	80
10.4								

	DELTA 10	ALFA 20	TIP 30	TOLH 40	TOLL 50	60	70	80
10.4								

	RHO 10	20	30	40	50	60	70	80
10.6								

CASE 2

X 10	Y 20	BP 30	DAMP 40	DEPTH 50	60	70	80

OMEGA 10	CP 20	DP 30	CAPM 40	DELTA 50	60	70	80

ALFA 10	TIP 20	30	40	50	60	70	80

APPENDIX D4 – TEST RUNS

Results obtained from the computer programs of Table 6 are given in Figures 16–18.

A test run for the dimensionless plate velocity spectral density $\phi_{\dot{\phi}}^{+}(x^{+}, y^{+}, \omega^{+})$ converted to the ratio of displacement spectral density to turbulent pressure spectral density $(\phi_d(\omega)/(\phi_f(\omega)$ is plotted logarithmically in Figure 16. Test runs for the plate velocity power spectrum and the cavity acoustic pressure power spectrum are plotted in Figures 17 and 18, respectively. Computer listings are given in Table 7.

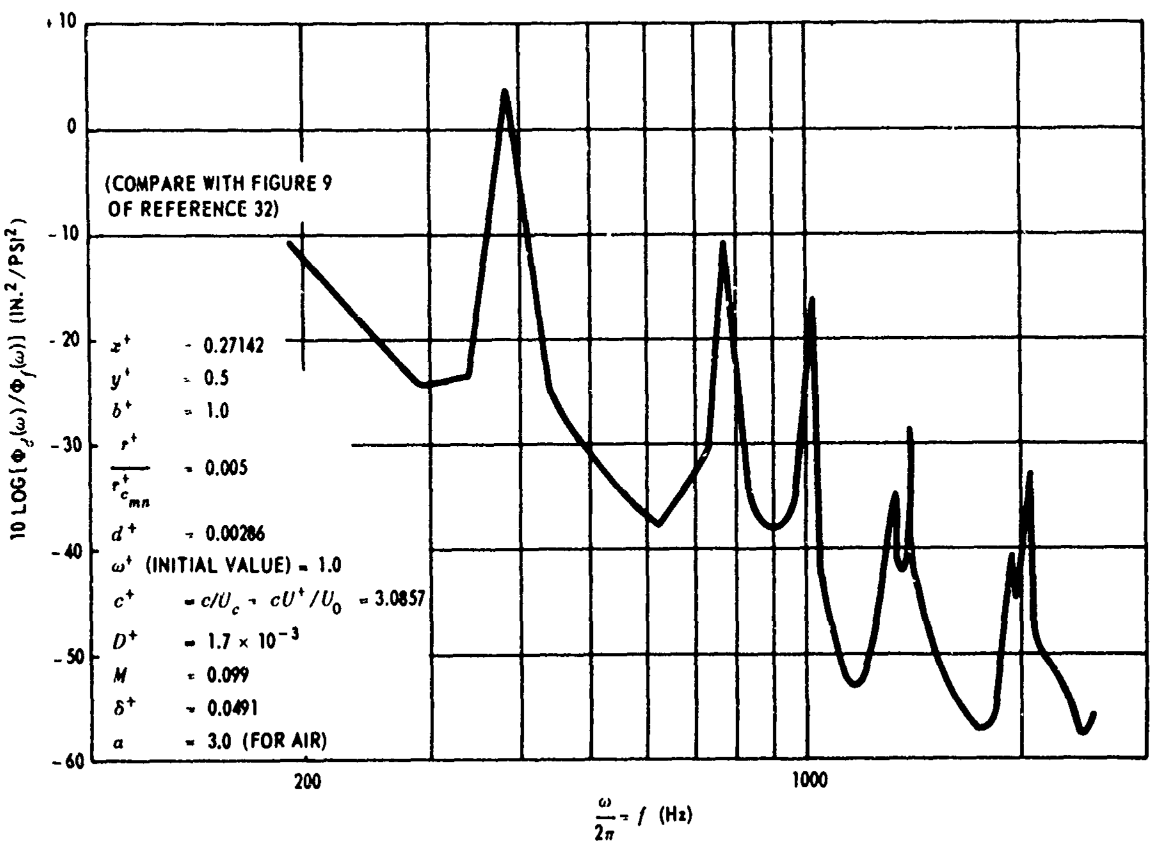

Figure 16 – Computed Response of a 3.5 × 3.5 × 0.1-Inch Steel Plate to Turbulent Boundary Layer Excitation

See pages 56–57 of Reference 32 for source of data used here.

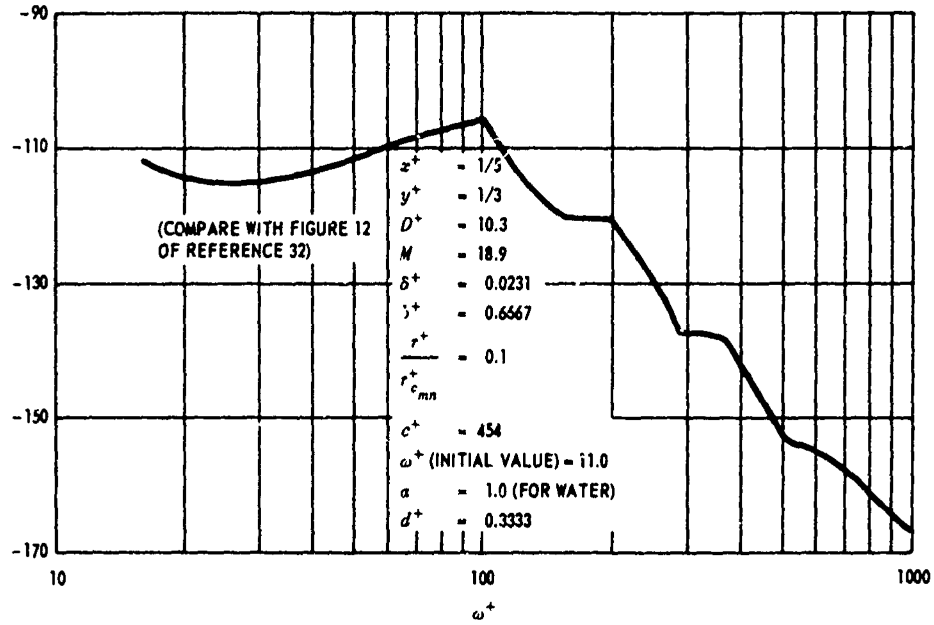

Figure 17 – Computed Dimensionless Plate Velocity Power Spectrum at Dimensionless Coordinates (1/5, 1/3); 10 Percent Critical Damping

See pages 60, 61 and 75 (Table 2, Case 1) of Reference 32 for source of data used here.

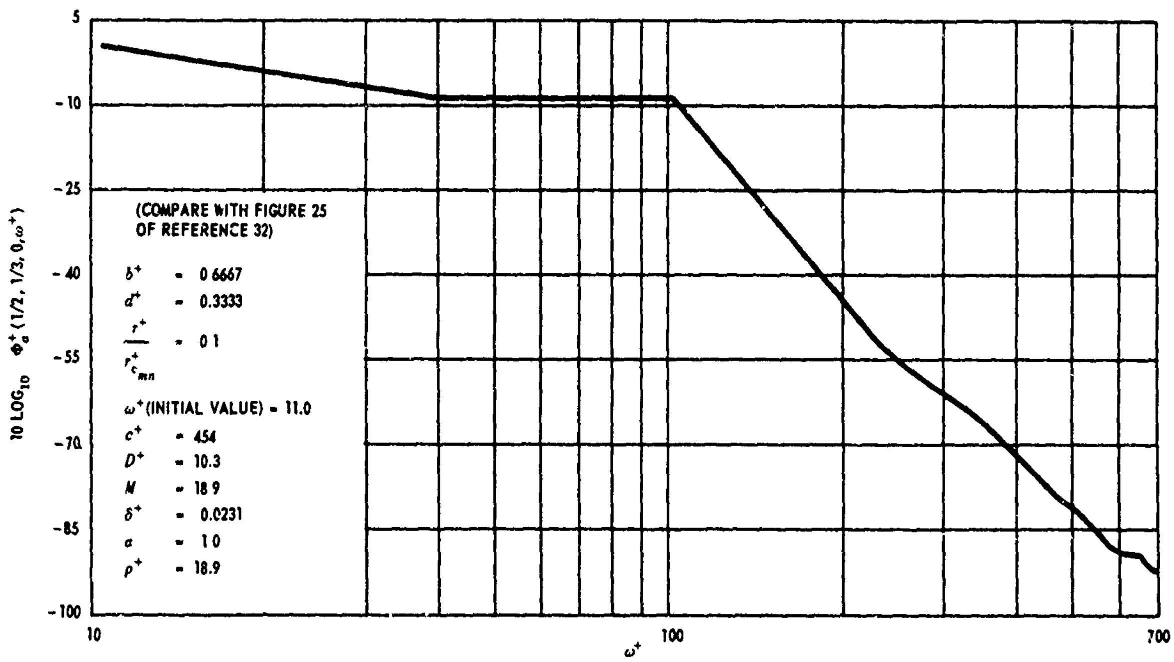

Figure 18 – Computed Dimensionless Cavity Acoustic Pressure Power Spectrum at Dimensionless Cavity Coordinates (1/2, 1/3, 0)

See page 75 (Table 2, Case 1) of Reference 32 for source of data used here.

TABLE 7

Computer Listings for USL Subprograms I and II – Strawderman

Table 7A – Plate Velocity Power Spectrum

```
$IBFTC STRTR2
      DIMENSION PNOME(20,20),FREQ(20,20),TMINO(20),PHIFY(100),SNX(20),
     1SNY(20),CSX(20),CSY(20),G(20,20),T(20,20),P(20),CAPR(20)
      DIMENSION PNOND(20,20),GNU(20),PLDA(20,20)
      DIMENSION IDUMP(18)
  402 READ (5,403) X,Y,BP,DAMP,DEPTH,OMEGA,CP,DP,CAPM,DELTA,
     1ALFA,TIP
  403 FORMAT(5F10.8/5F10.4/2F10.4)
  406 Q=0.0
      PI=3.14159265
      PISQ=PI**2.0
      E=2.71828183
      IPEN=+80000
      SINEX=SIN(PI*X)
      COSEX = COS(PI*X)
      SINEY = SIN((PI*Y)/BP)
      COSEY = COS((PI*Y)/BP)
      IF (ABS(SINEX)-10.0**(-7.0)) 800,800,801
  800 SINEX=0.0
  801 IF (ABS(SINEY)-10.0**(-7.0))802,802,803
  802 SINEY=0.0
  803 IF (ABS(COSEX)-10.0**(-7.0))804,804,805
  804 COSEX=0.0
  805 IF (ABS(COSEY)-10.0**(-7.0))806,806,807
  806 COSEY=0.0
  807 CONTINUE
      SNX(1)=SINEX
      SNY(1)=SINEY
      CSX(1)=COSEX
      CSY(1)=COSEY
      DO 701 I=2,20
      J=I-1
      SNX(I)=SNX(J)*COSEX+CSX(J)*SINEX
      SNY(I)=SNY(J)*COSEY+CSY(J)*SINEY
      CSX(I)=CSX(J)*COSEX-SNX(J)*SINEX
      CSY(I)=CSY(J)*COSEY-SNY(J)*SINEY
      IF  (ABS(SNY(I))-10.0**(-7.0))  80,80,81
```

```
 80 SNY(I)=0.0
 81 IF (ABS(SNX(I))-10.0**(-7.0))82,82,83
 82 SNX(I)=0.0
 83 IF (ABS(CSY(I))-10.0**(-7.0))84,84,85
 84 CSY(I)=0.0
 85 IF (ABS(CSX(I))-10.0**(-7.0))86,86,87
 86 CSX(I)=0.0
 87 CONTINUE
701 CONTINUE
    WRITE(6,7)
  7 FORMAT(1H1/26HW. STRAWDERMAN JOB NO 0775)
    DO 100 I=1,20
    DO 101 J=1,20
    F=I
    H=J
    PNOME(I,J)=(DP**0.5)*(((F*PI)**2.0)+((H*PI/BP)**2.0))
101 CONTINUE
100 CONTINUE
    CALL SSWTCH(4,KOOOFX)
    IF(KOOOFX.EQ.2)  GO TO 521
520 WRITE(6,522)X,Y,BP,DAMP,DEPTH,OMEGA,CP,DP,CAPM,DELTA ,
   1ALFA,TIP
522 FORMAT(5F10.8/5F10.4/2F10.4)
521 CONTINUE
    WRITE(6,142)((PNOME(I,J),J=1,10),I=1,10)
142 FORMAT(10E12.4)
160 DO 106 K=1,20
    DO 107 L=1,20
    FREQ(K,L)=0.0
107 CONTINUE
106 CONTINUE
    DO 102 I=1,20
    DO 103 J=1,20
    IF(OMEGA-PNOME(I,J))104,103,103
104 K=I
    L=J
    FREQ(K,L)=PNOME(K,L)
```

```
      GO TO 102
  103 CONTINUE
  102 CONTINUE
      DO 700 I=1,20
      TMINO(I)=0.0
  700 CONTINUE
      M=0
      DO 109 I=1,20
      DO 108 J=1,20
      IF(FREQ(I,J))99,110,111
  111 M=M+1
      TMINO(M)=FREQ(I,J)
  110 CONTINUE
  108 CONTINUE
  109 CONTINUE
      S=TMINO(1)
      DO 112 L=1,19
      IF(S-TMINO(L+1))112,121,121
  121 S=TMINO(L+1)
  112 CONTINUE
      DO 130 L=1,20
      IF(S-TMINO(L))130,132,130
  132 N=L
      GO TO 180
  130 CONTINUE
  180 DOMEG=(S-OMEGA)/4.0
      Z=N
      ITOP=Z+1.5
      MU=1
  300 CONTINUE
      DO 2171 I=1,100
      PHIFY(I)=0.0
 2171 CONTINUE
  217 CONTINUE
      SUM=0.00
      TOP=0.0
      EXPB=E**(-0.7*OMEGA*BP)
```

TABLE 7A (Continued)

```
      DO 702 I=1,20
      DO 703 J=1,20
      B=I
      D=J
      IF(B-D)11,12,11
   11 G(I,J)=B*D*PISQ*(((-1.0)**I)*((-1.0)**J)-1.0)+(2.0-(((-1.0)**I)
     1+((-1.0)**J))*EXPB))
      GO TO 703
   12 G(I,J)=(0.35*OMEGA*BP)*(2.0*((0.7*OMEGA*BP)**2.0)+PISQ*((B**2.0)+
     1(D**2.0)))+B*D*PISQ*(2.0-(((-1.0)**I)+((-1.0)**J))*EXPB)
  703 CONTINUE
  702 CONTINUE
      CALL OVERFL(J)
      IF(J.EQ.2)  GO TO 751
  750 WRITE(6,752)EXPB
  752 FORMAT(O12)
  751 CONTINUE
      DO 705 I=1,20
      DO 704 J=1,20
      PNOND(I,J)=PNOME(I,J)/OMEGA
      T(I,J)=((((PNOND(I,J)**2  )-1.0)**2  )+(2.0*DAMP*PNOND(I,J))**2  )
     1**0.5
  704 CONTINUE
  705 CONTINUE
      DO 706 I=1,20
      A=I
      P(I)=(A**2  )*PISQ+(0.7*OMEGA*BP)**2
  706 CONTINUE
      DO 707 I=1,20
      A=I
      CAPR(I)=((((A**2  )*PISQ-0.987*(OMEGA**2  ))**2  )+0.0529*(OMEGA**
     14  ))**0.5
  707 CONTINUE
      PNGNU=0.23*(OMEGA**2)
      DO 708 I=1,20
      A=I
      DGNU   =(A**2  )*PISQ-0.987*(OMEGA**2  )
```

TABLE 7A (Continued)

```
      CALL ACTN(DGNU    ,PNGNU,GNU(I),IOTA)
      IF(IOTA)13,14,13
   13 GO TO 216
   14 CONTINUE
  708 CONTINUE
      DO 710 I=1,20
      DO 709 J=1,20
      PNLDA=2.0*DAMP*PNOME(I,J)*OMEGA
      DLDA=(PNOME(I,J)**2  )-(OMEGA**2  )
      CALL ACTN(DLDA,PNLDA,PLDA(I,J),ILDA)
      IF(ILDA)19,20,19
   19 GO TO 216
   20 CONTINUE
  709 CONTINUE
  710 CONTINUE
  740 CONTINUE
      DO 714 J=1,ITOP
      DO 713 K=1,ITOP
      DO 712 M=1,ITOP
      DO 711 N=1,ITOP
      A=J
      B=K
      C=M
      D=N
      TMAX = AMAX1(A,B,C,D)
      IF(TMAX-TOP)711,711,737
  737 CONTINUE
      IF(SNY(N))716,715,716
  715 PNUM=0.0
      DEN=1.0
      GO TO 310
  716 IF(SNX(M))718,717,718
  717 PNUM=0.0
      DEN=1.0
      GO TO 310
  718 IF(SNY(K))720,719,720
  719 PNUM=0.0
```

TABLE 7A (Continued)

```
      DEN=1.0
      GO TO 310
  720 IF(SNX(J))722,721,722
  721 PNUM=0.0
      DEN=1.0
      GO TO 310
  722 CONTINUE
      IF(J-M)21,22,21
   21 W=A*C*PISQ*(2.0*(COS(GNU(J)+GNU(M)))*(COS
     X(PLDA(J,K)-PLDA(M,N)))+
     1((((-1.0)**J)*((-1.0)**M)-1.0)*(CAPR(J)*(COS(GNU(M)+PLDA(J,K)-
     2PLDA(M,N)))-CAPR(M)*(COS(GNU(J)+PLDA(M,N)-PLDA(J,K))))
     X/(PISQ*(
     3(A**2.0)-(C**2.0))))-((E**(-0.115*OMEGA))*
     X(((-1.0)**J)*(COS(OMEGA
     4+GNU(J)+GNU(M)+PLDA(J,K)-PLDA(M,N)))+((-1.0)**
     XM)*(COS(OMEGA+GNU(J
     5)+GNU(M)+PLDA(M,N)-PLDA(J,K))))))
      GO TO 33
   22 W = 1.0066*OMEGA*CAPR(J)*(COS(GNU(J)-0.463*PI))
     X*(COS(PLDA(J,K)-
     1PLDA(M,N)))+A*C*PISQ*(2.0*(COS(GNU(J)+
     XGNU(M)))*(COS(PLDA(J,K)-
     2PLDA(M,N)))-((E**(-0.115*OMEGA))*(((-1.0)**J)*
     X(COS(OMEGA+GNU(J)+
     3GNU(M)+PLDA(J,K)-PLDA(M,N)))+((-1.0)**M)*(COS
     X(OMEGA+GNU(J)+GNU(N)
     4+PLDA(M,N)-PLDA(J,K))))))
   33 CONTINUE
      PNUM=SNX(J)*SNY(K)*SNX(M)*SNY(N)*G(K,N)*W
      DEN=T(J,K)*T(M,N)*P(K)*P(N)*CAPR(J)*CAPR(M)
  310 SUM=SUM+(PNUM/DEN)
      CALL SSWTCH(2,KOOOFX)
      IF(KOOOFX.EQ.2)  GO TO 501
  500 WRITE(6,23) SUM,PNUM,DEN,G(K,N),W,T(J,K),T(M,N),P(K),
     1P(N),CAPR(J),CAPR(M),A,B,C,D
   23 FORMAT(5E17.8/5E17.8/5E17.8//)
```

```
501 CONTINUE
    CALL SSWTCH(6,KOOOFX)
    IF(KOOOFX.EQ.2)  GO TO 51
 50 WRITE(6,52)SNX(J),SNY(K),SNX(M),SNY(N)
 52 FORMAT(4E17.8)
 51 CONTINUE
711 CONTINUE
712 CONTINUE
713 CONTINUE
714 CONTINUE
    IF((OMEGA*DELTA)-1.932)202,202,203
202 PHIFY(MU)=4.38*(10.0**(-4.0))*(ALFA**2.0)*(CAPM**2.0)*DELTA*(OMEGA
   1**(-2.0))*SUM
    GO TO 204
203 PHIFY(MU)=3.2*(10.0**(-3.0))*(ALFA**2.0)*(CAPM**2.0)*(DELTA**(-2.0
   1))*(OMEGA**(-5.0))*SUM
204 CONTINUE
    CALL SSWTCH(4,KOOOFX)
    IF(KOOOFX.EQ.2)  GO TO 531
530 WRITE(6,532)X,Y,BP,DAMP,DEPTH,OMEGA,CP,DP,CAPM,DELTA,
   1ALFA,TIP
532 FORMAT(5F10.8/5F10.4/2F10.4)
531 CONTINUE
    CALL SSWTCH(4,KOOOFX)
    IF(KOOOFX.EQ.2)  GO TO 505
504 WRITE(6,502)PHIFY(MU),TOP,MU
502 FORMAT(2E17.8,1I2)
505  CONTINUE
    IF(TOP)206,205,206
205 CONTINUE
    TOP=ITOP
    MU=MU+1
    ITOP=ITOP+2
    GO TO 740
206 CONTINUE
    K=MU-1
    RATIO=ABS((PHIFY(MU))/PHIFY(K))
```

```
      CALL SSWTCH(4,KOOOFX)
      IF(KOOOFX.EQ.2)  GO TO 511
  510 WRITE(6,512)RATIO,PHIFY(MU),PHIFY(K),MU,K
  512 FORMAT(3E17.8,2I2)
      WRITE(6,515)(PHIFY(J),J=1,10)
  515 FORMAT(5E17.8)
  511 CONTINUE
      IF(RATIO-0.97)207,208,208
  207 CONTINUE
      TOP=TOP+2.0
      ITOP=ITOP+2
      MU=MU+1
      GO TO 740
  208 CONTINUE
      IF(RATIO-1.03)209,209,210
  209 CONTINUE
      GO TO 211
  210 CONTINUE
      TOP=TOP+2.0
      ITOP=ITOP+2
      MU=MU+1
      GO TO 740
  211 CONTINUE
      PHIP=PHIFY(MU)
      CALL SSWTCH(1,KOOOFX)
      IF(KOOOFX.EQ.2)  GO TO 4002
 4001 WRITE(6,4000)PHIP,OMEGA
 4000 FORMAT(2E17.8)
 4002 CONTINUE
      PHIDB = (10.0*ALOG(PHIP))/2.30258509
      WRITE(6,212)PHIP,PHIDB,OMEGA,ITOP,MU
  212 FORMAT(3E17.8,2I2)
      IF(PHIDB)3001,3000,3000
 3000 PHIDB=0.0
 3001 CONTINUE
      IF(OMEGA-TIP)215,216,216
  215 CONTINUE
```

TABLE 7A (Continued)

```
      IF(Q-3.0)213,214,214
  213 OMEGA=OMEGA+DOMEG
      Q=Q+1.0
      ITOP=Z+1.5
      MU=1
      GO TO 300
  214 OMEGA=S+0.001*DAMP
      Q=0.0
      GO TO 160
  216 END FILE 4
      WRITE(6,3009)IPEN,IPEN
 3009 FORMAT(2I6)
      END FILE 5
      END FILE 5
      STOP 5
   99 STOP 7
      END
$IBFTC ACTN    REF
CACTN
       SUBROUTINE ACTN (A,B,THETA,I)
      I=0
      IF (ABS(A)+ABS(B)) 27,28,27
 27   THETA= ATAN(ABS(B/A))
       IF (A) 22,21,23
 22    IF (B) 32,24,31
 23    IF (B) 33,25,34
 24    THETA=3.1415927
       GO TO 34
 25    THETA=0.0
       GO TO 34
 21    IF (B) 26,28,29
 26    THETA=4.7123890
       GO TO 34
 29    THETA=1.5707963
       GO TO 34
 31    THETA=3.1415927-THETA
       GO TO 34
 32    THETA=THETA+3.1415927
       GO TO 34
 33    THETA=6.283154-THETA
       GO TO 34
 28   WRITE (6,315)
315.   FORMAT (40HOPROGRAM-CANNOT-CONTINUE,ARCTAN OF (0/0) )
       I=1
 34    RETURN
      END
```

Table 7B – Subprogram II – Cavity Acoustic Pressure Power Spectrum

```
$IBFTC STRTR1
      DIMENSION PNOME(20,20),FREQ(20,20),TMINO(20),PHIFY(100),SNX(20),
     1SNY(20),CSX(20),CSY(20),G(20,20),T(20,20),P(20),CAPR(20)
      DIMENSION PNOND(20,20),GNU(20),PLDA(20,20),CKAYZ(20,20),SINKD(20,
     120),COSKZ(20,20),ACRES(10,10),COKAP(20,20),COGNU(20,20)
      DIMENSION IDUMP(18)
 402  READ(5,403) X,Y,ZP,BP,DEPTH,DAMP,OMEGA,CP,DP,CAPM,DELTA,
     1ALFA,TIP,TOLH,TOLL
  403 FORMAT(5F10.8/5F10.4/5F10.4)
      READ(5,410)   RHO
  410 FORMAT(F10.6)
  406 Q=0.0
      PI=3.14159265
      PISQ=PI**2.0
      E=2.71828183
      EXPA=E**(-0.115*OMEGA)
      IPEN=+80000
      SINEX=SIN(PI*X)
      COSEX = COS(PI*X)
      SINEY = SIN((PI*Y)/BP)
      COSEY = COS((PI*Y)/BP)
      IF (ABS(SINEX)-10.0**(-7.0)) 800,800,801
  800 SINEX=0.0
  801 IF (ABS(SINEY)-10.0**(-7.0))802,802,803
  802 SINEY=0.0
  803 IF (ABS(COSEX)-10.0**(-7.0))804,804,805
  804 COSEX=0.0
  805 IF (ABS(COSEY)-10.0**(-7.0))806,806,807
  806 COSEY=0.0
  807 CONTINUE
      SNX(1)=0.0
      SNY(1)=0.0
      CSX(1)=1.0
      CSY(1)=1.0
      DO 701 I=2,20
      J=I-1
      SNX(I)=SNX(J)*COSEX+CSX(J)*SINEX
```

```
      SNY(I)=SNY(J)*COSEY+CSY(J)*SINEY
      CSX(I)=CSX(J)*COSEX-SNX(J)*SINEX
      CSY(I)=CSY(J)*COSEY-SNY(J)*SINEY
      IF  (ABS(SNY(I))-10.0**(-7.0))  80,80,81
   80 SNY(I)=0.0
   81 IF (ABS(SNX(I))-10.0**(-7.0))82,82,83
   82 SNX(I)=0.0
   83 IF (ABS(CSY(I))-10.0**(-7.0))84,84,85
   84 CSY(I)=0.0
   85 IF (ABS(CSX(I))-10.0**(-7.0))86,86,87
   86 CSX(I)=0.0
   87 CONTINUE
  701 CONTINUE
      WRITE(6,7)
    7 FORMAT(1H1/26HW. STRAWDERMAN JOB NO 0775)
      DO 100 I=1,20
      DO 101 J=1,20
      F=I
      H=J
      PNOME(I,J)=(DP**0.5)*(((F*PI)**2.0)+((H*PI/BP)**2.0))
  101 CONTINUE
  100 CONTINUE
      CALL SSWTCH(4,JSSTCH)
      IF(JSSTCH.EQ.2) GO TO 521
  520 WRITE(6,522) X,Y,ZP,BP,DEPTH,DAMP,OMEGA,CP,DP,CAPM,
     1DELTA,ALFA,TIP
  522 FORMAT(5F10.8/5F10.4/3F10.4)
      WRITE(6,590)   RHO
  590 FORMAT(1X,F10.6)
  521 CONTINUE
      WRITE(6,142)((PNOME(I,J),J=1,10),I=1,10)
  142 FORMAT(10E12.4)
  160 DO 106 K=1,20
      DO 107 L=1,20
      FREQ(K,L)=0.0
  107 CONTINUE
  106 CONTINUE
```

```
      DO 102 I=1,20
      DO 103 J=1,20
      IF(OMEGA-PNOME(I,J))104,103,103
  104 K=I
      L=J
      FREQ(K,L)=PNOME(K,L)
      GO TO 102
  103 CONTINUE
  102 CONTINUE
      DO 700 I=1,20
      TMINO(I)=0.0
  700 CONTINUE
      M=0
      DO 109 I=1,20
      DO 108 J=1,20
      IF(FREQ(I,J))99,110,111
  111 M=M+1
      TMINO(M)=FREQ(I,J)
  110 CONTINUE
  108 CONTINUE
  109 CONTINUE
      S=TMINO(1)
      DO 112 L=1,19
      IF(S-TMINO(L+1))112,121,121
  121 S=TMINO(L+1)
  112 CONTINUE
      DO 130 L=1,20
      IF(S-TMINO(L))130,132,130
  132 N=L
      GO TO 180
  130 CONTINUE
  180 DOMEG=(S-OMEGA)/3.0
      Z=N
      ITOP=Z+1.5
      MU=1
      DO 901 I=1,10
      DO 900 J=1,10
```

TABLE 7B (Continued)

```
      A=I-1
      B=J-1
      ACRES(I,J)=PI*CP*((A**2  )+((B/BP)**2  ))**0.5
  900 CONTINUE
  901 CONTINUE
      WRITE(6,902)  ((ACRES(I,J),J=1,10),I=1,10)
 902  FORMAT(//10E12.4)
  300 CONTINUE
      DO 2171 I=1,100
      PHIFY(I)=0.0
 2171 CONTINUE
  217 CONTINUE
      SUM=0.00
      TOP=0.0
      EXPB=E**(-0.7*OMEGA*BP)
      DO 702 I=1,20
      DO 703 J=1,20
      B=I
      D=J
      IF(B-D)11,12,11
   11 G(I,J)=B*D*PISQ*((((-1.0)**I)*((-1.0)**J)-1.0)+(2.0-(((-1.0)**I)
     1+((-1.0)**J))*EXPB))
      GO TO 703
   12 G(I,J)=(0.35*OMEGA*BP)*(2.0*((0.7*OMEGA*BP)**2  )+PISQ*((B**2  )+
     1(D**2  )))+B*D*PISQ*(2.0-(((-1.0)**I)+((-1.0)**J))*EXPB)
  703 CONTINUE
  702 CONTINUE
      CALL OVERFL(J)
      IF(J.EQ.2)  GO TO 751
  750 WRITE(6,752)EXPB
  752 FORMAT(O12)
  751 CONTINUE
      DO 705 I=1,20
      DO 704 J=1,20
      PNOND(I,J)=PNOME(I,J)/OMEGA
      T(I,J)=((((PNOND(I,J)**2  )-1.0)**2  )+(2.0*DAMP*PNOND(I,J))**2  )
     1**0.5
```

TABLE 7B (Continued)

```
 704 CONTINUE
 705 CONTINUE
     DO 706 I=1,20
     A=I
     P(I)=(A**2   )*PISQ+(0.7*OMEGA*BP)**2
 706 CONTINUE
     DO 707 I=1,20
     A=I
     CAPR(I)=((((A**2   )*PISQ-0.987*(OMEGA**2   ))**2   )+0.0529*(OMEGA**
    14   ))**0.5
 707 CONTINUE
     PNGNU=0.23*(OMEGA**2)
     DO 708 I=1,20
     A=I
     DGNU    =(A**2   )*PISQ-0.987*(OMEGA**2   )
     CALL ACTN(DGNU    ,PNGNU,GNU(I),IOTA)
     IF(IOTA)13,14,13
  13 GO TO 216
  14 CONTINUE
 708 CONTINUE
     DO 7080 I=1,20
     DO 7081 J=1,20
     COGNU(I,J) = COS(GNU(I)+GNU(J))
7081 CONTINUE
7080 CONTINUE
     DO 710 I=1,20
     DO 709 J=1,20
     PNLDA=2.0*DAMP*PNOME(I,J)*OMEGA
     DLDA=(PNOME(I,J)**2   )-(OMEGA**2   )
     CALL ACTN(DLDA,PNLDA,PLDA(I,J),ILDA)
     IF(ILDA)19,20,19
  19 GO TO 216
  20 CONTINUE
 709 CONTINUE
 710 CONTINUE
     CQR=(OMEGA/CP)**2
     DO 811 I=1,20
```

```
      DO 810 J=1,20
      A=I-1
      B=J-1
      EQR=PISQ*((A**2  )+((B/BP)**2  ))
      IF(EQR-CQR)812,812,813
  812 CKAYZ(I,J)=(CQR-EQR)**0.5
      ARGD=CKAYZ(I,J)*DEPTH
      ARGZ=CKAYZ(I,J)*ZP
      SINKD(I,J)=SIN(ARGD)
      COSKZ(I,J)=COS(ARGZ)
      GO TO 810
  813 CKAYZ(I,J)=(EQR-CQR)**0.5
      ARGD=CKAYZ(I,J)*DEPTH
      ARGZ=CKAYZ(I,J)*ZP
      SINKD(I,J)=(0.5)*((E**ARGD)-(E**(-ARGD)))
      COSKZ(I,J)=(0.5)*((E**ARGZ)+(E**(-ARGZ)))
  810 CONTINUE
  811 CONTINUE
      DO 5002 I=1,20
      DO 5001 J=1,20
      A=I
      B=J-1
      K=I
      L=J-1
      IF(A-B)5003,5004,5003
 5004 COKAP(I,J)=0.0
      GO TO 5001
 5003 AHAF=(A+B)/2.0
      IHAF=AHAF
      AIH=IHAF
      IF(AHAF-AIH)4001,4002,4001
 4002 COKAP(I,J)=0.0
      GO TO 5001
 4001 IF(B) 5005,5006,5005
 5005 DIJ=1.0
      GO TO 5007
 5006 DIJ=2.0
```

TABLE 7B (Continued)

```
5007 COKAP(I,J)=A*(1.0-((-1.0)**K)*((-1.0)**L))/(DIJ*((A**2)-(B**2)))
5001 CONTINUE
5002 CONTINUE
 740 CONTINUE
     DO 714 J=1,ITOP
     DO 713 K=1,ITOP
     DO 712 M=1,ITOP
     DO 711 N=1,ITOP
     A=J
     B=K
     C=M
     D=N
     IF(J-M)21,22,21
 21  W=A*C*PISQ*(2.0*COGNU(J,M)*(COS(PLDA(J,K)-PLDA(M,N)))+
    1((((-1.0)**J)*((-1.0)**M)-1.0)*(CAPR(J)*(COS(GNU(M)+PLDA(J,K)-
    2PLDA(M,N)))-CAPR(M)*(COS(GNU(J)+PLDA(M,N)-PLDA(J,K)))))/(PISQ*(
    3(A**2)-(C**2))))-(EXPA*(((-1.0)**J)*(COS(OMEGA
    4+GNU(J)+GNU(M)+PLDA(J,K)-PLDA(M,N)))+((-1.0)**M)*(COS(OMEGA+GNU(J
    5)+GNU(M)+PLDA(M,N)-PLDA(J,K))))))
     GO TO 33
  22 W=1.0066*OMEGA*CAPR(J)*(COS(GNU(J)-0.463*PI))*(COS(PLDA(J,K)-
    1PLDA(M,N)))+A*C*PISQ*(2.0*COGNU(J,M)*(COS(PLDA(J,K)-
    2PLDA(M,N)))-(EXPA*(((-1.0)**J)*(COS(OMEGA+GNU(J)+
    3GNU(M)+PLDA(J,K)-PLDA(M,N)))+((-1.0)**M)*(COS(OMEGA+GNU(J)+GNU(N)
    4+PLDA(M,N)-PLDA(J,K))))))
  33 CONTINUE
     DO 824 JQ=1,ITOP
     DO 823 KR=1,ITOP
     DO 822 MS=1,ITOP
     DO 821 NT=1,ITOP
     AQ=JQ
     BR=KR
     CS=MS
     DT=NT
     TMAX = AMAX1(A,B   ,C,D,AQ,BR,CS,DT)
     IF(TMAX-TOP)821,821,737
 737 CONTINUE
```

```
      IF(CSY(NT))716,715 ,716
  715 PNUM=0.0
      DEN=1.0
      GO TO 310
  716 IF(CSX(MS))718,717,718
  717 PNUM=0.0
      DEN=1.0
      GO TO 310
  718 IF(CSY(KR))720,719,720
  719 PNUM=0.0
      DEN=1.0
      GO TO 310
  720 IF(CSX(JQ))722,721,722
  721 PNUM=0.0
      DEN=1.0
      GO TO 310
  722 CONTINUE
      IF(COKAP(J,JQ)) 602,601,602
  601 CKAPA=0.0
      PNUM=0.0
      DEN=1.0
      GO TO 310
  602 IF(COKAP(K,KR)) 604,603,604
  603 CKAPA=0.0
      PNUM=0.0
      DEN=1.0
      GO TO 310
  604 IF(COKAP(M,MS))606,605,606
  605 CKAPA=0.0
      PNUM=0.0
      DEN=1.0
      GO TO 310
  606 IF(COKAP(N,NT))608,607,608
  607 CKAPA=0.0
      PNUM=0.0
      DEN=1.0
      GO TO 310
```

TABLE 7B (Continued)

```
 608 CONTINUE
     CKAPA=COKAP(J,JQ)*COKAP(K,KR)*COKAP(M,MS)*COKAP(N,NT)
     UQRST=CKAYZ(JQ,KR)*CKAYZ(MS,NT)*SINKD(JQ,KR)*SINKD(MS,NT)
     PNUM=CSX(JQ)*CSY(KR)*CSX(MS)*CSY(NT)*COSKZ(JQ,KR)*COSKZ(MS,NT)
    1*G(K,N)*W*CKAPA
     DEN=T(J,K)*T(M,N)*P(K)*P(N)*CAPR(J)*CAPR(M)*UQRST
 310 SUM=SUM+(PNUM/DEN)
     CALL SSWTCH(2,JSSTCH)
     IF(JSSTCH.EQ.2)  GO TO 501
 500 WRITE(6,23) SUM,PNUM,DEN,G(K,N),W,T(J,K),T(M,N),P(K),
    1P(N),CAPR(J),CAPR(M),CKAPA,UQRST,JQ,KR,MS,NT,J,K,M,N
  23 FORMAT(5E17.8/5E17.8/3E17.8/8I10//)
 501 CONTINUE
 821 CONTINUE
 822 CONTINUE
 823 CONTINUE
 824 CONTINUE
 711 CONTINUE
 712 CONTINUE
 713 CONTINUE
 714 CONTINUE
     IF((OMEGA*DELTA)-1.932)202,202,203
 202 PHIFY(MU)=7.008*(10.0**(-3.0))*(ALFA**2.0)*(CAPM**2.0)*DELTA*SUM
    1*(RHO**2)/(PISQ**2)
     GO TO 204
 203 PHIFY(MU)=5.112*(10.0**(-2.0))*(ALFA**2.0)*(CAPM**2.0)*(DELTA**
    1(-2.0))*(OMEGA**(-3.0))*SUM *(RHO**2)/(PISQ**2)
 204 CONTINUE
     CALL SSWTCH(4,JSSTCH)
     IF(JSSTCH.EQ.2) GO TO 531
530  WRITE(6,532)  X,Y,ZP,BP,DEPTH,DAMP,OMEGA,CP,DP,CAPM,
    1DELTA,ALFA,TIP
 532 FORMAT(5F10.8/5F10.4/3F10.4)
 531 CONTINUE
     CALL SSWTCH(4,JSSTCH)
     IF(JSSTCH.EQ.2)  GO TO 505
504  WRITE(6,502)  PHIFY(MU),TOP,MU
```

```
 502 FORMAT(2E17.8,1I2)
     CALL SSWTCH(4,JSSTCH)
     IF(JSSTCH.EQ.2)  GO TO 99
505  CONTINUE
     IF(TOP)206,205,206
 205 CONTINUE
     TOP=ITOP
     MU=MU+1
     ITOP=ITOP+2
     GO TO 740
 206 CONTINUE
     K=MU-1
     RATIO = ABS((PHIFY(MU))/(PHIFY(K)))
     CALL SSWTCH(4,JSSTCH)
     IF(JSSTCH.EQ.2) GO TO 511
510  WRITE(6,512) RATIO,PHIFY(MU),PHIFY(K),MU,K
 512 FORMAT(3E17.8,2I2)
     WRITE(6,515) (PHIFY(J),J=1,10)
 515 FORMAT(5E17.8)
     CALL SSWTCH(4,JSSTCH)
     IF(JSSTCH.EQ.2)  GO TO 99
 511 CONTINUE
     IF(RATIO-TOLL)207,208,208
 207 CONTINUE
     TOP=TOP+2.0
     ITOP=ITOP+2
     MU=MU+1
     GO TO 740
 208 CONTINUE
     IF(RATIO-TOLH)209,209,210
 209 CONTINUE
     GO TO 211
 210 CONTINUE
     TOP=TOP+2.0
     ITOP=ITOP+2
     MU=MU+1
     GO TO 740
```

```
  211 CONTINUE
      PHIP=PHIFY(MU)
      PHIDB = (10.0*ALOG(PHIP))/2.30258509
      WRITE(6,212) PHIP,PHIDB,OMEGA,ITOP,MU
  212 FORMAT(3E17.8,2I2)
      CALL SSWTCH(4,JSSTCH)
      IF(JSSTCH.EQ.2)  GO TO 99
      IF(PHIDB)3001,3000,3000
 3000 PHIDB=0.0
 3001 CONTINUE
      IF(OMEGA-TIP)215,216,216
  215 CONTINUE
      IF(Q-2.0)213,214,214
  213 OMEGA=OMEGA+DOMEG
      Q=Q+1.0
      ITOP=Z+1.5
      MU=1
      GO TO 300
  214 OMEGA=S+0.001*DAMP
        0.0
       , TO 160
  216 END FILE 4
      WRITE(6,3009)    IPEN,IPEN
 3009 FORMAT(2I6)
      END FILE 5
      END FILE 5
      STOP 5
   99 STOP 7
      END
$IBFTC ACTN    REF
CACTN
      SUBROUTINE ACTN (A,B,THETA,I)
      I=0
      IF (ABS(A)+ABS(B)) 27,28,27
   27 THETA= ATAN(ABS(B/A))
      IF (A) 22,21,23
   22 IF (B) 32,24,31
   23 IF (B) 33,25,34
   24 THETA=3.1415927
      GO TO 34
   25 THETA=0.0
      GO TO 34
   21 IF (B) 26,28,29
   26 THETA=4.7123890
      GO TO 34
   29 THETA=1.5707963
      GO TO 34
   31 THETA=3.1415927-THETA
      GO TO 34
   32 THETA=THETA+3.1415927
      GO TO 34
   33 THETA=6.283154-THETA
      GO TO 34
   28 WRITE (6,315)
  315 FORMAT (40HOPROGRAM-CANNOT-CONTINUE,ARCTAN OF (0/0) )
      I=1
   34 RETURN
      END
```

APPENDIX E

BOEING PROGRAM II (JACOBS AND LAGERQUIST)

APPENDIX E1 – MATHEMATICAL ANALYSIS

APPENDIX E2 – METHOD FOR DETERMINING INPUT DATA

APPENDIX E3 – PROGRAM IDENTIFICATION

APPENDIX E4 – TEST RUNS

NOTATION

$\lceil A \rfloor$	Diagonal matrix of elemental areas on structure associated with nodal points
A_i, A_j, A_k	Elemental area on structure associated with i, j, and k node points (in.^{2})
A_n	A constant, $A_1 = 26.5$, $A_2 = 7.20$, $A_3 = 0.5$
a	$1/U_c\theta$ (in.$^{-1}$)
B	$1/0.8\delta^*$ (in.$^{-1}$)
b	ω/U_c (in.$^{-1}$)
$[C]$	Damping matrix
$[C_F(\omega)]$	Force co-power spectral density matrix (lb^2 · sec)
$C_{F_{ij}}(\omega)$	Force co-power spectral density (co-PSD) acting on plate pairs i and j (lb^2 · sec)
C_f	Local coefficient of frictions τ_w/q
$C_p(\xi,\eta;\omega)$	Pressure co-power spectral density function (psi^2 · sec)
$[C_p(\omega)]$	Pressure co-power spectral density matrix (psi^2 · sec)
$[C_\delta(\omega)]$	Deflection co-power spectral density matrix (in.^{2} · sec)
$\lceil D \rfloor$	Diagonal matrix, real factor in admittance matrix
$\lceil E \rfloor$	Diagonal matrix, imaginary factor in admittance matrix
$\{F(t)\}$	Column force matrix (lb)
g	Structural damping coefficient
$H_j^{(i)}(i\omega), H_j^{(k)}(i\omega)$	Complex frequency response function defining deflection at j due to unit harmonic forcing at i and k, respectively
$\{I\}$	Column matrix, Laplace transform of force column matrix with unit impulse at particular point, zero forces at other points
$[H(i\omega)]$	Complex frequency response matrix
i	$\sqrt{-1}$
i,j	Finite node points
$[K]$	Stiffness matrix
K^2	Equals $\dfrac{\overline{p^2}}{\tau_w^2}$; also equals $\sum_{n=1}^{3} \dfrac{A_n}{K_n} = 9.56$ (a normalization constant for power spectral density)

K_n	A constant; $K_1 = 6.1$, $K_2 = 0.91$, $K_3 = 0.26$
$k(\tau)$	Impulse response function defined at time t due to a unit impulse applied τ time units earlier
$[L(\delta)]$	Matrix of the Laplace transform of the deflection
M	Mach number
$[M]$	Mass matrix
M_i	Generalized mass
m_{ij}, n_{ij}	Integers used to denote separation distance between the i and j node in x and y-directions respectively
N	Number of frequencies used to define the pressure cross power spectral density
n	Integer denoting spectral component; allowable values are 1, 2, and 3
$p_j(t)$, $p_1(t)$, $p_2(t)$	Pressure at positions j, 1, and 2, respectively
$\overline{p^2}$ or $<p^2>$	Mean square fluctuating pressure at the wall in turbulent boundary layer (psi^2)
$[Q_F(\omega)]$	Force quad power spectral density matrix (lb^2 · sec)
$Q_{F_{ij}}(\omega)$	Force quad-power spectral density acting on plate pairs i and j (lb^2 · sec)
$Q_p(\xi, \eta; \omega)$	Pressure quad-power spectral density function
$[Q_p(\omega)]$	Pressure quad-power spectral density matrix (psi^2 · sec)
$[Q_\delta(\omega)]$	Deflection quad-power spectral density matrix (in.^{2} · sec)
$q(t)$	Dynamic pressure (psi)
$\{q(t)\}$	Column matrix of principal coordinates
$R_{p_{jk}}(\tau)$	Cross correlation of pressures at points j and k (psi^2)
$R_{\delta_q^j \delta_r^k}(\tau)$	Cross correlation of deflections at points q and r resulting from loads at points j and k respectively (in.^{2})
S	$\omega\delta^*/U$, Strouhal number, dimensionless frequency
s	Laplace dummy variable
t	Time (sec)
U	Free-stream air flow velocity or aircraft speed (in./sec)
U_c	Convection velocity (in./sec)
x,y	Cartesian coordinates (in.)

x_i, y_i	Cartesian coordinates of ith node point (in.)
$Y_n(K_n S)$, $Y_n\left(\frac{\omega K_n}{BU_c}\right)$	A correction factor (equals 1 unless otherwise defined)
γ	C_p/C_v, ratio of specific heats of air, 1.41 when p_a = 14.7 psi
ζ	Critical damping ratio
$\{\zeta(t)\}$	Column matrix of deflection distance of structure normal to the surface of the structural plate (in.)
δ^*	Boundary layer displacement thickness (in.)
η	Separation distance in y-direction (in.)
$\hat{\eta}$	$\eta/0.8K_n\delta^*$, normalized separation distance
η'	$\eta + \eta_j - \eta_i$ (in.)
η_i, η_j	Distance in y-direction between node and dummy variable on ith and jth nodal areas respectively (in.)
$\hat{\eta}_i, \hat{\eta}_j$	$\eta_i/0.8K_n\delta^*$, $\eta_j/0.8K_n\delta^*$, normalized separation distance
η_0	Smallest basic separation distance in y-direction (in.)
$\hat{\eta}_0$	$\eta_0/0.8K_n\delta^*$, normalized separation distance
θ	Eddy lifetime (sec^{-1})
$\kappa_0(K_n S), \kappa_0\left(\frac{\omega K_n}{BU_c}\right)$	Modified Bessel function of order zero with argument $K_n S$ and $\omega K_n/BU_c$ respectively
λ, μ	Proportionality factor between damping and stiffness and inertias respectively
ξ	Separation distance in x-direction (in.)
ξ'	$\xi + \xi_j - \xi_i$ (in.)
ξ_i, ξ_j	Distance in x-direction between node and dummy variable on ith and jth nodal areas respectively (in.)
ξ_0	Smallest basic separation distance in x-direction
$\Pi_{F_{ij}}(i\omega)$	Normalized cross power spectral density of forces acting on plate pair i and j, a complex function of ω (sec)
$\Pi_{F(n)_{ij}}(i\omega)$	nth component of normalized cross power spectral density of forces acting on plate pair i and j, a complex function of ω (sec)
$\Pi_n(\xi, \eta; i\omega)$	nth component of the normalized pressure cross power spectral density, a complex function of ω (sec)
$\Pi(\xi, \eta; i\omega)$	Normalized pressure cross power spectral density, a complex function of ω (sec)
$\Pi(\omega)$, $\Pi_n(\omega)$	Normalized pressure power spectral density and the nth component of normalized pressure power spectral density respectively

$\rho_n(\xi, \eta; \tau)$	nth component of pressure cross-correlation coefficient (psi^2)
$\rho(\xi, \eta; \tau)$	Cross-correlation coefficient, $-1 \leq \rho(\xi, \eta; \tau) \leq +1$
τ	Time delay (sec)
τ_w	Local fluid shearing stress of air measured at wall (psi)
$[\Phi_F(i\omega)]$	Force cross power spectral density matrix (lb^2 · sec)
$\Phi_{F_{ii}}(\omega)$	Force power spectral density acting on the ith structural plate (lb^2 · sec)
$\Phi_{F_{ij}}(i\omega)$	Cross power spectral density of forces acting on plate pair i and j, a complex function of ω (lb^2 · sec)
$\Phi_p(\xi, \eta; i\omega)$	Pressure cross power spectral density function (psi^2 · sec)
$\Phi_p(\omega)$	Pressure power spectral density (psi^2 · sec)
$[\phi]$	Matrix of eigenvectors
$\left\{\phi^{(r)}\right\}$	Eigenvector column matrix (rth normal mode shape)
ψ	Phase angle (radians)
ω	Angular frequency, $2\pi f$ (radians/sec)
ω_i	Eigenfrequency of ith mode of structure, modal frequency (radians/sec)
$\omega_k, \{\omega_k\}$	Frequency and a set of frequencies respectively at which pressure cross power spectral density is defined (radians/sec)
ω_r	Angular eigenfrequency or eigenvalue (radians/sec)
$[\ ]^T$	Transpose of matrix
$(\ )^*$	Complex conjugate
$(\dot{\ })$	First derivative with respect to time
$(\ddot{\ })$	Second derivative with respect to time
$(\overline{\ })$	Time average
$(\bar{\ })$	Vector
$[\searrow(\ )\searrow]$ or $[\diagdown(\ )\diagdown]$	Denotes diagonal matrix

APPENDIX E1 - MATHEMATICAL ANALYSIS

This section presents equations developed by means of a finite element analysis[34-37] for the deflection cross power spectral density response of a simple *clamped* panel to a turbulent boundary layer.

Consider a plate idealized into a finite number of discrete structural elements connected at node points having prescribed freedoms (Figure 19). The physical properties of the plate are assumed to be lumped into individual elements. The equations of motion of each panel element is written in the form of a matrix equation[13]

$$[M]\{\ddot{\delta}(t)\} + [C]\{\dot{\delta}(t)\} + [K]\{\delta(t)\} = \{F(t)\} \tag{E1}$$

where $\delta(t)$ and $F(t)$ are column matrices of time dependent *nodal* displacements and applied forces, respectively.

The square matrices $[M]$,$[C]$, and $[K]$ are inertia, viscous damping, and stiffness coefficients, respectively.

Elements of the inertia matrix $[M]$ correspond to inertia forces associated with the freedoms at each node. For small panel deflections, rotary and inplane inertia forces are small in comparison to the forces corresponding to translational freedoms. Hence the inertia of the elements are treated by assuming their masses to be concentrated at their respective nodes, thereby *diagonalizing* the inertia matrix. The accuracy of the concentrated mass assumption depends primarily on the number of elements used to represent the panel; accuracy increases with the number of elements used (for some quantitative data on accuracy, see pages 22, 23 and 34 of Reference 34).

The *viscous* damping is assumed to be proportional to inertia and stiffness; the significance of this assumption is discussed below.* Hence

$$[C] = \mu[M] + \lambda[K] \tag{E2}$$

where μ and λ are proportionality factors.

For the jth mode:

$$C_j = \mu M_j + \lambda K_j$$

It is convenient to represent the damping factor ζ_j which represents the fraction of critical viscous damping for the jth mode

$$2\zeta_j \equiv \frac{C_j}{\sqrt{K_j M_j}} = \frac{C_j}{M_j \omega_j} = \frac{\mu M_j + \lambda K_j}{M_j \omega_j} = \frac{\mu}{\omega_j} + \lambda\omega_j \tag{E3}$$

or

$$2\zeta_j \omega_j = \mu + \lambda\omega_j^2$$

*Viscous and structural damping are forms of damping which allow the equations of motion to be uncoupled when displacements are expressed in terms of normal mode shapes.

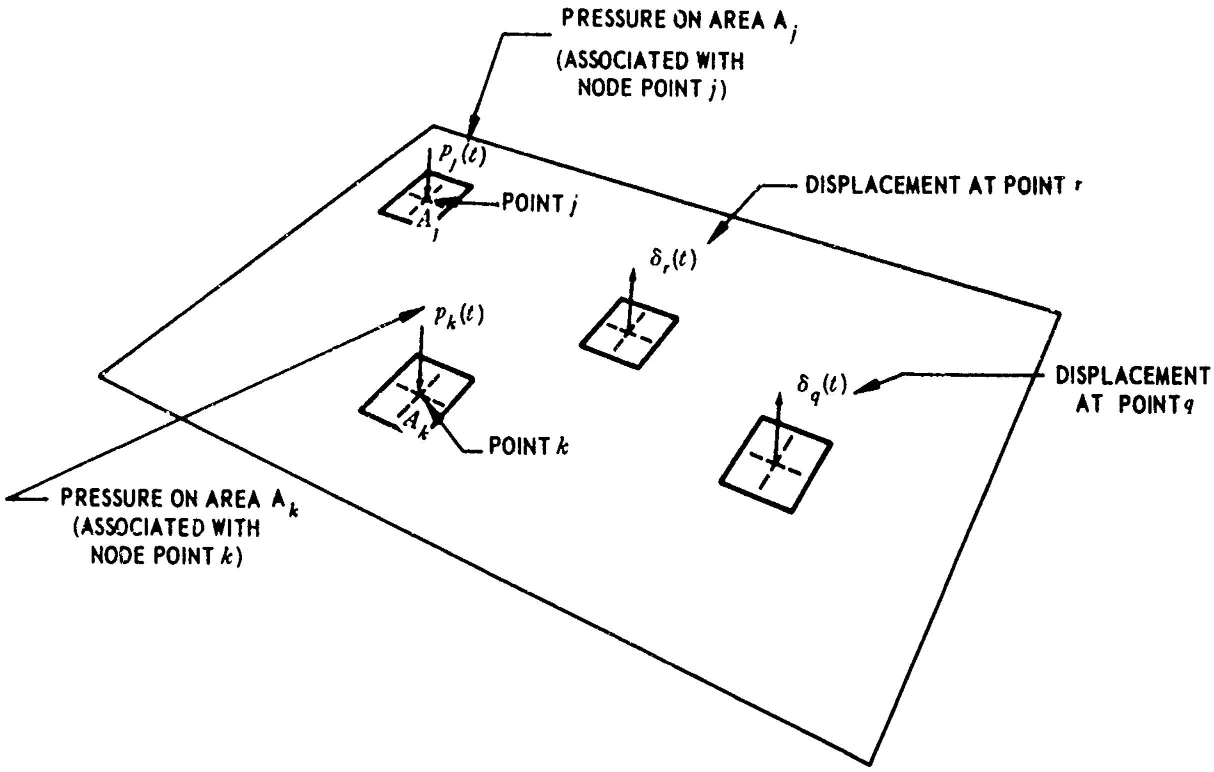

Figure 19 – Random Pressure Loads

Alternatively, when *structural* damping is used, the equations of motion for this damping are (see pages 83–86 of Reference 18)*

$$[M]\{\ddot{\delta}(t)\} + (1 + ig)[K]\{\delta(t)\} = \{F(t)\} \tag{E4}$$

When the structural damping coefficient is small ($g << 1$), then (see page 88, Equation XI and page 16, Equation (27) of Reference 18) the coefficient g is related to an equivalent viscous damping factor

$$g \simeq 2\,\zeta_j \tag{E5}$$

Total panel damping includes both acoustic radiation and structural damping. This total damping based on *experimental* panel-displacement power spectral density measurements is assumed to have the following mass-proportional viscous-damping representation as in Equations (E2) and (E3) (see pages 24–25 and 34 of Reference 34)

$$\zeta = \frac{\Delta f}{2f} = \frac{7.5}{f}$$

The symmetric stiffness matrix $[K]$ for the plate is generated by a computer program based on the displacement or stiffness method of static matrix structural analysis.[37] Both applied loading and inertia forces of the panel correspond only to translational freedoms, but the stiffness matrix is formulated with all freedoms included. Through matrix manipulation, the stiffness matrix can also be expressed solely in terms of translational deflections of the panel. Obtaining this "reduced" stiffness matrix in no way restrains the displacements of the unloaded freedoms;[37] thus the accuracy of the stiffness coefficients is unaffected. In the displacement method the panel is idealized as a system of finite plate elements connected at node points. For any point on the plate

$$F_r = K_{r1}\,\delta_1 + K_{r2}\,\delta_2 + \cdots + K_{rr}\,\delta_r + \cdots + K_{rn}\,\delta_n$$

where the K_r's are force influence coefficients that relate the external force at one point on the plate to deflections at that and other points. The collection of these force equations is represented as

$$\begin{Bmatrix} F_1 \\ F_2 \\ \cdot \\ \cdot\cdot \\ F_n \end{Bmatrix} = \begin{bmatrix} K_{11} & K_{12} & \cdots & K_{1n} \\ K_{21} & K_{22} & \cdots & K_{2n} \\ \cdot & \cdot & \cdots & \\ \cdot & \cdot & \cdots & \\ K_{n1} & K_{n2} & \cdots & K_{nn} \end{bmatrix} \begin{Bmatrix} \delta_1 \\ \delta_2 \\ \cdot \\ \cdot \\ \delta_n \end{Bmatrix} \tag{E6}$$

*See footnote on page 271.

or

$$\{F\} = [K]\{\delta\} \tag{E6}$$

where the matrix of force influence coefficients is called the stiffness matrix and the individual terms in the matrix are called the stiffness coefficients. The coefficient (or element) K_{rs} of $[K]$ is the static force at nodal point i corresponding to a unit displacement at point j, all other points held fixed. The foregoing is more fully discussed in Reference 37.

We determine the system response from the equations of motion, (E1) or (E4), for an excitation random in time using the frequency response method of analysis. The method specifies the characteristics of the systems behavior by a matrix of complex frequency response functions, i.e., the admittance matrix now derived.

Let $\delta(t)$, the response at time t due to a *unit* impulse applied at an earlier time t', be expressed by a unit impulse function $h(t-t')$.[33] Then the response to an *arbitrary input* $F(t')$ is, by use of the superposition or convolution integral

$$\delta(t) = \int_0^t F(t')\, h(t-t')\, dt'$$

since $h(t-t') = 0$ for $t' > t$ and since $F(t')$ can be defined for all negative t', the limits of integration can be extended (see Equation 2.8 of Reference 33) so that

$$\delta(t) = \int_{-\infty}^{\infty} F(t')\, h(t-t')\, dt'$$

If $F(t') = e^{i\omega t'}$, then

$$\delta(t) = \int_{-\infty}^{\infty} h(t-t')\, e^{i\omega t'}\, dt'$$

Let $\tau = t - t'$, $-d\tau = dt'$. Then since $-\int_{\infty}^{-\infty} \ldots d\tau = \int_{-\infty}^{\infty} \ldots d\tau$,

$$\delta(t) = e^{i\omega t} \int_{-\infty}^{\infty} h(\tau)\, e^{-i\omega\tau}\, d\tau = e^{i\omega t} H(i\omega)$$

where $H(i\omega) = \int_{-\infty}^{\infty} h(\tau)\, e^{-i\omega\tau}\, d\tau$ is defined as the complex frequency response function $= 2\pi$ times the Fourier transform of the unit impulse response function.

The Laplace transform of Equation (E1) is

$$\mathfrak{L}\Big[[M]\{\ddot{\delta}(t)\} + [C]\{\dot{\delta}(t)\} + [K]\{\delta(t)\}\Big] = \mathfrak{L}\{F(t)\}$$

where $\mathfrak{L}\{F(t)\} = \int_0^\infty F(t)\, e^{-st} dt$, s being the Laplace dummy variable.

For a system at rest at time $t = 0$, this may be written

$$\Big[s^2[M] + s[C] + [K]\Big]\mathfrak{L}\{\delta(t)\} = \mathfrak{L}\{F(t)\}$$

If a unit impulse is applied at time $t = 0$ to *one* load point of the structure, then since the Laplace function of a unit impulse function is unity

$$\Big[s^2[M] + s[C] + [K]\Big]\mathfrak{L}\{\delta(t)\} = \{I\}$$

where $\{I\}$ is a null column matrix except for a *unit entry* corresponding to the excitation point. If a unit impulse is consecutively applied to *each* load point and the resulting displacement column matrices are arranged in a square matrix, then[38]

$$\Big[\mathfrak{L}(\delta)\Big] = \Big[s^2[M] + s[C] + [K]\Big]^{-1}$$

Let $s \to i\omega$. Then $\mathfrak{L}(\delta) = \int_0^\infty \delta(t)\, e^{-i\omega t} dt = \int_0^\infty \delta(\tau)\, e^{-i\omega\tau} d\tau$ and $H(i\omega) =$

$\int_{-\infty}^{\infty} h(\tau)\, e^{i\omega\tau} d\tau = \int_{-\infty}^{\infty} \delta(\tau)\, e^{-i\omega\tau} d\tau = \int_0^\infty \delta(\tau)\, e^{-i\omega\tau} d\tau$ since as previously stated $h(\tau) =$

$\delta(\tau) = 0$ for $t' > t$ or $\tau < 0$. Thus,

$$\Big[H(i\omega)\Big] = \lim_{s \to i\omega} \Big[L(\delta)\Big] = \Big[-\omega^2[M] + i\omega[C] + [K]\Big]^{-1} \tag{E7}$$

is the admittance matrix which is a square complex matrix dependent on frequency ω. In general (for a large number of elements), the evaluation of this matrix inversion involves extensive computer time. The inversion can be avoided if we assume the damping to be proportional to inertia, to stiffness, or to both (see Equation (E2)). This assumption permits the displacements to be expressed in terms of the normal modes, thereby uncoupling the equations of motion. The decoupling of the equations of motion results in the diagonalization of the admittance matrix, thus eliminating matrix inversion.

The following procedure is used to find an admittance matrix $[H(i\omega)]$ which will not involve matrix inversion when the equations of motion are decoupled, the displacements being expressed in terms of the normal mode shapes. The mode shapes are determined from the undamped, unforced equations of motion[18]

$$\{M\}\{\ddot{\delta}(t)\} + [K]\{\delta(t)\} = 0$$

The solutions to this equation are expressed in terms of normal modes

$$\{\delta(t)\} = \{\phi^{(j)}\}\, e^{i(\omega_j t + \psi)}$$

Substitution of the latter into the former equation yields

$$\Big[[K] - \omega_j^2 [M]\Big] \{\phi^{(j)}\}\, e^{i(\omega_j t + \psi)} = 0$$

Equating the determinant of the square matrix to zero yields the nontrivial solutions to the *classic eigenvalue equation*, i.e., set

$$\Big|[K] - \omega_j^2 [M]\Big| = 0$$

Corresponding to each degree of freedom of the system, we can solve for an eigenvalue ω_j^2 . Associated with each eigenfrequency ω_j is an eigenvector $\{\phi^{(j)}\}$.

By use of a coordinate transformation,[18] we write

$$\{\delta(t)\} = [\phi]\,[q(t)]$$

where each *column* of $[\phi]$ is a normal mode $\{\phi^{(j)}\}$ and $\{q(t)\}$ is a column matrix of coordinates called principal (or generalized) coordinates[18]. Substituting this equation into Equation (E1)* and premultiplying by the transpose of $[\phi]$ results in

$$[\phi]^T[M][\phi]\{\ddot{q}(t)\} + [\phi]^T[C][\phi]\{\dot{q}(t)\} + [\phi]^T[K][\phi]\{q(t)\} = [\phi]^T\{F(t)\} \ .$$

Since the modes are assumed orthogonal with respect to inertia and stiffness, the generalized inertia and stiffness matrices become diagonal (see page 132 of Reference 18). Since the damping matrix $[C]$ is proportional to $[M]$, $[K]$, or both (Equation (E2)), it also results in a diagonal matrix, i.e.,

$$\begin{aligned}
[\phi]^T [M] [\phi] &= \lceil\!-M_j-\!\rfloor \\
[\phi]^T [K] [\phi] &= \lceil\!-K_j-\!\rfloor = \lceil\!-\omega_j^2 M_j-\!\rfloor \\
[\phi]^T [C] [\phi] &= \lceil\!-C_j-\!\rfloor
\end{aligned}$$

where M_j, $K_j = \omega_j^2 M_j$, and C_j are the generalized mass, stiffness, and damping, respectively.

Hence, substituting these quantities into the previous equation of motion, we get the decoupled equation of motion

---

*Recall that Equation (E1) includes *viscous* damping.

$$\lceil M_j \rfloor \{\ddot{q}(t)\} + \lceil C_j \rfloor \{\dot{q}(t)\} + \lceil \omega_j^2 M_j \rfloor \{q(t)\} = [\phi]^T \{F(t)\}$$

Thus, if *viscous damping* is used, then by means of the unit impulse excitations and the Laplace transform as in the derivation of Equation (E7), the admittance matrix is found from the foregoing equation to be

$$[H(i\omega)] = [\phi] \left[\diagdown \frac{1}{-\omega^2 M_j + i\omega C_j + \omega_j^2 M_j} \diagdown \right] [\phi]^T \qquad \text{(viscous damping)}$$

$$= [\phi] \left[\diagdown \frac{1}{M_j(-\omega^2 + i\omega(\mu + \lambda\omega_j^2) + \omega_j^2)} \diagdown \right] [\phi]^T \qquad \text{(E8)}$$

where μ and λ are constants, ω_j is the jth natural circular frequency of the plate, and each column of $[\phi]$ is a normal mode $\{\phi^{(j)}\}$. The term M_j is the jth generalized mass defined by

$$M_j = \{\phi^{(j)}\}^T [M] \{\phi^{(j)}\} \qquad \text{(E9)}$$

Since ω_j and ϕ_j(and therefore $[\phi]$ and $[\phi]^T$) are solutions to the classic eigenvalue problem and $[M]$ is a known quantity, then for each value j, M_j is computed from Equation (E9) as a number lying along a diagonal[18] and $H(i\omega)$ is obtained from Equation (E8). Note that in Equation (E8) the quotient of a scalar quantity, i.e., $1/[M_j(-\omega^2 + i\omega(\mu + \lambda\omega_j^2) + \omega_j^2)]$, for a given value of j is quite easily determined by a computer for a range of ω's. Hence evaluation of the product of the three matrices in Equation (E8) is generally much simpler (requires less computer time) than the evaluation of the inverse matrix, Equation (E7).

If *structural damping* is used as in Equation (E4), then since $\omega_j^2 M_j = K_j$, the quotient in the first of Equations (E8) becomes

$$\frac{1}{-\omega^2 M_j + \omega_j^2 M_j(1 + ig)} = \frac{1}{M_j(-\omega^2 + ig\omega_j^2 + \omega_j^2)}$$

so that

$$[H(i\omega)] = [\phi] \left[\diagdown \frac{1}{M_j(-\omega^2 + ig\omega_j^2 + \omega_j^2)} \diagdown \right] [\phi]^T \qquad \text{(structural damping)} \quad \text{(E10)}$$

Equations (E8) or (E10) are *decoupled* admittance matrices and do not involve matrix inversions.

The admittance function will now be used in determining the response to turbulence excitation which is treated as an ergodic stationary random process. For such processes the relationship between response cross spectral density and pressure-loading cross spectral density of the turbulent boundary layer pressures is obtained as follows:

As in the derivation of $H(i\omega)$, the displacement of point q of a plate to a pressure p_j applied over an area A_j at point j is (see Figure 19)

$$\delta_q^j(t) = A_j \int_{-\infty}^{\infty} p_j(t_1')\, h_q^j(t-t_1')\, dt'$$

Similarly the displacement at point r due to pressure at point k is

$$\delta_r^k(t) = A_k \int_{-\infty}^{\infty} p_k(t_2')\, h_r^k(t-t_2')\, dt'$$

The cross correlation of the two responses is

$$R_{\delta_q^j \delta_q^k}(\tau) = \lim_{T\to\infty} \frac{1}{2T} \int_{-T}^{T} \delta_q^j(t)\, \delta_r^k(t+\tau)\, dt$$

$$= A_j A_k \int_{-\infty}^{\infty} \int_{-\infty}^{\infty} \left[\lim_{T\to\infty} \frac{1}{2T} \int_{-T}^{T} p_j(t-\xi_1)\, p_k(t+\tau-\xi_2)\, dt \right] \cdot h_q^j(\xi_1)\, h_r^k(\xi_2)\, d\xi_1 d\xi_2$$

$$= A_j A_k \int_{-\infty}^{\infty} \int_{-\infty}^{\infty} R_{p_{jk}}(\tau-\xi_2+\xi_1)\, h_q^j(\xi_1)\, h_r^k(\xi_2)\, d\xi_1\, d\xi_2$$

where the order of the integrations has been interchanged and $\xi_1 = t - t_1'$, $\xi_2 = t - t_2' + \tau$ and $R_{p_{jk}}$ is the cross correlation of the pressures at points j and k.

The cross spectral density of the two displacements is the Fourier transform of this quantity

$$\Phi_{\delta_q^j \delta_r^k}(i\omega) = \frac{1}{2\pi} \int_{-\infty}^{\infty} R_{\delta_q^j \delta_r^k}(\tau)\, e^{-i\omega\tau}\, d\tau$$

$$= A_j A_k \frac{1}{2\pi} \int_{-\infty}^{\infty} R_{p_{jk}}(\tau-\xi_2+\xi_1)\, d\tau\, e^{-i\omega(\tau-\xi_2+\xi_1)} \int_{-\infty}^{\infty} h_q^j(\xi_1)\, e^{i\omega\xi_1}\, d\xi_1 \int_{-\infty}^{\infty} h_r^k(\xi_2)\, e^{-i\omega\xi_2} d\xi_2$$

$$= A_j A_k \Phi_{p_{jk}}(i\omega)\, H_q^{j*}(i\omega) \cdot H_r^k(i\omega)$$

where $\Phi_{p_{jk}}$ is the cross spectral density of pressures j and k and H_q^{j*} is the complex conjugate of H_q^j.

When all points of the structure are loaded, the displacement at point q is the sum of the components resulting from each load

$$\delta_q(t) = \sum_{j=1}^{n} \delta_q^j(t)$$

where n is the number of load points. The cross correlation of two displacements when all points are loaded is therefore

$$R_{\delta_{qr}}(\tau) = \sum_{j=1}^{n} \sum_{k=1}^{n} R_{\delta_r^j \delta_s^k}(\tau)$$

and the corresponding cross spectral density function for displacements at q and r is

$$\Phi_{\delta_{qr}}(i\omega) = \sum_{j=1}^{n} \sum_{k=1}^{n} A_j A_k \Phi_{p_{jk}}(i\omega)\, H_q^{j*}(i\omega)\, H_r^k(i\omega)$$

which can be expressed conveniently in matrix form for *all* pairs of node displacements*

$$[\Phi_\delta(i\omega)] = [H^*(i\omega)] \left\lceil A \right\rfloor [\phi_p(i\omega)] \left\lceil A \right\rfloor [H(i\omega)]^T \tag{E11}$$

where $[\phi_\delta(i\omega)]$ and $[(\phi_p(i\omega)]$ are cross power spectral density matrices of displacement and pressure, respectively. The diagonal elements of the resulting matrix in Equation (E11) are power spectral density functions of the displacements. The off-diagonal terms are displacement cross power spectral density terms.

Now substituting Equation (E3) into (E8) we get

$$H(i\omega) = [\phi] \left\lceil \frac{1}{M_j\left((\omega_j^2 - \omega^2) + i\omega(2\zeta_j\omega_j)\right)} \right\rfloor [\phi]^T$$

$$= [\phi] \left\lceil \frac{(\omega_j^2 - \omega^2) - 2\zeta_j\omega_j\omega}{M_j\,(\omega_j^2 - \omega^2)^2 + (2\zeta_j\omega_j\omega)^2} \right\rfloor [\phi]^T$$

*The matrices in Equation (E11) are easily expanded to yield the foregoing summation.

$$= [\phi]\left[\lceil D \rfloor - i\lceil E \rfloor\right][\phi]^T \qquad \text{(E12)}$$

where

$$D_j = \frac{1}{M_j}\,\frac{\omega_j^2 - \omega^2}{(\omega_j^2 - \omega^2)^2 + (2\zeta_j\omega_j\omega)^2}$$

$$E_j = \frac{1}{M_j}\,\frac{2\zeta_j\omega_j\omega}{(\omega_j^2 - \omega^2) + (2\zeta_j\omega_j\omega)^2}$$

Both pressure and deflection cross power spectral density matrices are Hermitian matrices which can be decomposed into a real symmetric matrix (co-power spectral density) $[C(\omega)]$ and a skew symmetric imaginary matrix (quad-power spectral density) $i[Q(\omega)]$

$$[\phi_p(\omega)] = [C_p(\omega)] + i[Q_p(\omega)] \qquad \text{(E13)}$$

$$[\phi_\delta(\omega)] = [C_\delta(\omega)] + i[Q_\delta(\omega)] \qquad \text{(E14)}$$

Pre-and post-multiplying by $\lceil A \rfloor$, we have

$$[\Phi_F(\omega)] = [C_F(\omega)] + i[Q_F(\omega)] \qquad \text{(E15)}$$

where

$$[\Phi_F(\omega)] = \lceil A \rfloor [\phi_p(\omega)] \lceil A \rfloor$$

$$[C_F(\omega)] = \lceil A \rfloor [C_p(\omega)] \lceil A \rfloor$$

$$[Q_F(\omega)] = \lceil A \rfloor [Q_p(\omega)] \lceil A \rfloor$$

Substituting Equations (E12) and (E15) into Equation (E11), we get (noting that $[\phi]$, $[\phi]^T$ are real quantities)

$$[\Phi_\delta(i\omega)] = [C_\delta(\omega)] + i[Q_\delta(\omega)]$$

$$= \left[[\phi]\left[\lceil D \rfloor - i[\ E\ ]\right][\phi]^T\right]^* [C_F(\omega) + iQ_F(\omega)] \cdot \left[[\phi]\left[[\ D\ ] - i[\ E\ ]\right][\phi]^T\right]^T$$

$$= [\phi]\left[[\ D\ ] + i[\ E\ ]\right][\phi]^T[C_F + iQ_F][\phi]\left[[\ D\ ] - i[\ E\ ]\right][\phi]^T$$

The equation consists of the sum of eight terms. Consider one of these terms $[\phi] \lceil D \rfloor [\phi]^T [C_F] [\phi] \lceil D \rfloor [\phi]^T$. For convenience we treat the term as a 3×3 matrix. The results can then be extended to an $m \times m$ matrix.

Thus

$$[\phi] \lceil D \rfloor [\phi]^T = \phi \begin{pmatrix} D_1 & 0 & 0 \\ 0 & D_2 & 0 \\ 0 & 0 & D_3 \end{pmatrix} \phi^T = [\phi] \begin{pmatrix} D_1 & 0 & 0 \\ 0 & 0 & 0 \\ 0 & 0 & 0 \end{pmatrix} [\phi]^T +$$

$$[\phi] \begin{pmatrix} 0 & 0 & 0 \\ 0 & D_2 & 0 \\ 0 & 0 & 0 \end{pmatrix} [\phi]^T + [\phi] \begin{pmatrix} 0 & 0 & 0 \\ 0 & 0 & 0 \\ 0 & 0 & D_3 \end{pmatrix} [\phi]^T$$

$$= D_1 [\phi] \begin{pmatrix} 1 & 0 & 0 \\ 0 & 0 & 0 \\ 0 & 0 & 0 \end{pmatrix} [\phi]^T + D_2 [\phi] \begin{pmatrix} 0 & 0 & 0 \\ 0 & 1 & 0 \\ 0 & 0 & 0 \end{pmatrix} [\phi]^T +$$

$$D_3 [\phi] \begin{pmatrix} 0 & 0 & 0 \\ 0 & 0 & 0 \\ 0 & 0 & 1 \end{pmatrix} [\phi]$$

If

$$[\phi] = \begin{bmatrix} \phi_{11} & \phi_{12} & \phi_{13} \\ \phi_{21} & \phi_{22} & \phi_{23} \\ \phi_{31} & \phi_{32} & \phi_{33} \end{bmatrix} = \left(\phi^{(1)} \ \phi^{(2)} \ \phi^{(3)} \right)$$

where

$$\left\{ \phi^{(1)} \right\} = \begin{pmatrix} \phi_{11} \\ \phi_{12} \\ \phi_{13} \end{pmatrix}, \left\{ \phi^{(2)} \right\} = \begin{pmatrix} \phi_{12} \\ \phi_{22} \\ \phi_{23} \end{pmatrix}, \left\{ \phi^{(3)} \right\} = \begin{pmatrix} \phi_{13} \\ \phi_{23} \\ \phi_{33} \end{pmatrix}$$

$$\left\{ \phi^{(1)} \right\}^T = \left(\phi_{11} \ \phi_{12} \ \phi_{13} \right), \left\{ \phi^{(2)} \right\}^T = \left(\phi_{12} \ \phi_{22} \ \phi_{23} \right), \left\{ \phi^{(3)} \right\}^T = \left(\phi_{13} \ \phi_{23} \ \phi_{33} \right)$$

then

$$[\phi]^T = \begin{bmatrix} \phi_{11} & \phi_{21} & \phi_{31} \\ \phi_{12} & \phi_{22} & \phi_{32} \\ \phi_{13} & \phi_{23} & \phi_{33} \end{bmatrix} = \begin{bmatrix} \left\{ \phi^{(1)} \right\}^T \\ \left\{ \phi^{(2)} \right\}^T \\ \left\{ \phi^{(3)} \right\}^T \end{bmatrix} ; \ \phi_{jk} = \phi_{kj}$$

Hence

$$[\phi][\ulcorner D \lrcorner][\phi]^T = D_1 \begin{pmatrix} \phi_{11} & \phi_{12} & \phi_{13} \\ \phi_{21} & \phi_{22} & \phi_{23} \\ \phi_{31} & \phi_{32} & \phi_{33} \end{pmatrix} \begin{pmatrix} 1 & 0 & 0 \\ 0 & 0 & 0 \\ 0 & 0 & 0 \end{pmatrix} \begin{pmatrix} \phi_{11} & \phi_{21} & \phi_{31} \\ \phi_{12} & \phi_{22} & \phi_{32} \\ \phi_{13} & \phi_{23} & \phi_{33} \end{pmatrix} + \cdots$$

$$= D_1 \begin{pmatrix} \phi_{11} & 0 & 0 \\ \phi_{21} & 0 & 0 \\ \phi_{31} & 0 & 0 \end{pmatrix} \begin{pmatrix} \phi_{11} & \phi_{21} & \phi_{31} \\ \phi_{12} & \phi_{22} & \phi_{32} \\ \phi_{13} & \phi_{23} & \phi_{33} \end{pmatrix} + \cdots$$

$$= D_1 \begin{pmatrix} \phi_{11}^2 & \phi_{11}\ \phi_{21} & \phi_{11}\ \phi_{31} \\ \phi_{21}\ \phi_{11} & \phi_{21}^2 & \phi_{21}\ \phi_{31} \\ \phi_{31}\ \phi_{11} & \phi_{31}\ \phi_{21} & \phi_{31}^2 \end{pmatrix} + \cdots\cdots\cdots$$

$$= D_1 \begin{pmatrix} \phi_{11} \\ \phi_{12} \\ \phi_{13} \end{pmatrix} \begin{pmatrix} \phi_{11} & \phi_{12} & \phi_{13} \end{pmatrix} + \cdots\cdots$$

$$= D_1 \left\{\phi^{(1)}\right\} \left\{\phi^{(1)}\right\}^T + D_2 \left\{\phi^{(2)}\right\} \left\{\phi^{(2)}\right\}^T + D_3 \left\{\phi^{(3)}\right\} \left\{\phi^{(3)}\right\}^T$$

which is the sum of dyadic products.* Hence

---

*We have shown that if A, B, C, D, E, F are vectors and a, b, c are scalars in a diagonal matrix then

$(ABC) \begin{pmatrix} a & 0 & 0 \\ 0 & b & 0 \\ 0 & 0 & c \end{pmatrix} \begin{pmatrix} D^T \\ E^T \\ F^T \end{pmatrix} = aAD^T + bBE^T + cCF^T$. And the dyadic product $p \cdot q^T$ of two vectors

$p = \begin{pmatrix} p_1 \\ p_2 \\ p_3 \end{pmatrix}$, $q = \begin{pmatrix} q_1 \\ q_2 \\ q_3 \end{pmatrix}$ is $p \cdot q^T = \begin{pmatrix} p_1 \\ p_2 \\ p_3 \end{pmatrix} (q_1\ q_2\ q_3) = \begin{pmatrix} p_1 q_1 & p_1 q_2 & p_1 q_3 \\ p_2 q_1 & p_2 q_2 & p_2 q_3 \\ p_3 q_1 & p_3 q_2 & p_3 q_3 \end{pmatrix}$. The dyadic product should

not be confused with the inner product of two vectors $p \cdot q = p_1 q_1 + p_2 q_2 + p_3 q_3 = (p_1 p_2 p_3) \begin{pmatrix} q_1 \\ q_2 \\ q_3 \end{pmatrix} = p^T \cdot q$.

$$[\phi]\lceil D \rfloor[\phi]^T[C_F][\phi]\lceil\cdot\rfloor\lceil\phi\rfloor^T = \left(D_1\{\phi^{(1)}\}\{\phi^{(1)}\}^T + D_2\{\phi^{(2)}\}\{\phi^{(2)}\}^T + D_3\{\phi^{(3)}\}\{\phi^{(3)}\}^T\right)$$

$$\cdot [C_F]\left(D_1\{\phi^{(1)}\}\{\phi^{(1)}\}^T + D_2\{\phi^{(2)}\}\{\phi^{(2)}\}^T + D_3\{\phi^{(3)}\}\{\phi^{(3)}\}^T\right)$$

$$= \sum_{j=1}^{3}\sum_{k=1}^{3} D_j D_K C_F^{(jk)}(\omega)$$

where $\left[C_F^{(jk)}(\omega)\right] = \{\phi^{(j)}\}\{\phi^{(j)}\}^T[C_F(\omega)]\{\phi^{(k)}\}\{\phi^{(k)}\}^T$

Extending these results to an m x m matrix or summation and treating the remaining seven terms of $[\phi_\delta(i\omega)]$ in a similar manner, we get

$$\begin{aligned}[\Phi_\delta(i\omega)] &= [C_\delta(\omega)] + i[Q_\delta(\omega)] \\ &= \sum_{j=1}^{m}\sum_{k=1}^{m}\Bigg\{(D_jD_k + E_jE_k)[C_F^{(jk)}(\omega)] \\ &+ D_jE_k\left([Q_F^{(jk)}(\omega)] + [Q_F^{(jk)}(\omega)]^T\right) \\ &+ i\Bigg[D_kE_j\left([C_F^{(jk)}(\omega)] - [C_F^{(jk)}(\omega)]^T\right) \\ &+ (D_jD_k + E_jE_k)[Q_F^{(jk)}(\omega)]\Bigg]\Bigg\}\end{aligned} \tag{E16}$$

where

$$[C_F^{(jk)}(\omega)] = \{\phi^{(j)}\}\{\phi^{(j)}\}^T[C_F(\omega)]\{\phi^{(k)}\}\{\phi^{(k)}\}^T$$

$$[Q_F^{(jk)}(\omega)] = \{\phi^{(j)}\}\{\phi^{(j)}\}^T[Q_F(\omega)]\{\phi^{(k)}\}\{\phi^{(k)}\}^T$$

The summation in Equation (E16) is over m normal modes.

Equation (E16) can be approximated for lightly damped systems. The cross product terms $(j \neq k)$ $D_j D_k$, E_jE_k, and D_jE_k, which involve coupling between modes, are considered insignificant for small damping. Neglecting these terms and since $[Q_F^{(ii)}] = 0$ due to the skew symmetry of $[Q_F]$, whereas $[C_F^{(ii)}] = [C_F^{ii}]^T$ due to the real symmetry of $[C_F]$ (this will be shown later), we have

$$[\Phi_\delta(\omega)] \simeq [C_\delta(\omega)] - \sum_{j=1}^{m} (D_j^2 + E_j^2)\{\phi^{(j)}\}\{\phi^{(j)}\}^T C_F(\omega)\{\phi^{(j)}\}\{\phi^{(j)}\}^T \qquad \text{(E17)}$$

The average value of the product of two distinct responses at locations q and r is

$$\overline{\delta_q \delta_r} = \int_0^\infty \Phi_{\delta_{qr}}(\omega)\, d\omega$$

where $\overline{\delta_q \delta_r}$ is called the joint deflection moment of the two responses q and r and denotes the space cross correlation (zero time delay) of the two responses.* The joint deflection moments for all responses can be considered at once and written as a matrix integration

$$\overline{\delta_q \delta_r} = \int_0^\infty [\Phi_\delta(\omega)]\, d\omega \qquad \text{(E18)}$$

where the elements of $\left[\overline{\delta_q \delta_r}\right]$ are joint deflection moments for all pairs of structural node points. The diagonal elements are mean square values of the deflections, and the off-diagonal terms are time averages of products of deflections at different node points. For small uncoupled damping, $[\phi_\delta]$ is given by Equation (E17) and the response is predominantly narrowband occurring in the regions of the natural frequencies. If broad-band excitation is assumed, the variation of the excitation cross spectral density is small compared to the response variation near the natural frequencies and the force cross power spectral density can be treated as a constant near each natural frequency. Thus we have

$$\left[\overline{\delta_q \delta_r}\right] = \sum_{j=1}^{m} \{\phi^{(j)}\}\{\phi^{(j)}\}^T [C_F(\omega_j)]\{\phi^{(j)}\}\{\phi^{(j)}\}^T \int_0^\infty (D_j^2 + E_j^2)\, d\omega \qquad \text{(E19)}$$

For small damping, and from the definitions of D_j and E_j, this equation is evaluated as (see page 63, Equation (2.14) and page 72, Equation (ii) of Reference 18).

$$\left[\overline{\delta_q \delta_r}\right] = \sum_{j=1}^{m} \{\phi^{(j)}\}\{\phi^{(j)}\}^T [C_F(\omega_j)]\{\phi^{(j)}\}\{\phi^{(j)}\}^T \frac{\pi}{4 \bar{m}_j^2 \omega_j^3 \zeta_j} \qquad \text{(E20)}$$

The Maestrello mathematical model for the space-time cross correlation of the fluctuating turbulence boundary layer pressures measured in broad frequency bands for Mach numbers ranging from 0.52 to 0.57 is (see Equation (B9) and the corresponding notation as well as Equation (E23) below)

*For $j \neq K$, evaluation of the joint responses is given in Appendix II of Reference 37.

$$\rho(\xi,\eta;\tau) = \frac{e^{-|\tau|/\theta}}{\sum_{n=1}^{3} \frac{A_n}{K_n}} \left\{ \sum_{n=1}^{3} \frac{A_n K_n}{K_n^2 + B^2[(\xi - U_c\tau)^2 + \eta^2]} \right\} \tag{E21}$$

where

$$-1 \leq \rho(\xi,\eta;\tau) \leq 1$$

$$\sum_{n=1}^{3} \frac{A_n}{K_n} = K^2 = 9.56$$

and the mean (broad band) values of θ as a function of Mach number M is given in Figure 16 of Reference 34*; see also the method given later in this Appendix for determining computer program output.

The corresponding normalized pressure cross power spectral density is

$$\left.\begin{aligned} \pi(\xi,\eta;i\omega) &= \frac{1}{\pi}\int_{-\infty}^{\infty} \rho(\xi,\eta;\tau)\, e^{-i\omega\tau}\, d\tau \;;\; (0 \leq \omega \leq \infty) \\ &= \frac{1}{2\pi}\int_{-\infty}^{\infty} \rho(\xi,\eta;\tau)\, e^{-i\omega\tau}\, d\tau ;\; (-\infty \leq \omega \leq +\infty) \end{aligned}\right\} \tag{E22}$$

(multiplying the second of Equations (E22) by 2 yields the cross power spectral density in the positive frequency domain).

It has not been possible to solve Equation (E22) using ρ as defined by Equation (E21). However a solution is possible if we take an alternate approach which makes use of the frozen turbulence model known as the Taylor hypothesis, i.e., assume space and time variations are interrelated according to

$$\frac{|\tau|}{\theta} = \frac{|\xi|}{U_c\theta} \tag{E23}$$

Thus if the time decay is described as a spacial decay, the Maestrello space-time correlation function ρ has the form

*Measured values of θ for frequency band width centered at 1200 and 4800 cps are also plotted in Figure 16 of Reference (34).

$$\rho(\xi,\eta;\tau) = \frac{e^{-|\xi|/U_c\theta}}{9.56}\left\{\sum_{n=1}^{3} \frac{A_nK_n}{K_n^2 + B^2\left[(\xi - U_c\tau)^2 + \eta^2\right]}\right\}$$

$$= \sum_{n=1}^{3} \rho_n(\xi,\eta;\tau) \qquad \text{(E24)}$$

where

$$\rho_n(\xi,\eta;\tau) = \frac{A_nK_n\, e^{-|\xi|/U_c\theta}}{9.56\left\{K_n^2 + B^2\left[(\xi - U_c\tau)^2 + \eta^2\right]\right\}} \qquad \text{(E25)}$$

Then

$$\Pi(\xi,\eta;i\omega) = \sum_{n=1}^{3} \frac{1}{\pi}\int_{-\infty}^{\infty} \rho_n(\xi,\eta;\tau)\, e^{-i\omega\tau}\, d\tau \quad (0 \le \omega \le +\infty) \qquad \text{(E26)}$$

and the nth *component of the cross power spectral density* is

$$\Pi_n(\xi,\eta;i\omega) = \frac{1}{\pi}\int_{-\infty}^{\infty} \rho_n(\xi,\eta;\tau)\, e^{-i\omega\tau}\, d\tau \quad (0 \le \omega \le +\infty) \qquad \text{(E27)}$$

Substituting Equation (E25) in (E27) and putting Equation (E25) in the form $\rho_n = \dfrac{A_nK_n\, e^{-|\xi|/U_c\theta}}{9.56\,B^2U_c^2} \cdot \left[\dfrac{1}{\dfrac{K_n^2 + B^2\eta^2}{B^2U_c^2} + \left(\tau - \dfrac{\xi}{U_c}\right)^2}\right]$ yields upon taking the Fourier transform

$$\Pi_n(\xi,\eta;i\omega) = \frac{A_nK_n\, e^{-\frac{|\xi|}{U_c\theta} - \frac{\omega}{BU_c}\left[K_n^2 + B^2\eta^2\right]^{1/2}}\, e^{-\frac{i\omega\xi}{U_c}}}{9.56\,BU_c\left[K_n^2 + B^2\eta^2\right]^{1/2}}$$

$$(0 \le \omega \le +\infty) \qquad \text{(E28)}$$

Dimensionless forms of π_n are plotted in Figures 19 and 20 of Reference 34. The three components defined in Equation (E28) are used in Equation (E26) to define the fluctuating pressure loading function.

From Equation (B7) we have

$$\Pi(\omega) = \frac{\Phi_p(\omega)\, U}{\tau_w^2\, \delta^*}$$

and by definition

$$\int_0^\infty \Pi(\omega)\, d\omega = 1 = \frac{U}{\tau_w^2\, \delta^*}\int_0^\infty \Phi_p(\omega)\, d\omega = \frac{U}{\tau_w^2\, \delta^*}\,\overline{p^2}$$

Hence

$$\frac{\tau_w^2\, \delta^*}{U} = \overline{p^2}$$

or

$$\Pi(\omega) = \frac{\Phi_p(\omega)}{\overline{p^2}} \quad \text{or} \quad \Phi_p(\omega) = \overline{p^2}\, \Pi(\omega)$$

but in accordance with the experimental results shown in Figure 14 of Reference 34, $[(\overline{p^2})^{1/2} / \tau_w] = K(M)$ is a function of the Mach M so that $\overline{p^2} = K_m^2\, \tau_w^2$. Thus, the power spectrum in nondimensional form is described by:

$$\frac{\Phi_p(\omega)\, U}{\tau_w^2\, \delta^*} = \frac{\overline{p^2}\, \Pi(\omega)\, U}{\tau_w^2\, \delta^*} = \frac{\Pi(\omega)\, U K^2}{\delta^*} = \sum_{n=1}^{3} A_n\, e^{-K_n(\omega\delta^*/U)}$$

(see Equation (B7) and note that Figure 2 of Reference 15 and Figure 2 of Reference 39 are equivalent.); however, see Appendix E2 with respect to the value K used in practice.

Hence, using Equation (E28) and noting that $1/9.56 \cong 0.105$

$$\Phi_p(\xi,\eta;i\omega) = C_p(\xi,\eta;\omega) + iQ_p(\xi,\eta;\omega) = \overline{p^2}\, \Pi(\xi,\eta;i\omega)$$

$$= \frac{[K(M)\tau_w]^2}{BU_c}\, e^{-\frac{|\xi|}{U_c\theta} - \frac{i\omega\xi}{U_c}} \left[0.105 \sum_{n=1}^{3} \frac{A_n K_n\, e^{-\frac{\omega}{B U_c}(K_n^2 + B^2\eta^2)^{1/2}}}{(K_n^2 + B^2\eta^2)^{1/2}} \right]$$

$$(0 \le \omega \le +\infty) \qquad \text{(E29)}$$

Figure 3 of Reference 34 shows graphs of this function.

The complex pressure cross power spectral density describes pressure loading as a continuous function of separation distances in the x- and y-directions. Pressure loads from boundary layers are small in spacial scale. The load can change appreciably within a few inches or even less. Figure 21 of Reference (34) shows the variation of cross power spectral density over an element.* These rapid variations cause problems in using $\Phi_p(\xi,\eta;i\omega)$ to define a loading matrix for use with finite element structural methods. Matrix finite structural analysis methods generally assume that the pressure loads vary slowly over the distance of one element, i.e., that approximately constant pressure acts over the element. When this is true, pressure at the node points can be multiplied by area to approximate forces on the elements. But when the loads vary rapidly over an element, as do boundary layer pressure loads, the method is invalid since it results in large overestimates of the total forces on the element.

This rapid variation causes problems in trying to define a matrix of cross power spectral densities acting on pairs of finite element node points; proper application of the matrix would require a very fine grid of elements. Hence an alternate method has been developed to correctly calculate the cross power spectral density of net forces acting on pairs of finite structural elements. Terms of this type are gathered into a cross power spectral density matrix that is compatible with the structural idealization; the number of elements chosen is such that the desired number of modes can be adequately resolved. The infinitesimal forces are then summed to calculate the net force cross power spectral density on finite element pairs, i.e., the elemental loads are determined by summing the contribution of each infinitesimal area within an elemental pair.

We now evaluate the force cross power spectral density and construct matrices for its real and imaginary coefficients.

Consider the geometry of a pair of finite plate elements (Figure 20) and the more detailed drawing of ξ-direction separation distances (Figure 21); similar relations hold for η-direction separation distances. Let ξ_0 and η_0 be the dimensions of the finite elements in the x- and y-directions, respectively. The area of the structure represented at each node is $(\xi_0 \eta_0)$. The separation distances between the nodes are

$$\xi = (x_j - x_i) = n_{ij}\xi_0$$

$$\eta = (y_j - y_i) = m_{ij}\eta_0$$

The infinitesimal normalized cross power spectral density of the net forces acting on the infinitesimal areas dA_i and dA_j (which are on the finite areas A_i and A_j associated with the node points , i.e., nodal areas) is

*In Mach 0.52 (δ^* = 0.155 in.) flow in the Boeing boundary layer facility, the 990-cps frequency cross power spectral density varies by a factor of more than ten between pairs of points on an 0.75-in.-long finite element.

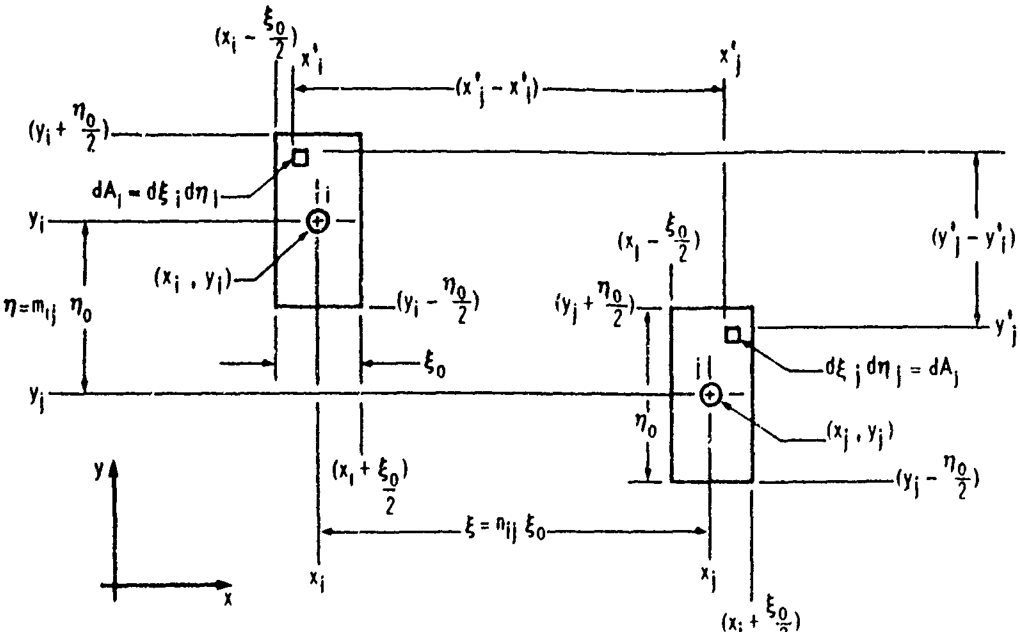

Figure 20 – Geometry of a Pair of Finite Plate Elements

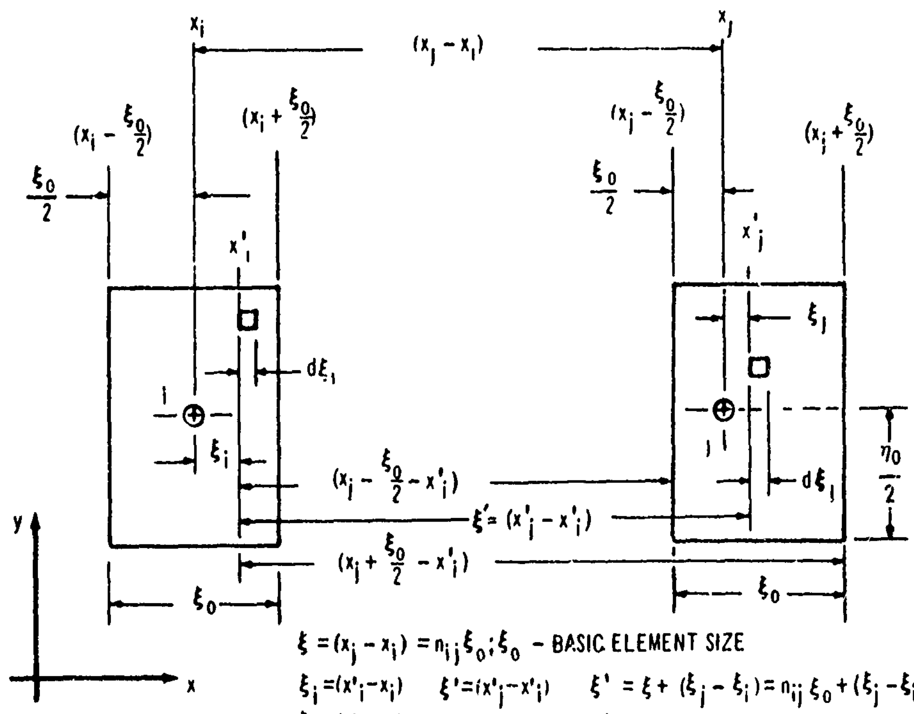

Figure 21 – Coordinates and Separation Distances in the x-Direction

$$d(\Pi_{F_{ij}}) = \Pi[(x_j' - x_i'), (y_j' - y_i'), i\omega] \, (dx_j' \, dy_j') \, (dx_i' \, dy_i')$$

where $\Pi[(x_j' - x_i'), (y_j' - y_i')]$ is the normalized pressure cross spectral density; (x_i', y_i') and (x_j', y_j') are points on the i th and j th elements, respectively, whose elemental areas are

$$dA_i = dx_i' \, dy_i' = d\xi_i \, d\eta_i$$

$$dA_j = dx_j' \, dy_j' = d\xi_j \, d\eta_j$$

The net force cross power spectral density on the (i,j) pair of nodes is then

$$\Pi_{F_{ij}}(i\omega) = \int_{A_i} \int_{A_i} \Pi[(x_j' - x_i')(y_j' - y_i') i\omega] \, dA_j \, dA_i \tag{E30}$$

where A_i and A_j are areas associated with the i and j nodes.

Figures 19 and 20 show that

$$\xi' = (x_j' - x_i') = n_{ij}\xi_0 + (\xi_j - \xi_i); \quad \xi = n_{ij}\xi_0$$

$$\eta' = (y_j' - y_i') = m_{ij}\eta_0 + (\eta_j - \eta_i); \quad \eta = m_{ij}\eta_0$$

where n_{ij} and m_{ij} are the integral numbers of incremental separation distances in the x- and y-directions, respectively.

Hence the force cross power spectral density of the net forces acting on the (i,j) pair of nodes is

$$\Pi_{F_{ij}}(i\omega) = \int_{-\frac{\eta_0}{2}}^{\frac{\eta_0}{2}} \int_{-\frac{\eta_0}{2}}^{\frac{\eta_0}{2}} \int_{-\frac{\xi_0}{2}}^{\frac{\xi_0}{2}} \int_{-\frac{\xi_0}{2}}^{\frac{\xi_0}{2}} \Pi[(\xi + \xi_j - \xi_i), (\eta + \eta_j - \eta_i); i\omega] \, d\xi_j \, d\xi_i \, d\eta_j \, d\eta_i \tag{E31}$$

Now rewrite Equation (E28) using the variables of Equation (E31), i.e., *replace the separation between nodes* ξ, η *by the separation between infinitesimal areas* $\xi + \xi_j - \xi_i$, $\eta + \eta_j - \eta_i$ *respectively.* Then

$$\Pi_n[(\xi+\xi_j-\xi_i),\ (\eta+\eta_j-\eta_i);i\omega] = \underbrace{\frac{A_n K_n}{9.56 B U_c}}_{3}\ \underbrace{e^{-\left\{\frac{|\xi+\xi_j-\xi_i|}{U_c\theta}\right\}}\ e^{-\left\{i\frac{\omega}{U_c}(\xi+\xi_j-\xi_i)\right\}}}_{2}$$

$$\underbrace{\frac{e^{-\left\{\frac{\omega}{B U_c}\left[K_n^2+B^2(\eta+\eta_j-\eta_i)^2\right]^{1/2}\right\}}}{\left[K_n^2+B^2(\eta+\eta_j-\eta_i)^2\right]^{1/2}}}_{1} \quad (0 \le \omega \le \infty) \qquad \text{E32)}$$

is the nth *component of* the *pressure* cross spectral density. Equation (E32) shows that the integrand of Equation (E31) is divided into parts so that the integration is over (1) η only, (2) ξ only, (3) constant. The first two parts are now discussed.

The integral of (1) in Equation [E32], which involves η integration only, is

$$\int_{-\frac{\eta_0}{2}}^{+\frac{\eta_0}{2}} \int_{-\frac{\eta_0}{2}}^{+\frac{\eta_0}{2}} \frac{e^{-\frac{\omega}{B U_c}\left[K_n^2+B^2(\eta+\eta_j-\eta_i)^2\right]^{1/2}}}{\left[K_n^2+B^2(\eta+\eta_j-\eta_i)^2\right]^{1/2}}\, d\eta_j\ d\eta_i \qquad \text{E33)}$$

To generalize the analysis, the following dimensionless separation distances are defined

$$\hat{\eta} = \frac{\eta}{0.8K_n\delta^*} = \frac{m_{ij}\eta_0}{0.8K_n\delta^*}$$

$$\hat{\eta}_0 = \frac{\eta_0}{0.8K_n\delta^*}$$

$$\hat{\eta}_i = \frac{\eta_i}{0.8K_n\delta^*}$$

$$\hat{\eta}_j = \frac{\eta_j}{0.8K_n\delta^*}$$

$$y = \hat{\eta}_j - \hat{\eta}_i$$

Since $\dfrac{\omega}{BU_c} = \dfrac{\omega}{\dfrac{1}{0.8\delta^* U_c}} = \dfrac{\omega\delta^*}{U} = S$, Equation (E33) may be rewritten as

$$\int_{-\frac{\eta_0}{2}}^{+\frac{\eta_0}{2}} \int_{-\frac{\eta_0}{2}}^{+\frac{\eta_0}{2}} \frac{e^{-K_n S\left[1+\frac{B^2}{K_n^2}\eta^2\left(1+\frac{\eta_j-\eta_i}{\eta}\right)^2\right]^{1/2}}}{K_n\left[1+\frac{B^2}{K_n^2}\eta^2\left(1+\frac{\eta_j-\eta_i}{\eta}\right)^2\right]^{1/2}} \, d\eta_j \, d\eta_i$$

but

$$\frac{B^2}{K_n^2}\eta^2 = \frac{\left(\frac{1}{0.8\delta^*}\right)^2}{K_n^2}(0.8K_n\delta^*\hat{\eta})^2 = \hat{\eta}^2$$

$$\frac{\eta_j-\eta_i}{\eta} = \frac{\hat{\eta}_j-\hat{\eta}_i}{\hat{\eta}} = \frac{y}{\hat{\eta}}$$

$$d\eta_j \, d\eta_i = (0.8K_n\delta^*)^2 \, d\hat{\eta}_j \, d\hat{\eta}_i$$

and the variables of integration are transformed by use of the Jacobian

$$d\hat{\eta}_i \, d\hat{\eta}_j = \left|\frac{\partial(\hat{\eta}_i, \hat{\eta}_j)}{\partial(\hat{\eta}_i, y)}\right| dy \, d\hat{\eta}_i = \begin{vmatrix} \dfrac{\partial\hat{\eta}_i}{\partial\hat{\eta}_i} & \dfrac{\partial\hat{\eta}_j}{\partial\hat{\eta}_i} \\ \dfrac{\partial\hat{\eta}_i}{\partial y} & \dfrac{\partial\hat{\eta}_j}{\partial y} \end{vmatrix} dy \, d\hat{\eta}_i$$

$$= \begin{vmatrix} 1 & 0 \\ -1 & 1 \end{vmatrix} dy \, d\hat{\eta}_i = dy \, d\hat{\eta}_i$$

Hence $d\eta_j \, d\eta_i \rightarrow (0.8K_n\delta^*)^2 \, dy \, d\hat{\eta}_i$.

For the limits when $\eta_i = \pm\dfrac{\eta_0}{2}$, $\hat{\eta}_i = \pm\dfrac{\eta_i}{0.8K_n\delta^*} = \pm\dfrac{\eta_0}{2(0.8K_n\delta^*)} = \pm\dfrac{\hat{\eta}_0}{2}$. Similarly

the upper and lower limits of η_j are $\pm \hat{\eta}_0 / 2$ respectively. Hence for the $y(= \hat{\eta}_j - \hat{\eta}_i)$ variable of integration, since η_i remains as a variable in the inner limits, the inner limits, the inner limits are $y = \pm \frac{\hat{\eta}_0}{2} - \hat{\eta}_i$.

Hence the previous integral in terms of the new coordinates $y, \hat{\eta}_i$ is

$$(0.8K_n\delta^*)^2 \int_{-\frac{\hat{\eta}_0}{2}}^{+\frac{\hat{\eta}_0}{2}} \int_{\left[\frac{-\hat{\eta}_0}{2} - \hat{\eta}_i\right]}^{\left[\frac{\hat{\eta}_0}{2} - \hat{\eta}_i\right]} \frac{e^{-K_n S[1 + (\hat{\eta} + y)^2]^{1/2}}}{K_n[1 + (\hat{\eta} + y)^2]^{1/2}} \, dy \, d\hat{\eta}_i$$

Now let

$$y' = \hat{\eta} + y$$

$$dy' = dy$$

when $y = \pm \frac{\hat{\eta}_0}{2} - \hat{\eta}_i$, $y' = \pm \frac{\hat{\eta}_0}{2} + \eta - \hat{\eta}_i$, hence the equation becomes

$$(0.8K_n\delta^*)^2 \int_{-\frac{\hat{\eta}_0}{2}}^{+\frac{\hat{\eta}_0}{2}} \int_{\left[\frac{-\hat{\eta}_0}{2} + \hat{\eta} - \hat{\eta}_i\right]}^{\left[\frac{\hat{\eta}_0}{2} + \hat{\eta} - \hat{\eta}_i\right]} \frac{e^{-K_n S[1 + (y')^2]^{1/2}}}{K_n[1 + (y')^2]^{1/2}} \, dy' \, d\hat{\eta}_i$$

Since y' is a dummy variable, we let $y' \rightarrow y$ so that the equation and symbols conform to those in Reference 34. The integral is then

$$(0.8K_n\delta^*)^2 \int_{-\frac{\hat{\eta}_0}{2}}^{\frac{\hat{\eta}_0}{2}} \int_{\left[\frac{-\hat{\eta}_0}{2} + \hat{\eta} - \hat{\eta}_i\right]}^{\left[\frac{\hat{\eta}_0}{2} + \hat{\eta} - \hat{\eta}_i\right]} \frac{e^{-K_n S[1 + y^2]^{1/2}}}{K_n[1 + y^2]^{1/2}} \, dy \, d\hat{\eta}_i \qquad \text{(E34)}$$

Equation (E33) or its equivalent Equation (E34) cannot be integrated in closed form. For the general case, a numerical approximation of this integral is necessary. For the special case of the integrand approaching small values within one incremental separation, a closed-form approximation is possible. Thus for S and $\hat{\eta}_0$ not too small and assuming $\hat{\eta} = 0$, the integrand of Equation (E34) is a rapidly decaying function. That is, we assume that the sphere of influence of all pressure points on the ith finite element does not extend beyond the element; the approximation is good when the boundary layer thickness is small compared

to the element size. We can then extend the limits of integration from $-\infty$ to $+\infty$ and take $\int_{-\infty}^{\infty} = 2\int_0^{\infty}$ since the integrand is an even function. With these approximations, Equation (E34) is equal to

$$2(0.8K_n\delta^*)^2 \int_{-\frac{\hat{\eta}_0}{2}}^{+\frac{\hat{\eta}_0}{2}} \int_0^{\infty} \frac{e^{-K_nS[1+y^2]^{1/2}}}{K_n[1+y^2]^{1/2}} \, dy \, d\hat{\eta}_i \tag{E35}$$

Equation (E35) may then be written as

$$1.28K_n(\delta^*)^2 \int_{-\frac{\hat{\eta}_0}{2}}^{+\frac{\hat{\eta}_0}{2}} d\hat{\eta}_i \int_0^{\infty} \frac{e^{-K_nS[1+y^2]^{1/2}}}{K_n[1+y^2]^{1/2}} \, dy$$

The value of the first integral is $\hat{\eta}_0$ and the value of the second integral obtained from Reference 40 (page 342, item 3.479.1 with $x = y^2$, $\beta = K_nS$ and $\nu = \frac{1}{2}$) is $\kappa_0(K_nS)$ the modified Bessel function of order zero with argument K_nS. Hence the solution to Equation (E35) is

$$1.28\, K_n(\delta^*)^2\, \hat{\eta}_0\, \kappa_0\, (K_nS) \tag{E36}$$

When the Bessel function approximation is used, it is assumed that the force cross power spectral density is approximately zero for all (i,i) pairs of finite elements except pairs (i,i).

The integral of 2 in Equation (E32) which involves ξ integration only must be handled as two special cases

Case I: $\xi = 0$

Case II: $\xi > 0, \xi < 0$

When $\xi = 0$, the region of integration is divided into two regions to properly represent the function with absolute value sign. The $\xi > 0$ and $\xi < 0$ cases have been reduced to a single expression which describes both cases.

Now rewriting Equation (E29)

$$\Phi_p(\xi,\eta;i\omega) = \overline{p^2}\,\Pi\,(\xi,\eta;i\omega) \tag{E29}$$

Similarly, using $\Pi_{F_{ij}}(i\omega)$ as defined in Equation (E31)

$$\Phi_{F_{ij}}(i\omega) = \overline{p^2}\,\Pi_{F_{ij}}(i\omega)$$

where i and j are node points with incremental separation distance in the x and y-directions such that $\xi = n_{ij}\xi_0$, $\eta = m_{ij}\eta_0$, where $\eta_{ij} = \dfrac{x_j - x_i}{\xi_0}$ and $m_{ij} = \dfrac{y_j - y_i}{\eta_0}$; n_{ij} and m_{ij} are integers so that all nodes are separated by increments of length ξ_0 and η_0 in the x-directions, respectively. But the force power spectral density is the sum of three spectral components as defined by Equations (E31) and (E32)

$$\Phi_{F_{ij}}(i\omega) = \overline{p^2}\,\Pi_{F_{ij}}(i\omega) = \overline{p^2}\left[\sum_{n=1}^{3} \Pi_{F(n)_{ij}}(i\omega)\right] \tag{E37}$$

where

$$\Pi_{F(n)_{ij}}(i\omega) = \frac{A_n K_n}{9.56\,B U_c}\int_{-\frac{\xi_0}{2}}^{+\frac{\xi_0}{2}}\int_{-\frac{\xi_0}{2}}^{+\frac{\xi_0}{2}}\int_{-\frac{\eta_0}{2}}^{+\frac{\eta_0}{2}}\int_{-\frac{\eta_0}{2}}^{+\frac{\eta_0}{2}} \cdot$$

$$\cdot \frac{e^{-\frac{|n_{ij}\xi_0 + \xi_j - \xi_i|}{U_c\theta} - \frac{i\omega}{U_c}(n_{ij}\xi_0 + \xi_j - \xi_i) - \frac{\omega}{B U_c}\left[K_n^2 + B^2(m_{ij}\eta_0 + \eta_j - \eta_i)^2\right]^{1/2}}}{\left[K_n^2 + B^2(m_{ij}\eta_0 + \eta_j - \eta_i)^2\right]^{1/2}} \cdot d\eta_j\, d\eta_i\, d\xi_j\, d\xi_i \tag{E38}$$

$$(0 \le \omega \le +\infty)$$

The integral of Equation (E38) is determined as discussed above. *Final equations* for the power and cross power spectral density of force acting on node points of a structure are summarized below [41] (because of the presence of the absolute value signs, evaluation of the integrals requires separate consideration of the various domains; see statement preceding Equation (E29).*

---

*Correction of the boundary layer load equations originally presented in Reference 34 were made by the authors of the present report. These corrections as well as certain other minor modifications were adopted in Reference 41 and the correct final results are given here.

FORCE POWER SPECTRAL DENSITY $(n_{ij} = m_{ij} = 0)$

$$\Phi_{F_{ii}}(\omega) = \Phi(\omega) = \hat{K}'\hat{P}(\omega)\hat{\Phi}$$

$$C_{F_{ii}}(\omega) = \hat{K}'\hat{P}(\omega)\hat{\Phi}\,; \qquad Q_{F_{ii}}(\omega) = 0 \tag{E39}$$

FORCE CROSS POWER SPECTRAL DENSITY $(n_{ij} \neq 0,\ m_{ij} \neq 0)$*

$$\Phi_{F_{ij}}(i\omega) = \Phi(n_{ij}, m_{ij};\, i\omega) = C_{F_{ij}}(\omega) + i\,Q_{F_{ij}}(\omega) \tag{E40}$$

FORCE CO-POWER SPECTRAL DENSITY $(n_{ij} \neq 0,\ m_{ij} \neq 0)$

$$C_{F_{ij}}(\omega) = C_F(n_{ij}, m_{ij};\, \omega) = \hat{K}'\hat{C}\hat{\Phi}\,e^{-|n_{ij}a\xi_0|} \tag{E41}$$

FORCE QUAD-POWER SPECTRAL DENSITY $(n_{ij} \neq 0,\ m_{ij} \neq 0)$

$$Q_{F_{ij}}(\omega) = Q_F(n_{ij}, m_{ij};\, \omega) = \hat{K}'\hat{Q}\hat{\Phi}\,e^{-|n_{ij}a\xi_0|} \tag{E42}$$

where $\hat{K}'$ = constant $= \overline{p^2}\eta_0 / 4.78\, U_c B^2$.

PRESSURE POWER SPECTRAL DENSITY

Setting $\xi = \eta = 0$ and letting $[K(m)r(\omega)]^2 = \overline{p^2}$ in Equation (E29) and using the foregoing equation for $\hat{K}'$, we obtain

$$\Phi_p(\omega) = \frac{\overline{p^2}}{9.56\,BU_c}\sum_{n=1}^{n=3} A_n\, e^{-\frac{K_n\omega}{BU_c}} = \frac{\hat{K}'B}{2\eta_0}\sum_{n=1}^{n} e^{-\frac{K_n\omega}{BU_c}} \tag{E42A}$$

$P(\omega)$ (power spectral density, dependent on ξ)

$$= \frac{2}{(a^2+b^2)^2}\{a\xi_0(a^2+b^2) + (b^2-a^2)[1-e^{-a\xi_0}\cos(b\xi_0)] - 2ab\,e^{-a\xi_0}\sin(b\xi_0)\} \tag{E43}$$

Φ = that part of Equation (E37) with dependence on η.

*If $n_{ij} = 0$, $m_{ij} \neq 0$, then $C_{F_{ij}}(\omega) = \hat{K}'\hat{P}\hat{\Phi}$ and $Q_{F_{ij}} = 0$.

There are two options for φ thus:

1. $\Phi(\omega)$ (uses Bessel function approximation)

$$= \sum_{n=1}^{N} A_n K_n Y_n \left(\frac{\omega K_n}{BU_c}\right) \kappa_0 \left(\frac{\omega K_n}{BU_c}\right) \quad \text{(Phi Hat Option 1)} \tag{E44}$$

2. $\hat{\Phi}(\omega)$ (uses numerical methods)

$$= \frac{B}{2n_0} \sum_{n=1}^{N} A_n K_n Z_n(m_{ij}, \omega) \quad \text{(Phi Hat Option 2)} \tag{E45}$$

$$Z_n(m_{ij},\omega) = \int_{\frac{-\eta_0}{2}}^{\frac{+\eta_0}{2}} \int_{\frac{-\eta_0}{2}}^{\frac{+\eta_0}{2}} \frac{e^{-\frac{\omega}{BU_c}[K_n^2 + B^2(m_{ij}n_0 + \eta_j - \eta_i)^2]^{1/2}}}{[K_n^2 + B^2(m_{ij}\eta_0 + \eta_j - \eta_i)^2]^{1/2}} \, d\eta_j \, d\eta_i \tag{E46}$$

$\hat{C}, \hat{Q}$ = those parts of Equation (E37) with dependence on ξ

$$\hat{C} = \frac{4}{(a^2 + b^2)^2} [V \cos(n_{ij} b\xi_0) + W \sin(n_{ij} b\xi_0)] \tag{E47}$$

$$\hat{Q} = \frac{4}{(a^2 + b^2)^2} [W \cos(n_{ij} b\xi_0) - V \sin(n_{ij} b\xi_0)] \tag{E48}$$

or

$$\begin{Bmatrix} \hat{C} \\ \hat{Q} \end{Bmatrix} = \frac{4}{(a^2 + b^2)^2} \begin{bmatrix} V & W \\ W & -V \end{bmatrix} \begin{bmatrix} \cos(n_{ij} b\xi_0) \\ \sin(n_{ij} b\xi_0) \end{bmatrix}$$

$$V = ab \sin(b\xi_0) \sinh(a\xi_0) + \frac{(b^2 - a^2)}{2} [1 - \cos(b\xi_0) \cosh(a\xi_0)]$$

$$\cdot \frac{(a^2 - b^2)}{2} \sin(b\xi_0) \sinh(a\xi_0) + ab[1 - \cos(b\xi_0) \cosh(a\xi_0)] \tag{E49}$$

$$= \frac{1}{U_c \theta}, \; b = \frac{\omega}{U_c} \tag{E50}$$

The C_F and Q_F matrices are each constructed separately by ordering terms to match the ordering of terms in the structural stiffness matrix, thus making the final expressions for the turbulent boundary layer loading function compatible with the finite element methods of structural analysis. If $\{\omega_K\}$ is the set of frequencies with N_ω total frequencies, then there are N_ω matrices $[C_F(\omega_K)]$ and $[Q_F(\omega_K)]$ as follows (for simplicity, the F subscript is dropped in the terms in the matrices so that $C_{F_{ij}}(\omega_k) \rightarrow C_{ij}(\omega_k)$ etc.).

$$[C_F(\omega_k)] = \begin{bmatrix} C_{11}(\omega_k) & C_{12}(\omega_k) & C_{13}(\omega_k) & --- & C_{1m}(\omega_k) \\ C_{21}(\omega_k) & C_{22}(\omega_k) & C_{23}(\omega_k) & --- & C_{2m}(\omega_k) \\ C_{31}(\omega_k) & C_{32}(\omega_k) & C_{33}(\omega_k) & --- & C_{3m}(\omega_k) \\ \vdots & \vdots & \vdots & & \vdots \\ C_{m1}(\omega_k) & C_{m2}(\omega_k) & C_{m3}(\omega_k) & --- & C_{mm}(\omega_k) \end{bmatrix} \tag{E51}$$

$$[Q_F(\omega_k)] = \begin{bmatrix} Q_{11}(\omega_k) & Q_{12}(\omega_k) & C_{13}(\omega_k) & --- & Q_{1m}(\omega_k) \\ Q_{21}(\omega_k) & Q_{22}(\omega_k) & Q_{23}(\omega_k) & --- & Q_{2m}(\omega_k) \\ Q_{31}(\omega_k) & Q_{32}(\omega_k) & Q_{33}(\omega_k) & --- & Q_{3m}(\omega_k) \\ \vdots & \vdots & \vdots & & \vdots \\ Q_{m1}(\omega_k) & Q_{m2}(\omega_k) & Q_{m3}(\omega_k) & --- & Q_{mm}(\omega_k) \end{bmatrix} \tag{E52}$$

Since $[\Phi_F(i\omega)]$ is Hermitian, then $[\Phi_F(i\omega)] = [\Phi_F^*(i\omega)]^T$ or $[C_F(\omega_k)] = [C_F(\omega_k)]^T$; $[Q_F(\omega)] = -[Q_F(\omega)]^T$ and terms in the matrices have the following properties

$$C_{F_{ii}}(\omega_k) = C_{F_{jj}}(\omega_k) = \Phi_F(\omega_k) \tag{E53}$$

$$C_{F_{ij}}(\omega_k) = C_{F_{ji}}(\omega_k) = C(n_{ij}, m_{ij}; \omega_k) = C(n_{ij} = -n_{ji}, m_{ij} = -m_{ji}; \omega_k) \tag{E54}$$

$$Q_{F_{ii}}(\omega_k) = Q_{F_{jj}}(\omega_k) = 0 \tag{E55}$$

$$Q_{F_{ij}}(\omega_k) = -Q_{F_{ji}}(\omega_k) \tag{E56}$$

Hence

$$[C_F(\omega_k)] = \begin{bmatrix} \Phi(\omega_k) & C_{12}(\omega_k) & C_{13}(\omega_k) & --- & C_{1m}(\omega_k) \\ C_{12}(\omega_k) & \Phi(\omega_k) & C_{23}(\omega_k) & --- & C_{2m}(\omega_k) \\ C_{13}(\omega_k) & C_{23}(\omega_k) & \Phi(\omega_k) & --- & C_{3m}(\omega_k) \\ \vdots & \vdots & \vdots & & \vdots \\ C_{1m}(\omega_k) & C_{2m}(\omega_k) & C_{3m}(\omega_k) & --- & \Phi(\omega_k) \end{bmatrix} \quad \text{(E57)}$$

$$[Q_F(\omega_k)] = \begin{bmatrix} 0 & Q_{12}(\omega_k) & Q_{13}(\omega_k) & --- & Q_{1m}(\omega_k) \\ -Q_{12}(\omega_k) & 0 & Q_{23}(\omega_k) & --- & Q_{2m}(\omega_k) \\ -Q_{13}(\omega_k) & -Q_{23}(\omega_k) & 0 & --- & Q_{3m}(\omega_k) \\ \vdots & \vdots & \vdots & & \vdots \\ -Q_{1m}(\omega_k) & -Q_{2m}(\omega_k) & -Q_{3m}(\omega_k) & --- & 0 \end{bmatrix} \quad \text{(E58)}$$

Diagonal terms of C_F are the collections of power spectral densities at all node points. Because the turbulent boundary layer is approximately a homogeneous random process and its thickness changes very slowly within a panel length, these diagonal terms are all equal.

The $[C_F(\omega)]$ and $[Q_F(\omega)]$ matrices are symmetric and skew symmetric, respectively. The diagonal terms of the $[\Phi_F(i\omega)]$ matrix are the diagonal terms of the $[C_F(\omega)]$ matrix, Equation (E57); hence the diagonal terms of the $[Q_F(\omega)]$ matrix are zero.

APPENDIX E2 – METHOD FOR DETERMINING INPUT DATA

In using the program described herein, it is necessary to calculate numerical values for boundary layer parameters δ^*, θ, $<p^2>$, and U_c.[41] These parameters and the associated quantities required for their calculation are defined below. The definitions assume incompressible flow and, therefore, are restricted to subsonic conditions. The Maestrello method (Appendix B2) may be used for computing additional input data.

Parameter	Description
c	Free-stream speed of sound (in./sec)
C_f	Local coefficient of skin friction (dimensionless), equal to $0.059\ R_x^{-1/5}$
K	Ratio of rms fluctuating pressure to local wall shearing stress (i.e., $<p^2>^{1/2}/\tau_w = 3.1$)
M	Mach number of the free stream
P_A	Ambient pressure (psi)
$<p^2>$	Mean square fluctuating pressure $(\text{psi})^2$, equal to $K^2 \tau_w^2$
q	Dynamic pressure (psi), equal to $\rho U^2/2$
R_x	Reynolds number based on x (dimensionless), equal to xU/ν
$R_{e\delta^*}$	Reynolds number based on δ^* (dimensionless), equal to $\delta^* U/\nu$
U_c	Mean convection velocity of pressure fluctuations in the boundary layer (in./sec)
x	Distance from leading edge, or nose, of body (in.)
γ	Ratio of specific heats, 1.4 at sea level; equal to c_p/c_v
δ	Boundary layer thickness (in.), equal to $0.37\ xR_x^{-1/5}$
δ^*	Boundary layer displacement thickness (in.), equal to $\delta/8$
θ	Mean eddy lifetime (sec)
μ	Viscosity (lb force sec/in.^{2})
ν	Kinematic viscosity (in^2/sec), equal to μ/ρ
ρ	Density of free stream (lb force sec^2/in.^{4})
τ_w	Local wall shearing stress (psi), equal to $C_f q = \frac{\gamma}{2} C_f P_A M^2$
$\sum_{n=1}^{3} \frac{A_n}{K_n}$	Equal to 9.56

The system of units is in inch-pound-seconds.

Measurements of the rms fluctuating pressure $\langle p^2 \rangle^{1/2}$ nondimensionalized with respect to the wall shear stress τ_w show considerable scatter (Figure 22). Different investigations show different relationships between $\langle p^2 \rangle^{1/2}/\tau_w$ and Mach number M, so it is difficult to predict the influence of Mach number on the rms pressure. It is assumed here that $\langle p^2 \rangle^{1/2}/\tau_w$ has the value 3.1 for all subsonic and low supersonic Mach numbers, and the model for the pressure power spectral density function, as shown in Figure 23, has been chosen accordingly. The value of $(\langle p^2 \rangle)^{1/2}/\tau_w$ was chosen to be close to the values measured in the majority of the investigations.

In the frequency domain, the convection velocity U_c and the eddy lifetime θ are functions of frequency. When the overall values of U_c and θ are considered, it is found that the effective values change with distance from the reference point. Complete representations of U_c and θ, which describe the spacial variation, greatly complicate the boundary layer model and, as a simple alternative, values of U_c and θ are chosen for a particular separation distance. Corrections to U_c and θ are proposed, depending on the frequency range of interest for the particular structure under consideration.

The mean convection velocity ratio U_c/U, taken as the asymptotic value for large separation distances, is not very sensitive to Mach number in subsonic and low supersonic flow. A value of $U_c/U = 0.82$ can be assumed for subsonic conditions as shown in Figure 24. This figure also indicates variation of subsonic convection velocity with frequency. The mean value is much closer to the low frequency value than it is to the high frequency value.

The mean eddy lifetime is shown in nondimensional form $U_c\,\theta/\delta^*$ in Figure 25 as a function of Reynolds number based on displacement thickness δ^*. The variation of θ with frequency is shown in Figure 26 where the results refer to measurements by Maestrello in fully developed turbulent pipe flow. The data in Figure 26 show that the low-frequency eddy lifetime will be longer by factors of 1.5 or greater than the mean lifetimes predicted in Figure 25.

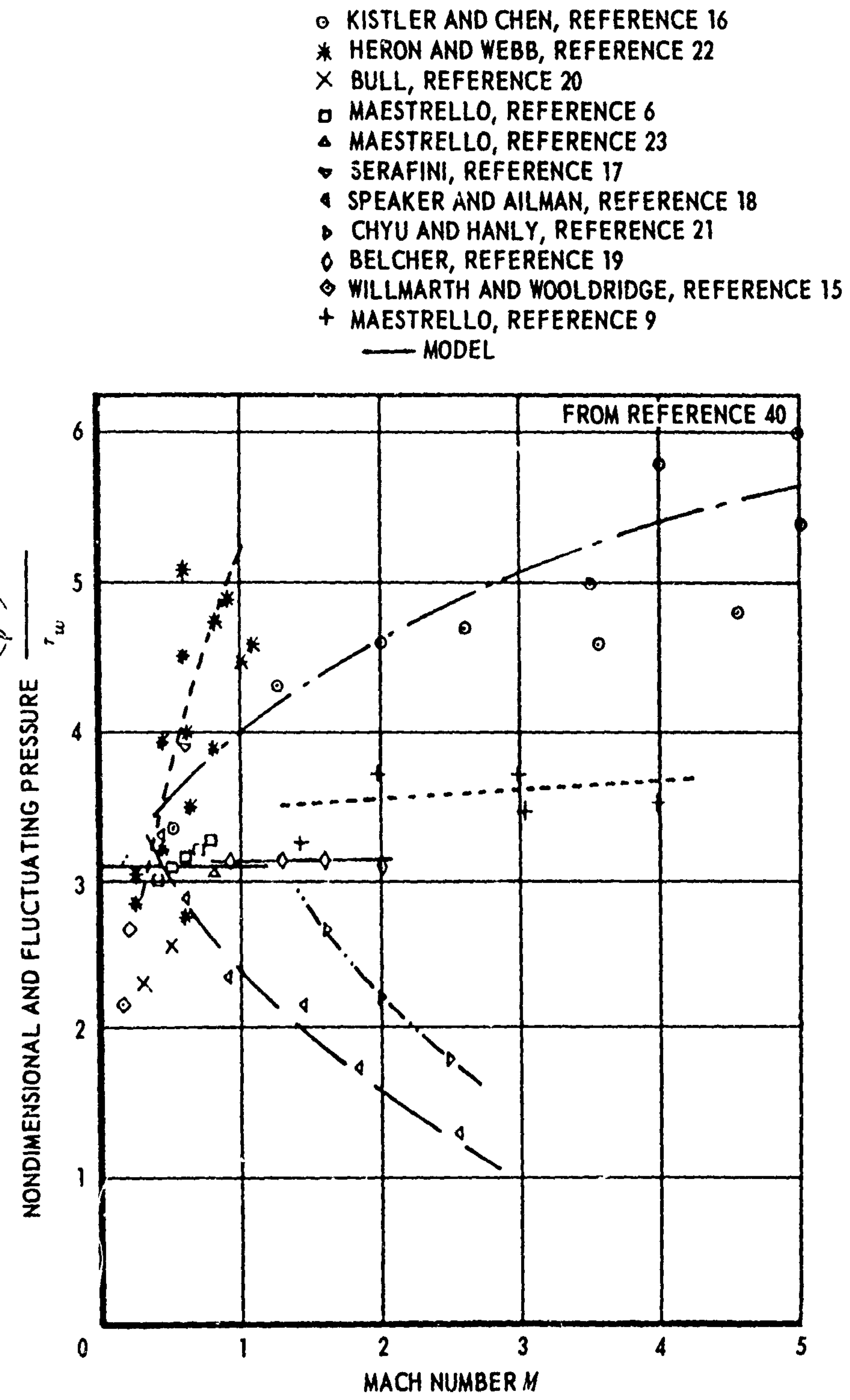

Figure 22 – Summary of Boundary Layer RMS Pressure Fluctuations

This figure is reproduced from Reference 41. The reference numbers indicated on this figure are those given in Reference 41.

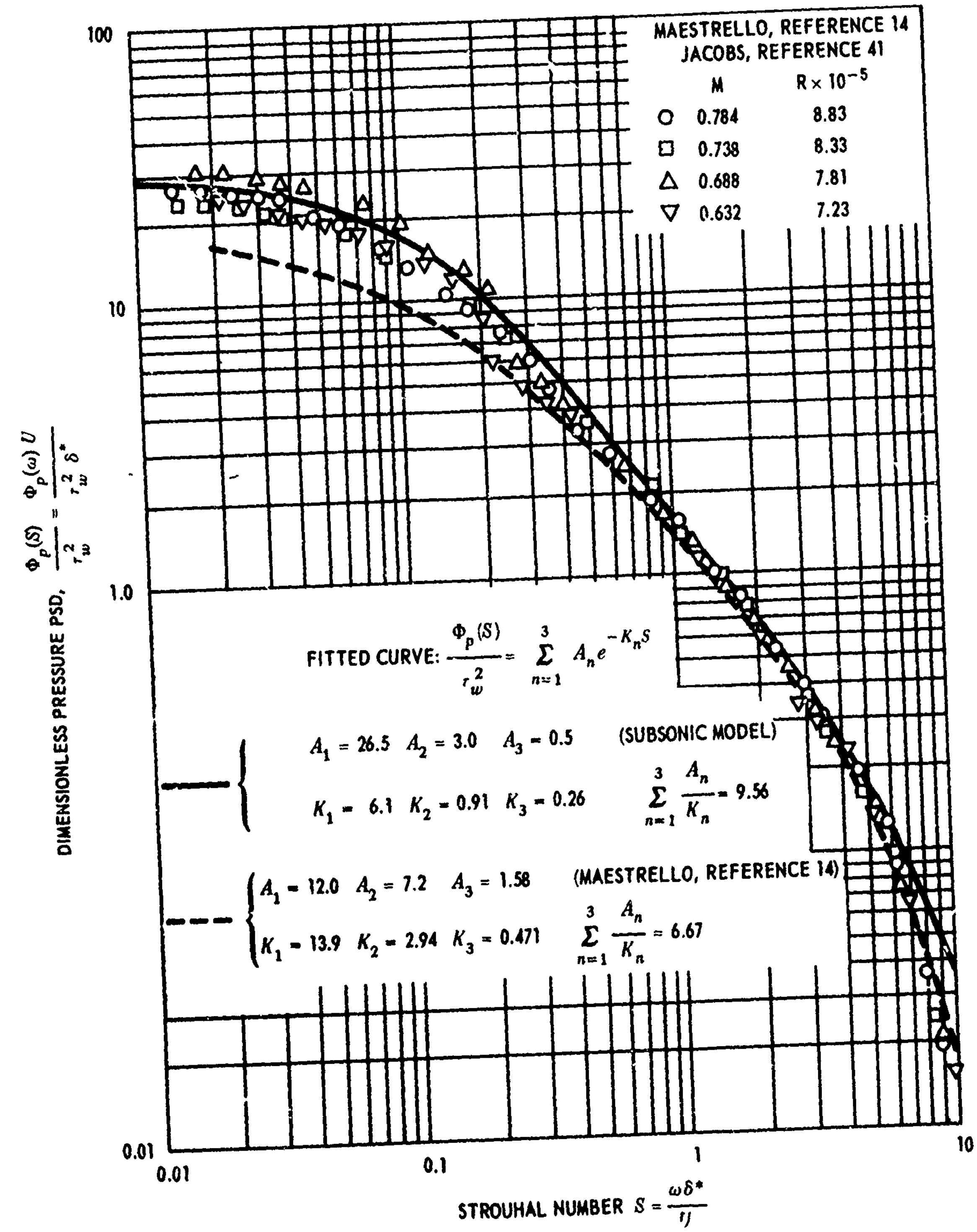

Figure 23 – Dimensionless Pressure Power Spectra

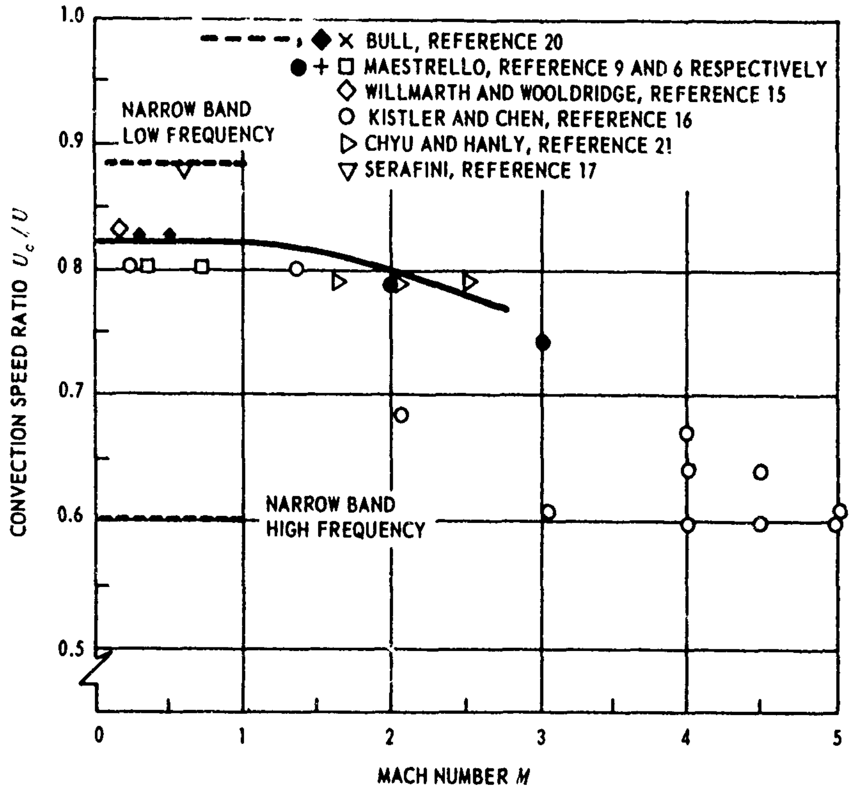

Figure 24 – Convection Speed Ratio

This figure is reproduced from Reference 41. The reference numbers indicated on the figure are those given in Reference 41.

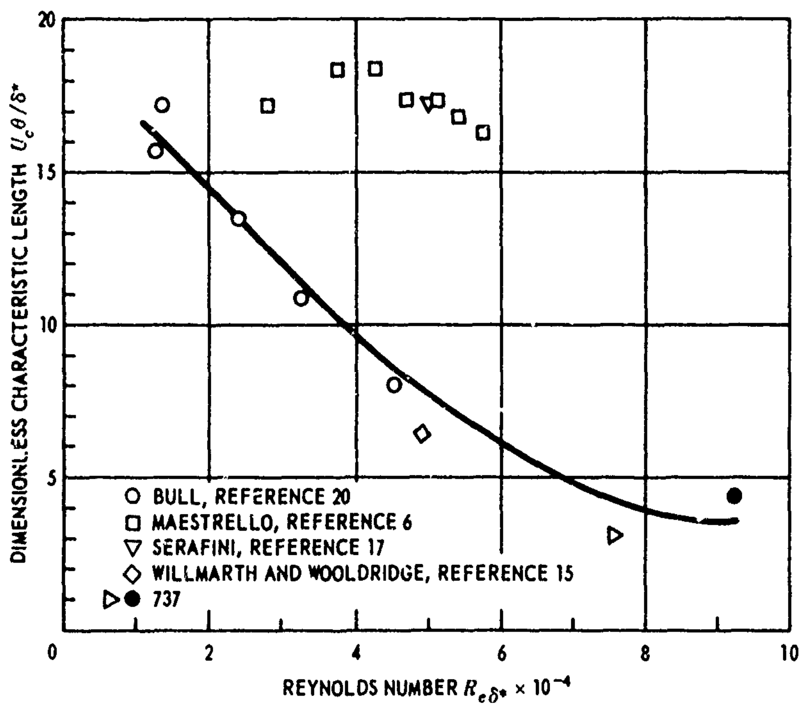

Figure 25 – Characteristic Length

This figure is reproduced from Reference 41. The reference numbers indicated on the figure are those given in Reference 41.

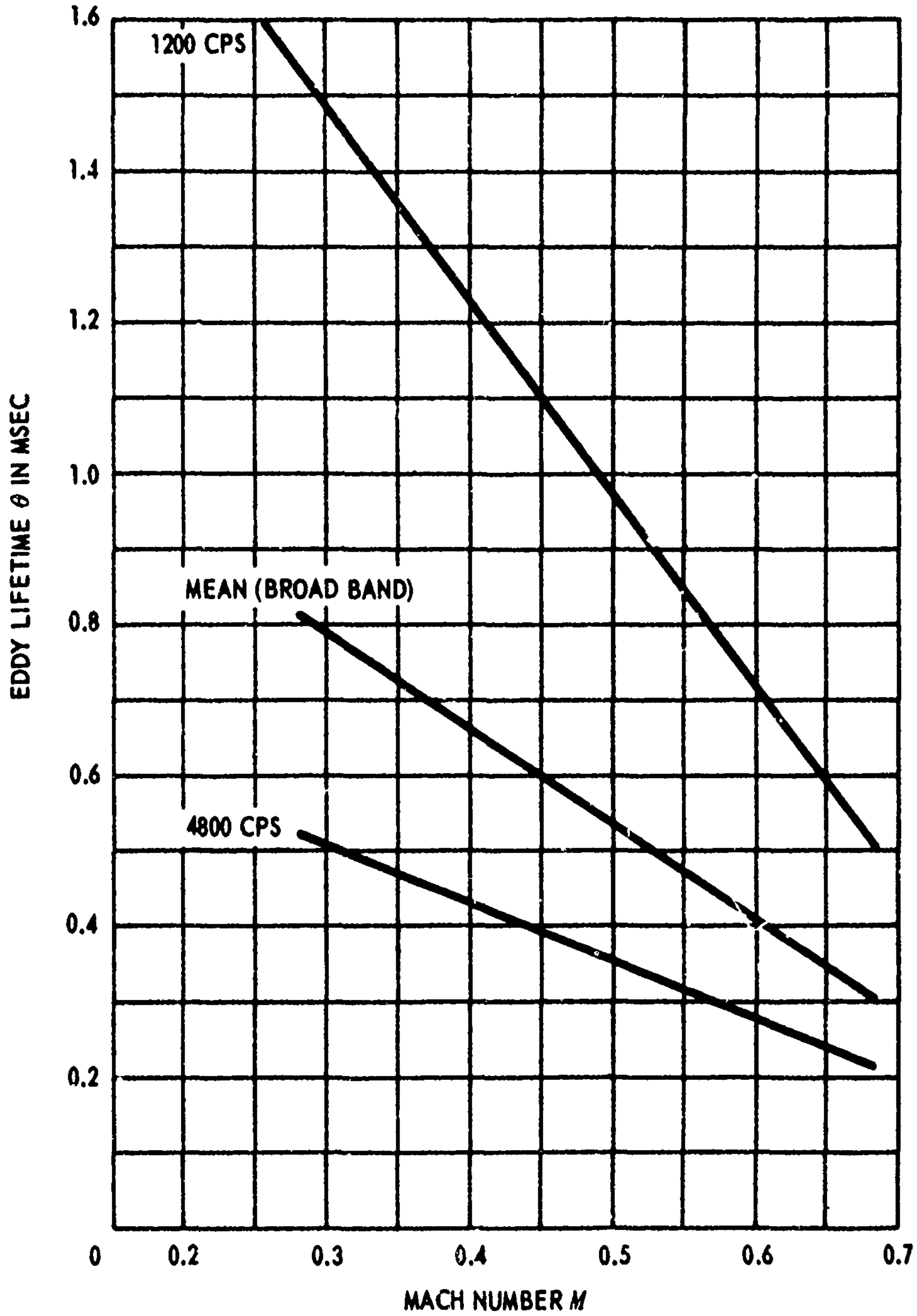

Figure 26 – Eddy Lifetime

Taken from Reference 14.

APPENDIX E3 – PROGRAM IDENTIFICATION

The reader is referred to References 36, 37, and 41 which present an extensive and detailed document of the computer program.

APPENDIX E4 – TEST RUNS

The computer printout of boundary layer input data is shown in Table 8a. Corresponding sample printouts of the computed force co-power spectral density matrix generated by these data are shown in Table 8b and 8c; note that the frequency associated with one sample differs from that of the other sample. The mean square displacement and displacement power spectral density of a 2024 aluminum alloy rectangular plate subject to this excitation are shown in Figures 27 and 28, respectively.*

*The set of force cross-PSD matrices define loads on a structure with certain geometric characteristics. Compatibility between the terms of both the loading and structural flexibility matrices can be achieved by using some of the structural geometry information and by specifying flow direction and the direction of cyclic structural node numbering (see page 25 of Reference 41 and References 36 and 37). For the convenience of the reader, a description of the numbering schemes used to achieve compatibility is given in Figure 29.

TABLE 8

Sample Printouts of Boundary Layer Input Data and Computed Force Co-Power Spectral Density Matrix – Jacobs

INPUT DATA

JACOBS BOUNDARY LAYER PLATE - AIAA PAPER 69-20 (SEE REFERENCE 42)

```
BOUNDARY LAYER FLOW MODEL OPTION - OPTION= 1
NUMBER OF FREQUENCIES FOR WHICH FORCE-CROSS-PSD MATRICES ARE TO BE PRINTED - NPRINT= 33
CYCLIC NODE NUMBERING DIRECTION - NCYCL= 2
FLOW DIRECTION - NFLOW= 1
ROW PRINT OPTION - RPRINT= -0
DISPLACEMENT THICKNESS - DELTA= 0.1550000E-00 IN.
MEAN EDDY CONVECTION VELOCITY - UC= 0.6200000E 04 IN./SEC
INCREMENTAL SEPARATION DISTANCE IN FLOW DIRECTION - XI= 0.1000000E 01 IN.
INCREMENTAL SEPARATION DISTANCE IN DIRECTION PERPENDICULAR TO FLOW - ETA= 0.1167000E 01 IN.
MEAN EDDY LIFETIME - THETA= 0.9100000E-03 SEC
NUMBER OF STRUCTURAL COORDINATES IN DIRECTION OF CYCLIC NODE NUMBERING -N1= 7
NUMBER OF STRUCTURAL COORDINATES IN DIRECTION PERPENDICULAR TO CYCLIC NODE NUMBERING DIRECTION - N2= 13
MEAN SQUARE FLUCTUATING PRESSURE RATIO - FPR= 0.4070000E-03 SQ. LBS


***** END OF INPUT DATA PRINTOUT *****
```

(Table 8A is used in Phase II of the RANVIB program with the ABLN load module. The force matrix CF(I,J) for this case is a 55x55 matrix, determined by the number of retained freedoms in Phase I, computed for frequencies specified by the user[36,37,41]. For any frequency, the number of rows of the matrix that are to be printed is either the first row or the total matrix.)

Table 8A – Turbulent Boundary Layer Pressure Loading on Finite Structural Elements

TABLE 8 (Continued)

FREQUENCY NO. 1 CF(I,J) MATRIX OMEGA = 0.27371982E 04

1	1.8343294E-08	9.5847473E-09	3.3228221E-09	1.3477665E-09	6.0726272E-10	1.4841135E-08
	7.7547979E-09	2.6884187E-09	1.0904468E-09	4.9132225E-10	8.8130685E-09	4.6050093E-09
	1.5964559E-09	6.4753686E-10	2.9176047E-10	2.9361496E-09	1.5341984E-09	5.3187302E-10
	2.1573248E-10	9.7202513E-11	-1.7357673E-09	-9.0697405E-10	-3.1442805E-10	-1.2753484E-10
	-5.7463333E-11	-4.6886978E-09	-2.4499409E-09	-8.4934087E-10	-3.4450029E-10	-1.5522138E-10
	-5.8835098E-09	-3.0742546E-09	-1.0657768E-09	-4.3228864E-10	-1.9477616E-10	-5.6215132E-09
	-2.9373560E-09	-1.0183170E-09	-4.1303854E-10	-1.8610265E-10	-4.3865067E-09	-2.2920398E-09
	-7.9460003E-10	-3.2229691E-10	-1.4521722E-10	-2.6998423E-09	-1.4107230E-09	-4.8906679E-10
	-1.9836989E-10	-8.9379456E-11	-1.0117252E-09	-5.2864721E-10	-1.8327041E-10	-7.4336127E-11
	-3.3493605E-11					

Table 8B — First Row 755 × 55 Matrix of the Forcing Function for the Frequency $w = 0.2737188ZE04$

FREQUENCY NO. 1 CF(I,J) MATRIX OMEGA = 0.20000000E 04

1	2.0364450E-08	1.1205248E-08	4.3956819E-09	2.0430298E-09	1.0565845E-09	1.7238963E-08
	9.4854932E-09	3.7210431E-09	1.7294705E-09	8.9442241E-10	1.2212589E-08	6.7198030E-09
	2.6360966E-09	1.2252079E-09	6.3363521E-10	7.3090158E-09	4.0216816E-09	1.5776566E-09
	7.3326495E-10	3.7921931E-10	3.0446401E-09	1.6752698E-09	6.5718786E-10	3.0544850E-10
	1.5796741E-10	-2.9035879E-10	-1.5976578E-10	-6.2674164E-11	-2.9129767E-11	-1.5064910E-11
	-2.5972299E-09	-1.4290887E-09	-5.6061403E-10	-2.6056280E-10	-1.3475408E-10	-3.9226527E-09
	-2.1583837E-09	-8.4670755E-10	-3.9353366E-10	-2.0352202E-10	-4.4100677E-09	-2.4265769E-09
	-9.5191646E-10	-4.4243278E-10	-2.2881095E-10	-4.2546174E-09	-2.3410425E-09	-9.1836239E-10
	-4.2683748E-10	-2.2074561E-10	-3.6657070E-09	-2.0170030E-09	-7.9124563E-10	-3.6775602E-10
	-1.9019071E-10					

Table 8C — First Row of 55 × 55 Matrix of the Forcing Function for the Frequency $w = 0.20000000E04$

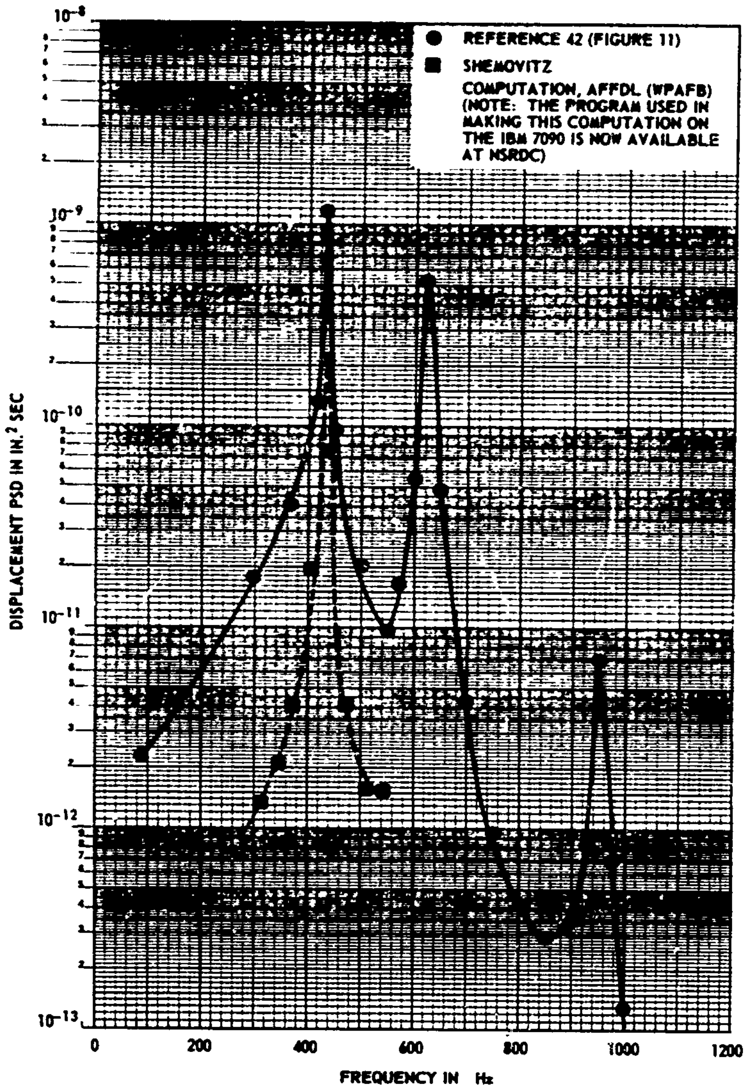

THE BOUNDARY LAYER AND PLATE PARAMETERS USED IN OBTAINING FIGURE 27 ARE

FLOW DATA
$<p^2> = 4.07 \times 10^{-4}$ (PSI)^2
$\delta^* = 0.155$ IN
$U_c = 0.88 U = 6200$ IN./SEC
$M = 0.52$
$Q = 9.1 \times 10^{-4}$ SEC
$\xi_0 = 1.00$ IN. } (SEPARATION DISTANCE
$\eta_0 = 1.167$ IN. } BETWEEN NODE POINTS)
FLOW IN x-DIRECTION

PLATE DATA: 12- × 7- × 0.08-IN. PLATE
$\xi_0 = 1.00$ IN.
$\eta_0 = 1.67$ IN.
MASS* = 0.000024 LB-SEC^2/IN.
E (YOUNGS MODULUS) = 1.05×10^7 PSI
ν OR γ (POISSONS RATIO) = 0.33
I_s (MOMENT OF INERTIA) = 4.267×10^{-5} IN^3

$t_x = 0$ $\quad I_x = 0$
$I_y = 0$ $\quad t_s = t_0$
$t_y = 0$ $\quad I_s = t_0^3/12 = (0.08)^3/12$ IN.^{3}

SEE PAGE 72 OF REFERENCE 36

*ELEMENT WEIGHT = (1.000) IN. × (1.167) IN. × (0.080) IN. × (0.1 LB/IN.^{3})
= 0.009336 LB

$$\text{MASS} = \frac{0.009336 \text{ LB}}{386 \text{ IN./SEC}^2} = 0.000024 \frac{\text{LB-SEC}^2}{\text{IN.}}$$

Figure 27 – Computed Displacement Power Spectral Density for a 12.0- × 7.0- × 0.08-Inch Aluminum Alloy Panel

Obtained at 38 th renumbered node—see Figure 29.

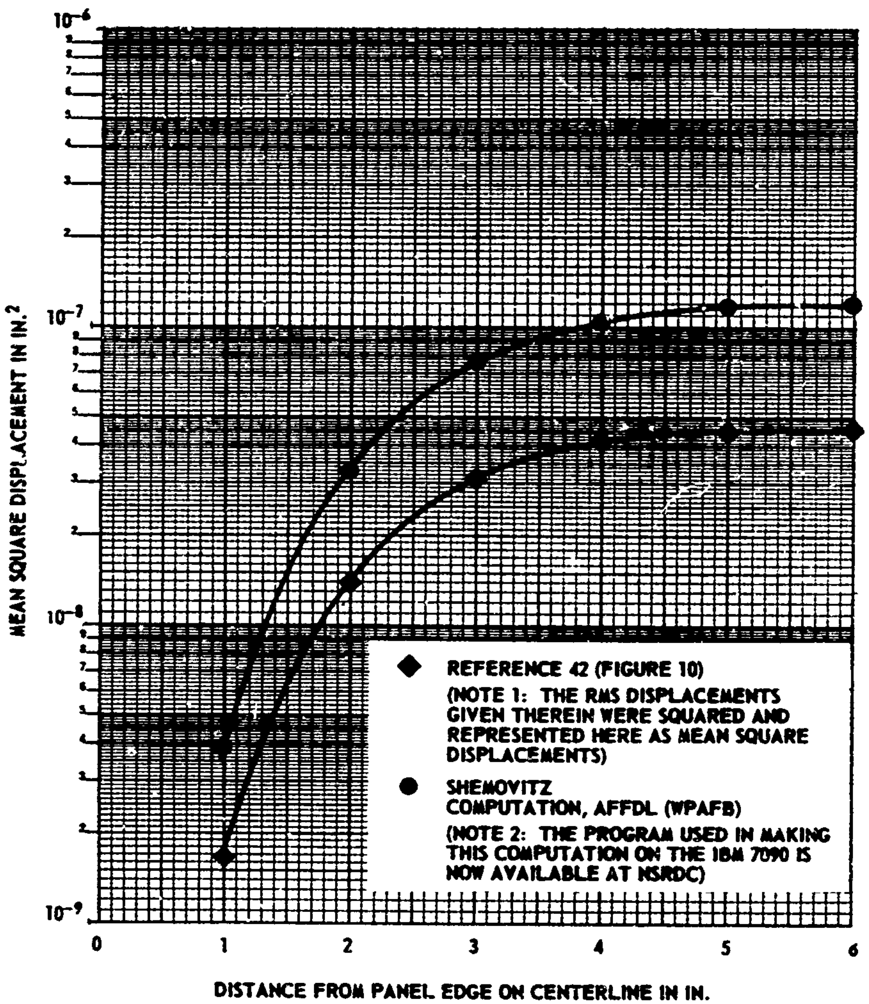

THE BOUNDARY LAYER AND PLATE PARAMETERS USED IN OBTAINING THE CENTERLINE RESPONSE SHOWN IN FIGURE 28 ARE*

FLOW DATA: $\langle p^2 \rangle = 4.07 \times 10^{-4}\ (\mathrm{PSI})^2$
$\delta^* = 0.155$ IN.
$U_c = 0.88\,U = 6200$ IN./SEC
$M = 0.52$
$Q = 9.1 \times 10^{-4}$ SEC
$\xi_0 = 1.00$ IN.
$\eta_0 = 1.167$ IN.
(SEPARATION DISTANCE BETWEEN NODE POINTS)
FLOW IN x-DIRECTION

PLATE DATA: 12- × 7- × 0.08-IN. PLATE
$\xi_0 = 1.00$ IN.
$\eta_0 = 1.67$ IN.
MASS* $= 0.000024$ LB-SEC²/IN.
E (YOUNGS MODULUS) $= 1.05 \times 10^7$ PSI
ν OR γ (POISSONS RATIO) $= 0.33$
I_z (MOMENT OF INERTIA) $= 4.267 \times 10^{-5}$ IN³

$t_x = 0$ $\quad I_x = 0$
$I_y = 0$ $\quad t_z = t_0$
$t_y = 0$ $\quad I_z = t_0^3/12 = (0.08)^3/12$ IN.³

SEE PAGE 72 OF REFERENCE 36

---

*ELEMENT WEIGHT = (1.000) IN. × (1.167) IN. × (0.080) IN. × (0.1 LB/IN.³)
= 0.009336 LB

$$\text{MASS} = \frac{0.009336\ \text{LB}}{386\ \text{IN./SEC}^2} = 0.000024\ \frac{\text{LB-SEC}^2}{\text{IN.}}$$

Figure 28 – Computed Mean Square Displacement for a 12.0- × 7.0- × 0.08-Inch Aluminum Alloy Panel

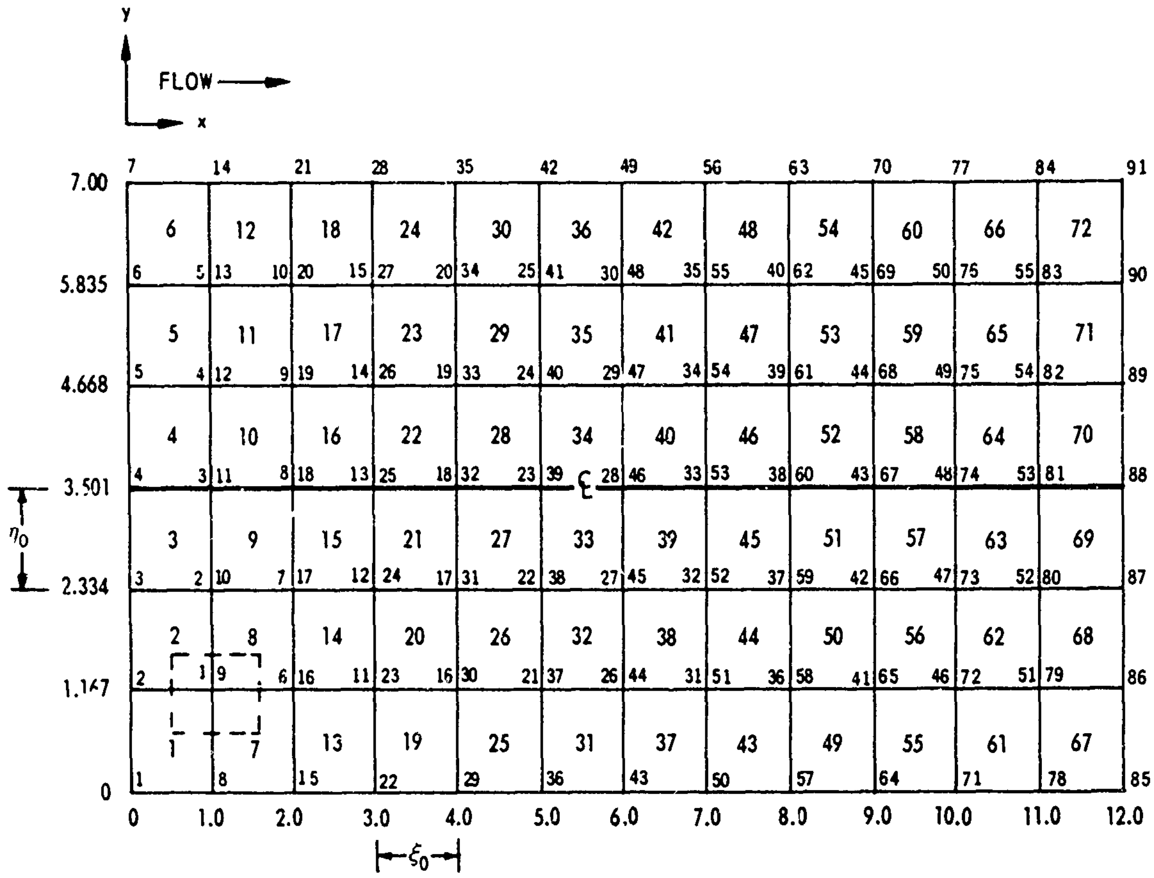

Note to Figure 29:

The area (12×7 in.^{2}) of the rectangular plate used in obtaining the results in Figures 27 and 28 was divided into 72 equal rectangles (1 × 1.167 in.) numbered consecutively in the y-direction as shown (1 through 72). The constraint conditions for each of the six degrees of freedom (θ_x, θ_y, θ_z, δ_x, δ_y, δ_z) are given for each node (free, fixed or attached to a spring).[36, 37, 41] The present example originally had 91 nodal points as shown (1 through 91), but only 55 of these nodes (inner nodes) have deflection δ_z free, which represent the retained freedoms. These (retained) nodes are renumbered in the y-direction as shown (1 through 55). The sizes of the solution matrices are determined by the number of retained freedoms, 55 in this example. Thus we use a 55 by 55 matrix. Note that the heavy line (centerline) in Figure 29 is the line along which the responses shown in Figures 27 and 28 were obtained.

The grid size ($\xi_0 \times \eta_0$) and the number of retained freedoms must be identical in Phases I and II of the computer program for compatibility to exist between the terms of both the loading and structural flexibility matrices. In the absence of compatibility, only the force co-power spectral matrices (Table 8) are generated, i.e., the computer will not generate response data, e.g., Figures 27 and 28.

Figure 29 – Cyclic Ordering of Nodes

(Area = $\xi_0 \times \eta_0$ = 1.167 in.^{2})

REFERENCES

1. Leibowitz, Ralph C., "Turbulence-Induced Vibrations and Radiations--A Projection of the State of the Art to Naval Research Needs," Acoustics and Vibrations Laboratory Technical Note AVL-185-942 (Jun 1967).*

2. Dyer, I., "Sound Radiation into a Closed Space from Boundary Layer Turbulence," Bolt Beranek and Newman, Inc., Report 602, ONR Contract Nonr-2321(00), Task NR 062-205 (Dec 1958).

3. Dyer, I., "Response of Plates to a Decaying and Convecting Random Pressure Field," Journal of the Acoustical Society of America, Vol. 31, No. 7 (Jul 1959).

4. Lin, Y.K., "Probabilistic Theory of Structural Dynamics," McGraw-Hill Book Company, New York (1967).

5. Morse, P.M. and Feshbach, H., "Methods of Theoretical Physics," Part 1, McGraw-Hill Book Company, New York (1953).

6. Dettman, J.W., "Mathematical Methods in Physics and Engineering," Chapter 4 , McGraw-Hill Book Company, New York (1962).

7. Campbell, G.A. and Foster R.M., "Fourier Integrals for Practical Applications," D. Van Nostrand Company, Inc., Princeton, N.J. (1951).

8. Lyon, R.H., "Propagation of Correlation Functions in Continuous Media," Journal of the Acoustical Society of America, Vol. 25, No. 1 (Jan 1953).

9. Nowacki, W., "Dynamics of Elastic Systems," John Wiley and Sons, Inc., New York (1963).

10. Smith, P.W., Jr., and Lyon, R.H., "Sound and Structural Vibration," National Aeronautics and Space Administration CR-160 (Mar 1965).

11. Kolsky, H., "Stress Waves in Solids," Dover Publications, Inc., New York (1963).

12. Willmarth, W.W., "Space-Time Correlations and Spectra of Wall Pressure in a Turbulent Boundary Layer," National Aeronautics and Space Administration Memorandum, 3-17-59W (Mar 1959).

13. Harrison, M.J., "Journal of the Acoustical Society of America 20:1252 (Abstract)" (1957). Also, "Pressure Fluctuations on the Wall Adjacent to a Turbulent Boundary Layer," TMB Report 1260 (Dec 1958).

14. Maestrello, L., "Measurement and Analysis of the Response Field of Turbulent Boundary Layer Excited Panels," Journal of Sound and Vibration, Vol. 2, No. 3, pp. 270–292 (1965).

*Reference 1 is available upon request to Dr. Don Ross, Head, Acoustics and Vibration Laboratory, Naval Ship Research and Development, Washington, D.C. 20007.

15. Maestrello, L., "Use of Turbulent Model to Calculate the Vibration and Radiation Responses of a Panel, with Practical Suggestions for Reducing Sound Level," Journal of Sound and Vibration, Vol. 15, No. 3, pp. 407–448 (1967).

16. Maestrello, L., "Design Criterion for Minimum Structural Response and Sound Radiation of a Panel Excited by a Turbulent Boundary Layer," Fifth Aerospace Sciences Meeting, American Institute of Aeronautics and Astronautics Paper 67-12 (23–26 Jan 1967).

17. Maestrello, L., "Test Results from the Boundary Layer Facility (Theory and Experimental Comparison)," Boeing Company Report D-6-9944 Vol. 3 (Jun 1966).

18. Tong, K.N., "Theory of Mechanical Vibration," John Wiley and Sons, Inc., New York (Jun 1963).

19. Apostol, T.M., "Mathematical Analysis," Addison-Wesley, Publishing Company, Inc., Reading, Mass. (1957).

20. Courant, R., "Differential and Integral Calculus," Vol. 2, formerly Interscience Publications, Inc., now John Wiley and Sons, Inc., New York (1947).

21. Pierce, B.O., "A Short Table of Integrals," Ginn and Company, Boston, Mass. (1929).

22. Maestrello, L., "Radiation from and Panel Response to a Supersonic Turbulent Boundary Layer," Boeing Scientific Research Laboratories Document D1-82-0719 (Sep 1968).

23. Coles, D., "The Law of the Wake in the Turbulent Boundary Layer," J. Fluid Mech., Vol. 1 (1956).

24. Maestrello, L., "Measurement of Noise Radiated by Boundary Layer Excited Panels," J. Sound Vib., 2(2), 100–115 (1965).

25. Schlicting, H., "Boundary Layer Theory," McGraw-Hill (1960).

26. Izzo, A.J. et al., "Sound Radiated from Turbulence Excited Finite Plates with Arbitrary Boundary Conditions," Report U411-67-045, General Dynamics/Electric Boat Division, Groton, Conn. (22 Aug 1967); also, U.S. Navy Journal of Underwater Acoustics, Vol. 18, No. 1 (Jan 1968).

27. Rayleigh J.W.S., "The Theory of Sound," Vol. 2, p. 107, Dover Publications, New York (1945).

28. Lee, Y.M., "Statistical Theory of Communication," John Wiley and Sons, Inc., New York (1963).

29. Izzo, A.J. et al., "Sound Radiated from Finite Plates Excited by a Turbulent Boundary Layer," Interim Report, General Dynamics/Electric Boat Division, Groton, Conn. (1 Sep 1966).

30. Young, D., "Vibration of Rectangular Plates by the Ritz Method," Trans. American Society of Mechanical Engineer, Vol. 72 (1956).

31. Bendat, J.S. et al., "Measurement and Analysis of Random Data," John Wiley and Sons, Inc., New York (1966).

32. Strawderman, W.A., "The Acoustic Field in a Closed Space Behind a Rectangular Simply Supported Plate Excited by Boundary Layer Turbulence," U.S. Navy Underwater Sound Laboratory Report 827 (11 May 1967).

33. Crandall, S.H. and Mark, W.D., "Random Vibration in Mechanical Systems," Academic Press, Inc., New York (1963).

34. Jacobs, L.D. and Lagerquist, D.R., "A Finite Element Analysis of Simple Panel Response to Turbulent Boundarys Layers," Technical Report AFFDL-TR-67-81, The Boeing Company, Commercial Airplane Division, Renton, Wash. (Jul and Dec 1967).

35. Jacobs, L.D. and Lagerquist, D.R., "Finite-Element Analysis of Complex Panel Response to Random Loads," Technical Report AFFDL-TR-68-44, The Boeing Company, Commercial Airplane Division, Renton, Wash. (Apr 1968).

36. Lagerquist, D.R., and Jacobs, L.D., "Random-Vibration Analysis System for Complex Structures," Technical Report AFFDL-TR-68-43, Part 1, Engineering Users Guide, The Boeing Company, Commercial Airplane Division, Renton, Wash. (Apr 1968).

37. Tsurusaki, K. and Wallace, F.S. "Random-Vibration Analysis System for Complex Structures," Technical Report AFFDL-TR-68-43, Part 2, Computer Program Description, The Boeing Company, Commercial Airplane Division, Renton, Wash. (Apr 1968).

38. Perlis, S., "Theory of Matrices," Addison-Wesley Publishing Company, Inc., Reading, Mass. (Mar 1956).

39. Maestrello, L., "Design Criterion of Panel Structure Excited by Turbulent Boundary Layer," Journal of Aircraft, Vol. 5, No. 4 (Jul-Aug 1968).

40. Gradshteyn, I.S. and Ryzhik, I.M., "Table of Integrals Series and Products," Academic Press, Inc., New York (1965).

41. Jacobs, L.D. et al., "A Computer Program on Turbulent Boundary Layer Loads for Use with Finite-Element Structural Analysis Systems," Boeing Commercial Airplane Division, Renton, Wash. D6-23769 (May 1969).

42. Jacobs, L. D. et al., "Response of Complex Structures to Turbulent Boundary Layers," American Institute of Aeronautics and Astronautics Seventh Aerospace Sciences Meeting, New York (20 Jan 1969).

BLANK PAGE

UNCLASSIFIED
Security Classification

DOCUMENT CONTROL DATA - R & D		
(Security classification of title, body of abstract and indexing annotation must be entered when the overall report is classified)		
1 ORIGINATING ACTIVITY (Corporate author) Naval Ship Research and Development Center Washington, D.C. 20034	2a. REPORT SECURITY CLASSIFICATION UNCLASSIFIED	
	2b. GROUP	
3 REPORT TITLE ENGINEERING GUIDE AND COMPUTER PROGRAMS FOR DETERMINING TURBULENCE-INDUCED VIBRATION AND RADIATION OF PLATES		
4 DESCRIPTIVE NOTES (Type of report and inclusive dates) Final Report 6/67 – 9/69		
5 AUTHOR(S) (First name, middle initial, last name) Ralph C. Leibowitz and Dolores R. Wallace		
6. REPORT DATE January 1970	7a. TOTAL NO OF PAGES 322	7b NO OF REFS 42
8a. CONTRACT OR GRANT NO	9a. ORIGINATOR'S REPORT NUMBER(S) Report 2976	
b. PROJECT NO S-R003 1001		
c. Task 11701	9b. OTHER REPORT NO(S) (Any other numbers that may be assigned this report)	
d.		
10 DISTRIBUTION STATEMENT This document is subject to special export controls and each transmittal to foreign governments or foreign nationals may be made only with prior approval of Naval Ship Systems Command, SHIPS 037.		
11 SUPPLEMENTARY NOTES	12 SPONSORING MILITARY ACTIVITY Naval Ship Systems Command, SHIPS 037	

13 ABSTRACT

This report is an engineering guide to the use of the Dyer method of manual computation and to several computer programs for determining turbulence-induced vibration and radiation of finite plates in air and in water. Both simple and clamped boundary conditions are treated. The Dyer method and the computer programs are presented in a series of appendixes:

A. Bolt Beranek and Newman Manual Method (Dyer)
B. Boeing Program I (Maestrello)
C. Electric Boat Program (Izzo)
D. Underwater Sound Laboratory Program (Strawderman)
E. Boeing Program II – Finite Element (Jacobs and Lagerquist)

The documentation is intended to facilitate the performance of flow-induced vibroacoustic computations as well as to furnish the groundwork for future research. It should also act as a theoretical guide for experimentalists. In the broader view, the documentation represents the initial steps of an effort to use computer programs to bridge the gap between vibroacoustic research results and design needs for structures that are subject to excitation by turbulence. Research tending to improve and extend the present program is recommended.

DD FORM 1 NOV 65 1473 (PAGE 1)

S/N 0101-807-6801

UNCLASSIFIED
Security Classification

14 KEY WORDS	LINK A		LINK B		LINK C	
	ROLE	WT	ROLE	WT	ROLE	WT
Turbulence-induced Vibration and Radiation of Plates						
1. Simply Supported and Clamped Boundaries						
2. Air and Water Fluid Media						
Manual Computation						
Digital Computer Programs						
Continuum and Finite Element Approach						
Theoretical and Experimental Recommendation						
Engineering Guide						